REPORT TO DECC

LONG-TERM ATMOSPHERIC MEASUREMENT AND INTERPRETATION

(OF RADIATIVELY ACTIVE TRACE GASES)

DECC contract number: GA0201

Annual Report (May 2012 - April 2013)

Date: 1st May 2013

University of Bristol: Simon O'Doherty, Aoife Grant

Met Office: Alistair J. Manning

rdscientific: Richard G. Derwent

INSCON: Peter Simmonds

Terra Modus: Dickon Young

Contents

1 Executive Summary 5
1.1 Project Summary 5
1.2 Summary of Headline Progress 5
2 Introduction 7
2.1 Objectives 7
2.1.1 For the measurement section of the project the objectives are: 7
2.1.2 For the interpretation part of the project the objectives are: 7
2.2 Detail on Specific Work Programme Items 8
2.3 Publications 12
2.4 Meetings 14
2.5 Related information 14
3 Instrumentation 15
3.1 Sites 16
3.1.1 Mace Head 16
3.1.2 Ridge Hill 16
3.1.3 Tacolneston 16
3.1.4 Angus 16
3.2 Calibration and Intercomparisons 16
3.2.1 AGAGE and NOAA comparisons 17
3.2.2 AGAGE and University of Heidelberg comparison 18
3.2.3 AGAGE-MD and LSCE-CRDS comparison 18
3.3 New Developments 20
3.3.1 Rolling SIM windows 20
3.3.2 Diagnostic measurements 22
3.3.3 Additional sample height at Tacolneston 22
3.3.4 Development of GCWerks for CRDS analysis 22
3.3.5 New Compounds 23
3.3.6 Isotopes 24
4 Description of data analysis methods 27
4.1 Introduction 27
4.2 Northern Hemisphere Atmospheric Baseline Trend Analysis 27
4.2.1 Introduction 27
4.2.2 Methodology 27
4.2.3 Baseline Concentrations 34
4.3 Regional emission estimation 34
4.3.1 InTEM (Inversion Technique for Emission Modelling) 34
4.4 Improvements to InTEM (April 2011 – April 2013) 40
4.4.1 Below baseline observations not fixed to zero 40
4.4.2 Each observation has an individual uncertainty 40
4.4.3 Alternate cost function has been developed 40
4.4.4 Solve with High and Low baseline possibilities 40
4.4.5 Baseline trends / Cycles 40
4.4.6 New inversion grid that conforms to country outlines 41
4.4.7 Overall impact of InTEM improvements 43
4.5 Incorporating new UK DECC network observations 44
4.6 Devolved Administration emission estimates 46
4.6.1 Methane Devolved Administration emissions 47
4.6.2 N_2O Devolved Administration emissions 50
5 Results and analysis of gases reported to the UNFCCC 53
5.1 Introduction 53
5.2 HFC-125 54
5.3 HFC-134a 57
5.4 HFC-143a 60
5.5 HFC-152a 63
5.6 HFC-23 66
5.7 HFC-32 69

5.8 HFC-227ea 72
5.9 PFC-14 (CF_4) 75
5.10 PFC-116 78
5.11 PFC-218 81
5.12 PFC-318 84
5.13 SF_6 85
5.13.1 SF_6 emissions estimated using the extended UK DECC network 88
5.14 Methane (CH_4) 89
5.14.1 CH_4 emissions estimated using the extended UK DECC network 93
5.15 Nitrous oxide (N_2O) 94
5.15.1 N_2O emissions estimated using the extended UK DECC network 97
5.16 Carbon dioxide (CO_2) 98
6 Results and analysis of additional gases 102
6.1 Introduction 102
6.2 CFC-11 103
6.3 CFC-12 106
6.4 CFC-113 109
6.5 CFC-115 112
6.6 HCFC-124 113
6.7 HCFC-141b 116
6.8 HCFC-142b 119
6.9 HCFC-22 122
6.10 HFC-236fa 125
6.11 HFC-245fa 128
6.12 HFC-365mfc 131
6.13 HFC-4310mee 133
6.14 SO_2F_2 134
6.15 CH_3Cl 135
6.16 CH_2Cl_2 138
6.17 $CHCl_3$ (chloroform) 141
6.18 CCl_4 (carbon tetrachloride) 144
6.19 CH_3CCl_3 (methyl chloroform) 147
6.20 $CHClCCl_2$ 150
6.21 CCl_2CCl_2 153
6.22 Methyl bromide (CH_3Br) 156
6.23 CH_2Br_2 157
6.24 Bromoform ($CHBr_{3)}$ 158
6.25 Halon-1211 159
6.26 Halon-1301 162
6.27 Halon-2402 165
6.28 CH_3I 166
6.29 Ethane (C_2H_6) 167
6.30 Carbon monoxide (CO) 168
6.31 Ozone (O_3) 171
6.31.1 Analysis of Mace Head ozone data 1987 - 2012 172
6.32 Hydrogen 173
7 References 174
8 Appendices 177
8.1 Instrumental 177
8.2 Sites 179
8.2.1 Mace Head 179
8.2.2 Ridge Hill 180
8.2.3 Tacolneston 181
8.2.4 Angus 183
8.3 PFC point source analysis 186
8.3.1 Introduction 186
8.3.2 PFC-14 (CF_4) 186
8.3.3 PFC-218 194

8.4 Stratospheric – Tropospheric exchange 199
8.4.1 Synopsis of paper submitted to the Journal of Geophysical Research 199
8.4.2 Potential Applications of this research. 206
8.5 SPARC (Stratospheric Processes And their Role in Climate) 207
8.5.1 Re-evaluation of Lifetimes of Dominant Stratospheric Ozone Depleting Substances 207

1 Executive Summary

1.1 Project Summary

Monitoring of atmospheric concentrations of gases is important in assessing the impact of international policies related to the atmospheric environment. The effects of control measures on chlorofluorocarbons (CFCs), halons and HCFCs introduced under the 'Montreal Protocol of Substances that Deplete the Ozone Layer' are now being observed. Continued monitoring is required to assess the overall success of the Protocol and the implication for atmospheric levels of replacement compounds such as HFCs. Similar analysis of gases regulated by the Kyoto Protocol on greenhouse gases will likewise assist policy makers.

Since 1987, high-frequency, real time measurements of the principal halocarbons and radiatively active trace gases have been made as part of the Global Atmospheric Gases Experiment (GAGE) and Advanced Global Atmospheric Gases Experiment (AGAGE) at Mace Head, County Galway, Ireland. For much of the time, the measurement station, which is situated on the Atlantic coast, monitors clean westerly air that has travelled across the North Atlantic Ocean. However, when the winds are easterly, Mace Head receives substantial regional scale pollution in air that has travelled from the industrial regions of Europe. The site is therefore uniquely situated to record trace gas concentrations associated with both the mid-latitude Northern Hemisphere background levels and with the more polluted air arising from Europe.

The observation network in the UK has been expanded to include three additional stations; Angus Tower near Dundee, Tacolneston near Norwich and Ridge Hill near Hereford. Ridge Hill became operational in February 2012, Tacolneston began operating in July 2012 and Angus Tower has been making measurements since late 2005.

The Met Office's Lagrangian atmospheric dispersion model, **NAME** (**N**umerical **A**tmospheric dispersion **M**odelling **E**nvironment), has been run for each 2-hour period of each year from 1989 so as to understand the recent history of the air arriving at Mace Head at the time of each observation. By identifying when the air is unpolluted at Mace Head, i.e. when the air has travelled across the Atlantic and the air concentration reflects the mid-latitude Northern Hemisphere baseline value, the data collected have been used to estimate baseline concentrations, trends and seasonal cycles of a wide range of ozone-depleting and greenhouse gases for the period 1989-2012 inclusive.

By removing the underlying baseline trends from the observations and by modelling the recent history of the air on a regional scale, estimates of UK, Irish and North West European (UK, Ireland, France, Germany, Denmark, the Netherlands, Belgium, Luxembourg) emissions and their geographical distributions have been made using **InTEM** (**In**version **T**echnique for **E**mission **M**odelling). The estimates are presented as yearly averages and are compared to the UNFCCC inventory.

The atmospheric measurements and emission estimates of greenhouse gases provide an important cross-check for the emissions inventories submitted to the United Nations Framework Convention on Climate Change (UNFCCC). This verification work is consistent with good practice guidance issued by the Intergovernmental Panel on Climate Change (IPCC).

1.2 Summary of Headline Progress

1. **All UK DECC Network sites are now operational**. The compounds measured at each site are shown in Table 1. This is the first network of its kind in the UK (and Europe) and has been a major achievement to get it to this stage within the time schedule outlined in the contract.
2. **Improved precision**. There have been a number of instrumental 'new developments' that have improved sample precision and ease of analysis/calibration. The development of software to allow 'rolling SIM windows' for the Medusa-MS is detailed in section 3, and the development of

software for processing the high volume cavity ringdown spectrometers (CRDS) data (1 Hz) will simplify data analysis and ensure acquisition of the highest quality dataset. This software is currently under development, but application to the Ridge Hill data looks very promising, as detailed in section 3.

3. **New compounds**: Significant work towards including additional compounds (NF_3 and C_6F_{14}) relevant to the Kyoto Protocol is detailed in 3.
4. **Mace Head** continues to be a baseline station at the forefront of global atmospheric research. This is demonstrated by the high volume of peer-reviewed publications related to work using the Mace Head observational record. A summary of publications related to this contract are detailed in the publication section of this report. In addition, the inclusion of Mace Head in many new EU funded atmospheric research programmes, such as ICOS, InGOS, ACTRIS, and continued support from other global programmes such as AGAGE and NOAA-ESRL indicates its international significance.
5. **New funding** has been secured by the University of Bristol to ensure that measurements of the key GHGs (CO_2, CH_4, N_2O and CO) continue at Tall Tower Angus (TTA) using state-of-the-art cavity ringdown spectrometers (CRDS).
6. **Inversion grid conforms to country (and Devolved Administration) regions**. The previous gridding method meant that in some instances a large grid box would overlap several countries and thereby all the emissions in that grid box would be split across multiple countries. By dividing the grid in a manner that is sensitive to country outlines this will no longer happen with the result that emissions near country borders are more likely to be assigned to the correct country. This is especially important given the requirement to report Welsh, Scottish, Northern Irish and English emissions separately.
7. **Baseline trend and seasonal cycle method.** The technique for splitting the baseline monthly mole fractions into a long-term trend and a seasonal component was improved. For each gas, two de-trending methods are now reported.
8. **Estimating UK CO_2 emissions.** The method for estimating UK CO_2 emissions was revised. Due to the strong biogenic CO_2 signal in the observations the current inversion method is not directly applicable to CO_2. For this report use has been made of the CO inversion estimates and the reported CO:CO_2 emission ratio to estimate UK emissions of CO_2.
9. **HFC-4310mee and PFC-318**. The monthly mole fractions of these gases are reported for the first time.
10. **Mid-latitude Northern Hemisphere baseline trends updated on website**. The trends are also presented in this report and have been extended up to and including December 2012.
11. **UK emission estimates**. Inversion emission estimates for the UK and North West Europe are reported up to and including 2012 and has been compared to the 2013 reported UK inventory (covers emissions up to and including 2011).
12. **UNFCCC verification appendix chapter** for the UK submission (National Inventory Report) delivered (March 2013).

2 Introduction

2.1 Objectives

2.1.1 For the measurement section of the project the objectives are:

1. To either lease, purchase or otherwise provide, and maintain instrumentation to obtain measurements of the gases listed in Annex 1 and to run the atmospheric observation site at Mace Head, Ireland.

2. To continue high quality real-time measurements of the gases listed in Annex 1 at Mace Head, Ireland, including routine in situ GC-MS measurements of perfluorocarbons (PFCs), hydrochlorofluorocarbons (HCFCs), hydrofluorocarbons (HFCs), methyl bromide, halons and other halogenated gases relevant to stratospheric ozone depletion and climate change.

3. To either lease, purchase or otherwise provide, and maintain instrumentation to obtain measurements of the major Kyoto gases (CO_2, CH_4, and N_2O) and to run atmospheric observation sites at any proposed additional site/s across the UK.

4. To make high-quality real time measurements of the major Kyoto gases at any additional observation site(s), consistent with the requirements set out above.

5. To continue international collaboration and data exchange within the global Advanced Global Atmospheric Gases Experiment (AGAGE) project. This will include, inter alia, the determination of global magnitude and latitudinal distribution of the surface sources of greenhouse gases

6. To provide data to help study the atmospheric behaviour of trace gases, to estimate source gas strengths in the UK and NW Europe and to study the concentrations and trends in the total chlorine/bromine content of the atmosphere and the oxidising capacity of the atmosphere

7. To maintain an up-to-date calibrated database of any of the trace gases measured under contract to DECC at Mace Head and any additional site/s, and to maintain a secondary database of any measurements made as part of the AGAGE global network.

8. To continue technical development of measurement methodologies to improve reliability and accuracy wherever possible.

2.1.2 For the interpretation part of the project the objectives are:

9. To quantify anthropogenic emissions (by source gas) of halocarbons, and anthropogenic emissions (by source gas, also source gas removal by sinks) of greenhouse gases, at the North West European, UK and Devolved Administrations (DA) levels and to use these for inventory verification.

10. To identify new substances with ozone depleting or radiative forcing properties, and quantify these where necessary.

11. To assess trends in emissions and concentrations of greenhouse gases and halocarbons and identify departure from expected trends, and the causes of any noted departure.

12. To identify additional sources of data for assessing compliance and verification of emissions inventories, particularly work initiated under the auspices of Working Group 1 of the EU Monitoring Mechanism and other EU programmes currently underway and report on these to DECC, with forewarning of upcoming meetings and their objectives.

2.2 Detail on Specific Work Programme Items

1. Assess and report concentrations of direct and indirect greenhouse gases measured at Mace Head and any additional site/s.

A majority of gases specified in Annex 1 of the original tender document are submitted to the Carbon Dioxide Information Analysis Center (CDIAC, http://cdiac.ornl.gov/) every six months. CDIAC is the primary climate-change data and information analysis cent of the U.S. Department of Energy. The CDIAC data are automatically reformatted and sent to the World Data Centre for Greenhouse Gases (WDCGG, http://ds.data.jma.go.jp/gmd/wdcgg/) which is one of the WDCs under the GAW programme that serve to gather, archive and provide data on greenhouse gases and other related gases in the atmosphere and ocean. As part of the EU InGOS project the AGAGE data submitted to CDIAC data will also be made available to the EBAS database (http://ebas.nilu.no/), as will all of the data from the new DECC Network sites. At present the format of Met data files and mole fraction data with errors are being finalised, with first submission of data scheduled for June 2013.

The reported baseline concentrations (mole fractions), annual growth rates and seasonal cycles along with instrumentation and calibration details are illustrated in the "UK DECC Network" website (http://www.metoffice.gov.uk/atmospheric-trends/). (Links to Objective 9).

2. Analyse and update annually global baseline atmospheric concentration trends and European emissions of the gases in Annex 1. Comparisons should be made with inventory data, and if relevant production and consumption figures provided by industry to the EU.

For each gas, baseline atmospheric concentration trends for the mid-latitude northern hemisphere have been reported quarterly through the website and are reported in Sections 5 and 6.

For each gas measured at Mace Head, an estimate of the UK and North West European (NWEU) (comprising of Ireland, UK, France, Belgium, The Netherlands, Luxembourg, Germany, Denmark) annual emissions have been made using the InTEM system (see Sections 5 and 6). The UK estimates for N_2O and CH_4 have been sub-divided to DA level. Where available the InTEM results have been compared against GHG inventory and other emission data.

3. Identify departure from expected trends in concentration and emissions of gases listed in Annex 1 and identify causes of these variations. Identify and assess the reasons for any departure from expected trends in concentration.

The trends in the mid-latitude northern hemisphere baseline concentrations of each gas are discussed in Sections 5 and 6. The UK emission trends of each gas are discussed and any departures from the expected have been highlighted.

4. Identify any additional sources of data for monitoring gases listed in Annex 1.

The additional UK DECC network stations, Ridge Hill, Tacolneston and Angus are discussed in Section 3 (for more detail see the Appendix, and the website www.metoffice.gov.uk/atmospheric-trends)

In the last year of the project, relevant observations from the wider ICOS network will be included within the InTEM analysis. This work will be facilitated through collaborations within the EU INGOS programme and the NERC GAUGE programme.

5. Make and update annually estimates of European and UK emissions of direct and indirect GHG and provide comparisons with the UKGHGI, EMEP and the EEA emissions inventories. Any discrepancies with emissions inventories should be highlighted and discussed.

InTEM has been applied to the direct and indirect greenhouse gases measured at Mace Head. Annual UK (and subdivided to DA level) and NW European emission estimates using Mace Head observations are reported in Sections 5 and 6 The observations from Ridge Hill and Tacolneston, along with the Mace Head observations from the same period, have been used within InTEM to estimate UK emissions of N_2O, CH_4 and SF_6, over a 6-month period (July 2012 – Dec 2012).

Where data are available these estimates have been compared to those reported elsewhere, most notably those reported through the UNFCCC programme, and the discrepancies are discussed. Due to the significant biogenic emissions and sinks of CO_2, estimating the anthropogenic emissions of CO_2 has been treated separately.

6. Identify new ozone depleting or global warming substances of potential policy interest, and provide details to DECC. Investigate the potential and feasibility for further expanding the policy relevance of Mace Head or any other sites' data, by considering other classes of atmospheric trace gases such as hydrocarbons, oxygenated species, perfluorocarbons, very long lived molecules, and oxygen concentrations.

It is a primary aim of the AGAGE program and UK DECC Network to identify new ozone depleting or global warming substances and where possible add these compounds to the ever increasing number of substances measured using the Medusa-MS at Mace Head, and more recently Tacolneston. However, with this type of activity there will always be a compromise between the number of substances measured and the precision of the measurement that can be achieved. For this reason, it normally takes a reasonable amount of time between identification of new compounds, assessment of the implication of adding the compound to the analysis list (i.e. degradation of measurement performance for existing compounds) and agreeing that the importance of the science questions that can be answered from the addition of the compound, warrant their inclusion. This process has taken place for two sets of compounds over the past year: nitrogen trifluoride (NF_3), and the higher molecular weight perfluorocarbons (PFCs). A discussion of these compounds is given in Section 3 (see Objective 10).

7. Identify any gaps in existing data from Mace Head and any additional site/s that could potentially be of policy relevance.

Isotope measurements of CO_2, CH_4 and N_2O have the potential to add further constraints to the inversion system, for example by providing additional information on the emissions from different source sector categories. The scope and challenges of isotope observations are discussed in Section 3.3.8.

8. Liaise with Hadley Centre over 3D atmospheric chemistry modelling being carried out at the Hadley Centre and provide data for model validation purposes, if required.

The monthly time-series of baseline concentrations and average seasonal cycles of all of the gases measured at Mace Head and the other AGAGE stations considered are provided to the Hadley Centre (part of the Met Office). Currently the data provided, although of direct relevance, is not widely used. To facilitate raising awareness of this useful source of data, the Met Office staff directly involved in this contract have been moved into the Hadley Centre, into the 'Earth System and Mitigation Science' group.

9. Investigate the use that could be made of new or additional sources of data such as isotope measurements or flux data, in conjunction with data from Mace Head and the additional site/s, or from any other sites that could potentially be of policy relevance, for verifying GHG emissions.

Through the new NERC funded GAUGE programme, new sources of data will become available. These include, inter-calibrated information from ground-based, airborne, ferry-borne, balloon-borne, and space-borne sensors, including new sensor technology and isotope measurements. (http://www.geos.ed.ac.uk/research/eochem/gauge.html). The contractors are also partners in this

new programme and will feed through the results from the use of these new data sources in a timely manner. As discussed above, use will also be made of relevant and available non-UK ICOS observations e.g. through the EU InGOS programme. (links to Objective 9). There are some isotope measurements made at Mace Head ($\Delta^{14}CO_2$ by University of Heidelberg and $\delta^{13}CO_2$ by NOAA) although, in isolation, these measurements do not provide a great deal of useful information about UK anthropogenic/biogenic emissions. As part of the NERC GAUGE programme we propose to use the existing "baseline" measurements at Mace Head, extend them and make new UK "pollution" measurements at an additional UK DECC network site, and from the FAAM aircraft, to provide information that will be more policy relevant for verifying GHG emissions. The revised GAUGE proposed isotope work is detailed in Section 3 and has recently been agreed by NERC (links to Objective 9).

10. Provide advice, as requested by DECC, on the relative roles of radiatively active trace gases in forcing climate change and, where possible, compute global warming potentials (GWPs) for any new substances identified.

This has taken place for the higher molecular weight PFCs, see Section 3.3.5.2, High molecular weight perfluorocarbons, for a full description of the work that has taken place.

11. Report on developments in the understanding of anthropogenic and natural sources and sinks of carbon dioxide, methane and nitrous oxide, using seasonal trends in emissions and analysis of annual trends

Annual UK and North West European emission estimates, through the use of inversion modelling, of carbon dioxide (CO_2), methane (CH_4) and nitrous oxide (N_2O) are reported in Section 5. The agreement between the anthropogenic inventory and the InTEM results for N_2O is good. The uncertainty ranges in the InTEM N_2O results are considerably smaller than those reported in the inventory. For CH_4 the UK InTEM results are consistently lower than the inventory pre-2000 estimates but agree, within the uncertainty, post-2000. The magnitude of the uncertainties in the InTEM CH_4 estimates are comparable to those reported for the inventory. For N_2O and CH_4 it has been assumed that on the NWEU scale the biogenic emissions are small compared to the anthropogenic contribution. For CO_2 the same assumption is not plausible and so an alternative route through the ratio to anthropogenic carbon monoxide has been used to estimate UK anthropogenic CO_2 emissions. The InTEM CO_2 estimates calculated through this method have very significant uncertainties compared to the reported inventory uncertainties.

In the final year of the project, using the observations from the extended network, 1, 2 or 3-monthly emission estimates and estimates using only daytime / night-time observations will be calculated. These additional emission estimates will provide some detail of the seasonal emissions and also may provide some indication of the biogenic – anthropogenic split in the emissions. A literature survey of the alternative methods of estimating anthropogenic emissions of CO_2 from observations will also be conducted. Isotopic measurements may also aid our understanding of this split, but the sparsity of observations will make this very challenging. The scope and challenges of isotope observations are discussed in Section 3.3.8.

12. Compare data from Mace Head and any additional site/s with data from other national and international studies, where appropriate.

The consortium is part of the AGAGE community and regularly compares analyses where appropriate. CSIRO (Australia) conducts comprehensive comparisons between all of the data measured by AGAGE (including Mace Head) and other global sites around the world. A selection of recent comparisons that have taken place at Mace Head are detailed in Section 3 (refer to Objective 9).

13. Provide assistance and as requested by DECC, on validation of European and national-level trace gas emission inventories, and on monitoring compliance with international protocols and agreements or other research conducted for the contract.

Each year a verification annex has been prepared under this contract and has been included in the UK National Inventory Report submission to the UNFCCC.

14. Ensure information-exchange and coordination with complementary European Union projects on verification of greenhouse gas emissions, for example CarboEurope, NitroEurope, IPCC reports, guidelines or studies, and attend inverse-modelling workshops arranged under the auspices of the EU Monitoring Mechanism.

The contractors are active members and share information with the AGAGE, ICOS, InGOS and GAUGE programmes and are available to contribute to IPCC reports, guidelines and studies and attend appropriate workshops as required.

.

15. Advise on developments in remote sensing techniques in general as applied to measurement of atmospheric trace gases and inventory verification.

Through the NERC GAUGE programme this area will be given great focus. Within GAUGE, specific use will be made of the methane GOSAT satellite data. The contractors will liaise with Dr. Hartmut Bosch of the University of Leicester who is leading this GAUGE work package. Satellite information will be used within the global inversion studies, the success of these efforts will be reported to DECC as they come to fruition.

16. Make provision for up to 5 days' ad-hoc policy support per year to DECC's Climate and Energy: Science and Analysis (CESA) team.

No work has been conducted under this item.

17. Provide quarterly project updates, annual project reports, and an end of contract project report.

Quarterly and annual contract reports have been produced as specified in the milestone plan. These reports, in addition to being delivered to DECC, have also been made available (when released by DECC) through the contract website (http://www.metoffice.gov.uk/atmospheric-trends).

18. Host a website containing information about Mace Head and any other observation sites. The website should contain up to date project reports, the interpreted and ratified observations data, and be updated at least once every three months.

A website has been launched that contains all relevant information relating to this work. Each observation site is described in detail, including geographical location, photographs and the gases measured. The record of monthly and annual baseline mass mixing ratios, the growth rates and the seasonal cycles for each gas (see Figure 85), together with relevant information about each gas, are displayed and updated quarterly. All contract reports, containing information on baseline trends and emission estimates, are available through the website.

2.3 Publications

Arnold, T., C.M. Harth, J. Mühle, A.J. **Manning**, P.K. Salameh, J. Kim, D.J. Ivy, L.P. Steele, V.V. Petrenko, J.P. Severinghaus, D. Baggenstos, and R.F. Weiss, Nitrogen trifluoride global emissions estimated from updated atmospheric measurements, PNAS 2013 110 (6) 2029-2034, 2013, doi:10.1073/pnas.1212346110.

Brunner, D, S. Henne, C.A. Keller, S. Reimann, M.K. Vollmer, S. **O'Doherty**, and M. Maione, An extended Kalman-filter for regional scale inverse emission estimation, Atmos. Chem. Phys., 12, 3455-3478, 2012. DOI: 10.5194/acp-12-3455-2012.

Derwent, R. G., P. G. **Simmonds**, S. **O'Doherty**, A. **Grant**, D. **Young**, M. C. Cooke, A. J. **Manning**, S. R. Utembe, M. E. Jenkin, and D. E. Shallcross, Seasonal cycles in short-lived hydrocarbons in baseline air masses arriving at Mace Head, Ireland, Atmospheric Environment, 62, 89–96, doi:10.1016/j.atmosenv.2012.08.023, 2012.

Ghalaieny, M, A. Bacak, M. McGillen, D. Martin, A.V. Knights, S. **O'Doherty**, D.E. Shallcross, C.J. Percival, Determination of gas-phase ozonolysis rate coefficients of a number of sesquiterpenes at elevated temperatures using the relative rate method, Physical Chemistry Chemical Physics, 14, 18, 6596-602, 2012. DOI: 10.1039/c2cp23988d.

Henne, S., D.E. Shallcross, S. Reimann, P. Xiao, D. Brunner, S. **O'Doherty**, B. Buchmann, Future emissions and atmospheric fate of HFC-1234yf from mobile air conditioners in Europe, Environ. Sci. Technol., 46, 3, 1650-1658, 2012. DOI: 10.1021/es2034608.

Keller, C.A, M. Hill, M.K. Vollmer, S. Henne, D. Brunner, S. Reimann, S. **O'Doherty**, J. Arduini, M. Maione, Z. Ferenczi, L. Haszpra, A.J. **Manning**, T. Peter, European Emissions of Halogenated Greenhouse Gases Inferred from Atmospheric Measurements, Environ. Sci. Technol., 46, (1), 217-225, 2012. DOI: 10.1021/es202453j.

Logan, J.A., Staehelin, J., Megretskaia, I.A., Cammas, J.-P, Thouret, V., Claude, H., De Backer, H., Steinbacher, M., Scheel, H.-E., Stubi, R.,Frohlich, M., and **Derwent,** R. Changes in ozone over Europe: Analysis of ozone measurements from sondes, regular aircraft (MOZAIC) and alpine surface sites. Journal of Geophys.Res., 117,D09301,doi:10.1029/2011JD016952.

Parrish, D.D., Law, K.S., Staehelin, J., **Derwent**, R., Cooper, O.R.,Tanimotot, H., Volz-Thomas, A., Gilge, S., Scheel, H.-E., Steinbacher, M., and Chan, E. Long-term changes in lower tropospheric baseline ozone concentrations at northern mid-latitudes. Atmos. Chem. Phys., 12, 11485-11504, 2012.

Parrish, D.D., Law, K.S., Staehelin, J., **Derwent**, R., Cooper, O.R.,Tanimotot, H., Volz-Thomas, A., Gilge, S., Scheel, H.-E., Steinbacher, M.,and Chan, E. Lower tropospheric ozone at northern mid-latitudes: Changing seasonal cycle. Geophys. Res. Letters, 40, 1-6, 2013, DOI: 10.1002/grl.50303, 2013.

Rigby, M., R. G. Prinn, S. **O'Doherty**, S. A. Montzka, A. McCulloch, C. M. Harth, J. Mühle, P. K. Salameh, R. F. Weiss, D. **Young**, P. G. **Simmonds**, B. D. Hall, G. S. Dutton, D. Nance, D. J. Mondeel, J. W. Elkins, P. B. Krummel, L. P. Steele, and P. J. Fraser, Re-evaluation of the lifetimes of the major CFCs and CH3CCl3 using atmospheric trends, Atmos. Chem. Phys., 13(5), 2691–2702, doi:10.5194/acp-13-2691-2013, 2013.

Rigby, M., A. J. **Manning**, and R. G. Prinn, The value of high-frequency, high-precision methane isotopologue measurements for source and sink estimation, Journal of Geophysical Research, 117(D12), D12312, doi:10.1029/2011JD017384, 2012.

Ruckstuhl, A.F, S. Henne, S. Reimann, M. Steinbacher, M.K. Vollmer, S. **O'Doherty**, B. Buchmann, and C. Hueglin, Robust extraction of baseline signal of atmospheric trace species using local regression, Atmospheric Measurement Tech., 5, 2613-2624, 2012.

Saikawa, E, M. Rigby, R. G. Prinn, S. A. Montzka, B. R. Miller, L. J. M. Kuijpers, P. J. B. Fraser, M. K. Vollmer, T. Saito, Y. Yokouchi, C. M. Harth, J. Mühle, R. F. Weiss, P. K. Salameh, J. Kim, S. Li, S. Park, K.-R. Kim, D. **Young**, S. **O'Doherty**, P. G. **Simmonds**, A. McCulloch, P. B. Krummel, L. P. Steele, C. Lunder, O. Hermansen, M. Maione, J. Arduini, B. Yao, L. X. Zhou, H. J. Wang, J. W. Elkins, and B. Hall, Global and regional emissions estimates for HCFC-22, Atmos. Chem. Phys., 12, 10033-10050, 2012. doi:10.5194/acp-12-10033-2012.

Tripathi, O.P, S.G. Jennings, C.D. O'Dowd, B. O'Leary, K. Lambkin, E. Moran, S.J. **O'Doherty**, and T.G. Spain, An assessment of the ozone trend in Ireland relevant to air pollution and environmental protection, Atmospheric Pollution Research, 3, 341-351, 2012.

Yao, B, Martin K. Vollmer, Lingjun Xia, Lingxi Zhou, Peter G. **Simmonds**, Frode Stordal, Michela Maionee, Stefan Reimann, Simon **O'Doherty**, A study of four-year HCFC-22 and HCFC-142b, in situ measurements at the Shangdianzi regional background station in China, Atmos. Environ., 63, 43–49, doi:10.1016/j.atmosenv.2012.09.011, 2012.

Yver, C., I. Pison, A. Fortems-Cheiney, M. Schmidt, F. Chevallier, M. Ramonet, A. Jordan, A. Søvde, A. Engel, R. E. Fisher, D. Lowry, E.G. Nisbet, I. Levin, S. Hammer, J. Necki, J. Bartyzel, S. Reimann, M. K. Vollmer, M. Steinbacher, T. Aalto, M. Maione, J. Arduini, S. **O'Doherty**, A. **Grant**, W.T. Sturges, G. L. Forster, C. R. Lunder, V. Privalov, N. Paramonova, A. Werner, and P. Bousquet. A new estimation of the recent tropospheric molecular hydrogen budget using atmospheric observations and variational inversion, Atmos. Chem. Phys., 11, 3375-3392, 2011. DOI: 10.5194/acp-11-3375-2011.

2.4 Meetings

AGAGE meeting (Boulder, Colorado, 12th -19th May 2012)

DECC meeting (London, 26th July 2012) – Progress meeting

Met Office meeting (Bristol, 15th August 2012)

NERC review panel for GAUGE project (London, 14th September 2012)

InGOS meeting (Amsterdam, 26th – 27th September 2012)

DECC meeting (London, 16th October 2012) – Progress meeting

Astrium meeting (London, 16th October 2012)

AEA Technology meeting (Bristol, 25th October 2012)

Parliamentary Office of Science and Technology meeting (Bristol 29th October 2012)

NPL meeting (Teddington, 6th November 2012)

Picarro meeting (Bristol, 8th November 2012)

AGAGE meeting (Urbino, Italy, 12th -16th November 2012)

NERC project integration meeting (London, 27th November 2012)

DECC meeting (University of East Anglia, Norwich, 26th July 2012) – New sites meeting

FAAM meeting (Cranfield University, 22nd January 2013) – aircraft sampling planning meeting

MIT meeting (MIT, Boston, 4th - 8th March 2013) – Thesis defence and DECC presentation

DECC meeting (London, 11th March 2013) – Progress meeting

InGOS meeting (Bremen 12th – 14th March 2013)

GAUGE KO meeting (University of Edinburgh, 19th – 20th March 2013)

EGU (Vienna 8th – 12th April 2013) – Presenting the DECC Network

2.5 Related information

Project website: www.metoffice.gov.uk/atmospheric-trends

3 Instrumentation

Sites -> Species	Mace Head MHD	Tacolneston TAC	Ridge Hill RGL	Angus TTA
CO_2	Picarro 2301*(1)*	Picarro 2301*(1)*	Picarro 2301*(1)*	LiCor 7000*(1)*
CH_4	Picarro 2301(1), GC-FID*(40)*	Picarro 2301*(1)*	Picarro 2301*(1)*	GC-FID*(40)*
N_2O	GC-ECD*(40)*	GC-ECD*(20)*	GC-ECD*(20)*	GC-ECD*(40)*
SF_6	Medusa*(120)*	GC-ECD*(20)*, Medusa*(120)*	GC-ECD*(20)*	GC-ECD*(40)*
H_2	GC-RGA*(40)*	GC-RGA*(20)*	-	-
CO	GC-RGA*(40)*	GC-RGA*(20)*	-	-
CF_4	Medusa*(120)*	Medusa*(120)*	-	-
C_2F_6	Medusa*(120)*	Medusa*(120)*	-	-
C_3F_8	Medusa*(120)*	Medusa*(120)*	-	-
c-C_4F_8	Medusa*(120)*	-	-	-
HFC-23	Medusa*(120)*	Medusa*(120)*	-	-
HFC-32	Medusa*(120)*	Medusa*(120)*	-	-
HFC-134a	Medusa*(120)*	Medusa*(120)*	-	-
HFC-152a	Medusa*(120)*	Medusa*(120)*	-	-
HFC-125	Medusa*(120)*	Medusa*(120)*	-	-
HFC-143a	Medusa*(120)*	Medusa*(120)*	-	-
HFC-227ea	Medusa*(120)*	Medusa*(120)*	-	-
HFC-236fa	Medusa*(120)*	Medusa*(120)*	-	-
HFC-43-10mee	Medusa*(120)*	-	-	-
HFC-365mfc	Medusa*(120)*	Medusa*(120)*	-	-
HFC-245fa	Medusa*(120)*	Medusa*(120)*	-	-
HCFC-22	Medusa*(120)*	Medusa*(120)*	-	-
HCFC-141b	Medusa*(120)*	Medusa*(120)*	-	-
HCFC-142b	Medusa*(120)*	Medusa*(120)*	-	-
HCFC-124	Medusa*(120)*	Medusa*(120)*	-	-
HCFC-123	-	Medusa*(120)*	-	-
CFC-11	Medusa*(120)*	Medusa*(120)*	-	-
CFC-12	Medusa*(120)*	Medusa*(120)*	-	-
CFC-13	Medusa*(120)*	Medusa*(120)*	-	-
CFC-113	Medusa*(120)*	Medusa*(120)*	-	-
CFC-114	Medusa*(120*	Medusa*(120)*	-	-
CFC-115	Medusa*(120)*	Medusa*(120)*	-	-
H-1211	Medusa*(120)*	Medusa*(120)*	-	-
H-1301	Medusa*(120)*	Medusa*(120)*	-	-
H-2402	Medusa*(120)*	Medusa*(120)*	-	-
CH_3Cl	Medusa*(120)*	Medusa*(120)*	-	-
CH_3Br	Medusa*(120)*	Medusa*(120)*	-	-
CH_3I	Medusa*(120)*	Medusa*(120)*	-	-
CH_2Cl_2	Medusa*(120)*	Medusa*(120)*	-	-
CH_2Br_2	Medusa*(120)*	Medusa*(120)*	-	-
$CHCl_3$	Medusa*(120)*	Medusa*(120)*	-	-
$CHBr_3$	Medusa*(120)*	Medusa*(120)*	-	-
CCl_4	Medusa*(120)*	Medusa*(120)*	-	-
CH_3CCl_3	Medusa*(120)*	Medusa*(120)*	-	-
$CHCl=CCl_2$	Medusa*(120)*	Medusa*(120)*	-	-
$CCl_2=CCl_2$	Medusa*(120)*	Medusa*(120)*	-	-

Table 1: Operational sites, instrumentation and observed species. Number in brackets indicates frequency of calibrated air measurement in minutes.

3.1 Sites

A brief summary of site operations is presented below; a more detailed account of operations over the past year is presented in the Appendices. A more detailed description of the instrumentation is detailed on the website.

3.1.1 Mace Head

- Medusa-MS: Overall, the Medusa performed well during the reporting period with no major issues.
- GC-MD: The MD proved yet again to be a most reliable system and performed well for the reporting period. Most of the data loss resulted from ancillary equipment failure or late gas delivery.

3.1.2 Ridge Hill

- Ridge Hill began operation in February 2012 and has collected 14 months of data
- GC-ECD: The ECD instrument at the site underwent modifications which resulted in an improvement in precision of SF_6 and N_2O measurements in July 2012. Two months of data was lost from December 2012 – January 2013 due to water ingress. This was resolved by replacing the detector within the instrument.
- CRDS: The CRDS has been running well over the last 14 months with a few days of data lost on two occasions due to pump failure

3.1.3 Tacolneston

- Tacolneston began operation in July 2012 and has collected 9 months of data
- Medusa-MS: The Medusa has performed well during the sites operation. CF_4 data was lost during January 2013 due to coolant problems. Significant improvement in precision has been found for many species after the introduction of the rolling SIM windows.
- GC-MD: The MD has operated well during the sites operation with only a week of data lost due to carrier gas contamination
- CRDS: The CRDS sampling from 54 and 100 m has operated without problems during the period. In January additional measurements from the 185 m line were initiated

3.1.4 Angus

- From the start of the contract, April 2011 to December 2012 Angus was run by the University of Edinburgh and data was provided to the project
- Licor: CO_2 data from the LiCor has been provided for this period and the instrument ran without interruptions
- GC-FID: CH_4 data from the FID has been provided for this period and ran without interruptions
- GC-ECD: N_2O and SF_6 data have been provided for the period however the data is short and does not compare well with Mace Head data and thus has not been used in modelling of emissions estimates
- The running of Angus was handed over to the University of Bristol (UoB) in January 2013. Operation continues using a Picarro G1301 CRDS instrument which measures CH_4 and CO_2 and is on loan from the Centre for Ecology and Hydrology
- Equipment was built and tested at UoB to set-up and run the CRDS in an identical way to the CRDS' at Tacolneston and Ridge Hill. This equipment was installed at a site visit on the 18th of April 2013.
- The University of Bristol have recently been awarded £171K from NERCs capital equipment fund to purchase new sampling equipment for Angus - Picarro CRDS for CO_2 and CH_4, Los Gatos CRDS for N_2O and CO, and a flask-sampling package to provide the capability of isotope analysis (note there are at present no funds for the analysis of isotopes).

3.2 Calibration and Intercomparisons

The calibration scales employed by AGAGE are used for all species measured in the network with the exception of CO_2 at all sites and CH_4 at Ridge Hill and Tacolneston, which are measured on

the CRDS instrument. The calibration methodology used at these sites is discussed in the Appendix (and on the website, http://www.metoffice.gov.uk/atmospheric-trends/).

3.2.1 AGAGE and NOAA comparisons

The Mace Head data is continuously compared to data from other groups within Europe and across the globe to ensure data consistency and comparability. Figure 1(a)-(c) shows examples of a comparison of the AGAGE *in situ* data with NOAA flask samples from Mace Head for three of the key species we measure (CH_4, N_2O and SF_6). Although not shown here, comparisons of all AGAGE MD and Medusa species are conducted where both networks make concurrent measurements.

The plots illustrate the excellent agreement in measured values (and calibration). For CH_4 the difference between NOAA and AGAGE data is 1.07 ± 4.48 ppb (0.06 ± 0.24%), for N_2O it is −0.22 ± 0.37 ppb (−0.07 ± 0.12%), and for SF_6 0.04 ± 0.06 ppt (0.6 ± 0.91%).

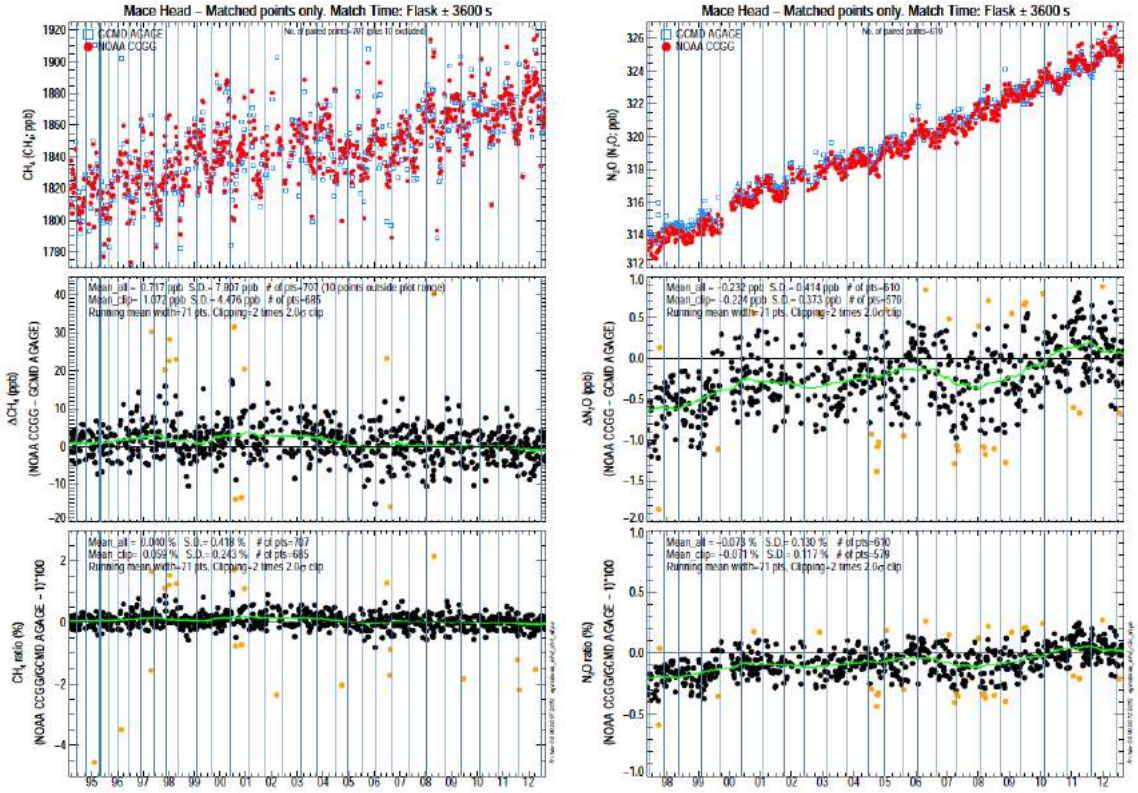

(a) (b)

Figure 1(a) and (b) Comparison of AGAGE MHD in situ date with NOAA flaks data. Top plot is the matched data, middle shows a difference plot and bottom plot shows the percentage difference.

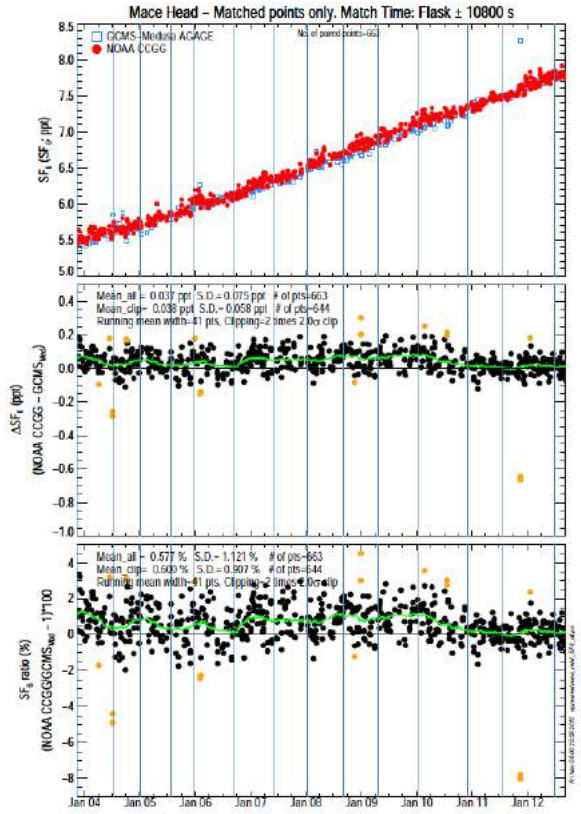

(c)

Figure 1(c) Comparison of AGAGE MHD in situ data with NOAA flaks data. Top plot is the matched data, middle shows a difference plot and bottom plot shows the percentage difference

3.2.2 AGAGE and University of Heidelberg comparison

The InGOS (Integrated non-CO_2 greenhouse gases) project aims at harmonizing the current measurement techniques to assure high quality and compatibility of the non-CO_2 greenhouse gas measurements in Europe. In this context a research group from the University of Heidelberg have developed an travelling Fourier Transform Infrared spectrometer (FTIR) for the detection of a range of GHG's (CO_2, CH_4, N_2O, CO and $\delta^{13}CO_2$). This equipment was installed at Mace Head in February 2013 for an intercomparison experiment with the long-term AGAGE sampling equipment. The Heidelberg group propose to show results at the WMO conference in Beijing in June 2013 detailing the first *in situ* comparisons of continuous atmospheric N_2O measurements of the Heidelberg Fourier Transform Infrared (FTIR) Spectrometer [Hammer *et al*., 2012] and gas chromatographic (GC) system in Heidelberg as well as at Mace Head. In Heidelberg, excellent agreement was found, of about 0.01 ± 0.07 ppb in atmospheric N_2O over a period of eight weeks. In Mace Head N_2O is routinely measured with the well-established technique and calibration of the global AGAGE network [Prinn *et al*., 2000] Comparison with the Heidelberg "travelling FTIR" system showed that the continuous atmospheric N_2O measurements differed by about 0.2 ± 0.12 ppb. A large portion of the difference is most likely due to a scale difference between the NOAA2006a scale used for the FTIR calibration and the SIO98 scale of the AGAGE network (Hall, pers. comm., 2013) which is in agreement with the difference for AGAGE vs NOAA scales. When accounting for the scale difference, both measurements agree within 0.1ppb, which is the WMO compatibility target. The exact scale differences still need to be confirmed. The results clearly show that with modern analytical techniques excellent precision of N_2O measurements to better than 0.1 ppb can be achieved. However, compatibility of results could be improved further by comparability of calibration scales in different networks. A more detailed analysis of results will be presented once the inetrcomparison exercise is completed later this year.

3.2.3 AGAGE-MD and LSCE-CRDS comparison

A Picarro G2301 Cavity Ringdown Spectrometer (CRDS) has been used by the LSCE group to measure CO_2 and CH_4 at Mace Head since 2011. The University of Bristol and LSCE groups

signed a memorandum of understanding to allow transfer of CO_2 data to UoB for inclusion in the UK DECC Network project, and also for comparison of CH_4 acquired by the CRDS and the AGAGE GC-MD system, which uses gas chromatography with flame ionisation detection. The sample detection methods are distinctly different and reporting a comparison between such instruments provides useful information about systematic differences in ambient mixing ratios. Figure 2 illustrates the comparison of data in 2012/2013. In the top plot the CRDS data in black (minute average data) corresponding to the closest GC-MD data point (red) are overlaid, indicating what appears to be excellent temporal agreement between the two data sets. The lower plot illustrates at the difference between the GC-MD and CRDS.

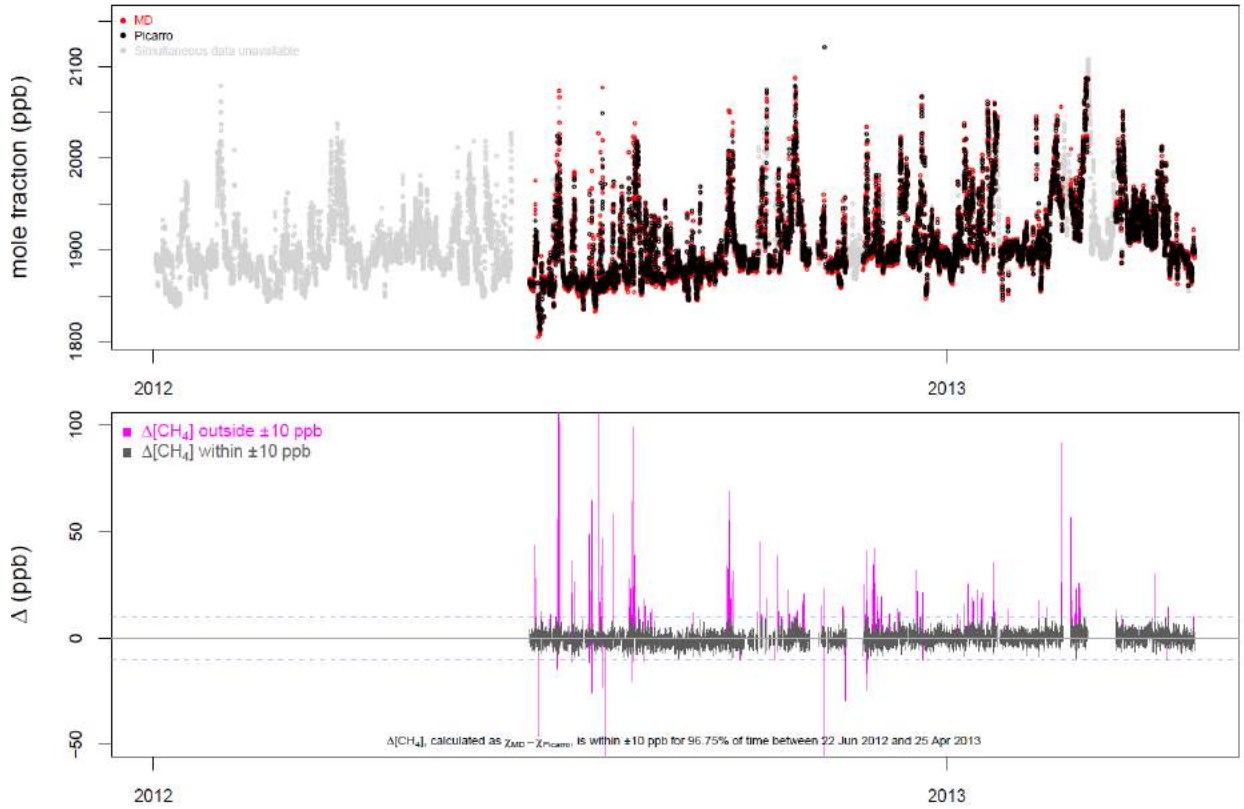

Figure 2 Comparison of CH_4 data at Mace Head from 2012-2013 with the GC-MD (red) and CRDS (black) instruments (above). Difference between the datasets where the pink points indicate a difference of >10 ppb (below).

The data plotted in grey in the lower plot are where the two datasets agree to within 10 ppb of each other; this occurred 96.75% of the time between 22 June 2012 and 25 April 2013. Interestingly, there are times where larger deviations occur (>100 ppb) as shown by the pink data points. These larger deviations occur when air transported from high emission regions are sampled at Mace Head, and the mixing ratios experienced are changing rapidly. Interestingly, the frequency of these deviations has reduced over the time period sampled, however, the magnitude and frequency of the pollution events has not decreased. This possibly suggests a non-linearity in either dataset or a feature in the data processing that has changed over time. These differences need to be explored further. It should be noted that both instruments use different calibration scales, NOAA 2004 (CRDS) and Tohoku University (GC-MD) however the conversion factor between these two scales is very small and would only cause a systematic difference of 1.0003 (NOAA04/TU; Dlugockencky et al., 2005).

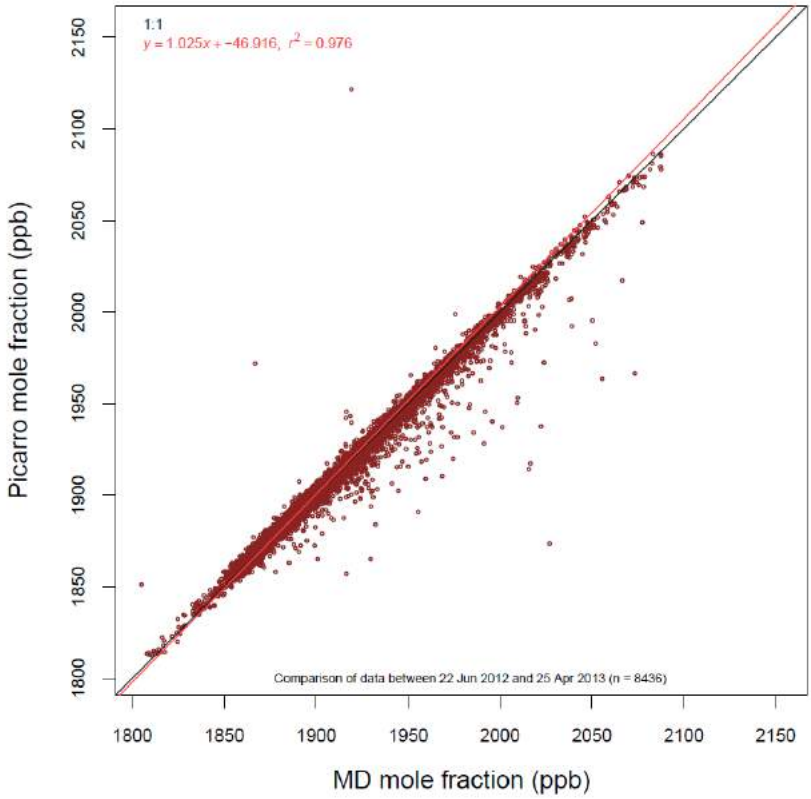

Figure 3: Correlation plot of the matched data between MD mole fraction and Picarro (CRDS) mole fraction

Figure 3 illustrates a correlation plot of the matched data from both instruments, the correlation coefficient (r^2) is high, indicating good correlation across the concentration range, however, the scatter of datapoints below the 1:1 line indicate that the Picarro CRDS tends to periodically report lower values than the AGAGE GC-MD instrument in the 1900-2100ppb range. These individual data points will be examined more fully to determine if this is an instrumental bias or incorrect assignment of mole fractions whilst data processing. However, it should also be noted that the Picarro CRDS only measures the ^{12}C isotope and so CH_4 events that are anomalously high in the lesser isotopes of ^{13}C and ^{14}C will not be reported by the CRDS whereas the GC-MD FID will account for all isotopes together.

3.3 New Developments

There have been many new developments in the past year, a new method of non-discrete SIM windows during MS data acquisition on the Medusa was implemented, measurement of new species at Tacolneston, the 185 metre air line at Tacolneston was attached to the CRDS and significant work has been carried out on software developments for analysis of the large amounts of data produced by CRDS instrumentation. These developments are discussed in further detail below.

3.3.1 Rolling SIM windows

In December, 2012 the Medusa mass spectrometer parameters were customised to measure the mass of ions by ‘rolling’ windows instead of the previous default method of static, discrete SIM windows more usual to mass spectrometry. This means that when species separation and retention times change, due to ageing of the gas chromatography column, the ‘rolling’ windows can be adjusted so each species continues to be measured accurately. Due to the retention time of different species often changing at differing rates it meant that in the past when a species moved out of a specific static window it could lie between two discrete SIM windows for some time with measurements of the less significant species not being possible for some time, until it fully entered another SIM window. The change to ‘rolling’ windows allows each species to effectively obtain its own unique SIM window that moves with the peak as its retention time shifts and means that peaks no longer become truncated in the chromatogram. Historically, due to overlapping of multiple

peaks in the chromatogram, a static SIM window had to monitor a multitude of ions before a baseline period in the chromatogram allowed a new SIM window to be started. The new method no longer requires this and as a result it means that in general fewer ions have to be measured at any given time in the chromatogram. This significantly improved the precision of measurements of many species. Figure 4 shows the improvement in precision of concurrent standard analyses when the change to 'rolling' windows was implemented at Tacolneston.

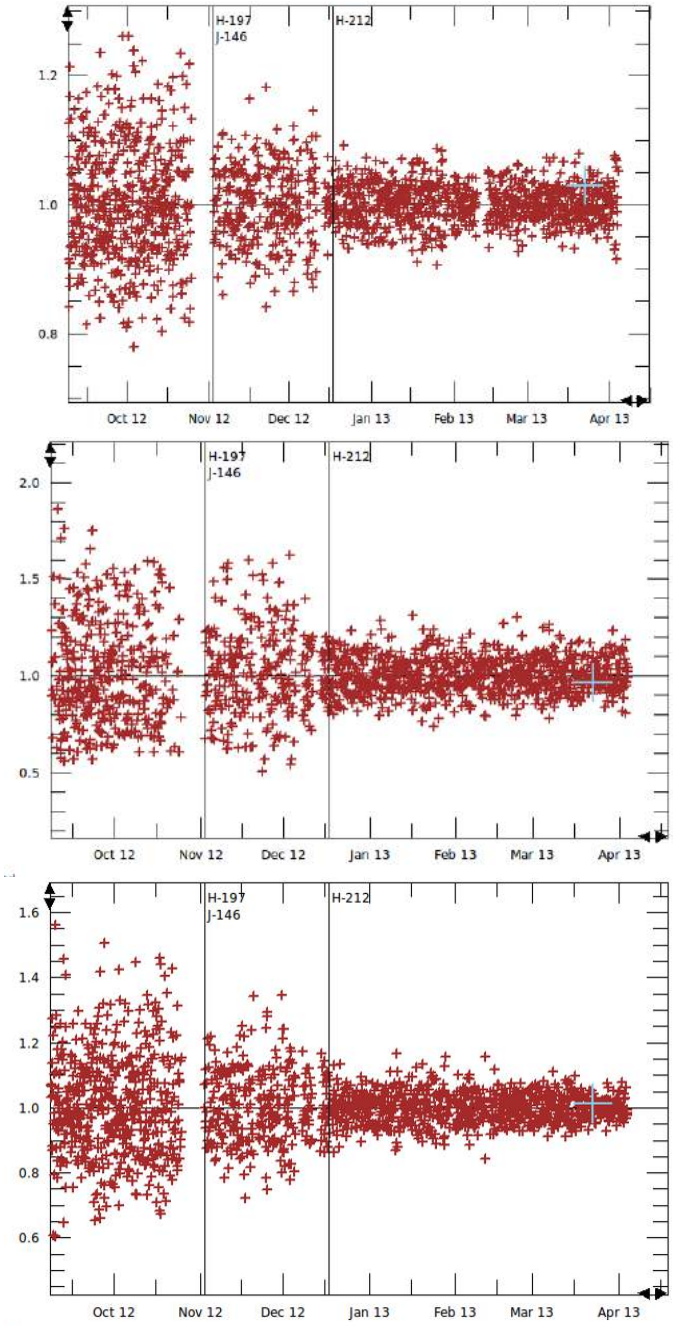

Figure 4: Improvement in precision seen in mid-December for PFC-218 (top), HFC-236fa (middle) and HFC-365mfc (bottom) on changing the Medusa from static to 'rolling' SIM ion windows at Tacolneston.

New species have also been added to the list of compounds measured on the Medusa at Tacolneston. These new species were added gradually to ensure that the precision of other species already measured were not affected by their addition. Table 2 shows the new species added the measurement list and on what dates they were added.

Species	Chemical Formula	GWP (IPCC AR4)	Target ion mass	Qualifier ion mass	Date Added
HFC-43-10mee	$C_5F_{10}H_2$	1,640	183	-	13/02/13
propane	C_3H_8	Indirect GHG	41	43	06/03/13
c-propane	C_3H_8	Indirect GHG	41	39	05/03/13
i-butane	C_4H_{10}	Indirect GHG	42	43	22/03/13
n-butane	C_4H_{10}	Indirect GHG	43	42	22/03/13
i-pentane	C_5H_{12}	Indirect GHG	43	-	22/03/13
n-pentane	C_5H_{12}	Indirect GHG	43	-	22/03/13

Table 2: New species added to the Tacolneston Medusa.

3.3.2 Diagnostic measurements

During the site visit to Tacolneston on the 30th of January 2013 additional diagnostic analyses were implemented on the Medusa, similar to the analyses that routinely take place at Mace Head. A filter was fitted to the inlet of a port on the Medusa so that lab air measurements could be made on a weekly basis. These measurements check for contamination in the lab and have been particularly useful at other AGAGE sites to detect leaks of HFC species from air conditioning (AC) units. Large leaks from the AC of these refrigerant species can contaminate ambient air measurements and monitoring the lab air allows early detection of problems and enables earlier resolution of these issues. During this site visit the measurement of 'blank' samples were also initiated. These samples measure just the carrier gas used in the measurement and thus tests for any 'carry over' (compounds that may remain on the traps from a previous run). This informs us of any species that have a residual blank in the system and thus allows correction for the amount of blank carried over from one sample to the next.

3.3.3 Additional sample height at Tacolneston

From site set-up at Tacolneston in July 2012 until January 2012 the CRDS on site was measuring from air sampling lines at 54 m and 100 m up the tall tower. From the end of January a new line at 185 m was connected to the CRDS. CO_2 and CH_4 measurements are now made for 20 minutes every hour from each of the three sample heights.

3.3.4 Development of GCWerks for CRDS analysis

Raw data from the CRDS instruments at Ridge Hill and Tacolneston is currently automatically transferred from the instrument computers to the ICOS server for calibration and processed data is returned daily to a server at the University of Bristol. This large volume of data, with a data point every second, is returned in raw data files with columns for the date, time and concentration of trace gas species. Data analysis and verification using the ICOS software is quite laborious. Flagging suspect data, e.g. for times when a rigger was climbing the tall tower and breathed near the inlet line is not a trivial task.

All other AGAGE instruments (Medusa and MD) use customised software developed by GCSoft, a software developer who is part of the AGAGE network. This software, called GCWerks (http://gcwerks.com/), is used to control the instruments, and import data for quick and easy data verification and quality control.

We have worked with GCSoft to develop a new data processing GCWerks package for the CRDS instrument, and ultimately a package that will control the CRDS sampling and communication. The new software is still in the developmental stage, but initial tests are very promising. We have transferred all Ridge Hill data to the new software and can now view and flag data. It is hoped that we can used this software to calibrate the CRDS data independently from the ICOS method and then compare the two methods. We also hope to use this software on the CRDS instrument at Tacolneston. This would mean that all data streams from the UK DECC network sites were in an identical format and undergo the same processing and quality control.

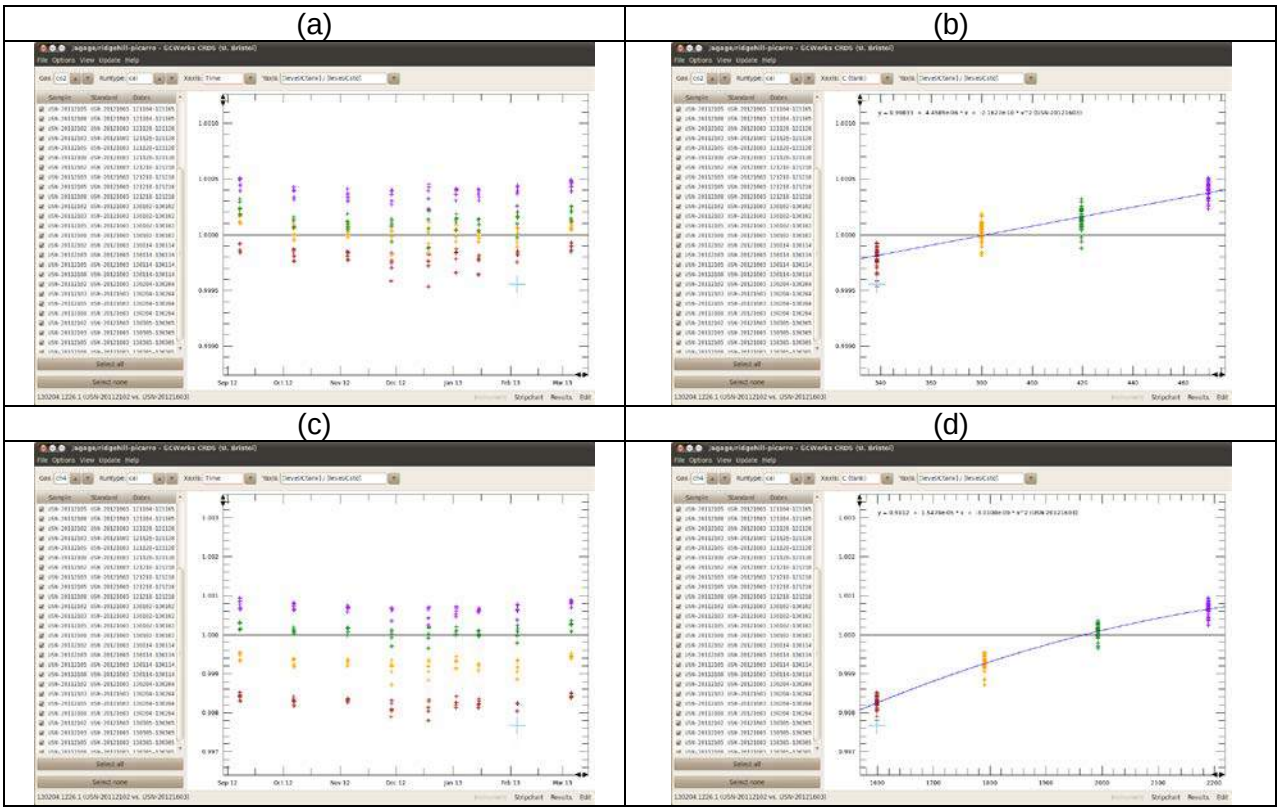

Figure 5: Calibration and linearity plots for CO_2 and CH_4

The software at Ridge Hill has already been used to highlight some potential linearity issues with the CRDS. It appears from the data that either the CRDS is slightly non-linear (especially for CH_4) or there is non-linearity in the preparation or assignment of values to the standard cylinders prepared at MPI Jena. In Figure 5, one of the near ambient standards (USN-20121603) is used to track the CRDS drift over time and other standards (USN-20112102, 103, 105 and 108) to measure the CRDS linearity as a function of concentration. The y-axis in the plots shows the ratio of CRDS response to tank concentration (level/Ctank) divided by the same quantity from the daily standard (level/Cstd, used for drift correction). With a linear response the CRDS level would be proportional to tank concentration and the y-axis for all points would be at 1.0 (the same level/C ratio for all tanks as for the standard). The first column (Figure 5 (a) and (c)) shows CO_2 and CH_4 concentrations as a function of time, and the colours match the 4 span tanks (102, 103 105 and 108). The second column (Figure 5, (b) and (d)) shows the same data as a function of tank concentration, which shows an apparent nonlinearity. For CO_2 the nonlinearity appears to be very small (0.06% between 340 and 470 ppm), but for CH_4 it is somewhat larger (almost 0.3% between 1600 and 2200 ppb). The plots as a function of time show that this nonlinearity has been fairly stable over the period that USN-20121603 has been in use (from Sep 2012 to present).

We are looking into the following ideas, (a) could it be the CRDS? (b) is there anything in the preparation or measurement of the ICOS calibration tanks which could produce non-linearity in the assigned values (e.g. a detector nonlinearity in the instrument used to measure the tanks or isotopic differences in the tanks that have been spiked to produce higher concentrations)?

3.3.5 New Compounds

Development of the sampling devices, specifically the Medusa-MS for the detection of new compounds in the atmosphere is an on-going process within the AGAGE network. Over the past year we have worked with other groups within the AGAGE network and InGOS program to identify such compounds.

3.3.5.1 NF_3 (Nitrogen Trifluoride)

NF_3 has been called the "missing greenhouse gas" [Prather and Hsu., 2008], it has a very long atmospheric lifetime of ~550 years and a GWP_{100} of 17,200. It is used as a replacement for PFC-116 in CVD chamber cleaning (part of semiconductor production), it also has a growing market in liquid-crystal displays and a minor use in photovoltaic cells. The Medusa-MS instrument was modified for NF_3 analysis by Weiss *et al*. [2008] to measure 11 AGAGE air archive samples from 1977 to 2008; they showed that it was growing in the atmosphere at a rate of 11% in 2008. A detailed assessment of NF_3 measurements in La Jolla's air was published by Arnold *et al*. [2012]. The Bristol Medusa was modified for the addition of NF_3 in December 2011, and it is expected that the Mace Head Medusa will be modified in 2013.

3.3.5.2 High molecular weight perfluorocarbons

High molecular weight perfluorocarbons (PFCs, C_4F_{10}, C_5F_{12}, C_6F_{14}, C_7F_{16} and C_8F_{18}) were reported as part of the AGAGE program, using Medusa-MS technology and air archive measurements from the Northern and Southern hemisphere [Ivy *et al*., 2012a]. The 100-yr GWPs as reported in the IPCC 4th Assessment Report (4AR) are 8,860 (C_4F_{10}), 9,160 (C_5F_{12}) and 9,300 (C_6F_{14}) and have lifetimes of 2,600 yr, 4,100 yr and 3,200 yr respectively. Emissions of these high molecular weight PFCs are predominantly used as solvents and precision cleaning chemicals in the electronics industry, although other minor uses also exist (Ivy et al., 2012b). Their atmospheric histories were based on measurements of 36 Northern Hemisphere and 46 Southern Hemisphere archived air samples collected between 1973 and 2011. A new calibration scale was prepared for each PFC, with estimated accuracies of 6.8% for C_4F_{10}, 7.8% for C_5F_{12}, 4.0% for C_6F_{14}, 6.6% for C_7F_{16} and 7.9% for C_8F_{18}. Based on the observations, the 2011 globally averaged dry air mole fractions of these heavy PFCs were: 0.17 parts-per-trillion (ppt, i.e., parts per 10^{12}) for C_4F_{10}, 0.12 ppt for C_5F_{12}, 0.27 ppt for C_6F_{14}, 0.12 ppt for C_7F_{16} and 0.09 ppt for C_8F_{18}. These atmospheric mole fractions combine to contribute to a global average radiative forcing of 0.35 mW m^{-2}, which is 6% of the total anthropogenic PFC radiative forcing [Montzka and Reimann, 2011; Oram *et al*., 2012]. The growth rates of the heavy perfluorocarbons were largest in the late 1990s peaking at 6.2 parts per quadrillion (ppq, i.e., parts per 10^{15}) per year (yr) for C_4F_{10}, at 5.0 ppq yr^{-1} for C_5F_{12} and 16.6 ppq yr^{-1} for C_6F_{14} and in the early 1990s for C_7F_{16} at 4.7 ppq yr^{-1} and in the mid 1990s for C_8F_{18} at 4.8 ppq yr^{-1}. The 2011 globally averaged mean atmospheric growth rates of these PFCs are subsequently lower at 2.2 ppq yr^{-1} for C_4F_{10}, 1.4 ppq yr^{-1} for C_5F_{12}, 5.0 ppq yr^{-1} for C_6F_{14}, 3.4 ppq yr^{-1} for C_7F_{16} and 0.9 ppq yr^{-1} for C_8F_{18}. The more recent slowdown in the growth rates suggests that emissions are declining as compared to the 1980s and 1990s. In a later paper Ivy *et al*., [2012b] used these measurements in combination with a 3-dimensional chemical transport model and an inverse method that includes a growth constraint on emissions to determine the PFC emissions. The results indicate large deviation when compared to bottom-up estimates (EDGARv4.2).

In addition, infrared absorption spectra were measured for C_7F_{16} and C_8F_{18}, and estimates made for their radiative efficiencies and global warming potentials (GWPs). C_8F_{18}'s radiative efficiency is similar to trifluoromethyl sulfur pentafluoride's (SF_5CF_3) at 0.57 W m^{-2} ppb^{-1}, which is the highest radiative efficiency of any measured atmospheric species. Using the 100-yr time horizon GWPs, the total radiative impact of the high molecular weight perfluorocarbons emissions are also estimated; it was found that the high molecular weight PFCs peak contribution was in 1997 at 24000 Gg of carbon dioxide (CO_2) equivalents and has decreased by a factor of three to 7300 Gg of CO_2 equivalents in 2010. This 2010 cumulative emission rate for the high molecular weight PFCs is comparable to: 0.02% of the total CO_2 emissions, 0.81% of the total hydrofluorocarbon emissions, or 1.07% of the total chlorofluorocarbon emissions projected for 2010 [Velders *et al*., 2009]. In terms of the total PFC emission budget, including the lower molecular weight PFCs, the high molecular weight PFCs peak contribution was also in 1997 at 15.4% and was 6% of the total PFC emissions in CO_2 equivalents in 2009. At present only C_6F_{14} has been added to the list of compounds measured on the Medusa-MS at Mace Head.

3.3.6 Isotopes

It is hoped that the use of isotopes to provide additional information about source partitioning on a national scale compared to mole fraction observations will become a reality in the near future. It is

well known that gases such as CH_4, CO_2 and N_2O emitted from different sources have characteristic but different isotopic ratios. For example, wetlands emit CH_4 that is relatively depleted in $\delta^{13}C$ compared to CH_4 emitted in biomass burning, and fossil fuel and landfill sources generally emit with $\delta^{13}C$ values in between those of biomass burning and microbial sources (wetlands). At present the determination of sources and sinks of these gases using isotope data is limited by the number and frequency of the measurements. Currently the majority of measurements are restricted to infrequent flask samples that use a central laboratory for very precise analysis. In case of $\Delta^{14}CO_2$, this type of analysis is very expensive and therefore further limits the frequency of analysis.

The high frequency CRDS instruments currently available are not precise enough to provide useful information. New developments in quantum cascade laser spectroscopy, along with sample pre-concentration techniques are predicted to lead to a new generation of high-frequency and high-precision measurements of CH_4 ($^{14}CH_4$, CH_3D) and N_2O (^{15}N, $^{15}N_\alpha$, $15N_\beta$, ^{12}O). Such an instrument for the isotopologues of N_2O has recently been installed at Mace Head, Ireland. A similar instrument is being developed for $^{14}CH_4$ and CH_3D. It will take time to understand the extent to which these new measurements will improve the partitioning of sources and sinks. The modelling of isotopes for source/sink determination is still in its infancy with regards to regional applications. Rigby et al, 2012, describes the theoretical improvements a global network of high-frequency high-precision isotope measurements would have on understanding global sources and sinks of CH_4.

3.3.6.1 Revised GAUGE proposal for sampling and analysis of isotopes

Here we document a proposed revision of the funded work plan for the NERC funded GAUGE project, reflecting a new collaborative opportunity that will deliver isotope measurements that: 1) better match the accuracy/precision required to attribute observed atmospheric variations of GHGs to anthropogenic activities; 2) substantially increases the expected breadth of measurements for the same amount of money; and 3) will ensure measurements taken within GAUGE are automatically inter-calibrated with international partners and disseminated widely.

Impetus and description of the revised work plan:

The opportunity to collaborate with the NOAA ESRL in the US has been presented to the GAUGE project. This collaboration will involve the use of glass sample flasks for the measurement of a large range of GHGs and their isotopes, substantially increasing the science return of the project. The original GAUGE proposal detailed the use of NERC Radiocarbon facility at Kilbride for $\Delta^{14}C_{CO2}$ analysis and CEH Lancaster for $\delta^{13}C_{CH4}$ analysis.

At the NERC review panel a number of concerns were raised regarding the science that could be achieved with the planned isotope analysis due to the associated individual sample costs (£600/sample for $\Delta^{14}C_{CO2}$), which limited the number of samples that could be acquired and therefore the overall science return. There were also some concerns about the suitability of sorbent sampling for high precision $\Delta^{14}C_{CO2}$ measurements and the relative inexperience of the facility at Kilbride in dealing with routine analysis of relatively high volumes of ambient air samples. The use of the NOAA ESRL and INSTAAR facilities, described below, will provide a substantial improvement to the range of analyses achievable within the GAUGE program at no extra cost to the project. NOAA ESRL has for many decades operated a large network of sampling site across the globe (*in situ*, tall tower, aircraft), routinely making high precision measurements of key GHGs, halocarbons, hydrocarbons and, most relevant to this document, isotopes. Table 3 summarizes the measurement precision and associated costs of the isotope analyses. At Mace Head, Ireland, NOAA currently measures all of the gases listed in Table 3, with the exception of $\Delta^{14}C_{CO2}$, which we propose to add measurements of at Mace Head to provide a UK baseline measurement. Following closely the original GAUGE project, we will implement routine sampling of all gases in Table 3 at Tacolneston, East Anglia, and campaign sampling at Heathfield, East Sussex. We will sample the complete range of gases using the FAAM BAe-146 atmospheric research aircraft.

The University of Colorado INSTAAR laboratory for AMS Radiocarbon Preparation and Research (NSRL) began collaboration with NOAA ESRL in 2003 with the aim of developing an ultra-precise $\Delta^{14}C_{CO2}$ measurement capability in small (~2L) samples of whole air, for implementation within the NOAA Cooperative Air Sampling Network. They have maintained a long-term measurement repeatability of better than 1.8 ‰ (1-sigma) since 2004, as determined by repeat extraction and measurement of aliquots obtained from high-pressure surveillance cylinders [Turnbull *et al*., 2007; Lehman *et al*., 2012]. This equates to a detection capability for recently-added fossil fuel derived CO_2 in the atmosphere of less than 1 ppm, which is highly significant with respect to typical pollution signals [Miller *et al*., 2012]. They maintain both manual [Turnbull *et al*., 2007] and automated [Turnbull *et al*., 2010] CO_2 extraction lines, with an extraction capability of about 2000 samples/year. Currently, in collaboration with their AMS measurement partners at UC-Irvine, they perform about 1000 ultra-high precision $\Delta^{14}C_{CO2}$ measurements per year in connection with various atmospheric trace gas measurement programs around the world. Quantification of fossil fuel CO_2 from observations requires paired measurements of both CO_2 and $\Delta^{14}C_{CO2}$. CO_2 measurements in the flasks will be obtained separately, leaving at least 2 L air STP remaining for our analysis. INSTAAR also coordinate the International Atmospheric $\Delta^{14}C_{CO2}$ Intercomparison Program for the WMO.

The gases listed in Table 3 will be measured by the Measurement of Atmospheric Gases that Influence Climate Change (MAGICC) system on one of two near-identical automated analytical systems. The MAGICC systems consist of custom-made gas inlet systems, gas-specific analyzers, and system-control software. The flasks used for GAUGE sampling will be purchased in Europe but will be a similar design to the standard NOAA flask. These flasks will follow NOAA procedures and be subject to multiple levels of quality control for flask samples taken at each *in situ* and aircraft site. The sources of error to the flask measurement fall into three different categories: flask-induced bias, sampling errors and analysis errors. We will incur extra shipping costs for the higher volume of flasks, but expect these costs to be absorbed within the original GAUGE isotope budget. A subset of flasks taken during GAUGE will also be analysed for isotopes of CO_2 at the University of Colorado INSTAAR Stable Isotope Lab. An automated analysis system allows a ~450 cm^3 sample to be analyzed for 13C/12C ratio of CO_2, 18O/16O ratio of CO_2 and 13C/12C ratio of CH_4 [Vaughn *et al*., 2004].

Compound	Facility	Precision	Cost/sample (£ total)	Estimate number of samples	Sample Turnaround time
$\Delta^{14}C_{CO2}$ (‰)	NERC Killbride	±2.0	£600 (£124,800)	208	
$\delta^{13}C_{CH4}$ (‰)	NERC CEH Lancaster	±0.5	£32.74 (£38,184)	800	
$\Delta^{14}C_{CO2}$ (‰)	INSTARR	±1.8	$250 (£80,000)	500	1-2 weeks
$\delta^{13}C_{CH4}$ (‰)	INSTARR	±0.04	$100 (£23,680)	500*	1 month
$\delta^{13}C_{CO2}$ (‰)	INSTARR	±0.01	$50 (£11,840)	500*	1 month
$\delta^{18}O_{CO2}$ (‰)	INSTARR	±0.03		500*	1 month
CO_2 (ppm)	MAGICC	±0.03	$90(£21,312)	500*	1-2 weeks
CH_4 (ppb)	MAGICC	±1.2			
CO (ppb)	MAGICC	±0.3			
SF_6 (ppt)	MAGICC	±0.03			
H_2 (ppb)	MAGICC	±0.4			
N_2O (ppb)	MAGICC	±0.4			

*NOAA ESRL already take weekly flasks for these compounds at Mace Head, so there would be no charge for use of these data.

Table 3: List of measurements provided by the INSTAAR laboratory for the GAUGE project.

4 Description of data analysis methods

4.1 Introduction

This chapter discusses the methods used to analyse the observations from the UK DECC network. The following chapter presents the results for the key gases that are reported through the UNFCCC process and then, following that, the analysis of the remaining gases observed at Mace Head.

The first section describes the method for estimating the long-term Northern Hemisphere atmospheric baseline trend, the growth rate and the seasonal cycle of each gas measured at Mace Head given knowledge of the recent history of the air as it travels to the station.

The subsequent section presents the InTEM (Inversion Technique for Emission Modelling) inversion system. This is the tool that is used to estimate the UK and North West European (NWEU) emissions of each gas for each year from 1990 or from when the observations started.

The final section describes the preliminary work that has been undertaken to incorporate the new observations from the extended UK DECC network into the inversion system.

4.2 Northern Hemisphere Atmospheric Baseline Trend Analysis

4.2.1 Introduction

This section describes the method behind the analysis of the baseline concentrations of the Mace Head observations from 1989-2012 inclusive. Baseline concentrations are defined here as those that have not been influenced by significant emissions within ten days of the travel, i.e. those that are well mixed and are representative of the mid-latitude Northern Hemisphere background concentrations.

The observations at Mace Head from 1989 to December 2012 have been analysed for each gas measured. The principle tool used to estimate the baseline concentrations is the NAME dispersion model. The methodology used is presented first, followed by the analysis of each individual gas. The analysis considers the long term trend of the monthly and annual baseline concentrations, their rate of growth and their seasonal cycle.

4.2.2 Methodology

This section describes in detail how the monthly baseline concentrations for each gas observed at Mace Head were derived. There are several specific stages to the process and the section is broken down into these segments with examples were possible.

The NAME model is run in backwards mode to estimate the recent history (30 days) of the air en-route to Mace Head. An air history map, such as those shown in Figure 6, has been calculated for each 2-hour period from 2003 until Dec. 2012 using UM meteorology and from 1989-2002 using ERA-Interim meteorology, amounting to more than 100,000 maps. The model output estimates the 30-day time-integrated air concentration (dosage) at each grid box (40 km horizontal resolution and 0-100 m above ground level) from a release of 1 g/s at Mace Head (the receptor). The model is 3-D therefore it is not just surface transport that is modelled, an air parcel can travel from the surface to a high altitude and then back to the surface but only those times when the air parcel is within the lowest 100 m above the ground will it be recorded in the maps. The computational domain covers 100^{o} W to 45.125^{o} E longitude and 10^{o} N to 80.125^{o} N latitude and extends to more than 10 km vertically (actual height varies depending on version of meteorology used). For each 2-hour period 40,000 inert model particles were used to describe the dispersion. No chemical or deposition processes were modelled; this is realistic given the long atmospheric lifetimes of the vast majority of gases considered.

By dividing the dosage (gs/m^3) by the total mass emitted (3600 s/hr x 2hr x 1 g/s) and multiplying by the geographical area of each grid box (m^2), the model output is converted into a dilution matrix (s/m). Each element of this matrix *D* dilutes a continuous emission (*e*) of 1 g/m^{2}s from a given grid box over the previous 30 days to an air concentration (g/m^3) at the receptor (*o*) during a 2-hour period.

$$D\,\underline{e} = \underline{o} \qquad \ldots 1$$

Baseline concentrations are defined here as those that have not been influenced by significant emissions within the previous 30-days of travel en-route to Mace Head, i.e. those that are well mixed and are representative of the mid-latitude Northern Hemisphere background concentrations.

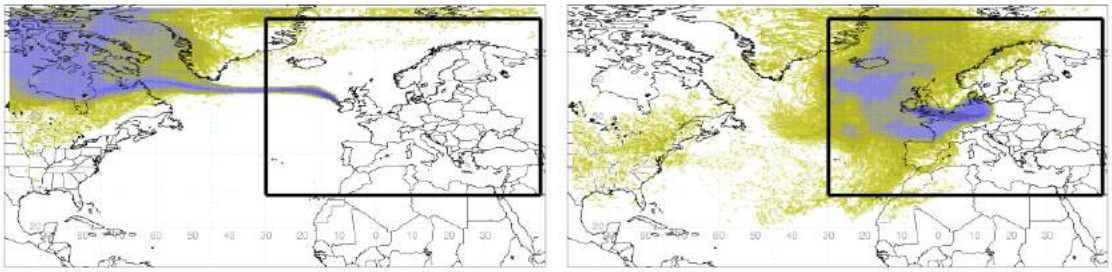

(a) (b)

Figure 6: Examples of 2-hour air history maps derived from NAME (a) baseline period (b) regionally polluted period. The air-history maps describe which surface areas (defined as within 100 m of the surface) in the previous 30-days impact the observation point at a particular time.

A 2-hour period is classed as 'baseline' if it meets the following criteria:

- The total air concentration from the nine grid boxes centred on and surrounding Mace Head is less than ten times the *dilution sensitivity limit* i.e. local emissions do not significantly contribute.
- The total air concentration contribution from a population map is less than an arbitrary limit. The limit is set so that it is clear that populated regions have not significantly contributed.
- The contribution from the southerly latitudes (south of 28^o latitude) is (arbitrarily) less than twice the *dilution sensitivity limit* indicating that southerly latitude air is not significantly present.

In order to define a *dilution sensitivity limit* it is necessary to arbitrarily decide on a level of emission that would produce an agreed response at the observation point. In this study we chose an emission of 100 kt CH_4 /yr/grid to produce a 10 ppb impact. As shown later, 10 ppb is approximately the noise found in the baseline signal for methane and an emission of 100 kt/year is about 4% of the estimated UK release of methane in 2006. 10 ppb CH_4 is equivalent to ~7 ug/m^3. Assuming a horizontal grid resolution of 40 km at a latitude of 50^o N, 100 kt CH_4 /yr/grid is approximately ~2 ug/m^2/s, thus the *dilution sensitivity limit* is calculated, using equation 1, to be 3.4 s/m (~2.2e-9 s/m^3 at Mace Head).

The *dilution sensitivity limit* is attempting to define a threshold above which an emission source would generate a concentration at Mace Head that would be discernible above the baseline noise. The same limit value is used for all of the gases analysed. The chosen limit is arbitrary but the impact of doubling it is small.

Figure 7 shows a three month extract of the methane observations measured at Mace Head. The observations have been colour coded to indicate whether, using the above classification, the air mass they were sampled from was considered baseline. For the baseline analysis all non-baseline observations are removed.

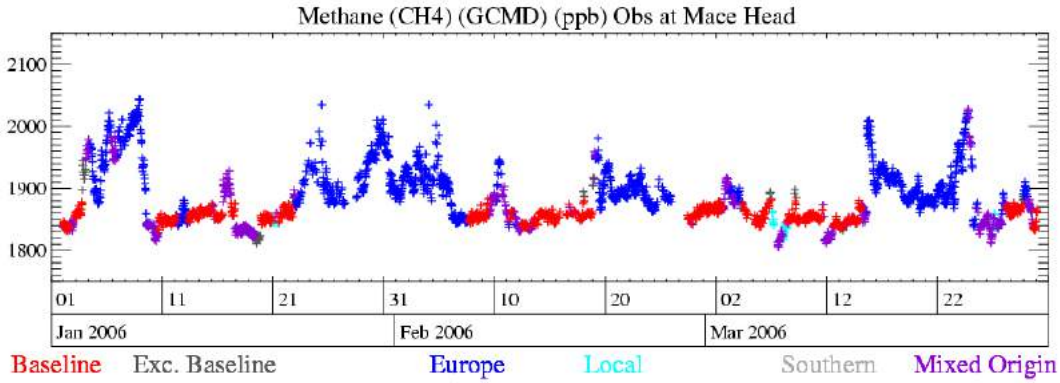

Figure 7: 3-month time-series of Mace Head methane observations showing the impact of the baseline and non-baseline classification. The baseline observations are shown in red.

The points defined as baseline using the above methodology still have a certain level of noise. The principle reasons for this are; unexpected short-lived emissions e.g. forest fires in Canada or from shipping, local emissions that are not identified using the above criteria above, incorrectly modelled meteorology or transport, i.e. European air defined as baseline by error.

Irrespective of the methodology used to identify these events some will inevitably be classed as baseline when it is inappropriate to do so. To capture such events the baseline data are statistically filtered to isolate and remove these non-baseline observations. For each baseline point in turn, the baseline points in a 40-day window surrounding this central value are considered and, provided that there are sufficient points (>11 with at least 4 in each third of the window or more than 18 in two thirds), a quadratic is fitted to these values. The standard deviation of the actual points and the fitted curve is calculated (*std*) and if the current baseline value is more than *x std* away from the fitted value it is marked for exclusion from the baseline observations. After all baseline points have been considered, those to be excluded are removed. The process is repeated nine times, each time the value for *x* is gradually reduced from 6 to 2, thus ensuring that those points statistically far from the fitted baseline do not unduly affect the points to be excluded by skewing the fitted curve. If there are insufficient baseline points in a 40-day window the values are only included if the spread in the points is small and there are at least 5. The observations removed through this statistical filter are shown in black in Figure 7.

For each hour in the time-series the baseline points in a running 40-day window are fitted using a quadratic function and the value extracted for the current hour in question. The process is then advanced by an hour and repeated. If there are insufficient baseline points well spaced within the window (at least 3 in each quarter) it is gradually extended up to 150-days.

For each hour within the observation time record a smoothed baseline concentration is estimated by taking the median of all fitted baseline values within a 20-day time window. If there are fewer than 72 baseline values in the time window then the window is steadily increased up to a maximum of 40 days. If there are still insufficient points then no smoothed baseline concentration is estimated for that hour.

The noise or potential error in the smoothed baseline concentration is estimated to be the standard deviation of the difference between the observations classed as baseline and the smoothed baseline concentrations at the corresponding times. Figure 8 shows, on a much expanded y-axis compared to Figure 7, the typical spread of baseline observations about the smoothed continuous baseline estimate.

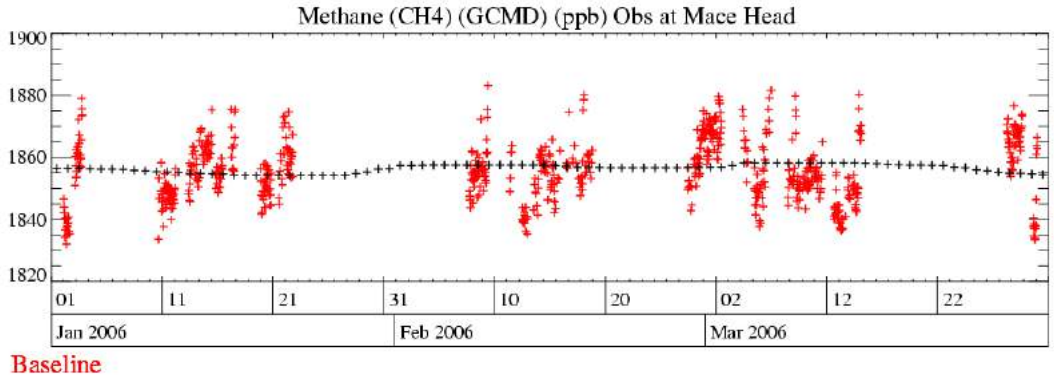

Figure 8: Observations of methane at Mace Head within a 3-month period classed as baseline (red) with the estimated daily baseline concentrations for the same period (black). Note: the y-axis has been expanded compared to Figure 7.

The hourly baseline concentrations are split into two components, a long-term trend and a residual component (seasonal cycle). Two methods have been used:

- **Kolmogorov–Zurbenko method**

A Kolmogorov–Zurbenko (KZ) filter involves *k* time iterations of a moving average of a given time duration and is ideally suited to this type of problem. For this application, the length of the moving average window was set to one year and the number of iterations was set to four. With these parameters a 12-month moving average was applied to the data four times, thereby approximately removing wavelengths smaller than 2-years. At each hour in the time-series the 12-month average of the baseline mass mixing ratios centred on this hour is calculated. This is the long-term trend component, subtracting this from the actual hourly baseline estimate at this time gives the residual.

- **3-year quadratic method**

At each hour calculate the 12-month average centred on this hour (y_a). For the three-year period centred on this hour calculate the quadratic line using standard value decomposition, that best-fits (minimises) the difference between the computed time-series and y_a. This is the long-term trend component, subtracting this from the actual hourly baseline estimate at this time gives the residual.

Monthly and annual baseline concentrations are estimated by averaging all of the long-term trend daily baseline values within the appropriate time window. A monthly value is estimated if there are at least 21 daily values within the month, this ensures a good representation of the whole month. An annual value is estimated if there are at least 330 daily values within the calendar year, ensuring a good representation of the whole year.

The annual growth rate on a particular day is defined as the local slope of the long-term trend on that day. The local slope is estimated by linearly fitting a best-fit line through the trend concentration values for the day before, current day and day after. Monthly averages of these growth rates for methane and nitrous oxide are shown in Figures 72 and 77.

The daily residual concentration values are averaged for each month over the data period studied to produce a seasonal cycle. The mean seasonal cycles for each gas are shown in Figures 85 - 155. The range of values for each month is also shown, along with the first, middle and last individual year seasonal cycles.

Gas	1990	1991	1992	1993	1994	1995	1996	1997	1998	1999
CFC-11 (GCMD)	264	267	268	269	268	267	266	264	263	261
CFC-12 (GCMD)	496	506	517	522	529	533	537	540	542	544
CFC-13										
CFC-113 (GCMD)	75.5	81.1	84.2	85	84.6	84.6	84.3	83.8	83.2	82.7
CFC-113										
CFC-115										8
HCFC-124										1.3
HCFC-141b						5.1	7.3		11.3	13.3
HCFC-142b						8	9.2	10.7	11.4	12.4
HCFC-22										145
HFC-125										1.3
HFC-134a						2.3	4.3	6.3	9.6	13.4
HFC-143a										
HFC-152a						1.2	1.2	1.3	1.9	2.2
HFC-23										
HFC-32										
HFC-227ea										
HFC-236fa										
HFC-245fa										
HFC-365mfc										
HFC-4310mee										
PFC-14										
PFC-116										
PFC-218										
PFC-318										
SF6										
SO2F2										
CH3Cl										535
CH2Cl2							36.3	36.1	35	31.8
CHCl3 (GCMD)						12.6	13	12.1	12.2	11.6
CHCl3							12.5	12	12.6	12.7
CH3CCl3 (GCMD)	151	152	150	139	125	111	95	80	66	55
CH3CCl3										
CCl4 (GCMD)			105	104	103	102	101	100	99	98
CHClCCl2										
CCl2CCl2										
CH3Br										11
Halon-1211						3.5	3.6		4	4.2
Halon-1301										2.8
Halon-2402										
CH2Br2										
CHBr3										
CH3I										
CH4 (ppb)	1792	1812	1804	1815	1818	1822	1827	1826	1836	1841
C2H6										
C6H6										
CO (ppb)						119	130	118	145	124
CO2 (ppm)				357	359	361	363	364	367	369
N2O (ppb)	309	310	310	311	312	312	313	314	314	315
O3 (ppb)	34.8	35.8	34.5	34.6	36.3	34.5	36.9	36.6	39.4	41.7
H2 (ppb)						496	502	494	507	507

Table 4: Annual Northern hemisphere baseline mass mixing ratios for all gases measured at Mace Head 1990-1999 (ppt unless stated).

Gas	2000	2001	2002	2003	2004	2005	2006	2007	2008	2009
CFC-11 (GCMD)	260	259	256	255	253	250	248	246	244	243
CFC-12 (GCMD)	546	546	546	546	545	544	543	541	539	536
CFC-13					2.8	2.8			2.9	2.9
CFC-113 (GCMD)	82.2	81.5	80.6	79.9	79.3	78.7	77.8	77.1	76.6	76
CFC-113						78.8	77.9		76.7	76
CFC-115	8.1	8.2	8.1	8.2	8.4	8.4	8.4	8.4	8.4	8.4
HCFC-124	1.4	1.6	1.6	1.6	1.6	1.6	1.6	1.6	1.6	1.6
HCFC-141b	15.2	16.4	17.6	18.6	19.1	19.1	19.6	20.2	20.9	21.3
HCFC-142b	13.6	14.6	15	15.5	16.2	17	18.1	19.3	20.6	21.4
HCFC-22	151	158	164	169	175	180	187	195	204	212
HFC-125	1.6	2.1	2.4	3.1	3.7	4.3	5	5.8	6.9	8
HFC-134a	17.2	20.8	25	29.6	34.7	39.3	43.8	47.9	53.3	58
HFC-143a					5.5	6.4	7.4	8.4	9.6	10.7
HFC-152a	2.5	2.9	3.4	4.2	4.8	5.6	6.8	7.9	8.8	8.9
HFC-23									22.5	23
HFC-32					1.1	1.6	2.1	2.7	3.4	4.1
HFC-227ea								0.4	0.5	0.6
HFC-236fa								0.1	0.1	0.1
HFC-245fa								0.9	1.1	1.2
HFC-365mfc					0.2	0.3	0.4	0.5	0.5	0.6
HFC-4310mee										
PFC-14					74.9	75.5	76.2	76.9	77.7	78.1
PFC-116					3.6	3.7	3.8	3.9	4	4.1
PFC-218					0.4	0.5	0.5	0.5	0.5	0.5
PFC-318										
SF6					5.6	5.8	6.1	6.3	6.6	6.9
SO2F2						1.5	1.5	1.6	1.6	1.7
CH3Cl	521	514	514	524	522	529	523	530	535	532
CH2Cl2	30.4	29.3	29.4	31.2	31	30.7	32.5	34.4	36.3	36.6
CHCl3 (GCMD)	11.1	11.1	11.2	11.4	11.4	11.3	11.4	11.4	11.5	11
CHCl3	11.6	10.9	10.4	11	10.8	11.1	11.1	10.6	10.6	10.2
CH3CCl3 (GCMD)	46	39	32	27	23	19	16	13	11	9
CH3CCl3		39.3	31.1	26.7	23.1	18.8	15.7	13.1	11	9.3
CCl4 (GCMD)	97	96	95	94	93	92	91	90	89	88
CHClCCl2	1.4	1.4	1.4	1.3	1.6	1	1	1.1	0.7	0.6
CCl2CCl2		5.1	4.7	4.8	4.7	3.9	3.8	3.6	3.4	3
CH3Br	10.5	9.9	9.1	8.9	9.1	9.9	9.5	9.1	9.2	8.6
Halon-1211	4.3	4.4	4.4	4.4	4.5	4.5	4.5	4.4	4.4	4.3
Halon-1301	2.9	3	3	3.1	3.1	3.2	3.2	3.2	3.3	3.3
Halon-2402						0.5	0.5	0.5	0.5	0.5
CH2Br2							1.6	1.7	1.6	1.6
CHBr3						5.7	6	4.8	4.8	4.9
CH3I		1.5	1.6	1.7	2	2	1.4	1.6	1.4	1
CH4 (ppb)	1842	1843	1844	1854	1848	1847	1847	1855	1864	1868
C2H6						1272	1300	1338	1339	1068
C6H6						66.3	64.2	61.8	65.7	61.7
CO (ppb)	119	117	127	137	123	123	123	120	120	114
CO2 (ppm)	369	371	373	375	378	379	382	384	386	387
N2O (ppb)	316	317	318	318	319	320	320	321	322	323
O3 (ppb)	40.1	39.4	39.8	40.7	40.3	39.6	40.8	39.5	40.5	39.9
H2 (ppb)	499	495	497	500	497	500	504	499	502	498

Table 5: Annual Northern hemisphere baseline mass mixing ratios for all gases measured at Mace Head 2000-2009 (ppt unless stated).

Gas	2010	2011	2012	AvGrow	AvGr12
CFC-11 (GCMD)	241	238	236	-1.17	-2.2
CFC-12 (GCMD)	533	531	528	1.68	-2.71
CFC-13	2.9	3	3	0.02	0.03
CFC-113 (GCMD)	75.3	74.9	74.3	0.04	-0.32
CFC-113	75.2	74.5	74	-0.68	-0.56
CFC-115	8.4	8.4	8.4	0.04	0.02
HCFC-124	1.5	1.4	1.4	0.02	-0.05
HCFC-141b	22	23.1	24.1	0.89	1.14
HCFC-142b	21.9	22.7	23	0.9	0.59
HCFC-22	219	226	231	6.72	5.46
HFC-125	9.2	10.8	12.4	0.81	1.59
HFC-134a	63.4	68.4	73.4	4.2	4.9
HFC-143a	11.9	13.2	14.5	1.13	1.31
HFC-152a	9.4	10	10.1	0.55	0.36
HFC-23	23.7	24.7	25.5	0.75	0.94
HFC-32	5.2	6.5	7.7	0.82	1.26
HFC-227ea	0.6	0.7	0.8	0.07	0.07
HFC-236fa	0.1	0.1	0.1	0.01	0.01
HFC-245fa	1.3	1.5	1.7	0.15	0.19
HFC-365mfc	0.6	0.7	0.8	0.08	0.08
HFC-4310mee		0.22	0.23		
PFC-14	78.7	79.5	80.3	0.68	0.79
PFC-116	4.1	4.2	4.3	0.08	0.08
PFC-218	0.6	0.6	0.6	0.02	0.02
PFC-318		1.32	1.36		
SF6	7.2	7.5	7.8	0.28	0.3
SO2F2	1.7	1.8	1.9	0.06	0.09
CH3Cl	531	521	528	-1.83	-3.59
CH2Cl2	40.2	39.7	41.9	0.24	-0.15
CHCl3 (GCMD)	12	11.6	11.7	-0.06	-0.19
CHCl3	11.2	10.9	10.9	-0.09	-0.14
CH3CCl3 (GCMD)	8	7	5	-6.56	-1.2
CH3CCl3	7.8	6.5	5.4	-3.03	-1.22
CCl4 (GCMD)	87	86	85	-0.99	-0.9
CHClCCl2	0.5	0.4	0.3	-0.09	-0.14
CCl2CCl2	3	2.7	2.5	-0.23	-0.31
CH3Br	8.3	8.4	8.3	-0.21	0.01
Halon-1211	4.2	4.2	4.1	0	-0.08
Halon-1301	3.3	3.3	3.3	0.04	0.03
Halon-2402	0.5	0.5	0.5	-0.01	0
CH2Br2	1.8	1.6	1.7	0	-0.08
CHBr3	5.6	4.5	4.5	-0.25	-0.63
CH3I	1	1	0.9	-0.07	-0.12
CH4 (ppb)	1872	1875	1882	4.11	5.29
C2H6	1068			-62.4	-144.4
C6H6	61.9			-1.12	-1.51
CO (ppb)	122	116	124	0.05	-1.33
CO2 (ppm)	390	392	394	1.93	2.09
N2O (ppb)	323	324	325	0.72	0.97
O3 (ppb)	39	39.6	39.9	0.22	0.02
H2 (ppb)	498	504	505	0.56	3.31

Table 6: Annual Northern hemisphere baseline mole fractions for all gases measured at Mace Head 2010-2012 (ppt unless stated) and (Kolmogorov–Zurbenko 2-year) Northern hemisphere baseline growth rates (ppt/yr unless stated): over all years (fifth) and most recent (last column).

4.2.3 Baseline Concentrations

For each gas observed at Mace Head a baseline analysis has been performed. ECMWF meteorology is used from 1989 – 2002 inclusive and Met Office meteorology from 2003-2012 inclusive. The figures that follow illustrate for each gas the monthly and annual baselines, the changing baseline growth rates and the average seasonal cycle seen within the observations. The gases are grouped into similar chemical families; CFC, HCFC, HFC, fluorine compounds (PFCs), chlorine compounds, bromine compounds (halons), hydrocarbons, oxides of carbon and finally nitrous oxide, ozone and hydrogen. Table 1 summaries the annual baseline mass mixing ratios within the observation period for each of the gases considered.

4.3 Regional emission estimation

By removing the time-varying baseline concentrations from the raw measurement data, a time-series of excursions from the baseline for each observed gas has been generated from 1990 onwards or from when observations were started. The observed deviations from baseline are averaged over each two-hour period. These perturbations are driven by emissions on regional scales that have yet to be fully mixed on the hemisphere scale. Henceforth these above-baseline measurements are referred to as simply the observations.

This chapter describes the inversion modelling technique (InTEM) that has been used to estimate the UK and North West European (NWEU) emissions. The results of the inversions when Mace Head observations are used are presented for each gas. The following chapter describes the impact of including the new data set from the enhanced UK DECC network. The estimates at DA level are presented in Section 5 and refer to inversions with Mace Head observations. In future reports one of the focuses will be on the use of the new observations to refine the DA emissions.

4.3.1 InTEM (Inversion Technique for Emission Modelling)

The observation time-series, together with the NAME model output predicting the recent history of the air, was used to estimate the emission distribution of each gas over North West Europe. The iterative best-fit technique, simulated annealing [Press *et al* 1992], was used to derive these regional emission estimates based on a statistical skill score (cost function) comparing the observed and modelled time-series at Mace Head. The technique, referred to as InTEM, starts from a set of random emission maps, it then searches for the emission map that leads to a modelled time series at Mace Head that most accurately mimics the observations.

The aim of InTEM is to estimate the spatial distribution of emissions across a defined geographical area (Figure 9). In the equation to solve (Equation 1) the set of observations (*o*) and the dilution matrix (*D*) as estimated using the NAME model are known. The observations are in volume mixing ratios. The dilution matrix has units (s/m) and is calculated from the time-integrated air concentrations produced by the NAME model. The dilution matrix has *t* rows equal to the number of 2-hour periods considered and has *n* columns equal to the number of grid points in the defined geographical domain. This matrix dilutes a continuous emission of 1 g/m^{2}s over a given grid to an air concentration (g/m^3) at the receptor during a 2-hour period. The observations are converted from volume mixing ratio [ppb] to air concentration (g/m^3) using the modelled temperature and pressure at the observation point.

The inversion domain is chosen to be a smaller subset of the full domain used for the air history maps. It covers 14.30^o W – 30.76^o E longitude and 36.35^o N – 66.30^o N latitude and is shown as the black box in Figure 6. The smaller domain covers all of Europe and extends into the Atlantic and has an intrinsic horizontal resolution of 0.352^o longitude by 0.234^o latitude. The inversion domain needs to be smaller to ensure re-circulating air masses are fully represented but also because emission sources very distant from Mace Head have little discernible impact on the concentration at the station, i.e. the signal would be too weak to be seen. The inversion method assumes baseline concentration air enters the inversion domain regardless of direction. For the eastern and southern edges in particular this will be incorrect. Emissions in Russia and around the Black Sea would be expected to elevate the atmospheric concentrations along the eastern edge, and due to

the latitudinal gradient it would be reasonable to assume below mid-latitudinal baseline concentration air enters from the south. This issue is overcome in the inversion by solving for, but not analysing, the estimated emissions in any grid on the edge of the inversion domain. It is assumed that the error of above or below baseline concentration air entering the domain will be absorbed into the solutions in these edge grids.

In order for the best-fit algorithm to provide robust solutions for every area within the domain, each region needs to significantly contribute to the air concentration at Mace Head on a reasonable number of time periods. If the signal from an area is only rarely or poorly seen at Mace Head, then its impact on the cost function is minimal and the inversion method has little skill at determining its true emission.

The contribution that different grid boxes make to the observed air concentration varies from grid to grid. Grid boxes that are distant from the observation site contribute little to the observation, whereas those that are close have a large impact. In order to balance the contribution from different grid boxes, those that are more distant are grouped together into increasingly larger blocks. The grouping varies for each time period considered and between the different gases due to varying meteorology and the impact of missing observations respectively. The underlying horizontal grid resolution is approximately 25 km (0.352^{o} longitude by 0.234^{o} latitude) and is equal to the resolution of the NAME output. The base grid used is shown in Figure 9(a) and conforms to country (and DA) boundaries. The country boundaries extend into the surrounding seas to reflect both emissions from shipping, off-shore installations and river runoff but also because the inversion has geographical uncertainty. Each area from the base grid is then considered in turn. If the contribution (impact) from an area at Mace Head is above a defined threshold then the area is sub-divided into two areas. This splitting process is continued until each area just falls below the threshold or the fine (25km) grid resolution is reached. An example grid used in the inversion process is shown in Figure 9(b). The threshold used for the splitting process has been arbitrarily defined as 600 (50 days x 12 [2-hour periods per day] = 600) times and the *dilution sensitivity limit* threshold is 3.4 s/m, as derived in the baseline analysis. The sensitivity of the emission results to this arbitrary choice of threshold is, through investigation, considered to be below the baseline sensitivity that is included in the inversions. However this uncertainty will be considered in more detail in the final year of the project and will be reported on in the final contract report.

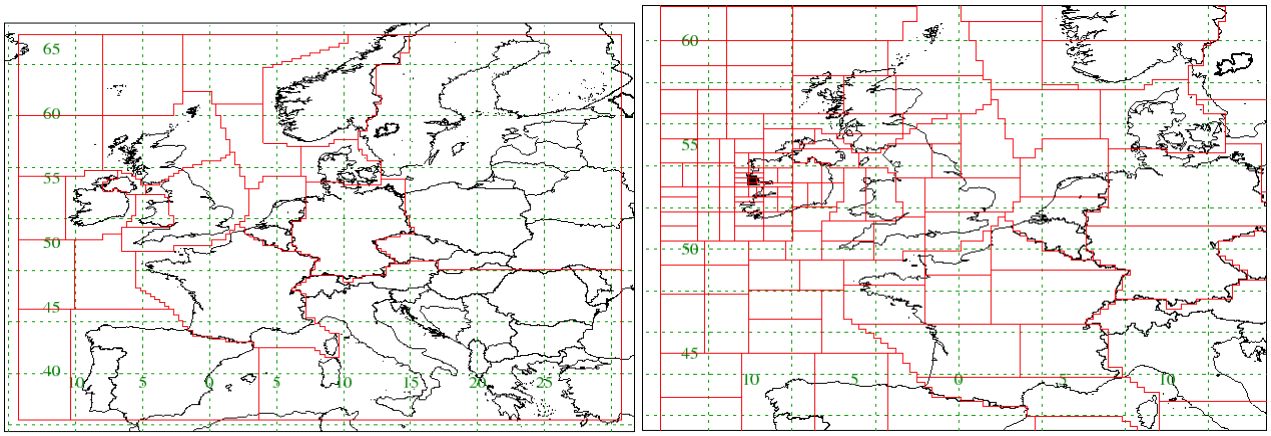

(a) (b)

Figure 9: (a) Base regions conforming to country (and Devolved Administration) boundaries (b) Example of the distribution of the different sized regions used by the inversion method to estimate regional emissions (Finest scale of the grid is ~25 km).

The modelled time-series at the measurement station is calculated by applying the current emission map to the dilution matrix (Equation 1).

The inversion process works by iteratively choosing different emissions, varying the emission magnitudes and distributions, with the aim of minimising the mismatch between the observations and the modelled concentrations. No *a priori* conditions are set. The relative skill of a derived

emission map is tested by comparing the modelled and observed time-series by using a cost function.

The cost function described here uses the baseline uncertainty as discussed and described in the previous chapter. This uncertainty varies from gas to gas depending on how well a smooth baseline can be constructed through the 'clean' observations.

An upper (lower) time-series of observations is constructed by adding (subtracting) the baseline uncertainty to the actual observations. These two time-series enclose a range of values that are entirely plausible within the uncertainty of the baseline definition. Given a modelled emission distribution (emission map), a modelled time-series is constructed. The sum of the absolute magnitudes of the modelled values outside of this acceptable range, normalised by the average observation value, is calculated and used as a measure of the skill of the current modelled emission map. This cost function has been extensively compared to the one previously used (see Figure 10 for an example using methane) and the differences are within the uncertainties reported. It is preferred as it is simpler and less esoteric. For each CFC and HCFC last year's InTEM estimates are presented alongside those for this year and show good agreement. Note, for methane, the average UK emissions are very marginally higher using the current cost function compared to those using the previous function, this observation is not universal for all gases. The final year of the project will revisit this area and a fuller investigation of the sensitivity of the results to the choice of the cost function will be reported.

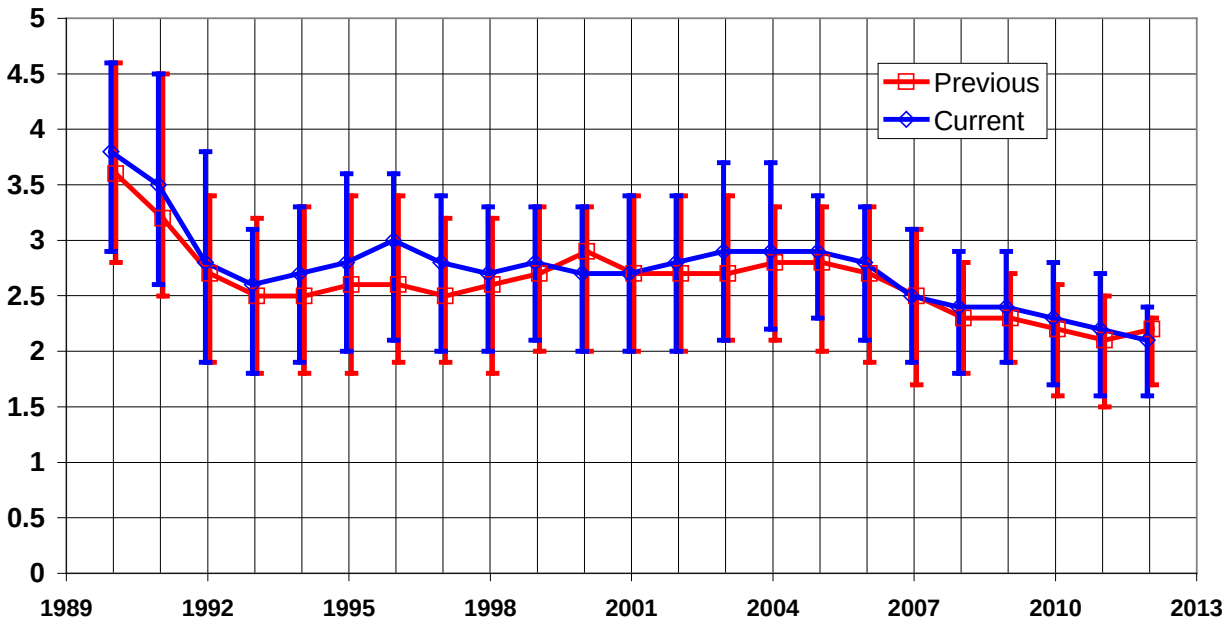

Figure 10: Comparing the UK emission estimates for methane (Mt/y) from InTEM using two different cost functions.

The iteration process is repeated until the future potential improvement in skill in the emission map is estimated to be negligible.

To simulate uncertainties in the meteorology, dispersion and observations the inversion process is applied to three observation time-series; (a) the actual observations (b) observations minus the baseline noise and (c) observations plus the baseline noise.

Any periods that were classed as baseline but were removed by the statistical filtering are removed from the analysis as these are considered to be unrepresentative of air from that sector. Times when the air is classed as 'local' are likewise removed from the analysis. A 2-hour period is classed as 'local' if the contribution from the 9 grids surrounding Mace Head is above fifteen times the *dilution sensitivity limit*. The local times represent periods when the emissions from the local area (75 km x 75 km area centred on Mace Head) would have a dominant effect on the

observations. These are typically characterised by low wind speeds, low boundary layer heights and thus poor dispersion conditions. During such times the meteorological models used, with horizontal resolutions of between 25 and 80 km, are poor at correctly resolving the local flows as they are dominated by sub-grid scale processes, e.g. land-sea breezes. For example, 86% (87%) of the CH_4 (N_2O) observations were retained for analysis.

Solutions are calculated for three-year periods covering the period when observations are available. After solutions have been estimated for a particular three-year period, the period is moved on by one month and the process repeated, e.g. Jan'95 – Dec'97, Feb'95 – Jan'98, etc.

An annual estimate of emission is calculated by averaging all of the solutions that contain a complete calendar year within the solved-for time period. The range for each year for each geographical region is calculated from the same sample of solutions and is taken as the 5th and 95th percentile solutions.

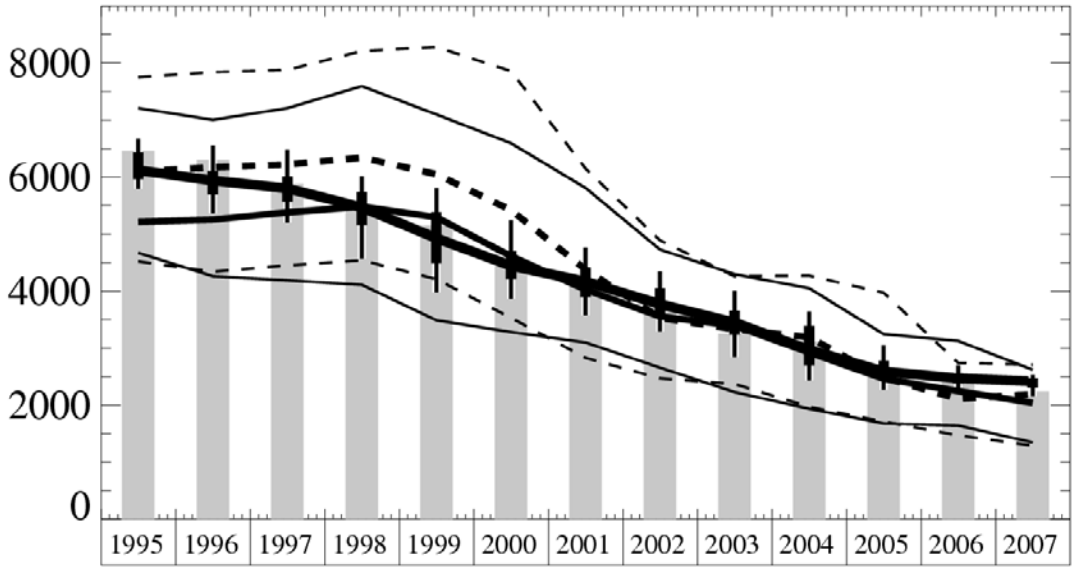

Figure 11: Time-series of annual emission estimates for NWEU (kt/y) using model-derived pseudo observations. The light grey columns are the EMEP inventory values. The solid line with 5th, 25th, median, 75th and 95th percentiles is the case with no noise and the same meteorology. The solid line is the case with noise and the same meteorology. The dashed line is with noise and different meteorology (UKMO used to create pseudo observations and ERAI dilution matrix used within the inversion). The 5th and 95th estimates provide the uncertainty ranges in each case and are shown as thinner lines with the same style.

To assess the ability of the inversion system to correctly estimate emissions on the regional scale it was first applied to model derived pseudo observations. The carbon monoxide (CO) emissions from the EMEP program (www.emep.int) were used to calculate a model time-series at Mace Head. Time-series' were derived using both ERAI (ECMWF re-analysis interim meteorlogy) and UKMO (UK Met Office meteorology). The inversion system was tested using the ERAI dilution matrix applied to, firstly, the pseudo observations derived using ERAI and then to the pseudo observations derived using UKMO. The latter test investigates the ability of the inversion system to estimate emissions with a system that has errors. The impact of applying random noise to the system is investigated by solving with and without noise. Figure 11 shows the time-series of emission estimates and true emissions for NWEU in this idealised case study.

The median emission total when no noise is added to the pseudo observations is excellent and the uncertainty bars are small. When noise is added to the measurements the median fit is still good but the uncertainty range is larger (solid lines). When a different meteorology is used to derive the pseudo observations and noise is added (dashed line) the fit is still good but the uncertainty range is at its largest. However in every case the uncertainty range completely encompasses the true

solution and gives confidence that the InTEM methodology is able to recreate the correct emission total within the estimated uncertainty range.

Figure 12 is an example of the observed and modelled time series of air concentration for CH_4 for 2010 at Mace Head. The magnitudes and patterns are similar and demonstrate that the inversion process is able to derive an emission map that produces a good match to the observations.

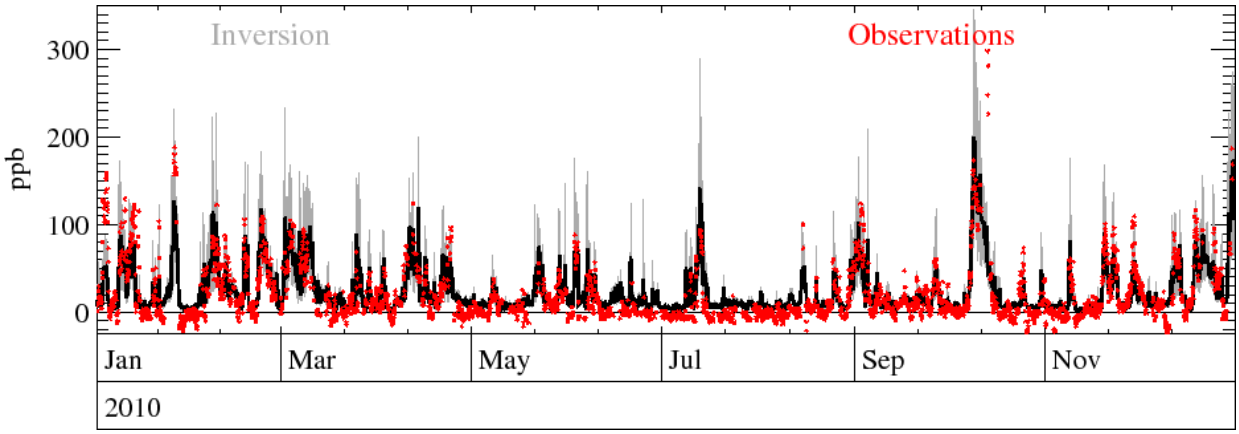

Figure 12: Time series of observed and best-fit modelled CH_4 concentrations (deviation from baseline) at Mace Head for the first three months of 2010 (solid black line = Inversion, grey = uncertainty in inversion, red crosses = observations).

Emission totals from specific geographical areas are calculated by summing the emissions from each 25 km grid box in that region (Figure 13). The emissions are also presented after they have been re-distributed by the population distribution in the inversion grid that has been used. The population distribution map used is shown in Figure 14. This final step does not in anyway alter the emissions per country, it is purely to demonstrate the likely distribution of the emissions. For some gases, such as HFC-134a, this re-distribution is entirely justified as all emissions are anthropogenic and are related to mobile air conditioning (e.g. cars) and therefore will have a strong correlation with population. For other gases, e.g. CH_4, the correlation with population is less strong as there is a significant contribution from the agricultural sector, primarily cattle.

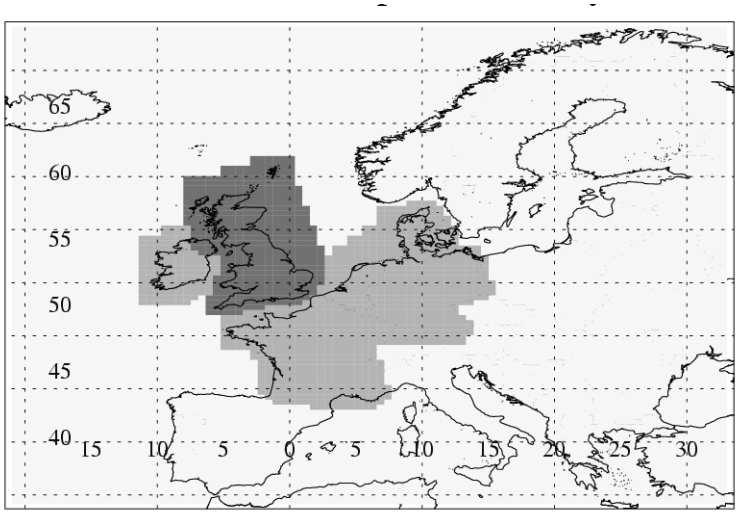

Figure 13: Geographical areas used to define UK and NWEU regional totals

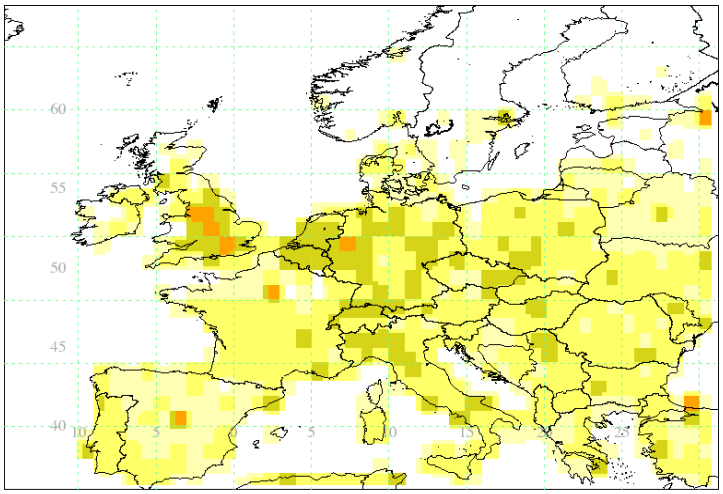

Figure 14: Population distribution used to re-distribute emissions within inversion grid.

All of the emissions are assumed constant in time and are geographically static within each 3-year study period. This is clearly a significant simplification. A sudden, but subsequently maintained, change in emission, will be picked up by solving multiple 3-year periods covering slightly different time periods, i.e. solving for a 3-year period and then advancing by one month. Enhanced emissions in any particular season, e.g. increased N_2O emissions in spring following fertilizer application, will not be resolved.

All areas of the domain are assumed to impact reasonably equally on Mace Head. The grouping of grid cells together, so that each area contributes approximately equally to the observations, attempts to ensure this but clearly there will be some variability. Also large grid cells could have significant variability actually within the grid itself especially if there are significant orographic features within the grid, e.g. the Alps. This may lead to errors if certain parts of the grid are more frequently sampled than others. However because of the large travel distances and therefore time elapsed between emission in these large grids and measurement the impact of this will be small. Also by only reporting emissions within NWEU this issue is assumed small.

The inversion method makes no distinction between anthropogenic and natural sources and thus its estimates are for the combined total, making direct comparisons with the UNFCCC inventory difficult. For most of the gases analysed here the natural emissions are estimated to be small in comparison to the anthropogenic emissions. For example, for CH_4 the natural emissions in NWEU are estimated to be 240 kt/yr [Bergamaschi *et al.* 2005].

It is also important to recognise that the release of certain gases to the atmosphere, e.g. N_2O released from agricultural practices, may occur many miles from its actual source and therefore adds to the uncertainty of using the maps to attribute emissions to particular regions. The area considered to be the UK includes the waters directly surrounding the UK (Figure 13), so the impact of this is considered to be small for the UK. This would be problematic if the individual contributions of Belgium or The Netherlands for example were presented and is the reason why only the NWEU total is considered. The most significant region in relation to this issue is the border between Northern Ireland and Ireland, however due to the proximity to Mace Head and the corresponding high resolution of the output there the impact is assumed small.

The transport modelling and thus the inversion algorithm also assume that the loss processes associated with each gas are negligible within the regional domain. Given the atmospheric lifetimes of the vast majority of the gases studied here this is considered to be a robust assumption. The clear exception is $CHClCCl_2$, which has a lifetime of around a week depending on the season of the year.

4.4 Improvements to InTEM (April 2011 – April 2013)

4.4.1 Below baseline observations not fixed to zero

Previously any observation that was below baseline, leading to a negative perturbation above baseline, was assigned a value of zero. This was because only the perturbation was available within the cost function routine. This has been altered so that the baseline is now also available. This means that the 2-hourly averaged observations can now be directly compared to the modelled deviations + estimated baseline, thereby removing the need for this zeroing step. The size of these negative deviations therefore now impact on the skill score assigned to each modelled emission map.

4.4.2 Each observation has an individual uncertainty

The uncertainty (+/- about the mean baseline) associated with each modelled observation is now available. This means that the uncertainty can change over the measurement period. Currently this uncertainty is limited to the uncertainty in the baseline within a time window (6-months) centred on the current time, but in time it will be expanded to include other factors such as; variable observational uncertainty, uncertainty per station, model transport uncertainty.

4.4.3 Alternate cost function has been developed

The distance of model time-series from the observations, outside of the baseline uncertainty, is a good measure of the quality of the current emission map and fully takes into account the allowable uncertainty at each observation time. Any modelled value that lies within the uncertainty is considered to be perfect and does not contribute to the cost of the emission map (a cost of zero is a perfect score).

4.4.4 Solve with High and Low baseline possibilities

The baseline that is used has an uncertainty. The inversion system is now solved three times, once with the mean baseline, once using the lower limit of the baseline possibility and once with the upper limit. Any systematic bias in the estimated baseline is thus considered within the uncertainty of the emission estimates.

4.4.5 Baseline trends / Cycles

The estimation of the long-term trend, growth rate and seasonal cycle of each gas has been improved. The hourly baseline concentrations are split into two components, a long-term trend and a residual component (seasonal cycle). Two methods are now used (to illustrate the uncertainty in this estimation process):

- **Kolmogorov–Zurbenko method**

Kolmogorov–Zurbenko (KZ) filter involves *k* time iterations of a moving average of a given time duration and is ideally suited to this type of problem. For this application the length of the moving average window was set to one year and the number of iterations was set to four. With these parameters a 12-month moving average was applied to the data four times, thereby approximately removing wavelengths smaller than 2-years. At each hour in the time-series calculate the 12-month average of the baseline mass mixing ratios centred on this hour. This is the long-term trend component, subtracting this from the actual hourly baseline estimate at this time gives the residual.

- **3-year quadratic method**

At each hour calculate the 12-month average centred on this hour (y_a). For the three year period centred on this hour calculate the quadratic line using standard value decomposition, that best-fits or minimises the difference between the computed time-series and y_a. This is the long-term trend component, subtracting this from the actual hourly baseline estimate at this time gives the residual.

4.4.6 New inversion grid that conforms to country outlines

Within the inversion system, InTEM, the basic core grid resolution of the maps is approximately 25 km. In order to balance the contributions from different regions these core grid boxes need to be grouped together as the distance from the observation point increases. In previous studies the grids have been grouped into 2x2, 4x4, 8x8, 16x16 and 32x32 larger grids. However this grouping takes no account of country borders therefore different countries will appear under the same large grid box, see Figure 15. This grouping has been improved so that the grouping ultimately conforms to the country borders. The largest the regions can become are now limited by those country borders of specific interest. Figure 16 shows extent of each of these large regions, each region is independently coloured (the actual colour is irrelevant). These large regions are sub-divided into smaller domains depending on the amount of information each region contributes to the observation point. Figure 17 shows the outcome of the new gridding process. Note that the country borders are extended into the surrounding seas and oceans to ensure a country's emissions are fully captured.

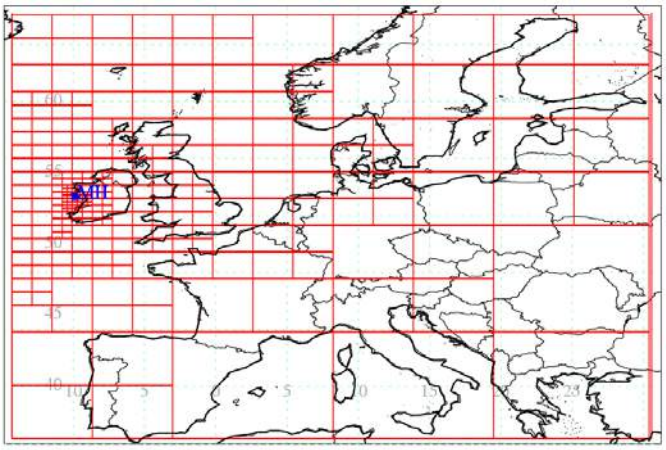

Figure 15: Grid resolution from old system for a 3-year inversion period with Mace Head observations.

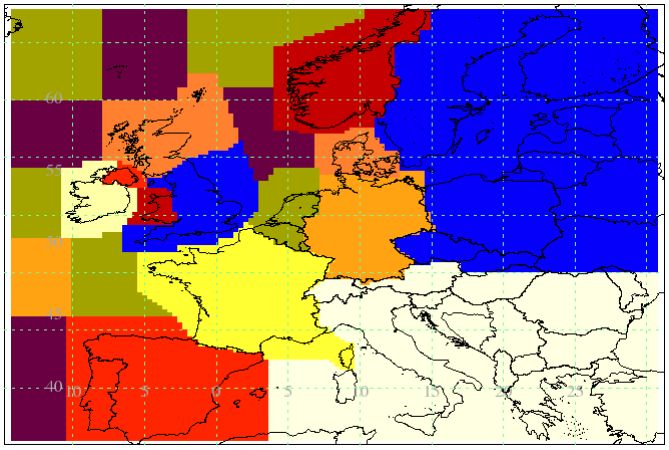

Figure 16: Extent of the large regions used to define the new inversion grid

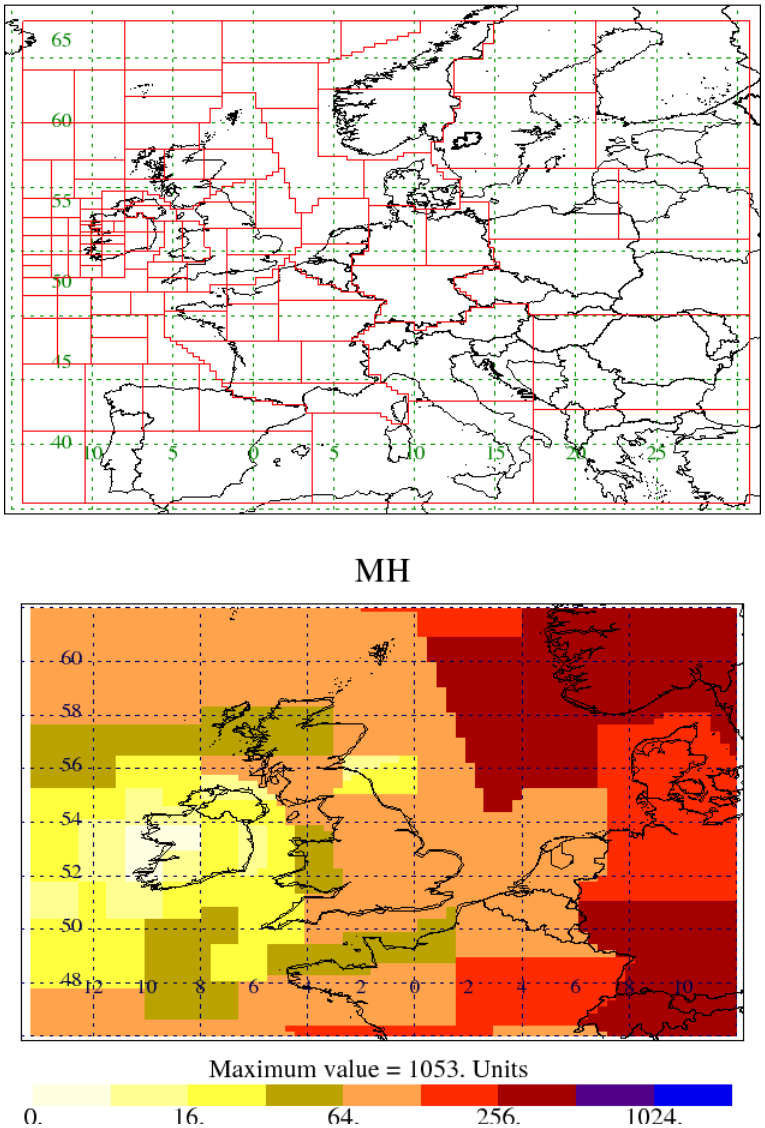

Figure 17: Top plot – new inversion grid (regions) that conforms to country boundaries; Lower plot – Example of the number of core basic grids in each of the inversion regions.

The new gridding system within InTEM allows a cleaner distinction between different countries and this is important when emissions are estimated from the Devolved Administrations (DAs).

4.4.7 Overall impact of InTEM improvements

Figures 18 and 19 show the InTEM results for CH_4 and N_2O respectively comparing the estimates from the final report from the previous contract (March 2011) and those produced using the improved INTEM system (April 2013). The GHG Inventory estimates submitted in 2011 and 2013 are also presented to show the changes within the inventory system as well.

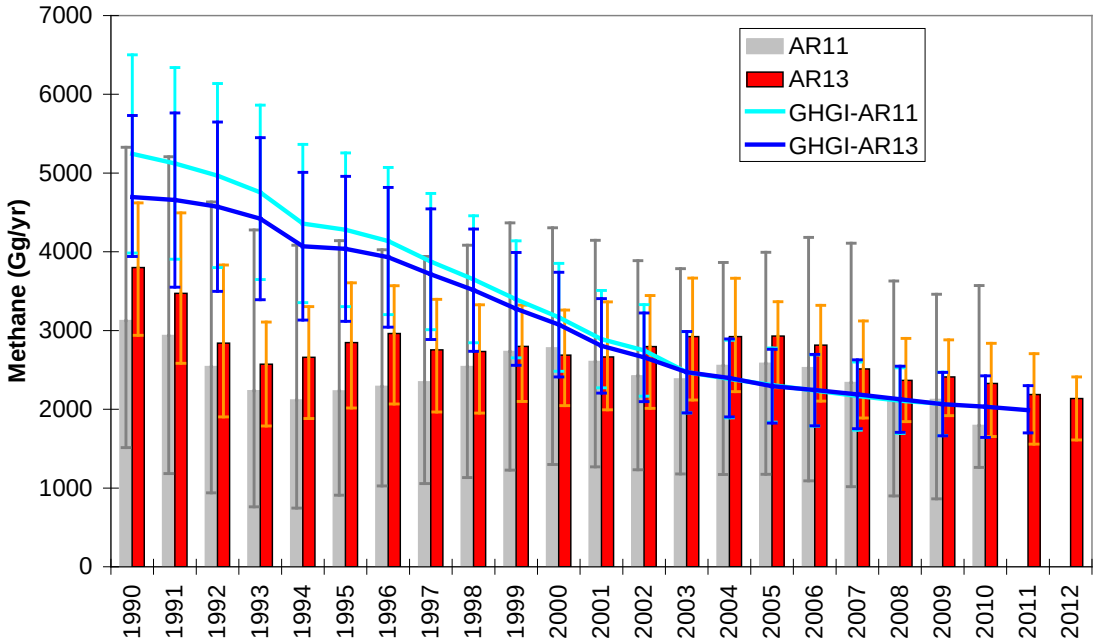

Figure 18: Comparison of UK methane emissions (Gg/yr) from InTEM (2011 annual report – grey and 2013 annual report – red) and from the GHG Inventory (2011 submission – cyan and 2013 submission - blue).

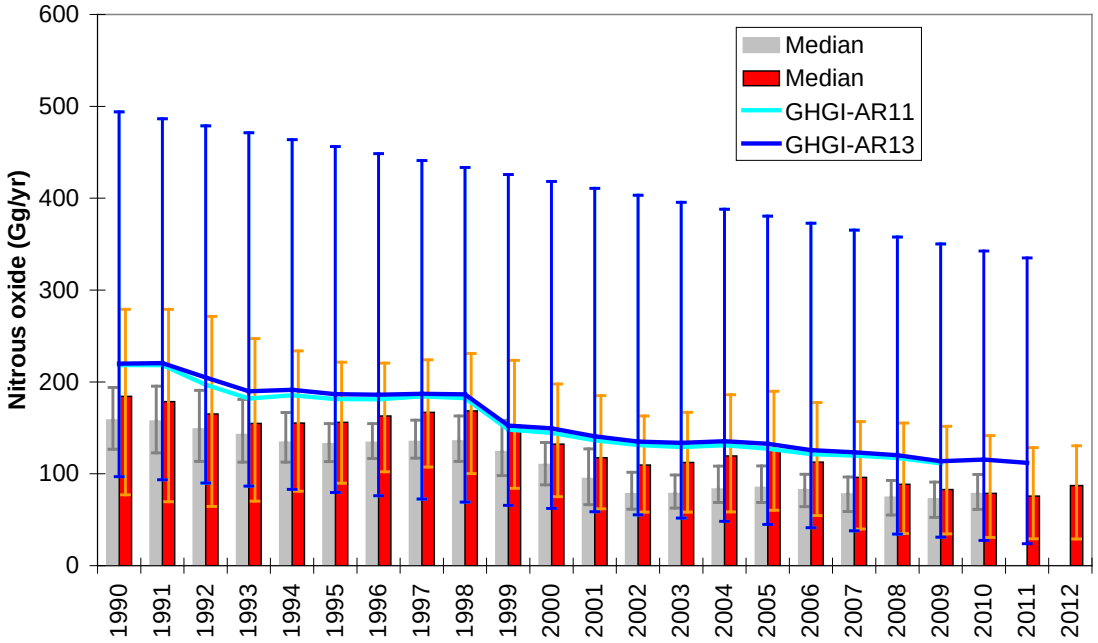

Figure 19: Comparison of UK nitrous oxide emissions (Gg/yr) from InTEM (2011 annual report – grey and 2013 annual report – red) and from the GHG Inventory (2011 submission – cyan and 2013 submission - blue).

4.5 Incorporating new UK DECC network observations

The observations from Ridge Hill and Tacolneston from July 2012 – December 2012 have been incorporated into the inversion system. The Ridge Hill observations prior to July 2012 were not used in this preliminary analysis because of the increased noise in the N_2O and SF_6 observations during the early part of the record. The baseline estimated from the Mace Head observations was assumed to be appropriate for both of the new sites and have been used throughout this analysis (see Figures 20 and 21). The close proximity of Mace Head to the new sites relative to the inversion domain justifies this approach.

No data from Tall Tower Angus have been included in the InTEM analysis. The quality of the reported N_2O observations have been shown to be insufficiently robust. The CH_4 Picarro data-set is currently being assessed and will be included if it is shown to be sufficiently robust. These data issues are discussed in the Annex section of this report. It is anticipated that CH_4 and CO_2 data will be available for the report in 2014.

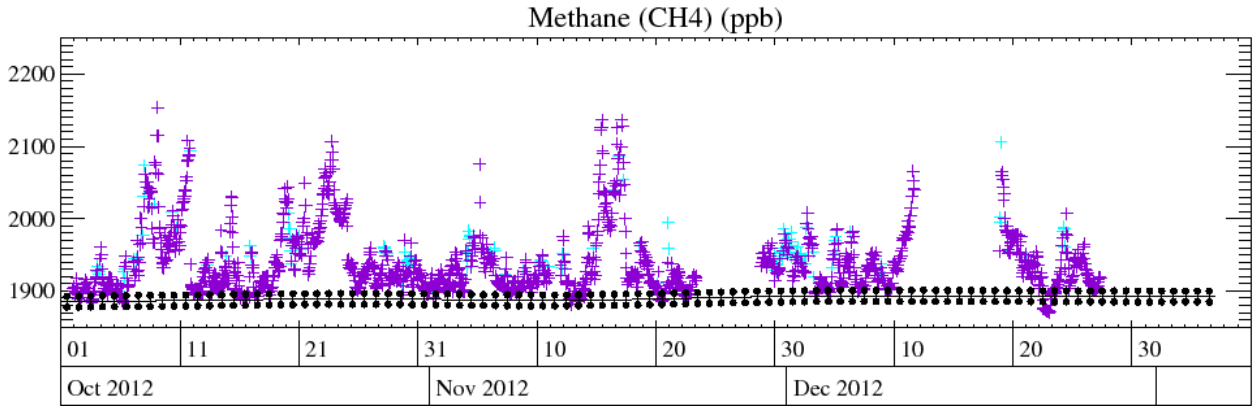

Figure 20: Portion of Ridge Hill CH_4 observations over-plotted with Mace Head baseline. Light blue points classed as local and not used in the inversion.

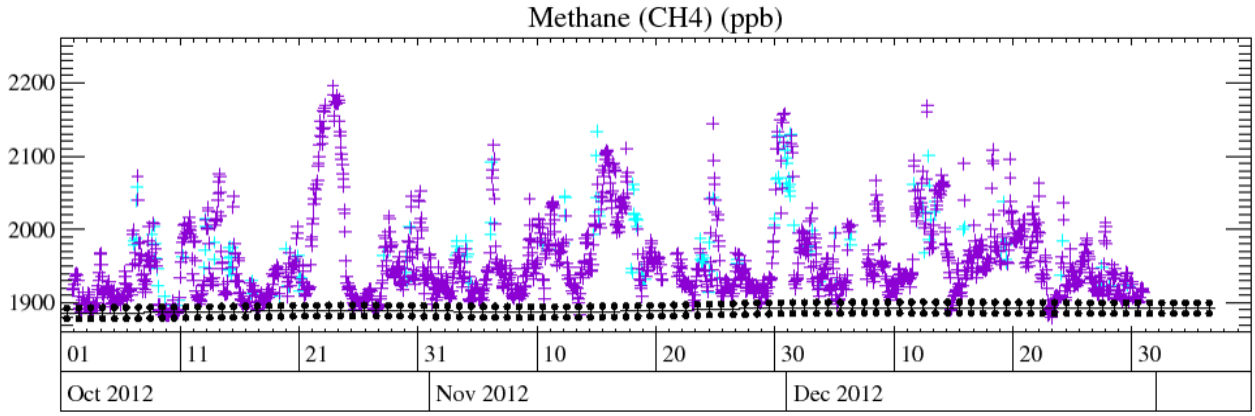

Figure 21: Portion of Tacolneston CH_4 observations over-plotted with Mace Head baseline. Light blue points classed as local and not used in the inversion.

CH_4 observations are recorded at two heights at both of the stations. When consecutive observations at the different heights are significantly different it implies that there is a strong gradient in the atmospheric concentration, which will occur if the atmosphere is very stratified and the vertical mixing is limited. During such times, usually during night time, the meteorological model will struggle to represent the local flow around the station because local effects, unresolved in the model, may be significant. These times were identified and flagged as being locally influenced (light blue in figures above) and have not been taken forward for use within InTEM. Figure 22 shows the inversion grid used for SF_6 for MHD-only for Jan 2010 – Dec 2012, along side that is the grid used for SF_6 for the 3-site inversion Jul 2012 – Dec 2012. The reduced number of

observations in the 3-site grid is seen through the reduced number of grid boxes overall, however the improved spatial distribution of the observations allows parts of England and Wales to be better resolved.

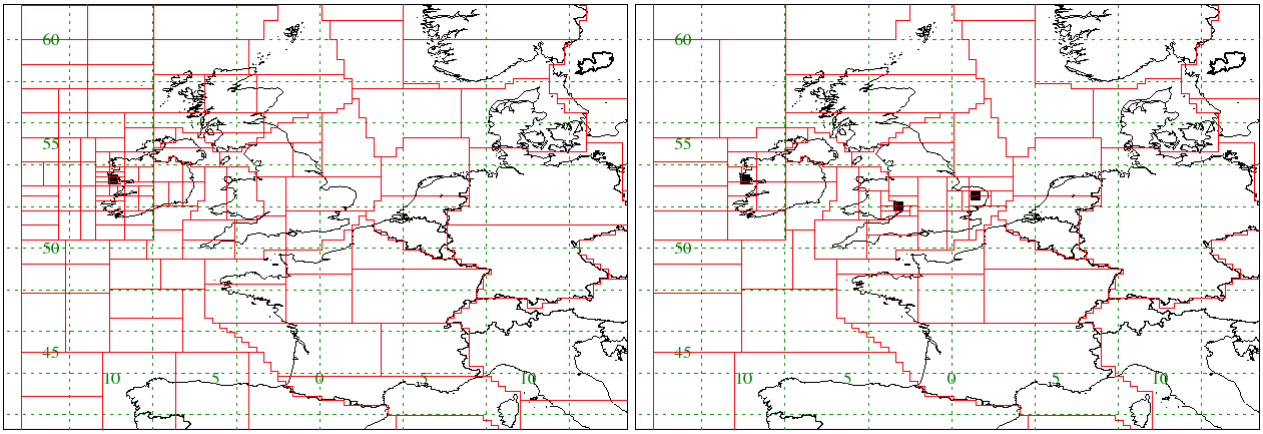

(a) (b)

Figure 22: (a) InTEM grid used for SF_6 for the period Jan 2010 – Dec 2012 MHD-only (b) InTEM grid used for SF_6 for the period Jul 2012 – Dec 2012 3-sites.

The inversion results for 2012 for SF_6, CH_4 and N_2O are presented in Sections 5.13.1, 5.14.1 and 5.15.1 respectively. The use of only 6-months of data from the new stations limits this analysis and these results are preliminary. Also, any seasonality in the emissions of these gases, which previously was smoothed out through the use of data covering 3-years, may be apparent in the inversion results, therefore direct comparison with the inventory or the results from the previous chapter may not be appropriate.

The 2014 report will provide a much more comprehensive analysis of the benefits of the enhanced DECC network. The areas of focus will be:

- The use of high-resolution meteorology to potentially better describe the flow of air to the stations. It will also allow an exploration into the impact of using a different meteorology on the results and partially quantify the uncertainty due to the meteorology used and the vertical resolution assumed with the NAME analysis.

- Include Tall Tower Angus in the analysis.

- The potential impact of unresolved local sources. Ridge Hill and Tacolneston are much closer to significant sources compared to Mace Head and this could have an impact on the inversion results. Appropriate data selection to those times which are well described by the model is the key.

- The seasonality of emissions can be explored given the significant increase in observations.

- The impact of the choice of grid for the inversion system and the sensitivity of the results to this choice.

- Incorporating the Tacolneston Medusa observations into the InTEM system.

4.6 Devolved Administration emission estimates

This section describes how the UK emission totals per year per gas have been sub-divided into four devolved administration (DA) areas; Scotland, Northern Ireland, Wales and England. Figure 23 shows the four regions that have been defined to make up the UK emission region. As previously noted the UK (and DA) region extends into the sea areas to reflect the fact that: (a) some of the anthropogenic emissions may occur out to sea for example oil/gas extraction or river run-off where material is transported out to sea before it is released to the atmosphere, and (b) the inversion system will have a degree of spatial error and so allowing some extension beyond the land-country areas is appropriate.

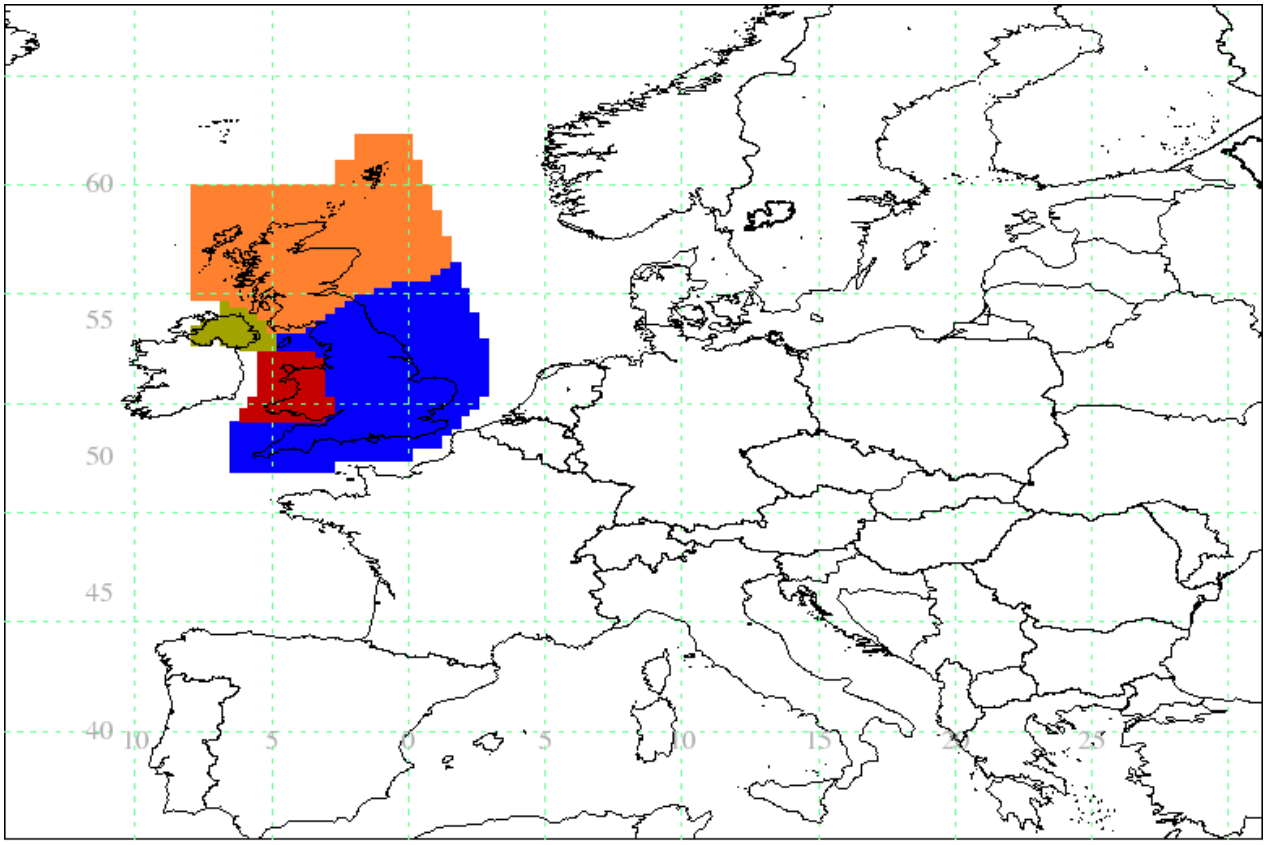

Figure 23: The UK region as defined in the inversion system. The separate colours indicate the four devolved administration areas.

The emissions per gas per year per DA for N_2O and CH_4 from a preliminary analysis are presented below. Only Mace Head observations have been used in this analysis to date because the extended UK DECC network only started in 2012 and this analysis shows the estimates from 1990 onwards. In the 2014 report the analysis will include DA estimates for 2012 and 2013 using the extended network for each of the Kyoto Protocol gases discussed in the next chapter. The UK emissions are usually dominated by the emissions from England. It is therefore interesting to also assess the emissions per million head of population taken from the 2011 census. The populations used (millions) are: England 53.013, Scotland 5.295, Wales 3.0635, Northern Ireland 1.789 and UK 62.641. For each gas a plot is also presented that shows the emissions per million head of population. For obvious reasons the relative uncertainty in the DA areas with smaller populations and/or smaller geographical areas are larger.

4.6.1 Methane Devolved Administration emissions

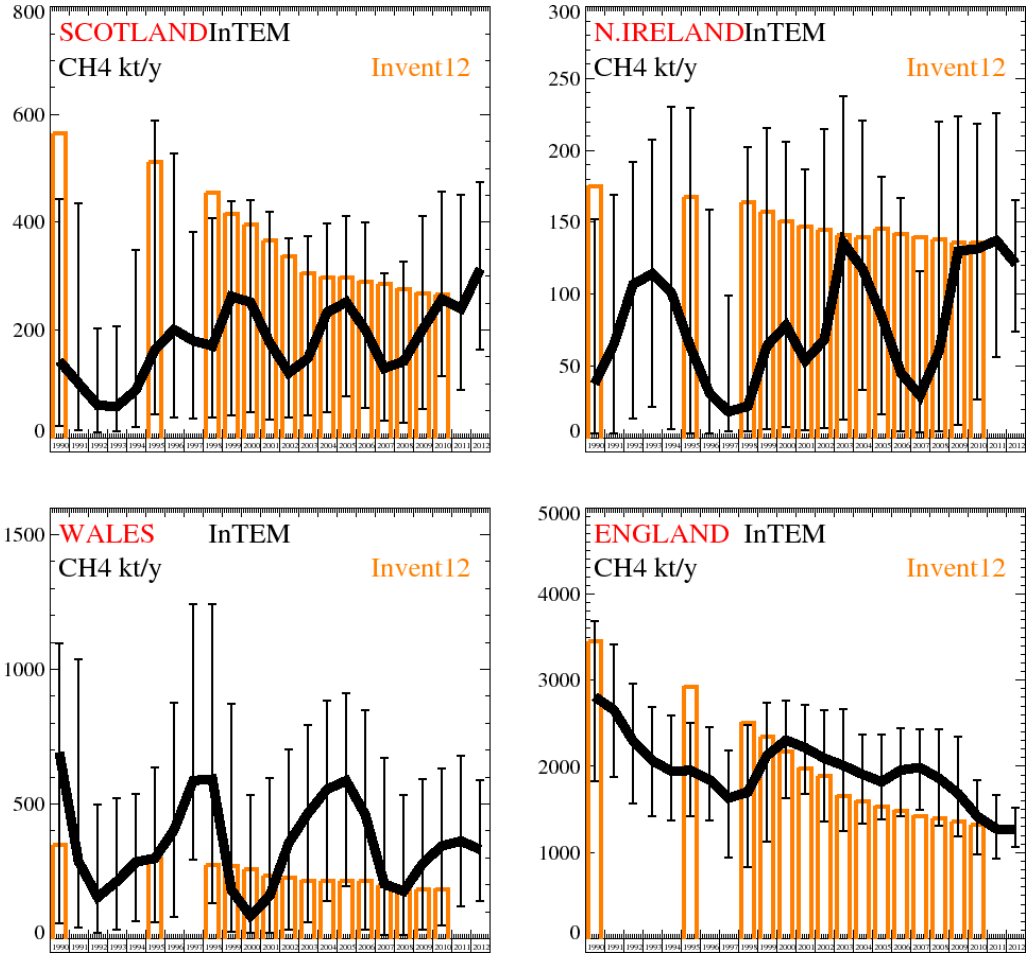

Figure 24: CH_4 devolved administration emission estimates using MH data. Black line with uncertainty bars (InTEM) and orange bars (Inventory).

The emissions of CH_4 in the UK are dominated by the emissions in England. The inversion results confirm this. Note that in the figures the Y-axis varies per plot. The uncertainties in the Welsh emissions are the largest in relative terms (in absolute terms the uncertainty in the English emissions are larger). This is unsurprising given the long border between England and Wales and the fact that this border area has significant emissions both due to farming and population. Given the uncertainty in the emissions from Scotland, Wales and Northern Ireland it is not possible to discern a trend over the years from 1990. The trend in the emissions from England mirrors that seen for the UK (as English emissions dominate the UK total), i.e. there is a downward trend but much less steep than reported in the inventory estimates. The introduction of additional monitoring will provide significantly more information to the relative split between the different DAs.

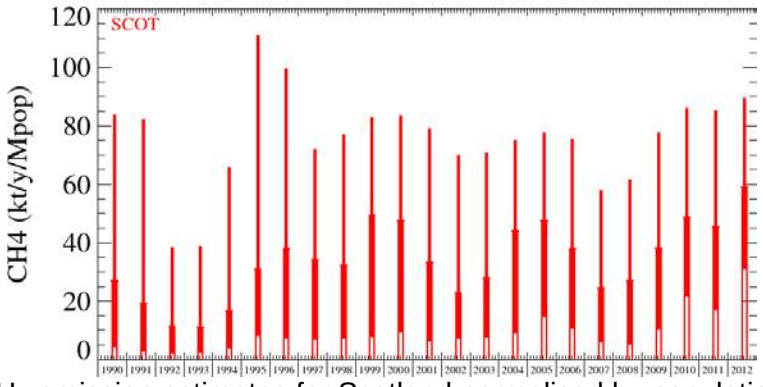

Figure 25: InTEM CH_4 emission estimates for Scotland normalised by population.

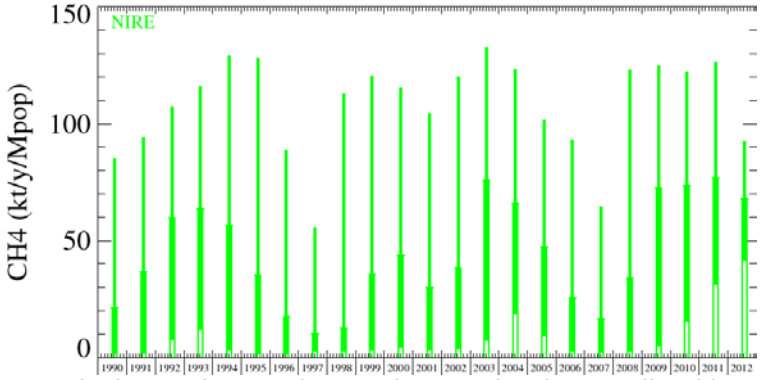

Figure 26: InTEM CH_4 emission estimates for Northern Ireland normalised by population.

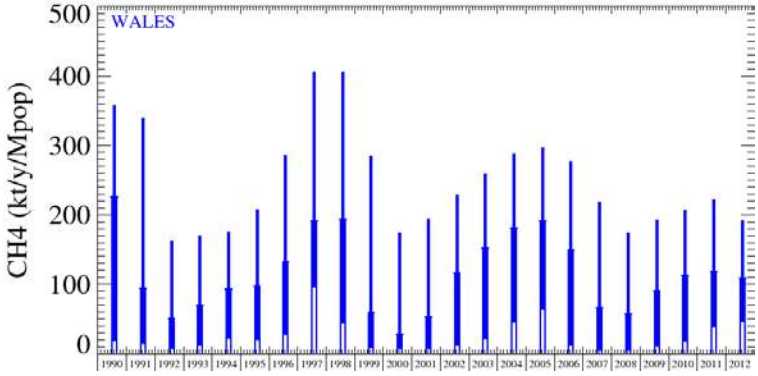

Figure 27: InTEM CH_4 emission estimates for Wales normalised by population.

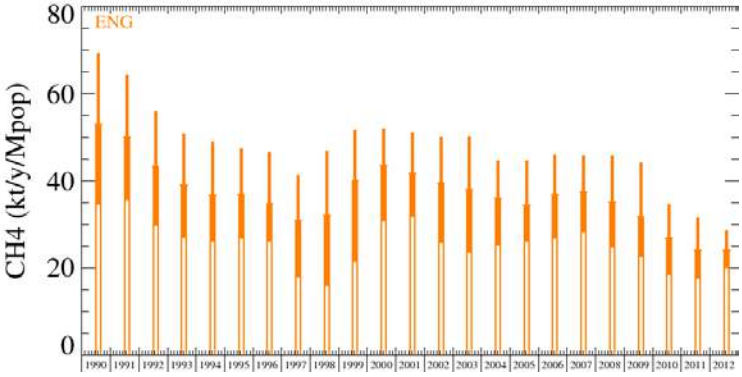

Figure 28: InTEM CH_4 emission estimates for England normalised by population.

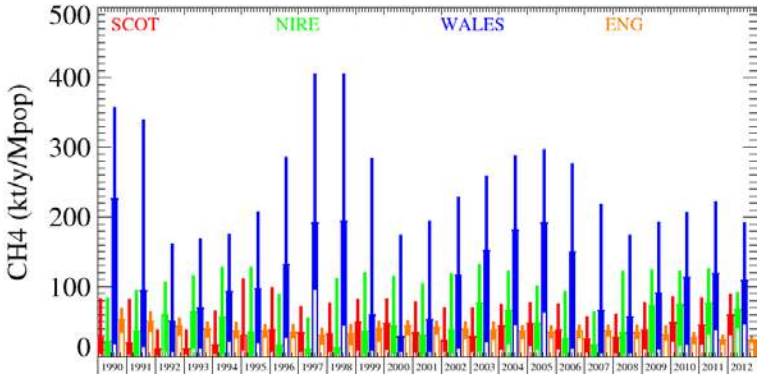

Figure 29: InTEM CH_4 devolved administration emission estimates normalised by the population of each DA – Composite picture for comparison.

Unit	Year	Scot	(5th-95th)	N.Ire	(5th-95th)	Wal	(5th-95th)	Eng	(5th-95th)
kt/y	1990	143	(22.- 443.)	38	(3.- 152.)	690	(57.-1095.)	2800	(1833.-3682.)
kt/y	1991	101	(14.- 436.)	65	(3.- 169.)	290	(42.-1039.)	2700	(1883.-3417.)
kt/y	1992	60	(11.- 204.)	107	(13.- 192.)	155	(21.- 497.)	2300	(1574.-2963.)
kt/y	1993	58	(12.- 207.)	114	(22.- 208.)	210	(35.- 521.)	2100	(1425.-2690.)
kt/y	1994	89	(21.- 348.)	101	(6.- 231.)	280	(67.- 539.)	1950	(1379.-2596.)
kt/y	1995	164	(43.- 589.)	63	(3.- 229.)	300	(60.- 637.)	1950	(1422.-2509.)
kt/y	1996	200	(38.- 527.)	31	(3.- 159.)	400	(83.- 877.)	1840	(1377.-2460.)
kt/y	1997	180	(36.- 381.)	18.2	(4.- 99.)	590	(292.-1243.)	1630	(942.-2189.)
kt/y	1998	171	(37.- 407.)	22	(5.- 202.)	590	(134.-1243.)	1700	(838.-2485.)
kt/y	1999	260	(42.- 439.)	64	(6.- 215.)	181	(24.- 872.)	2100	(1132.-2738.)
kt/y	2000	250	(48.- 442.)	78	(7.- 206.)	85	(22.- 535.)	2300	(1627.-2760.)
kt/y	2001	176	(34.- 419.)	54	(6.- 187.)	160	(24.- 597.)	2200	(1681.-2713.)
kt/y	2002	121	(38.- 370.)	68	(7.- 215.)	360	(35.- 702.)	2100	(1362.-2654.)
kt/y	2003	148	(41.- 374.)	136	(13.- 238.)	470	(62.- 795.)	2000	(1251.-2662.)
kt/y	2004	230	(48.- 397.)	117	(34.- 221.)	550	(138.- 883.)	1910	(1335.-2371.)
kt/y	2005	250	(78.- 412.)	85	(16.- 182.)	590	(194.- 911.)	1820	(1383.-2368.)
kt/y	2006	200	(56.- 400.)	45	(4.- 167.)	460	(35.- 847.)	1960	(1417.-2438.)
kt/y	2007	129	(31.- 306.)	30	(4.- 116.)	200	(15.- 672.)	1990	(1491.-2430.)
kt/y	2008	142	(28.- 327.)	60	(4.- 220.)	177	(15.- 532.)	1860	(1310.-2425.)
kt/y	2009	200	(54.- 412.)	130	(9.- 224.)	280	(33.- 591.)	1680	(1192.-2344.)
kt/y	2010	260	(114.- 457.)	132	(27.- 219.)	350	(52.- 632.)	1420	(974.-1840.)
kt/y	2011	240	(90.- 451.)	137	(56.- 226.)	360	(120.- 681.)	1270	(924.-1667.)
kt/y	2012	310	(164.- 475.)	121	(74.- 165.)	330	(140.- 589.)	1270	(1061.-1515.)

Table 7: InTEM CH_4 devolved administration emission estimates with uncertainty range using MHD observations only (provisional analysis results).

4.6.2 N_2O Devolved Administration emissions

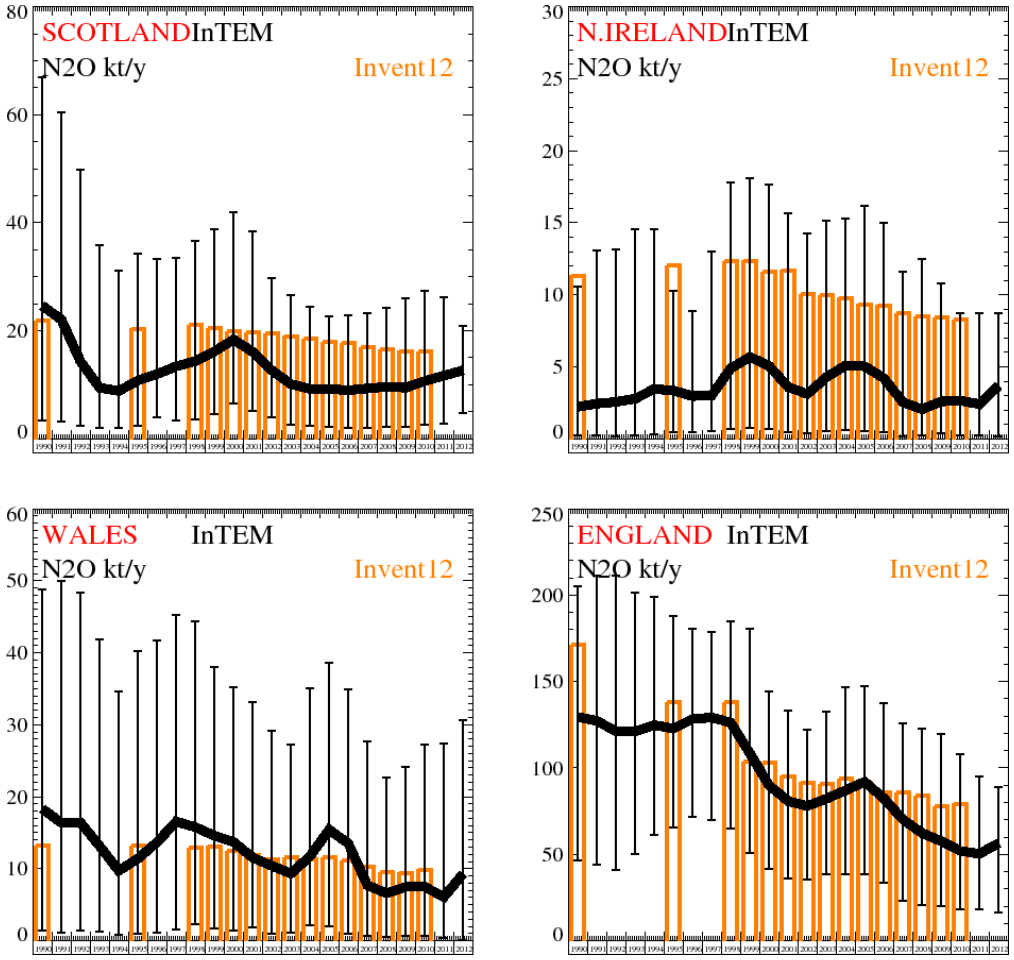

Figure 30: N_2O devolved administration emission estimates using MH data. Black line with uncertainty bars (InTEM) and orange bars (Inventory).

The discussion given in the CH_4 section preceding this are of equal relevance to N_2O and are not be repeated here.

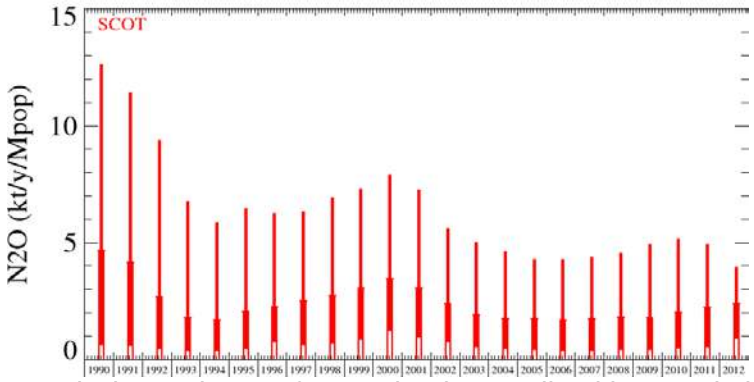

Figure 31: InTEM N_2O emission estimates for Scotland normalised by population.

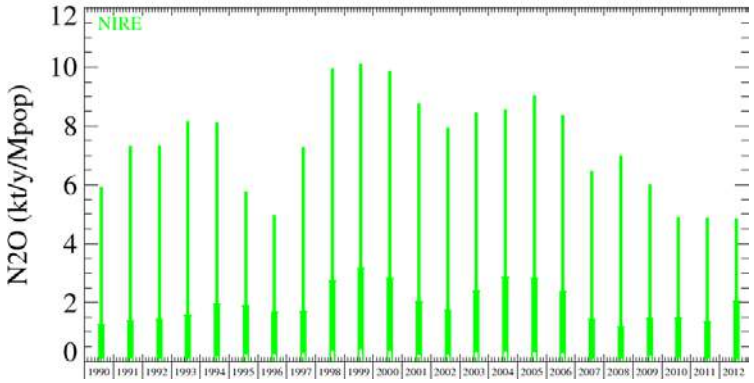

Figure 32: InTEM N_2O emission estimates for Northern Ireland normalised by population.

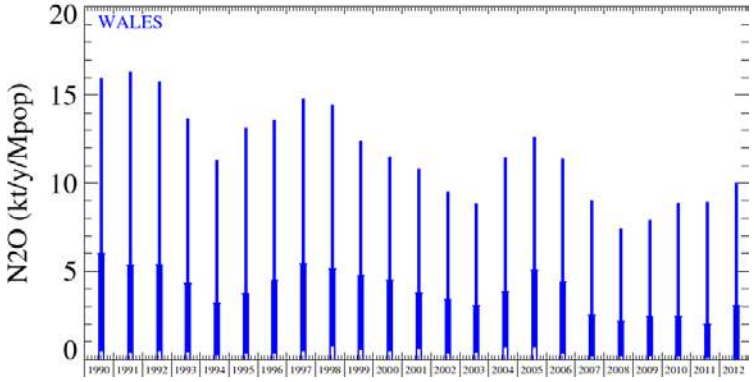

Figure 33: InTEM N_2O emission estimates for Wales normalised by population.

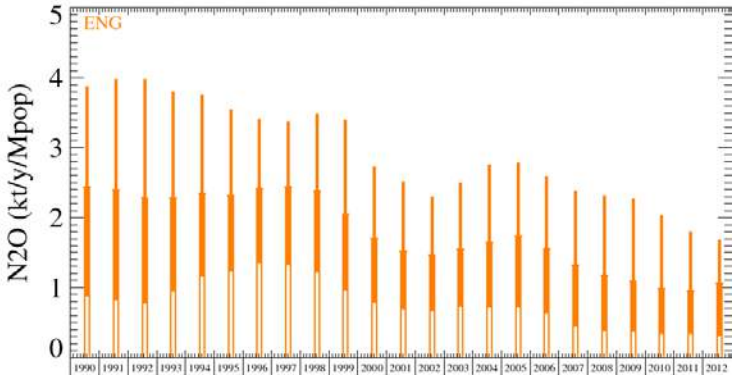

Figure 34: InTEM N_2O emission estimates for England normalised by population.

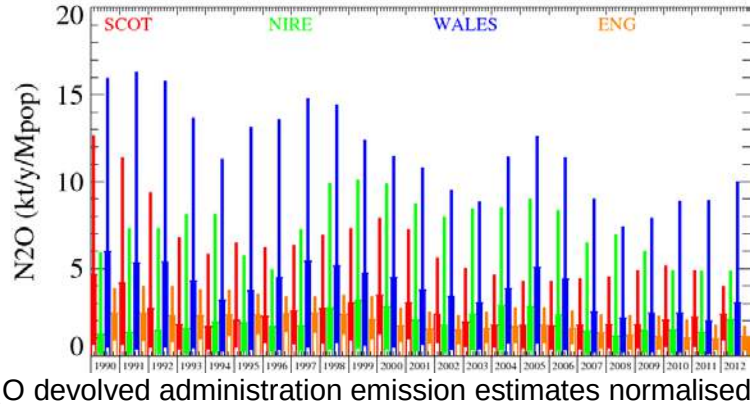

Figure 35: InTEM N_2O devolved administration emission estimates normalised by the population of each DA – Composite picture for comparison.

Unit	Year	Scot	(5th-95th)	N.Ire	(5th-95th)	Wales	(5th-95th)	Eng	(5th-95th)
kt/y	1990	25	(3.3- 67.)	2.2	(0.23- 11.)	18.3	(1.5- 49.)	130	(46.- 205.)
kt/y	1991	22	(3.1- 60.)	2.4	(0.22- 13.)	16.4	(1.2- 50.)	127	(44.- 211.)
kt/y	1992	14.3	(2.4- 50.)	2.6	(0.18- 13.)	16.4	(1.4- 48.)	121	(41.- 211.)
kt/y	1993	9.4	(2.1- 36.)	2.8	(0.21- 15.)	13.2	(1.3- 42.)	121	(50.- 202.)
kt/y	1994	8.9	(2.1- 31.)	3.5	(0.33- 15.)	9.7	(0.8- 35.)	125	(61.- 199.)
kt/y	1995	10.8	(2.5- 34.)	3.4	(0.44- 10.)	11.4	(1.0- 40.)	123	(66.- 188.)
kt/y	1996	12	(3.9- 33.)	3	(0.47- 9.)	13.7	(1.1- 42.)	128	(72.- 181.)
kt/y	1997	13.4	(3.3- 34.)	3	(0.51- 13.)	16.6	(1.5- 45.)	129	(70.- 179.)
kt/y	1998	14.4	(3.6- 37.)	4.9	(0.67- 18.)	15.8	(2.3- 44.)	126	(65.- 185.)
kt/y	1999	16.2	(4.5- 39.)	5.7	(0.74- 18.)	14.6	(1.7- 38.)	108	(51.- 180.)
kt/y	2000	18.4	(6.4- 42.)	5.1	(0.66- 18.)	13.7	(1.5- 35.)	90	(42.- 145.)
kt/y	2001	16.1	(5.1- 38.)	3.6	(0.42- 16.)	11.6	(1.9- 33.)	81	(36.- 133.)
kt/y	2002	12.7	(3.9- 30.)	3.1	(0.39- 14.)	10.4	(1.0- 29.)	78	(35.- 122.)
kt/y	2003	10.1	(2.7- 27.)	4.3	(0.56- 15.)	9.3	(1.1- 27.)	82	(39.- 133.)
kt/y	2004	9.2	(2.4- 24.)	5.1	(0.60- 15.)	11.8	(2.1- 35.)	87	(38.- 146.)
kt/y	2005	9.2	(2.2- 23.)	5	(0.55- 16.)	15.4	(2.1- 39.)	92	(38.- 147.)
kt/y	2006	9	(2.0- 23.)	4.2	(0.49- 15.)	13.5	(1.0- 35.)	82	(34.- 138.)
kt/y	2007	9.3	(2.0- 23.)	2.5	(0.17- 12.)	7.7	(0.7- 28.)	70	(23.- 126.)
kt/y	2008	9.6	(2.2- 24.)	2.1	(0.22- 12.)	6.6	(0.6- 23.)	62	(20.- 123.)
kt/y	2009	9.5	(2.3- 26.)	2.6	(0.36- 11.)	7.5	(0.6- 24.)	58	(20.- 120.)
kt/y	2010	10.7	(2.7- 27.)	2.6	(0.24- 9.)	7.5	(0.6- 27.)	52	(18.- 108.)
kt/y	2011	11.7	(2.7- 26.)	2.4	(0.22- 9.)	6.1	(0.3- 27.)	50	(18.- 95.)
kt/y	2012	12.7	(4.7- 21.)	3.7	(0.13- 9.)	9.3	(0.1- 31.)	56	(16.- 89.)

Table 8: InTEM N_2O devolved administration emission estimates with uncertainty range using MHD observations only (provisional analysis results).

5 Results and analysis of gases reported to the UNFCCC

5.1 Introduction

This section discusses the atmospheric trends and regional emissions of the gases that are measured at Mace Head and that are reported to the UNFCCC (United Nations Framework Convention on Climate Change). Table 9 describes the principle uses of each of the gases, their radiative efficiency, atmospheric lifetime and global warming potential in a 100-year framework (GWP_{100}).

Gas	Chemical Formula	Main Use	Radiative Efficiency (W $m^{-2}ppb^{-1}$)	Atmos. lifetime (years)	GWP_{100}
HFC-125	CHF_2CF_3	Refrigeration blend, fire suppression	0.23	28.2	3,420
HFC-134a	CH_2FCF_3	Mobile air conditiioner	0.16	13.4	1,370
HFC-143a	CH_3CF_3	Refrigeration blend	0.13	47.1	4,470
HFC-152a	CH_3CHF_2	Aerosol propellant, foam-blowing agent	0.09	1.5	133
HFC-23	CHF_3	Bi-product of manufacture of HCFC-22	0.19	222	14,200
HFC-32	CH_2F_2	Refrigeration blend	0.11	5.2	716
HFC-227ea	CF_3CHFCF_3	Fire suppression, inhalers, foam blowing	0.26	38.9	3,580
PFC-14	CF_4	Bi-product alum. production, electronics	0.08	>50,000	5,820
PFC-116	C_2F_6	Electronics, bi-product alum. production	0.26	>10,000	12,010
PFC-218	C_3F_8	Electronics, bi-product alum. production	0.26	2,600	8,690
PFC-318	C_4F_8	Semiconductor and electronics industries	0.32	3,200	10,300
SF_6	SF_6	Circuit breaker in high voltage switchgear	0.52	3,200	22,800
CH_4	CH_4	Landfill, farming, energy, wetlands	0.00037	12	25
CO_2	CO_2	Combustion	0.0000138	indefinite	1
N_2O	N_2O	Nylon manufacture, farming	0.00303	114	298

Table 9: The principle use, radiative efficiency, atmospheric lifetime and 100-year global warming potential of the gases measured at Mace Head and that are reported to the UNFCCC.

In this chapter InTEM results are presented for each of the gases. Apart from for SF_6, CH_4 and N_2O, only MHD observations have been used in all of the analyses. The limited availability (less than 1 year) of data from Tacolneston, the only other station that has a Medusa system and therefore measuring the full suite of HFCs, HCFCs and PFCs etc, only became operational in July 2012. For the 2014 report more than 18 months worth of data will be available and will be extensively analysed and presented. For SF_6, CH_4 and N_2O preliminary InTEM estimates for 2012 using Mace Head, Ridge Hill and Tacolneston observations are presented, Sections 5.13.1, 4.14.1 and 5.16.1 respectively.

For the majority of the gases, those considered to be significantly anthropogenic in origin, the InTEM emission estimates are also presented after a further post-processing step. This additional step redistributes the emissions within each solved-for region according to the population distribution within each region. The total emissions per region and country are unaffected by this post-processing step. It is considered that these population-weighted distributions give a good

indication of the actual spread of the emissions at horizontal resolutions that cannot be achieved through the use of just MHD observations. The statistical match between the observations and the modelled time-series at MHD are negligibly affected by this post-processing step.

5.2 HFC-125

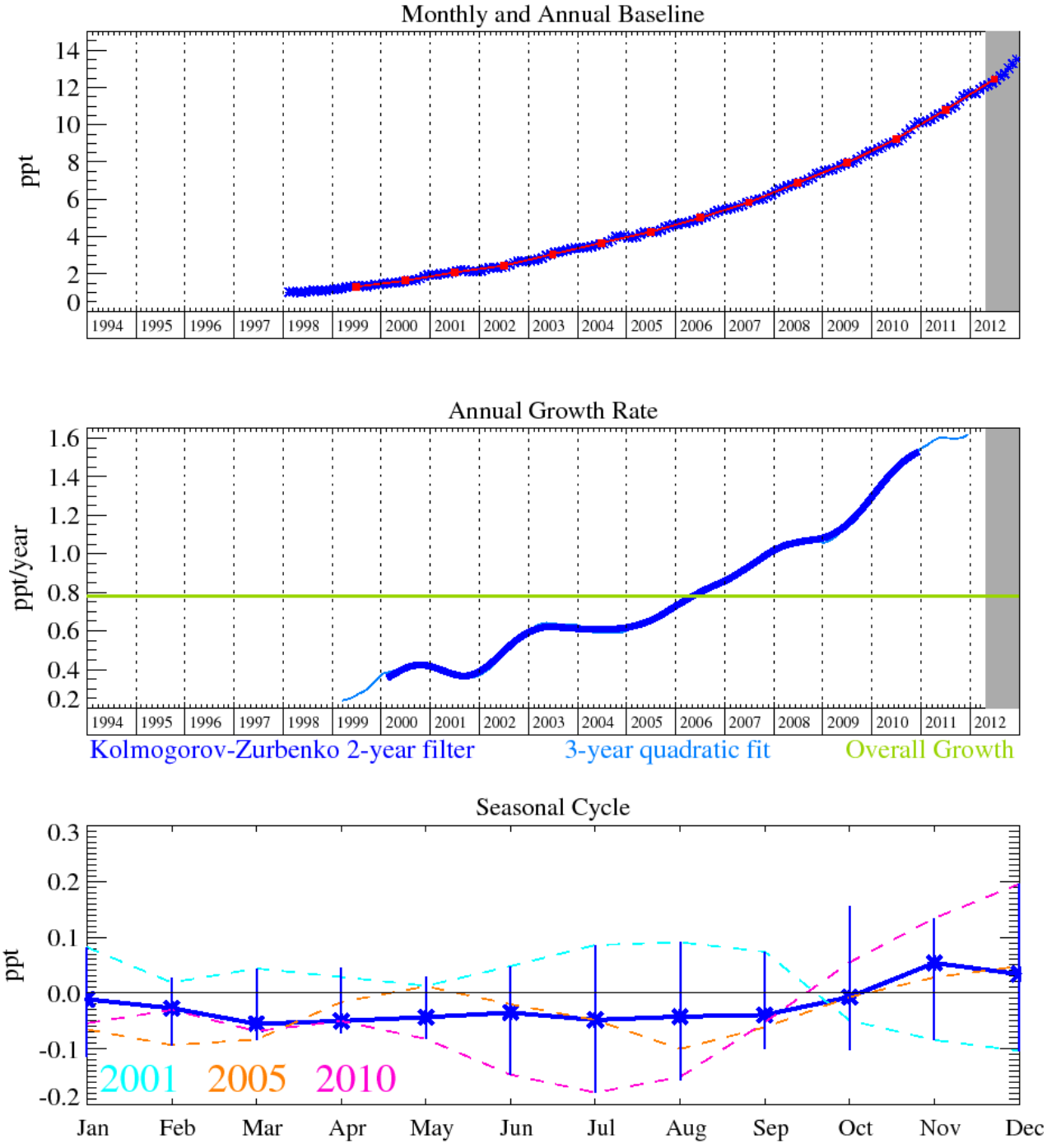

Figure 36: HFC-125 (CHF_2CF_3): Monthly (blue) and annual (red) baseline concentrations (top plot). Annual (blue) and overall average growth rate (green) (middle plot). Seasonal cycle (de-trended) with year-to-year variability (lower plot). Grey area covers un-ratified and therefore provisional data.

Hydrofluorocarbos (HFCs) are replacement chemicals for the long-lived ozone depleting substances in various applications such as refrigeration, fire extinguishers, propellants, and foam blowing. The most recent measurements of the HFCs at Mace Head indicate that the mixing ratios of all HFC compounds continue to grow, as is consistent with sustained emissions of these replacement compounds into the atmosphere. The baseline monthly mean, mixing ratios for all the

HFCs are shown in Figures 36-54 and the growth rates of these compounds, calculated from the data, are presented in Table 1c.

HFC-125 (CHF_2CF_3): This compound is used in refrigeration blends and for fire suppression. It has a GWP_{100} of 3420 and an atmospheric lifetime of 28.2 years. [O'Doherty *et al.*, 2009]. This compound is growing rapidly in the atmosphere reaching a level of 13.5 ppt in Dec. 2012 with a current growth rate of 1.6 ppt/yr.

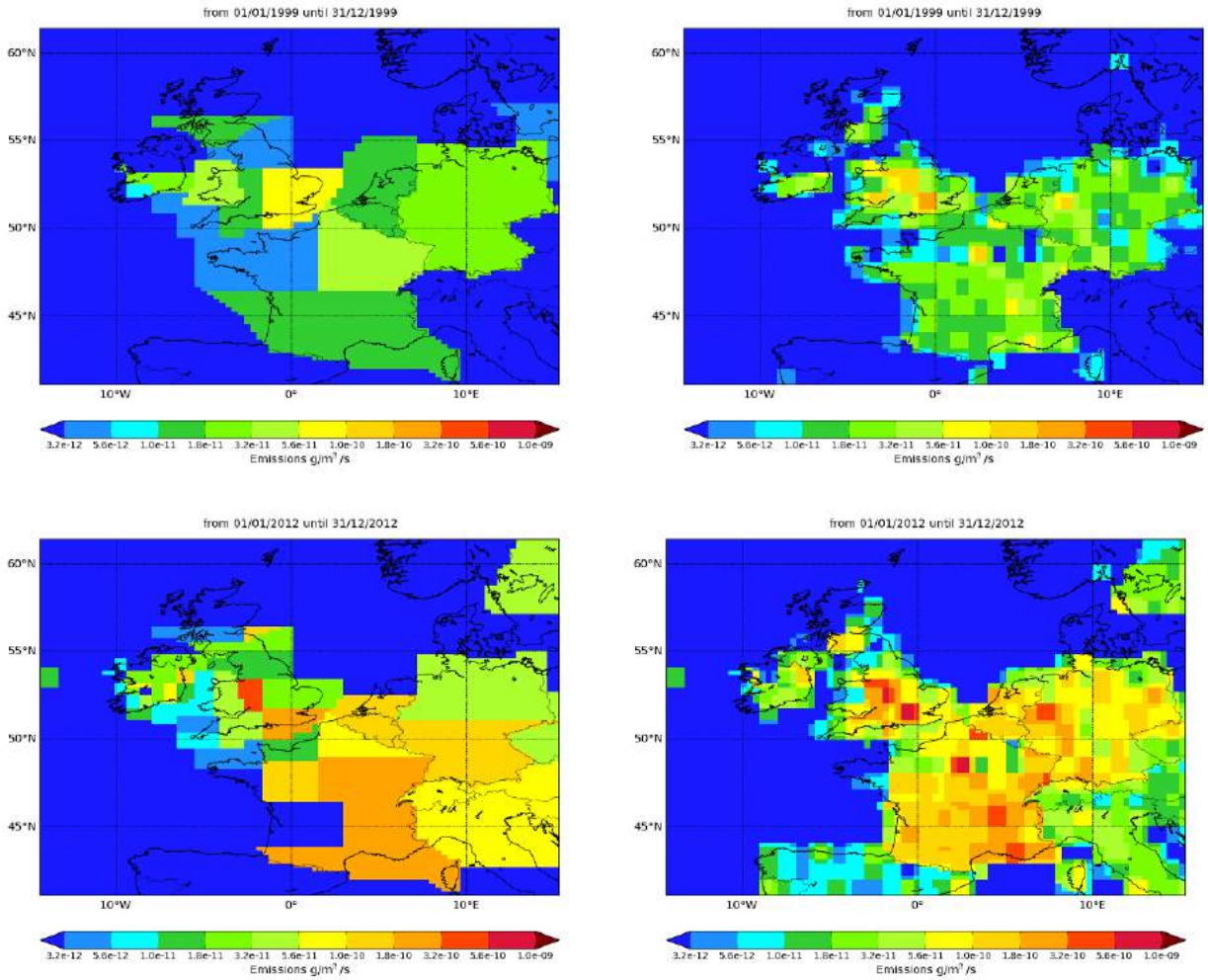

Figure 37: NAME-inversion emission estimates for 1999 (upper) and 2012 (lower). On the right hand side the emissions per grid box have been re-distributed based on population.

Relative to the magnitude of the baseline (growing rapidly but still currently less than 12 ppt) the pollution events are very significant. Therefore InTEM has plenty of clear information on which to base its emission estimates, consequently the statistical match between the model and measurements have remained good throughout, and the InTEM uncertainty is relatively small. The agreement between the inventory and InTEM for the UK is excellent up until 2009 – 2010 with a strong overlap of the uncertainty bars from both methods. It is interesting to note that with InTEM, the UK estimates started to decline in 2010 in contrast to the inventory that continues to grow strongly. However, it is also noticeable that the NWEU InTEM estimates have continued to grow and at a stronger rate than the inventory. It will be interesting to investigate the impact of including the Tacolneston data, especially on the split between UK emissions and those on the continent.

Year	RMSE (ppt)	Correlation	Max obs. above baseline (ppt)	% obs. above baseline noise	Mean obs. above baseline (ppt)
1999	0.27	0.76	3.8	38	0.23
2012	0.45	0.73	6.5	46	0.63

Table 10: Comparison between modelled and observed time-series

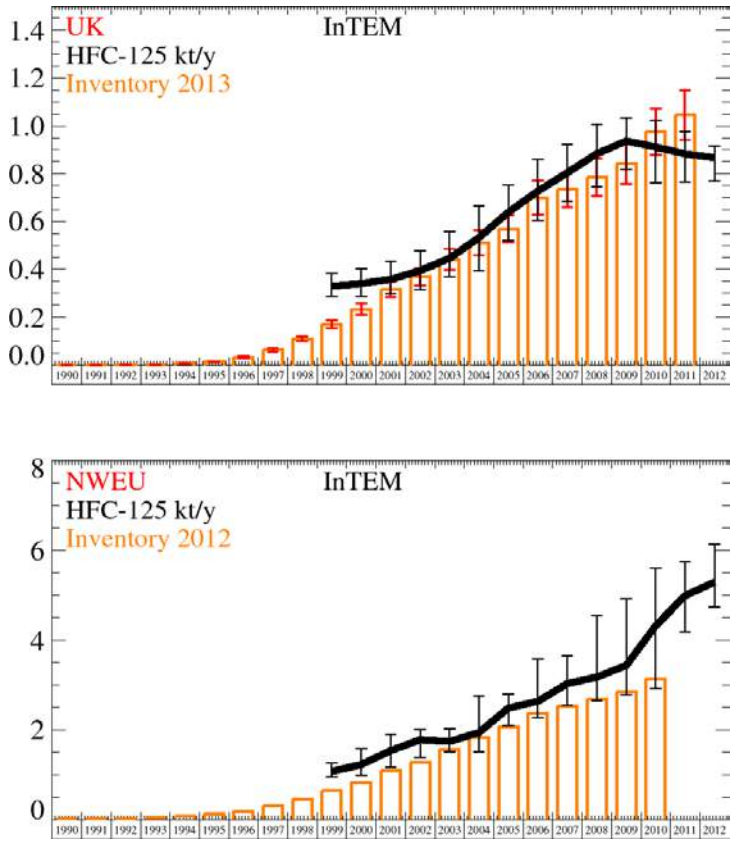

Figure 38: Emission (kt/y) estimates for UK and NWEU. The uncertainty bars represent the 5th and 95th percentiles.

Unit	Year	UK	(5th-95th)	NWEU	(5th-95th)
t/y	1999	330	(284.- 383.)	1070	(947.-1258.)
t/y	2000	340	(285.- 403.)	1220	(982.-1578.)
t/y	2001	360	(300.- 434.)	1530	(1158.-1907.)
t/y	2002	390	(318.- 476.)	1780	(1377.-2007.)
t/y	2003	450	(369.- 557.)	1740	(1496.-2016.)
t/y	2004	530	(392.- 667.)	1940	(1513.-2759.)
t/y	2005	640	(522.- 752.)	2500	(2097.-2792.)
t/y	2006	730	(604.- 861.)	2600	(2269.-3579.)
t/y	2007	800	(686.- 923.)	3000	(2547.-3654.)
t/y	2008	880	(745.-1007.)	3200	(2654.-4554.)
t/y	2009	940	(820.-1034.)	3400	(2770.-4918.)
t/y	2010	910	(762.-1025.)	4300	(2911.-5608.)
t/y	2011	880	(766.- 977.)	5000	(4192.-5752.)
t/y	2012	870	(769.- 916.)	5300	(4739.-6137.)

Table 11: Emission (t/y) estimates for UK and NWEU with uncertainty (5th – 95th %ile).

5.3 HFC-134a

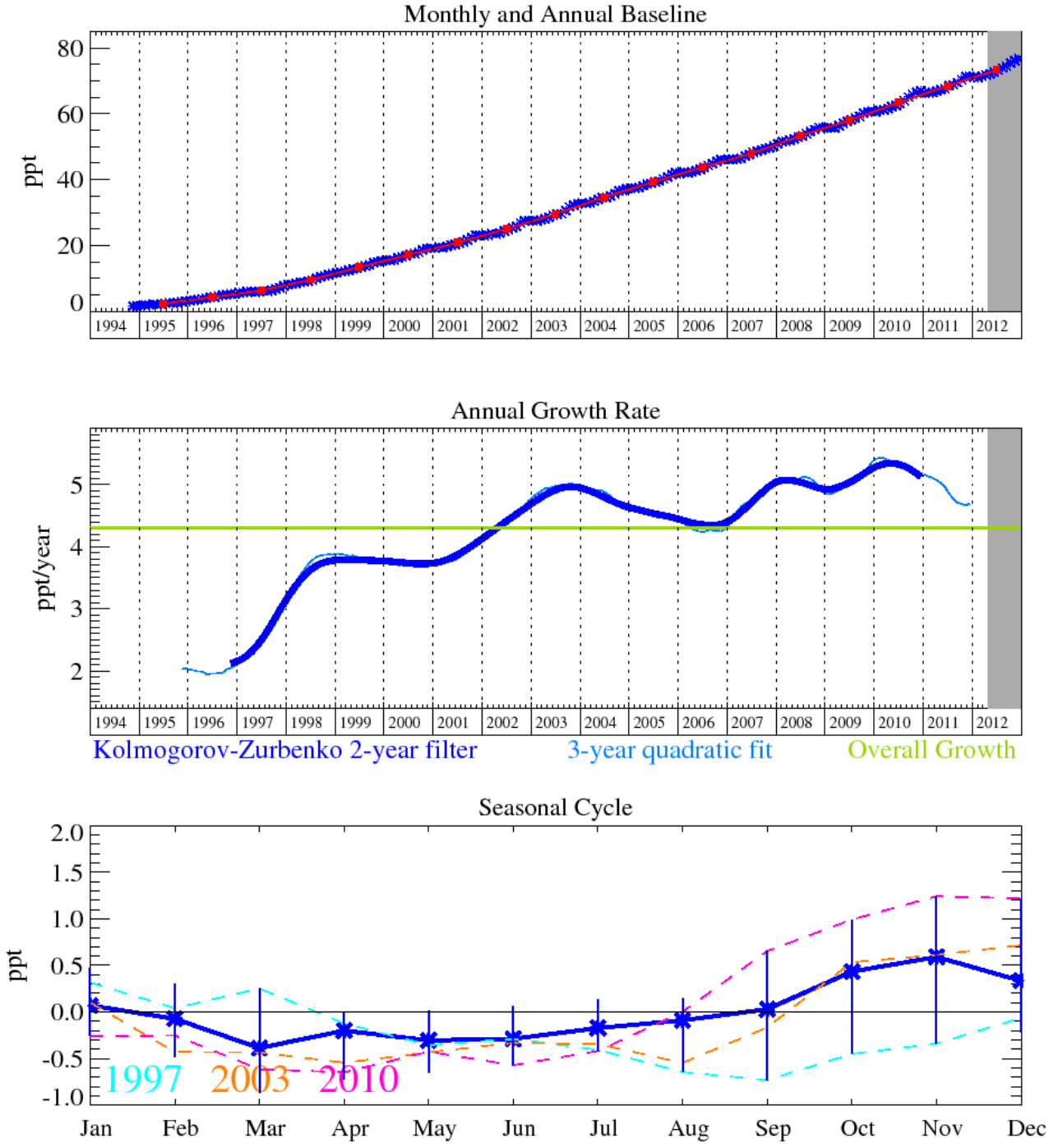

Figure 39: HFC-134a (CH_2FCF_3): Monthly (blue) and annual (red) baseline concentrations(top plot). Annual (blue) and overall average growth rate (green) (middle plot). Seasonal cycle (de-trended) with year-to-year variability (lower plot). Grey area covers un-ratified and therefore provisional data.

HFC-134a (CH_2FCF_3): Globally HFC-134a is the most abundant HFC present in the atmosphere and is used predominantly in refrigeration and mobile air conditioning (MAC). Due to its long lifetime, 13.4 years, and relatively high GWP_{100} 1370 [Forster *et al.*, 2007], the use of HFC-134a (and any other HFCs with a GWP_{100} >150) is being phased out in Europe between 2011 and 2017. It is proposed that a very gradual phase-out of the use of HFC-134a in cars will also take place outside Europe because of the global nature of the car industry. However in developing countries the potential for growth of HFC-134a is still large [Velders *et al.*, 2009]. As of December 2012 the

atmospheric mole fraction of HFC-134a was 76.7 ppt and recent growth is estimated to be 4.9 ppt/yr.

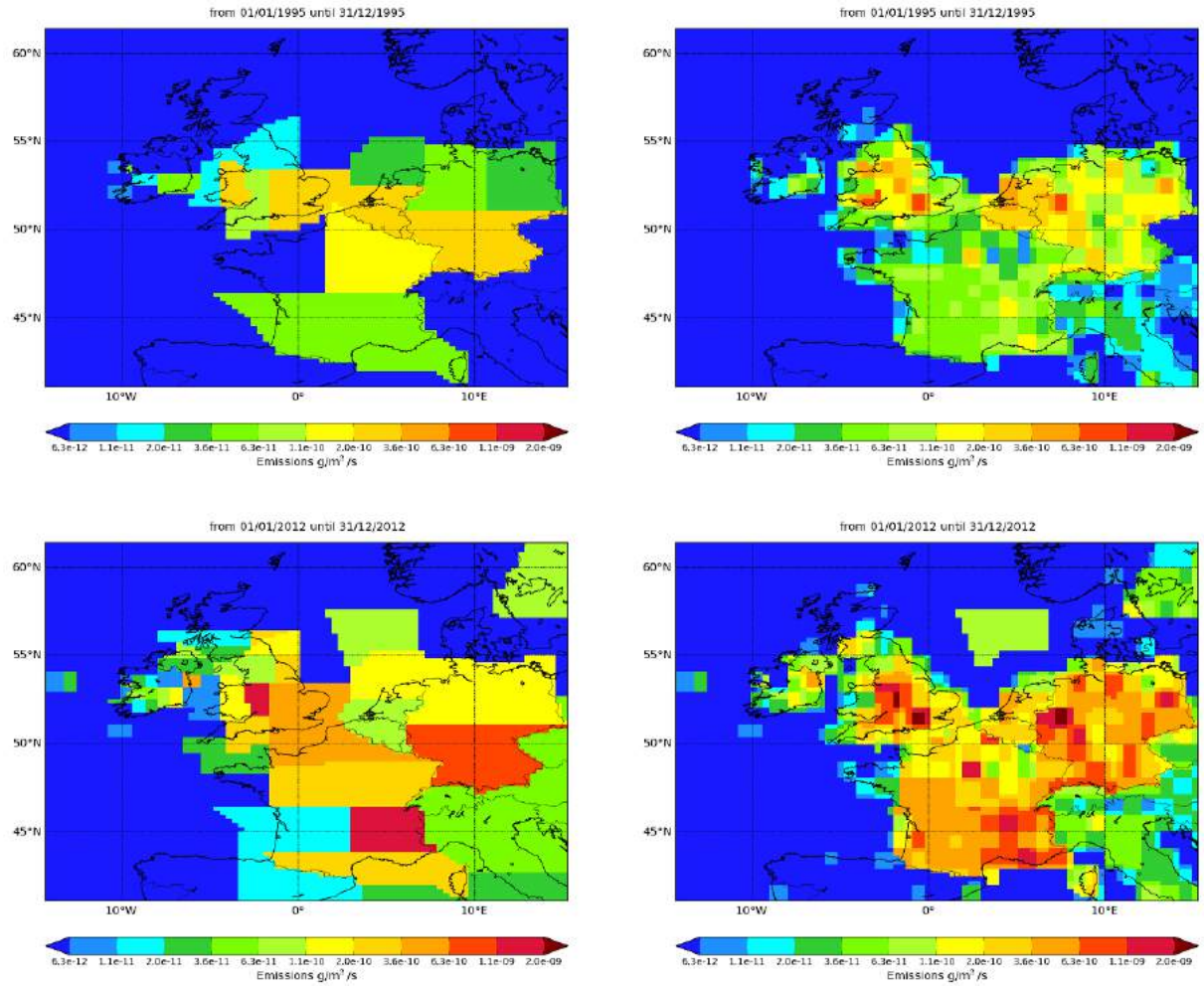

Figure 40: NAME-inversion emission estimates for 1995 (upper) and 2012 (lower). On the right hand side the emissions per grid box have been re-distributed based on population.

The UK inventory and InTEM estimates increased between the mid-1990s until 2009. Since then the UK inventory has very slightly decreased whereas the InTEM estimates have seen a more rapid decline. The InTEM estimates for the UK are consistently around two thirds of the inventory estimates. A different picture emerges in NWEU as a whole, both the inventory and InTEM show increasing emissions in recent years, especially InTEM. The statistical fit between the measurements and the modelling is relatively good throughout the time-series. A significant proportion of the HFC-134a emitted is estimated to come from in-use vehicles (it is used in mobile air conditioning units). Inspection of the inventory shows that different countries across the EU use surprisingly different values for the leakage rates from in-use vehicles. This discrepancy requires further investigation.

Year	RMSE (ppt)	Correlation	Max obs. above baseline (ppt)	% obs. above baseline noise	Mean obs. above baseline (ppt)
1995	0.72	0.59	11.3	40	0.43
2012	1.94	0.76	34.8	43	2.39

Table 12: Comparison between modelled and observed time-series

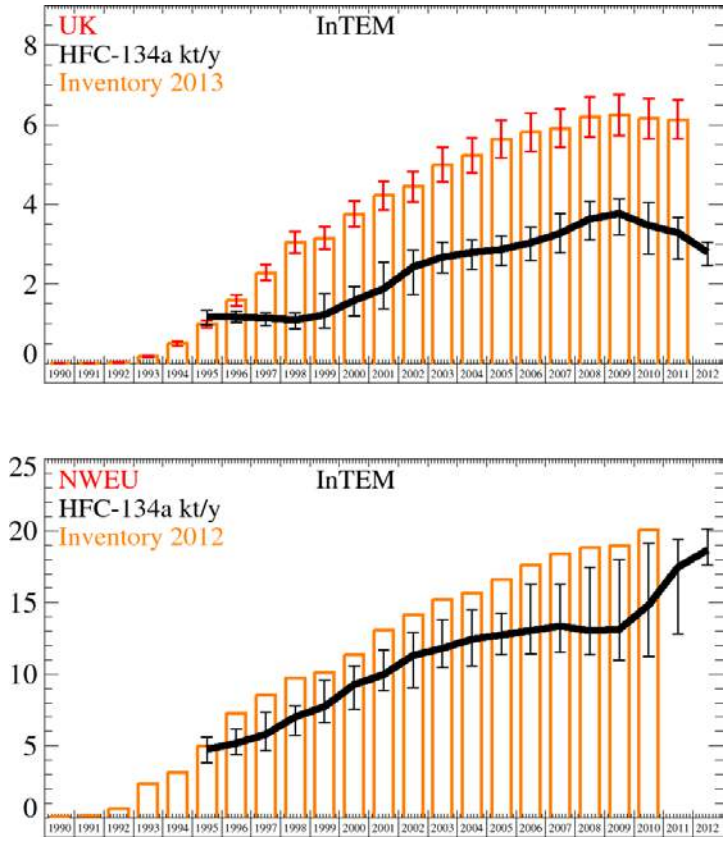

Figure 41: Emission (kt/y) estimates for UK and NWEU. The uncertainty bars represent the 5th and 95th percentiles.

Unit	Year	UK	(5th-95th)	NWEU	(5th-95th)
kt/y	1995	1.19	(1.0- 1.3)	4.8	(4.- 6.)
kt/y	1996	1.17	(1.0- 1.3)	5.2	(4.- 6.)
kt/y	1997	1.14	(1.0- 1.3)	5.8	(5.- 7.)
kt/y	1998	1.09	(0.9- 1.3)	7	(6.- 8.)
kt/y	1999	1.23	(0.9- 1.8)	7.7	(7.- 10.)
kt/y	2000	1.59	(1.2- 1.9)	9.3	(8.- 11.)
kt/y	2001	1.88	(1.4- 2.5)	10	(9.- 12.)
kt/y	2002	2.4	(1.7- 2.8)	11.3	(9.- 13.)
kt/y	2003	2.7	(2.3- 3.0)	11.8	(10.- 14.)
kt/y	2004	2.8	(2.4- 3.1)	12.4	(11.- 14.)
kt/y	2005	2.9	(2.5- 3.2)	12.7	(11.- 14.)
kt/y	2006	3	(2.6- 3.4)	13	(11.- 16.)
kt/y	2007	3.3	(2.8- 3.8)	13.4	(12.- 16.)
kt/y	2008	3.6	(3.1- 4.1)	13	(11.- 17.)
kt/y	2009	3.8	(3.2- 4.1)	13.1	(11.- 18.)
kt/y	2010	3.5	(2.8- 4.1)	14.8	(11.- 19.)
kt/y	2011	3.3	(2.6- 3.7)	17.5	(13.- 19.)
kt/y	2012	2.8	(2.5- 3.1)	18.7	(18.- 20.)

Table 13: Emission (kt/y) estimates for UK and NWEU with uncertainty (5th – 95th %ile).

5.4 HFC-143a

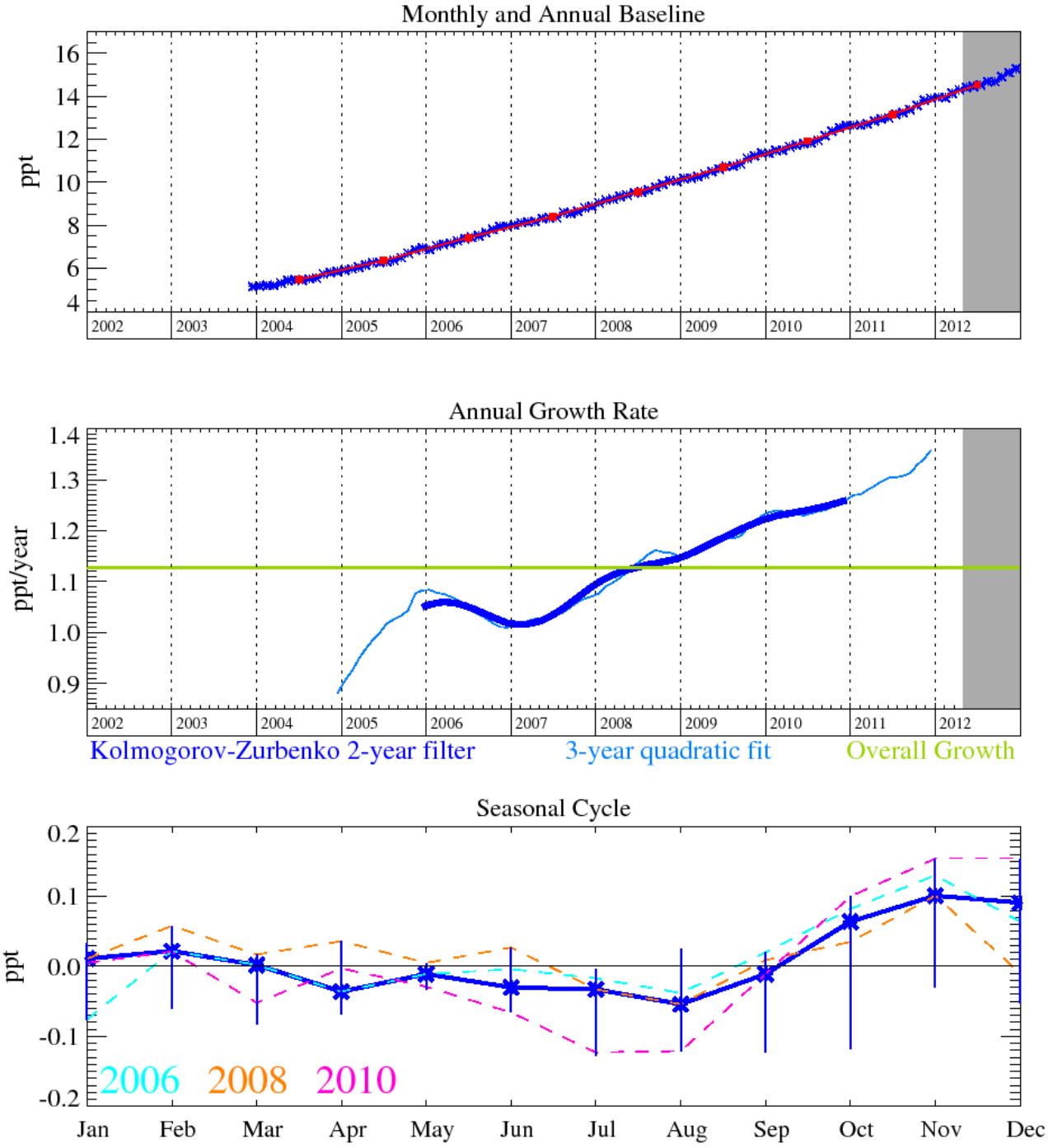

Figure 42: HFC-143a (CH_3CF_3): Monthly (blue) and annual (red) baseline concentrations (top plot). Annual (blue) and overall average growth rate (green) (middle plot). Seasonal cycle (de-trended) with year-to-year variability (lower plot). Grey area covers un-ratified and therefore provisional data.

HFC-143a is used mainly as a working fluid in refrigerant blends (R-404A and R-507A) for low and medium temperature commercial refrigeration systems. In December 2012 it reached levels of 15.3 ppt. These levels have increased dramatically from the low levels in 1997 with an increasing growth rate, currently estimated to be 1.3 ppt/yr. It has a relatively long atmospheric lifetime of 47.1 years and a significant radiative forcing value (third largest of all the HFCs) with a GWP_{100} of 4470.

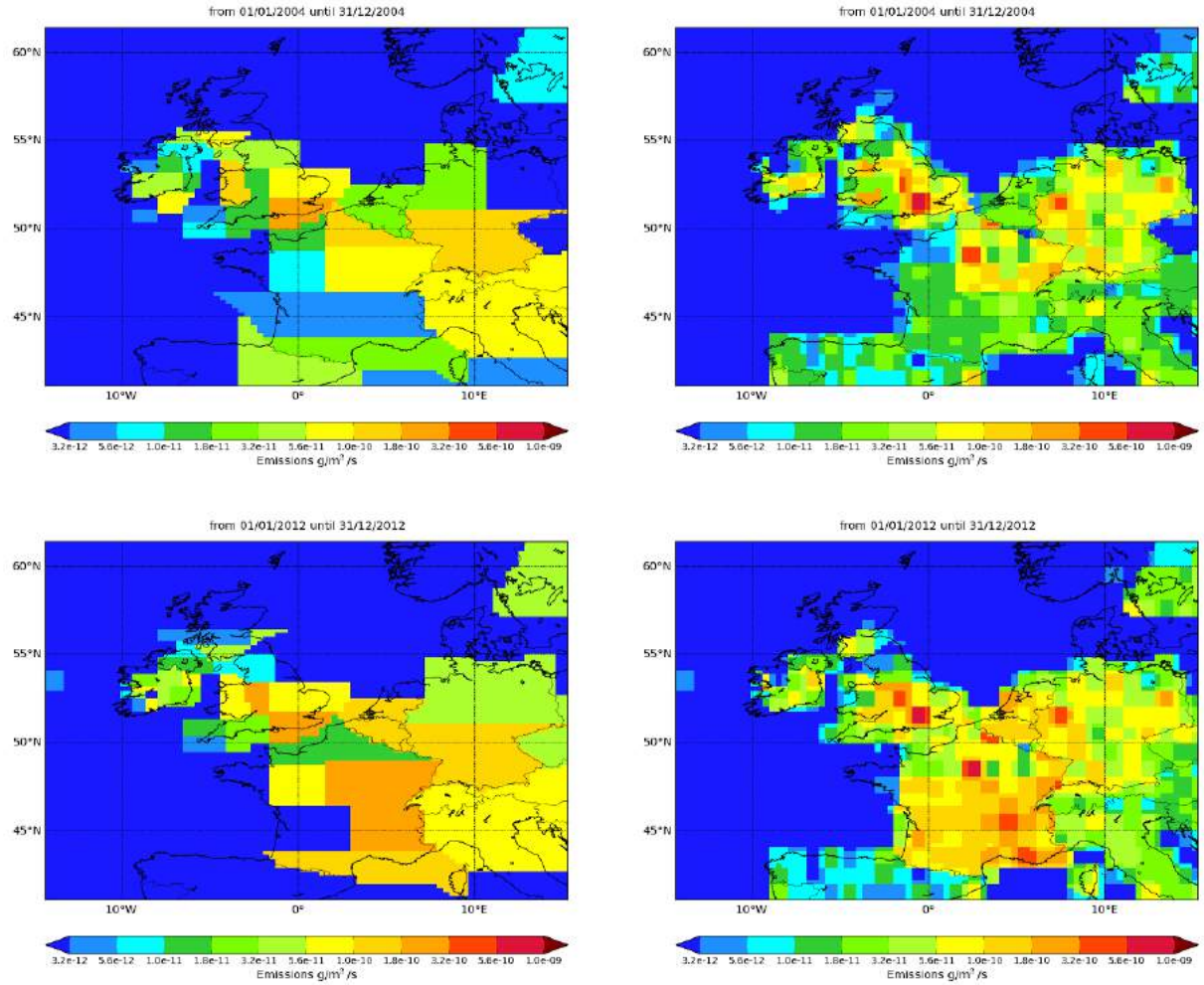

Figure 43: NAME-inversion emission estimates for 2004 (upper) and 2012 (lower). On the right hand side the emissions per grid box have been re-distributed based on population.

The InTEM emission estimates for the UK show a maximum was reached in 2008-09 after which they have started to decline. The inventory estimates an increase across the years. The table below shows that the maximum observation above baseline in 2004 was almost twice that seen in 2012, however on further inspection this is a misleading picture. The average perturbation above baseline in 2012 was 0.75 ppt compared to a smaller average in 2004 of 0.5 ppt, also the number of perturbations above the baseline noise in 2012 was greater (by 30%) than in 2004. The statistical match between the observations and model is good in both years.

Year	RMSE (ppt)	Correlation	Max obs. above baseline (ppt)	% obs. above baseline noise	Mean obs. above baseline (ppt)
2004	0.53	0.75	14.7	37	0.50
2012	0.52	0.82	7.9	44	0.75

Table 14: Comparison between modelled and observed time-series.

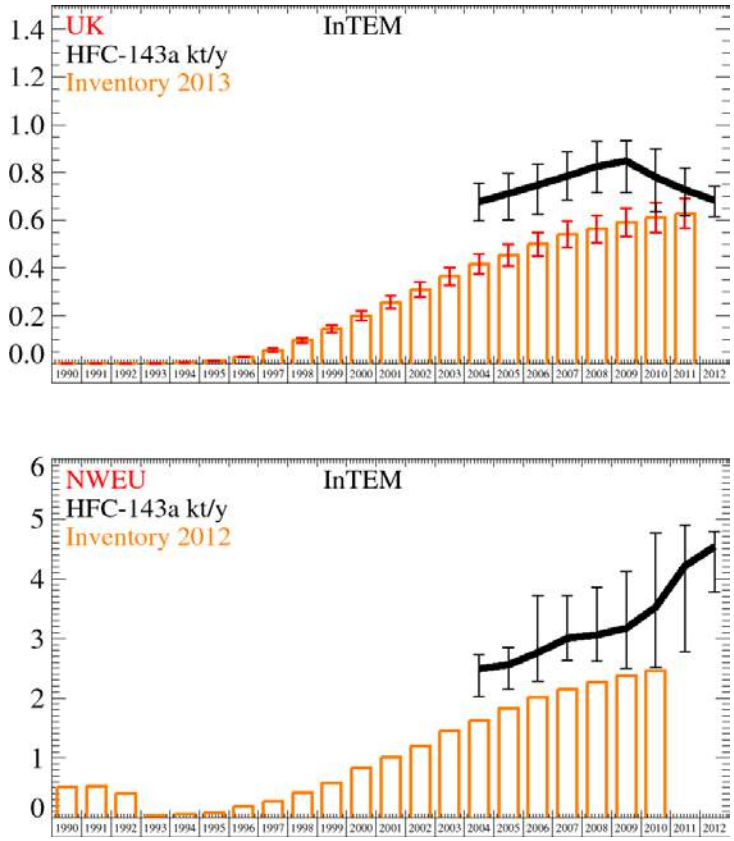

Figure 44: Emission (kt/y) estimates for UK and NWEU. The uncertainty bars represent the 5th and 95th percentiles.

Unit	Year	UK	(5th-95th)	NWEU	(5th-95th)
t/y	2004	680	(597.- 756.)	2500	(2021.-2732.)
t/y	2005	710	(602.- 797.)	2600	(2146.-2848.)
t/y	2006	750	(625.- 837.)	2800	(2285.-3724.)
t/y	2007	780	(685.- 886.)	3000	(2637.-3725.)
t/y	2008	830	(714.- 929.)	3100	(2621.-3854.)
t/y	2009	850	(716.- 933.)	3200	(2492.-4124.)
t/y	2010	780	(636.- 899.)	3500	(2516.-4761.)
t/y	2011	730	(619.- 821.)	4200	(2777.-4895.)
t/y	2012	680	(613.- 743.)	4500	(3778.-4798.)

Table 15: Emission (t/y) estimates for UK and NWEU with uncertainty (5th – 95th %ile).

5.5 HFC-152a

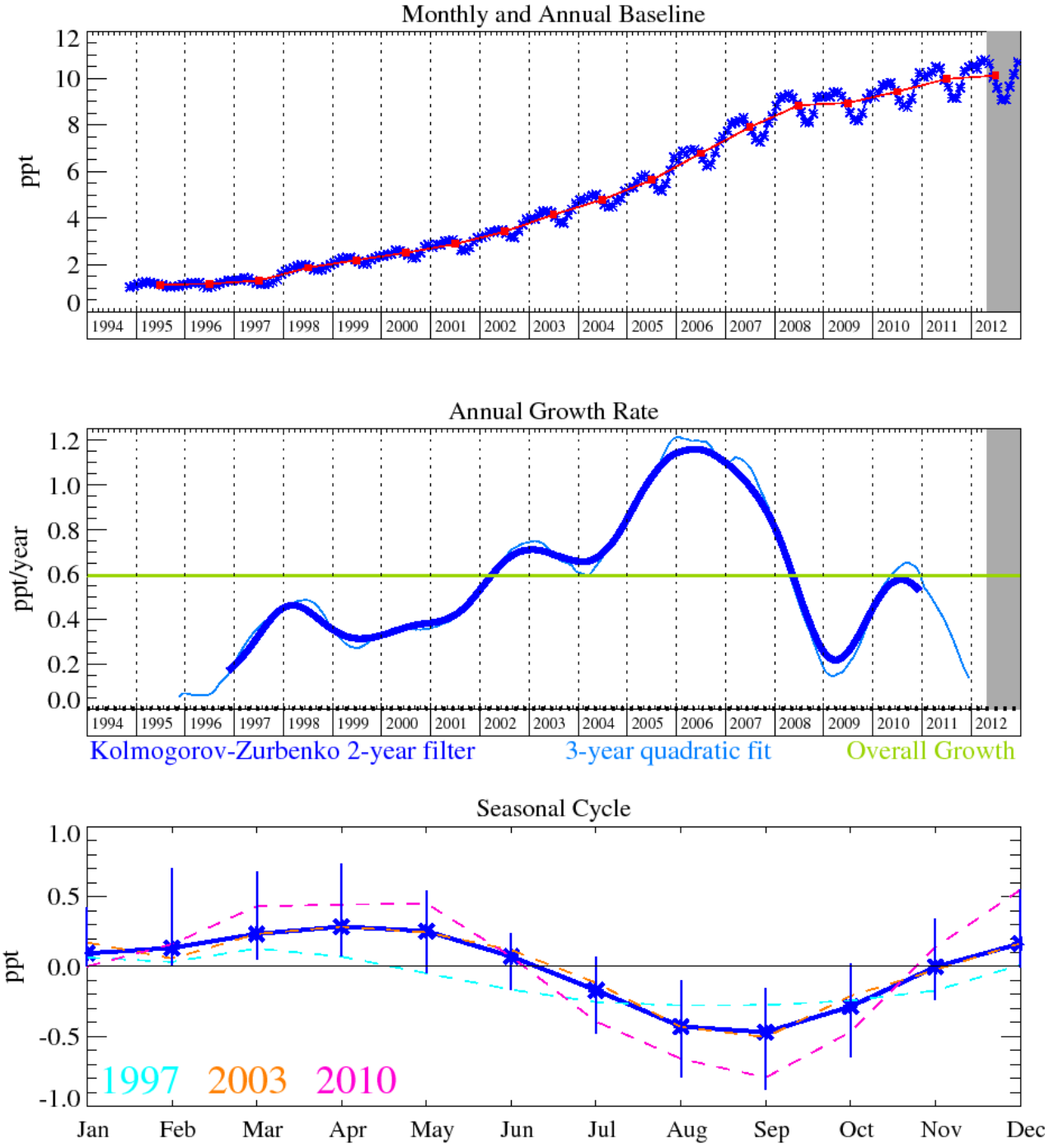

Figure 45: HFC-152a (CH_3CHF_2): Monthly (blue) and annual (red) baseline concentrations (top plot). Annual (blue) and overall average growth rate (green) (middle plot). Seasonal cycle (de-trended) with year-to-year variability (lower plot). Grey area covers un-ratified and therefore provisional data.

HFC-152a has a relatively short lifetime of 1.5 years due to its efficient removal by OH oxidation in the troposphere, consequently it has the smallest GWP_{100} at 133, of all of the major HFCs. It is used as a foam-blowing agent and aerosol propellant, and given its short lifetime has exhibited substantial growth in the atmosphere since measurement began in 1994, implying a substantial increase in emissions in these years. However, in the last few years the rate of growth has slowed somewhat to ~0.4 ppt/yr, reaching a mixing ratio in Dec 2012 of 10.7 ppt.

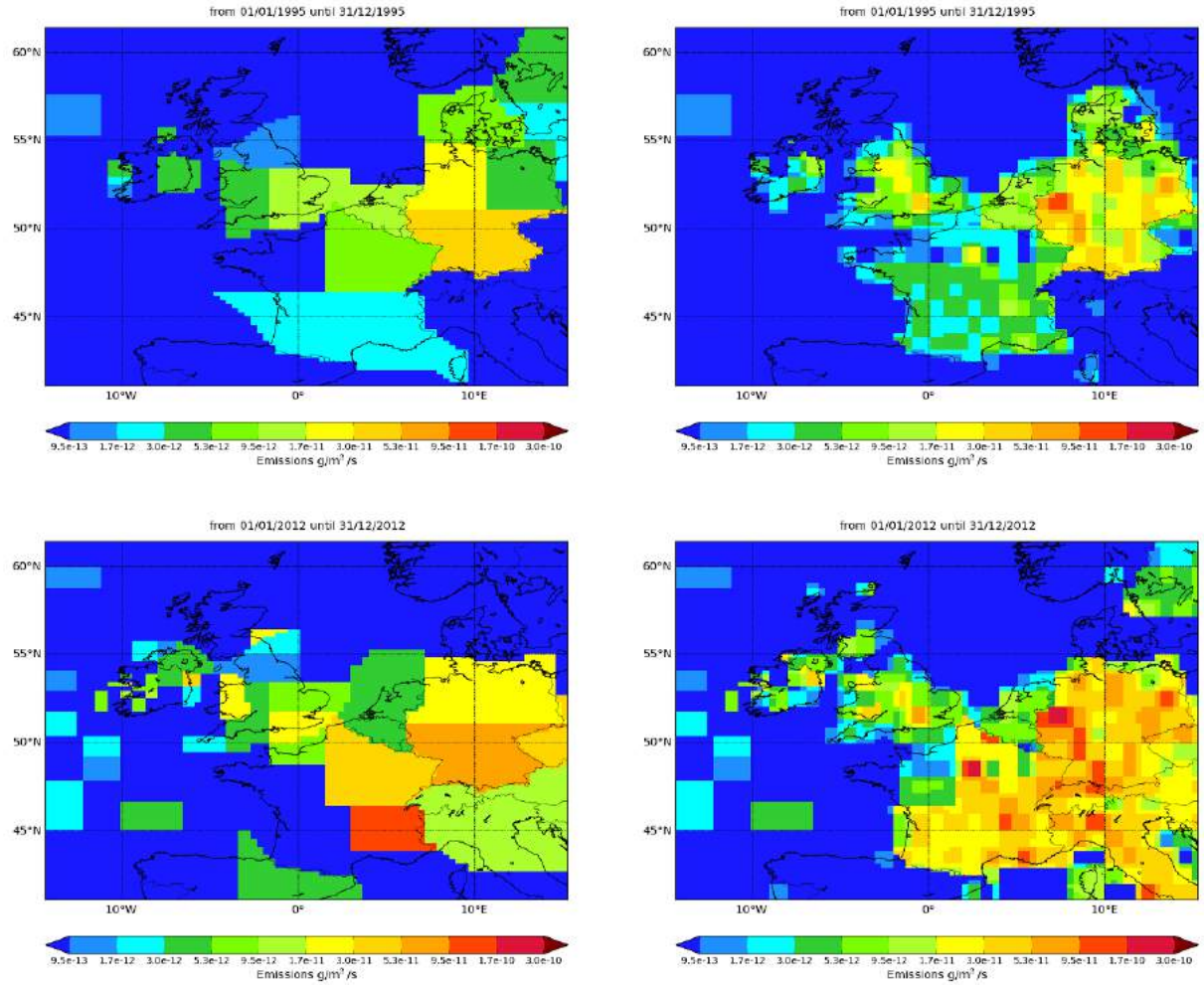

Figure 46: NAME-inversion emission estimates for 1995 (upper) and 2012 (lower). On the right hand side the emissions per grid box have been re-distributed based on population.

The NWEU emission estimates from both InTEM and the inventory match very well. The comparison for the UK is less well matched from 2002 onwards, when the inventory exhibited a substantial increase in emissions compared to InTEM. The shape of the annual emissions (the double peak, one in 2002 and the other in 2007) compares well, the InTEM estimates are lower than the inventory, although the uncertainty ranges do overlap in every year.

Year	RMSE (ppt)	Correlation	Max obs. above baseline (ppt)	% obs. above baseline noise	Mean obs. above baseline (ppt)
1995	0.12	0.64	1.3	44	0.12
2012	0.57	0.24	8.3	27	0.45

Table 16: Comparison between modelled and observed time-series.

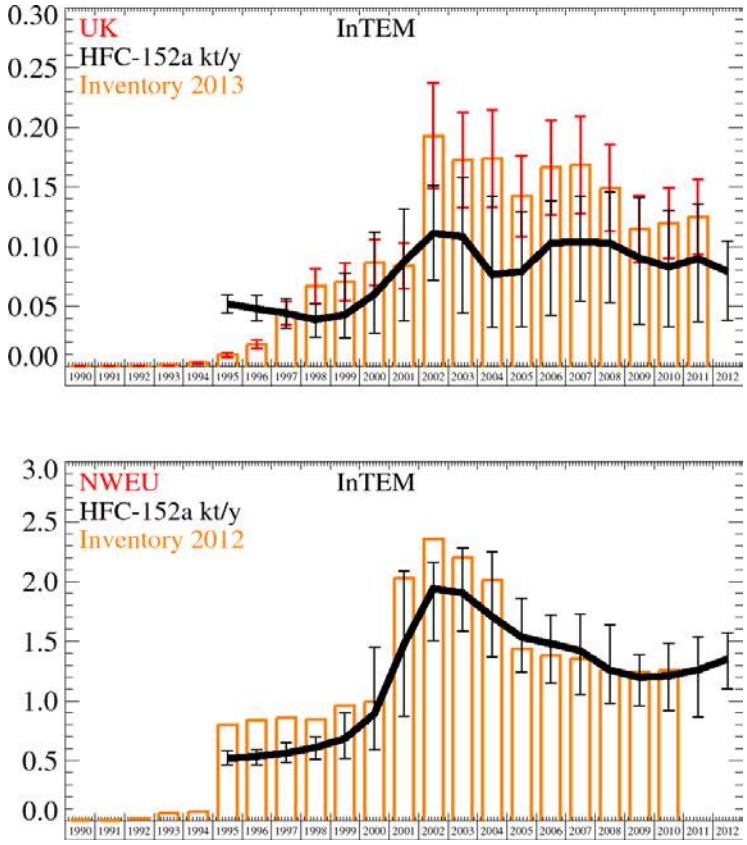

Figure 47: Emission (kt/y) estimates for UK and NWEU. The uncertainty bars represent the 5th and 95th percentiles.

Unit	Year	UK	(5th-95th)	NWEU	(5th-95th)
t/y	1995	52	(44.- 60.)	520	(467.- 582.)
t/y	1996	48	(38.- 59.)	540	(467.- 592.)
t/y	1997	44	(31.- 57.)	560	(483.- 649.)
t/y	1998	39	(25.- 51.)	610	(508.- 698.)
t/y	1999	43	(23.- 78.)	690	(519.- 902.)
t/y	2000	60	(28.- 112.)	890	(590.-1453.)
t/y	2001	87	(38.- 131.)	1470	(876.-2086.)
t/y	2002	111	(72.- 151.)	1940	(1505.-2163.)
t/y	2003	108	(44.- 158.)	1900	(1582.-2282.)
t/y	2004	77	(32.- 142.)	1710	(1368.-2246.)
t/y	2005	79	(33.- 129.)	1530	(1240.-1861.)
t/y	2006	103	(42.- 138.)	1480	(1150.-1721.)
t/y	2007	104	(55.- 142.)	1420	(1054.-1722.)
t/y	2008	103	(53.- 146.)	1260	(982.-1636.)
t/y	2009	91	(35.- 141.)	1200	(961.-1387.)
t/y	2010	83	(33.- 131.)	1210	(922.-1484.)
t/y	2011	90	(37.- 136.)	1260	(865.-1536.)
t/y	2012	79	(38.- 105.)	1350	(1103.-1569.)

Table 17: Emission (t/y) estimates for UK and NWEU with uncertainty (5th – 95th %ile).

5.6 HFC-23

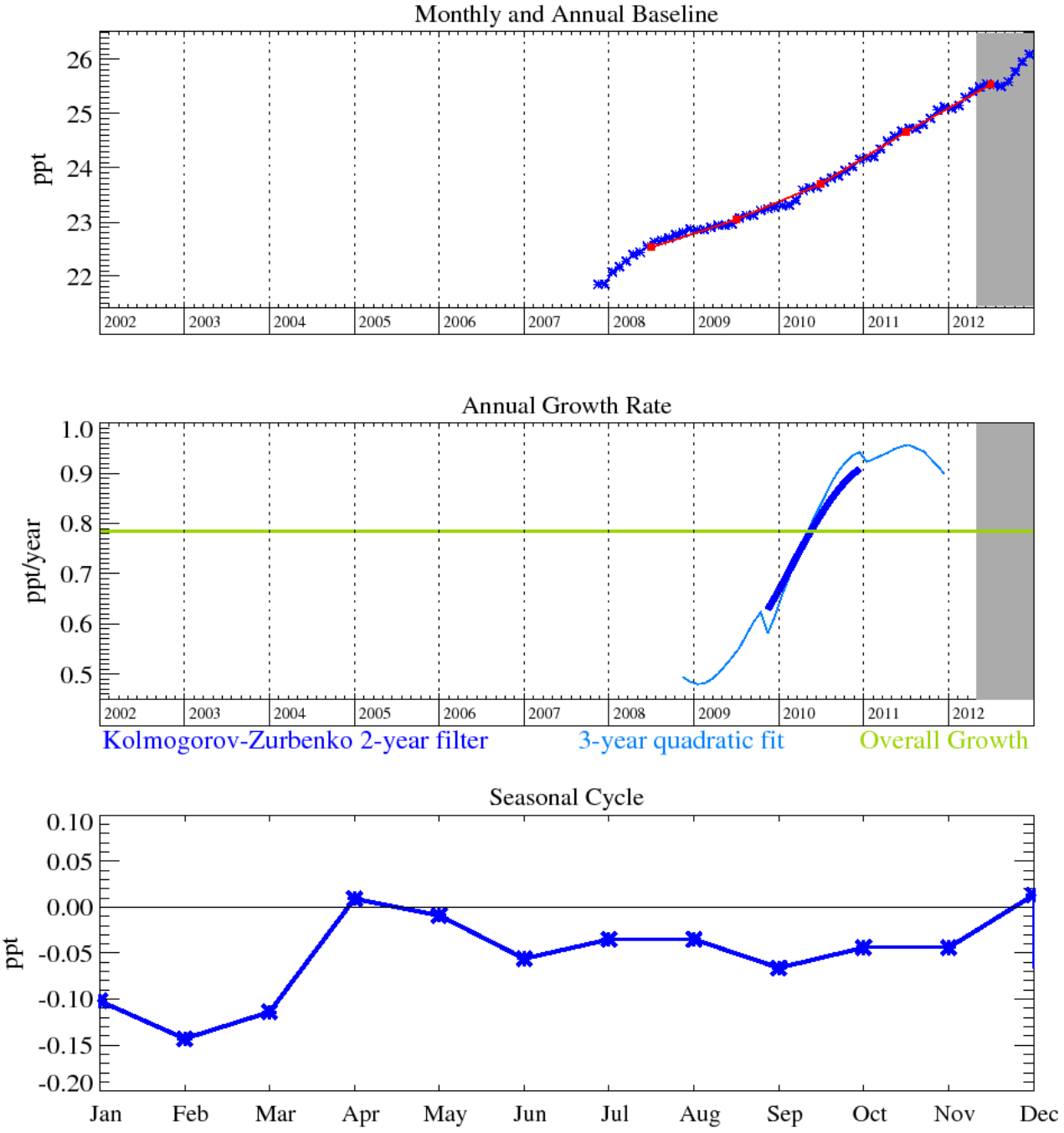

Figure 48: HFC-23 (CHF_3): Monthly (blue) and annual (red) baseline concentrations. Annual (blue) and overall average growth rate (green) (lower plot). Grey area covers un-ratified and therefore provisional data.

HFC-23 is primarily a by-product formed by the over fluorination of chloroform during the production of HCFC-22, other minor emissions arise from the electronic industry and fire extinguishers. For this reason it has grown at an average rate of 0.8 ppt/yr and by December 2012 had reached a mixing ratio of 26.1 ppt. It is the second most abundant HFC in the atmosphere after HFC-134a; this combined with a long atmospheric lifetime of 222 years makes this compound a potent GHG. Emissions of HFC-23 in developed countries has declined due to the Montreal Protocol phase-out schedule for HCFC-22, however, emissions from developing countries continues to drive global mixing ratios up, and will continue to do so until implementation of HFC-23 incineration through the Clean Development Mechanism is more widely used.

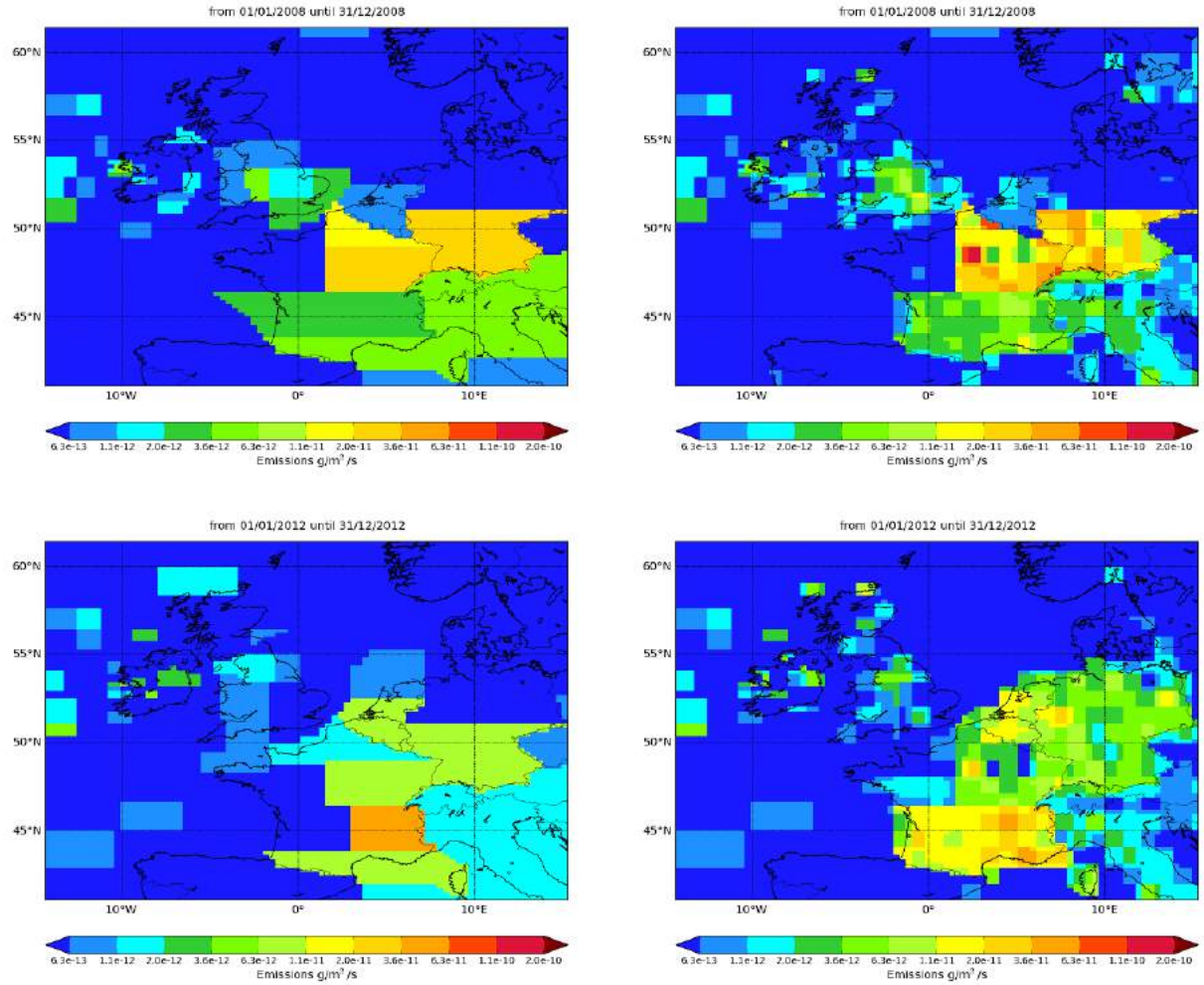

Figure 49: NAME-inversion emission estimates for 2008 (upper) and 2012 (lower). On the right hand side the emissions per grid box have been re-distributed based on population.

The statistical fit between the model time-series and the observations is not strong and this is reflected in the significant uncertainty bars for the InTEM emission estimates. Although the InTEM estimates on average are higher than the inventory estimates, the uncertainty ranges entirely overlap for the UK.

Year	RMSE (ppt)	Correlation	Max obs. above baseline (ppt)	% obs. above baseline noise	Mean obs. above baseline (ppt)
2008	0.19	0.47	2.9	22	0.17
2012	0.13	0.12	0.9	20	0.11

Table 18: Comparison between modelled and observed time-series.

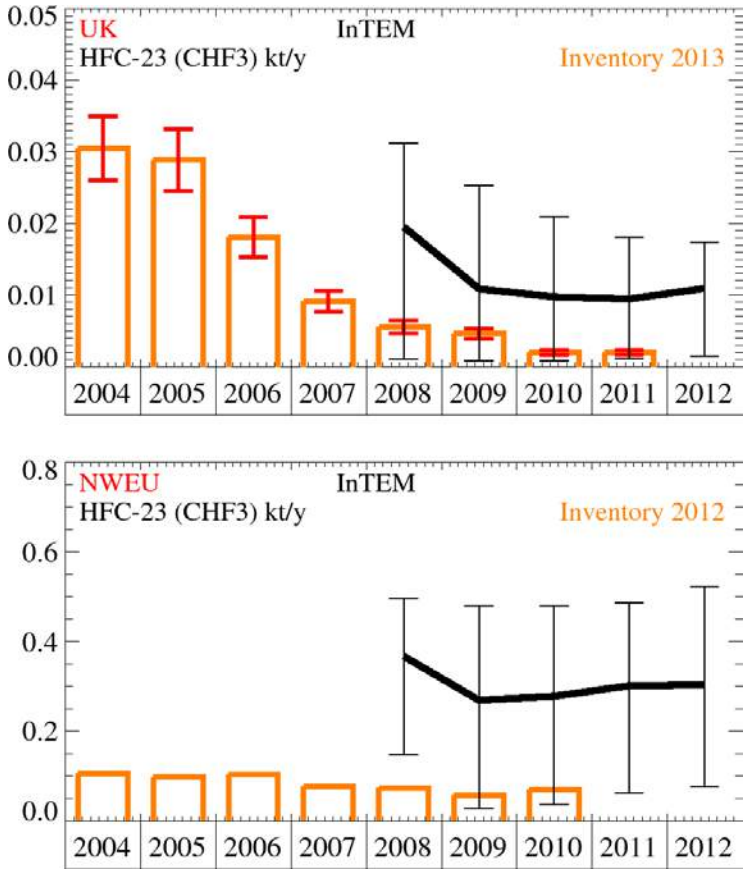

Figure 50: Emission (kt/y) estimates for UK and NWEU. The uncertainty bars represent the 5th and 95th percentiles.

Unit	Year	UK	(5th-95th)	NWEU	(5th-95th)
t/y	2008	19.5	(1.0- 31.)	370	(148.- 496.)
t/y	2009	10.9	(0.8- 25.)	270	(27.- 480.)
t/y	2010	9.8	(0.8- 21.)	280	(36.- 480.)
t/y	2011	9.5	(1.2- 18.)	300	(62.- 487.)
t/y	2012	11	(1.5- 17.)	300	(76.- 522.)

Table 19: Emission (t/y) estimates for UK and NWEU with uncertainty (5th – 95th %ile).

5.7 HFC-32

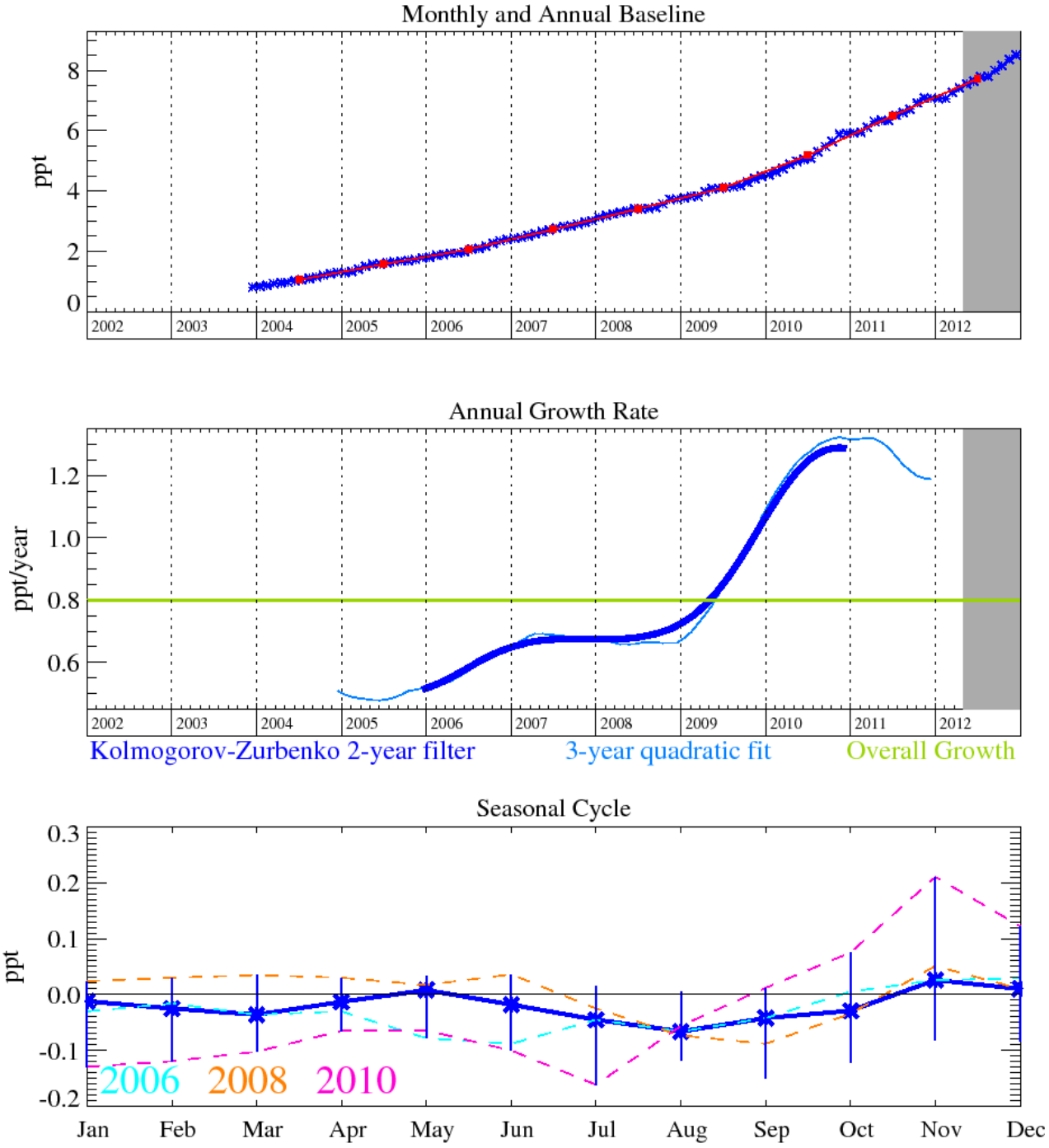

Figure 51: HFC-32 (CH_2F_2): Monthly (blue) and annual (red) baseline concentrations (top plot). Annual (blue) and overall average growth rate (green) (middle plot). Seasonal cycle (de-trended) with year-to-year variability (lower plot). Grey area covers un-ratified and therefore provisional data.

HFC-32 has an atmospheric lifetime of 5.2 years and a GWP_{100} of 716. It is used in air conditioning and refrigeration applications; azeotropic R-410A (50% HFC-32, 50% HFC-125 by weight) and R-407C (23% HFC-32, 52% HFC-134a, 25% HFC-125 by weight) are used to replace HCFC-22. As the phase-out of HCFC-22 gains momentum it might be expected that demand for these refrigerant blends will increase. The pollution events measured at Mace Head are highly correlated with that of HFC-125, and is used as a diagnostic for leakages in the on-site air conditioners.

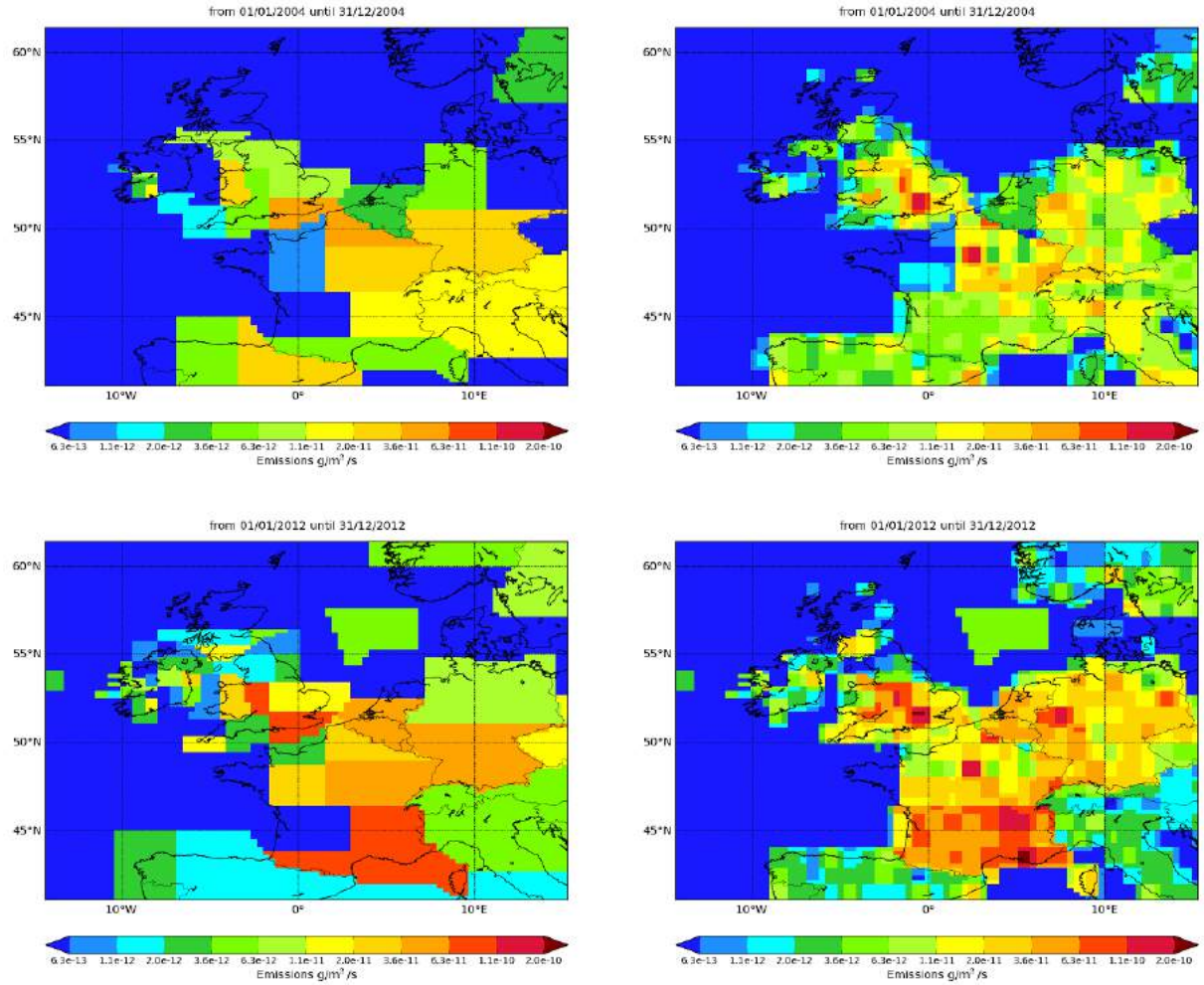

Figure 52: NAME-inversion emission estimates for 2004 (upper) and 2012 (lower). On the right hand side the emissions per grid box have been re-distributed based on population.

Year	RMSE (ppt)	Correlation	Max obs. above baseline (ppt)	% obs. above baseline noise	Mean obs. above baseline (ppt)
2004	0.23	0.56	5.5	34	0.17
2012	0.42	0.59	5.4	38	0.47

Table 20: Comparison between modelled and observed time-series.

Except for the last three years, the UK emission estimates from the inventory and InTEM agree extremely well. From 2009, InTEM shows a plateau and then a decline, whereas the inventory shows a continuing strong increase year on year. The NWEU estimates from InTEM are consistently higher than the inventory. The statistical match between the model time-series and the observations is reasonable across all years.

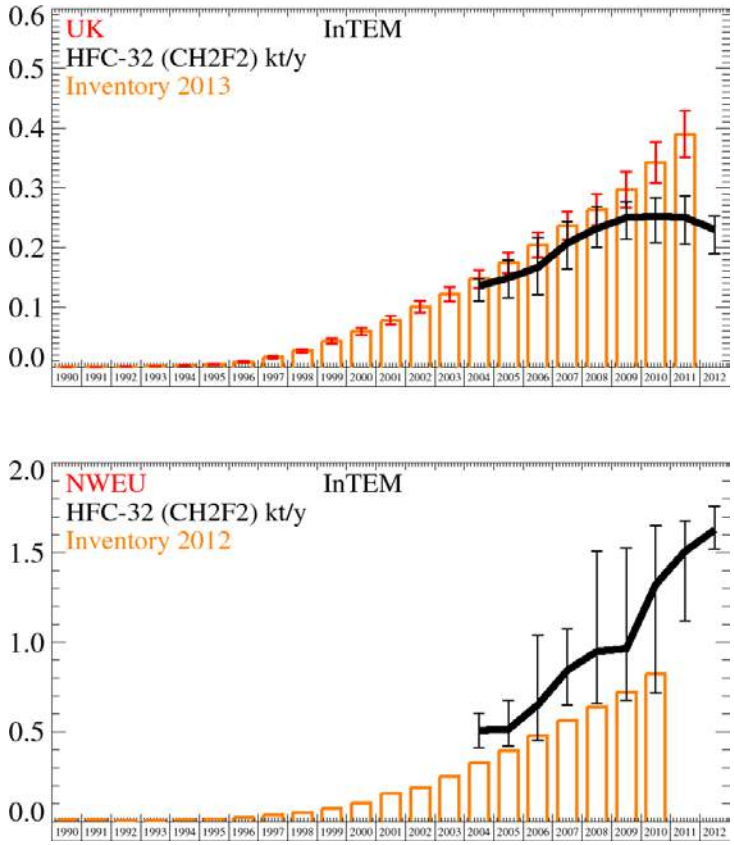

Figure 53: Emission (kt/y) estimates for UK and NWEU. The uncertainty bars represent the 5th and 95th percentiles.

Unit	Year	UK	(5th-95th)	NWEU	(5th-95th)
t/y	2004	136	(111.- 148.)	510	(412.- 605.)
t/y	2005	149	(115.- 178.)	510	(423.- 675.)
t/y	2006	167	(121.- 217.)	650	(451.-1038.)
t/y	2007	210	(164.- 243.)	840	(649.-1072.)
t/y	2008	230	(200.- 269.)	950	(657.-1506.)
t/y	2009	250	(214.- 276.)	960	(677.-1526.)
t/y	2010	250	(208.- 283.)	1320	(715.-1652.)
t/y	2011	250	(205.- 286.)	1510	(1119.-1676.)
t/y	2012	230	(190.- 253.)	1630	(1523.-1758.)

Table 21: Emission (t/y) estimates for UK and NWEU with uncertainty (5th – 95th %ile).

5.8 HFC-227ea

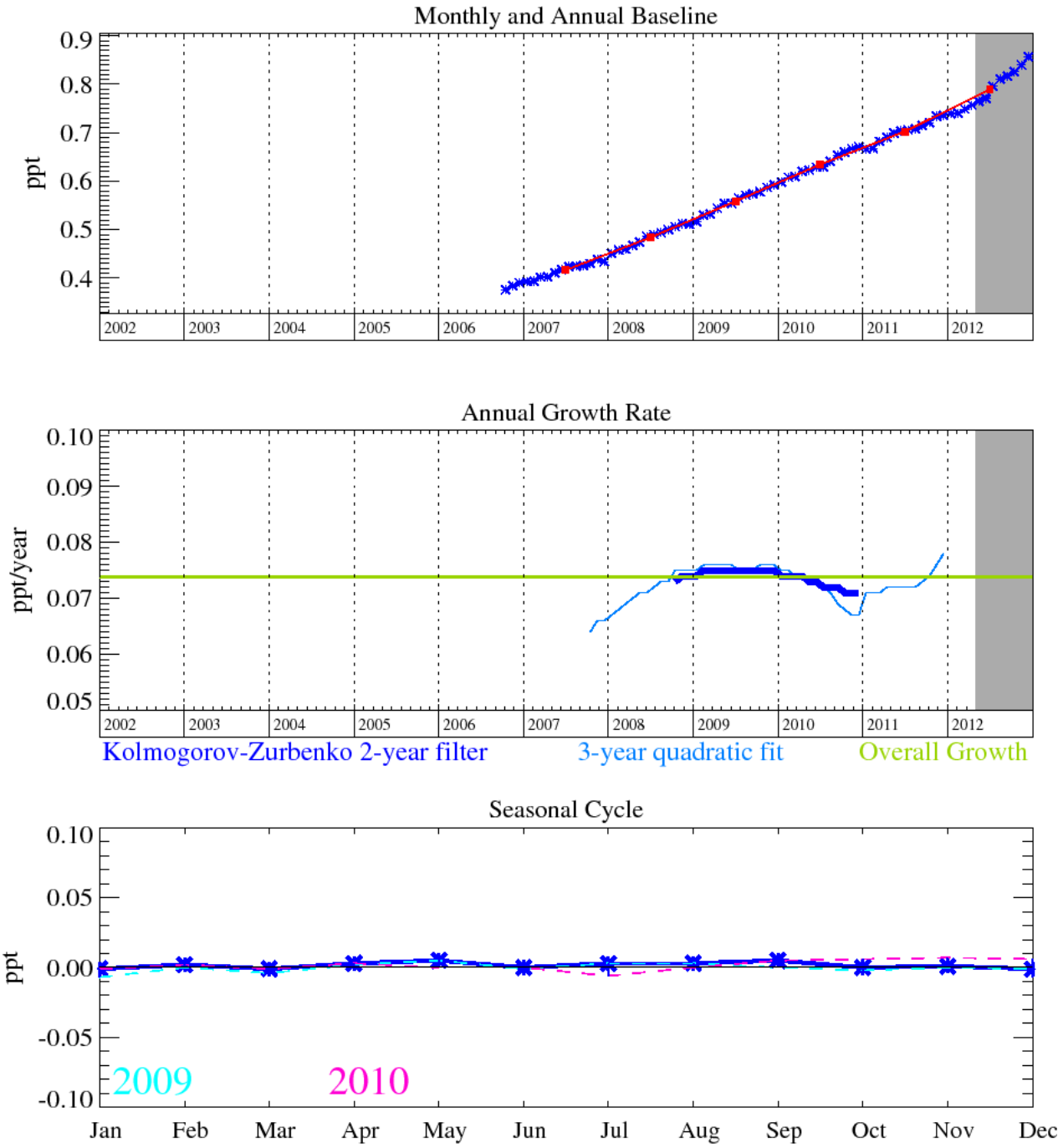

Figure 54: HFC-227ea (C_3HF_7): Monthly (blue) and annual (red) baseline concentrations (top plot). Annual (blue) and overall average growth rate (green) (middle plot). Seasonal cycle (de-trended) with year-to-year variability (lower plot). Grey area covers un-ratified and therefore provisional data.

HFC-227ea was added to the Medusa analysis in January 2008. HFC-227ea is used as a propellant for medical aerosols and a fire-fighting agent and to a lesser extent in metered-dose inhalers, and foam blowing (atmospheric lifetime 38.9 years and GWP_{100} of 3580). It has reached a mole fraction of 0.86 ppt with a growth rate of 0.07 ppt/yr.

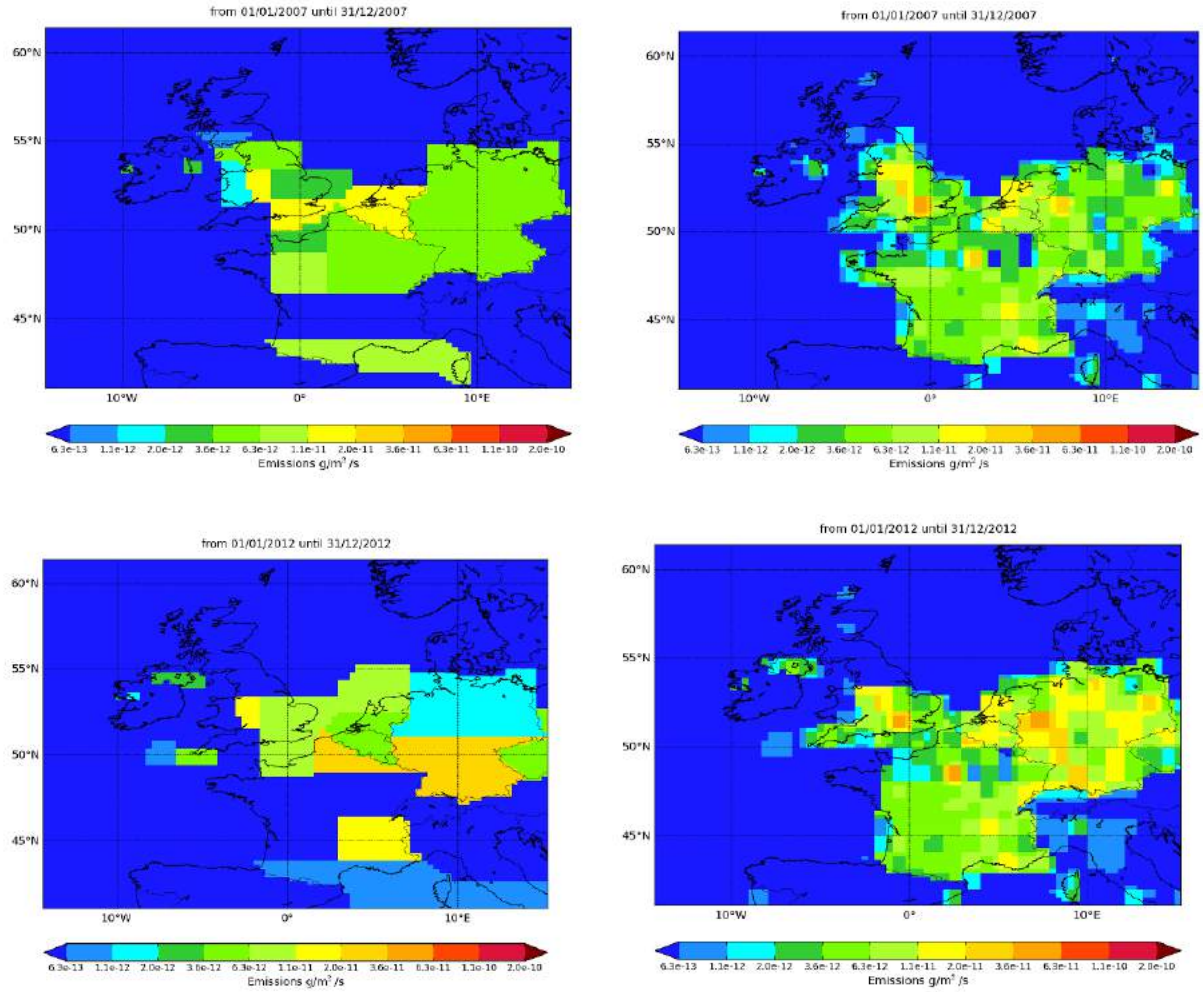

Figure 55: NAME-inversion emission estimates for 2007 (upper) and 2012 (lower). On the right hand side the emissions per grid box have been re-distributed based on population.

The InTEM results are significantly lower than the inventory estimates. The reason for this difference is unknown. The new observations from Tacolneston will prove extremely useful in further investigating this discrepancy. The statistical match between the model time-series and the observations is reasonable.

Year	RMSE (ppt)	Correlation	Max obs. above baseline (ppt)	% obs. above baseline noise	Mean obs. above baseline (ppt)
2007	0.03	0.65	0.5	30	0.03
2012	0.09	0.34	4.2	33	0.03

Table 22: Comparison between modelled and observed time-series.

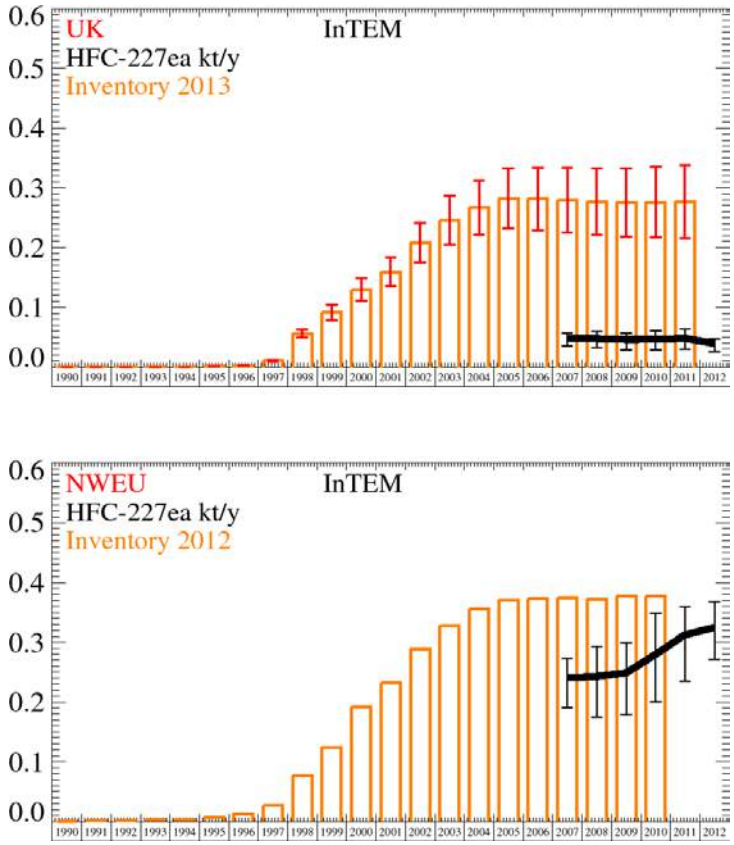

Figure 56: Emission (kt/y) estimates for UK and NWEU. The uncertainty bars represent the 5th and 95th percentiles.

Unit	Year	UK	(5th-95th)	NWEU	(5th-95th)
t/y	2007	48	(36.- 56.)	240	(191.- 273.)
t/y	2008	47	(32.- 59.)	240	(175.- 293.)
t/y	2009	46	(28.- 57.)	250	(178.- 299.)
t/y	2010	46	(28.- 60.)	280	(200.- 349.)
t/y	2011	48	(29.- 63.)	310	(235.- 360.)
t/y	2012	39	(25.- 48.)	320	(271.- 368.)

Table 23: Emission (t/y) estimates for UK and NWEU with uncertainty (5th – 95th %ile).

5.9 PFC-14 (CF_4)

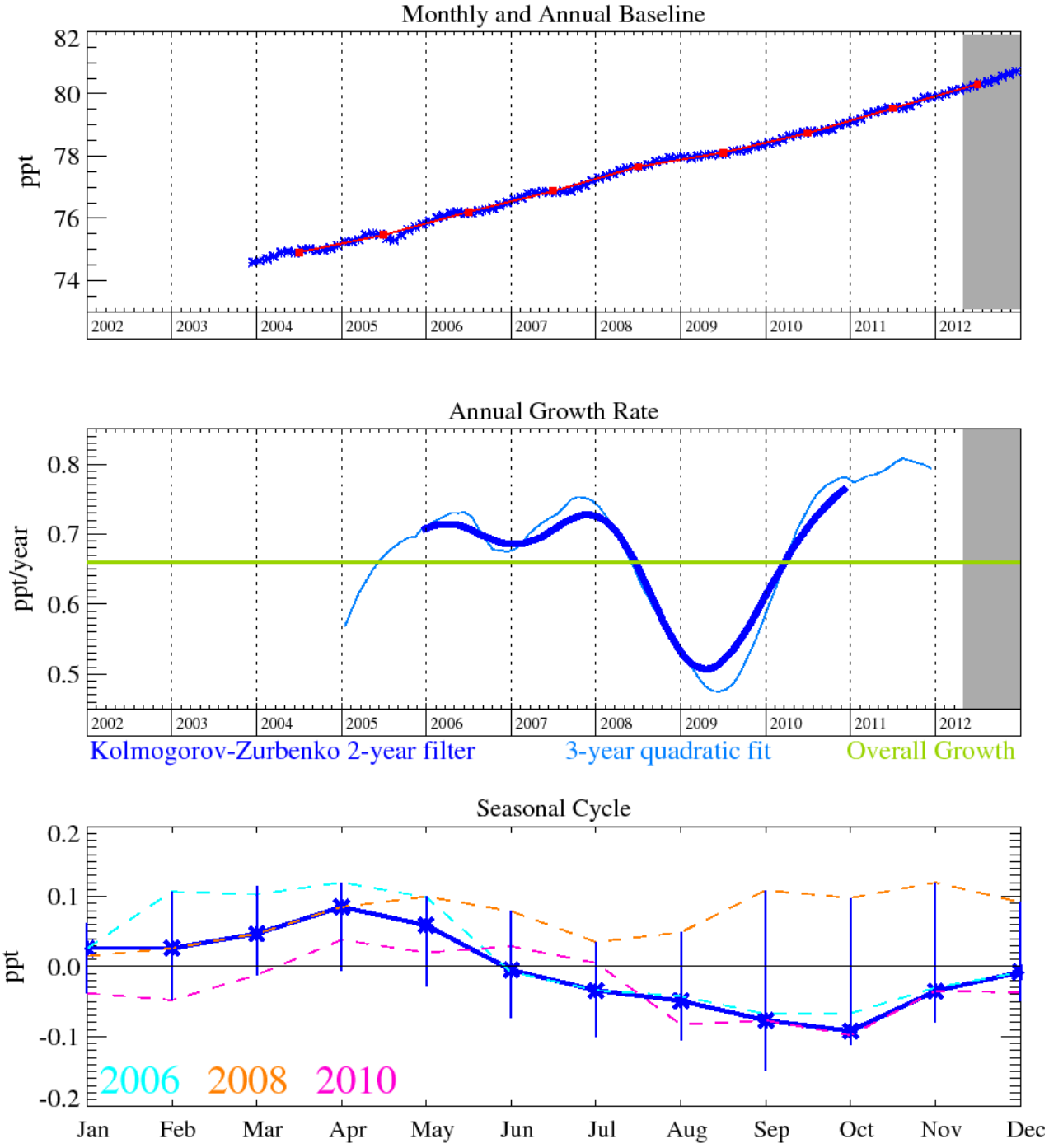

Figure 57: PFC-14 (CF_4): Monthly (blue) and annual (red) baseline concentrations (top plot). Annual (blue) and overall average growth rate (green) (middle plot). Seasonal cycle (de-trended) with year-to-year variability (lower plot). Grey area covers un-ratified and therefore provisional data.

PFC-14 (CF_4) possesses the longest known lifetime of anthropogenic molecules (>50,000 yrs), which, when coupled with its high absolute radiative forcing (0.08 W m^{-2} ppb^{-1}) gives rise to a high GWP_{100} of 5,820 and can equate to upwards of 1% of total radiative forcing. Its primary emission source is as an unwanted by-product of aluminium smelting during a fault condition known as the Anode Effect. Thus the frequency of occurrence and duration of an Anode Effect event will determine the regional and global CF_4 emission. CF_4 has some additional minor applications in the semiconductor industry (as a source of F radicals), but industry has shied away from using CF_4 knowing that its GWP is so high. The aluminium industry has recognised the CF_4 (and C_2F_6)

emission problem and has been undergoing processes of replacement of older, less efficient aluminium production cells with more efficient designs, and automated and quicker intervention policies to prevent the occurrence of these Anode Effects. It is also thought that CF_4 has a natural source from crustal degassing.

The current growth rate of atmospheric CF_4 is 0.79 ppt/yr. This compound will continue to accumulate in the atmosphere due to its very long atmospheric lifetime. In December 2012 the mixing ratio of CF_4 was 80.7 ppt.

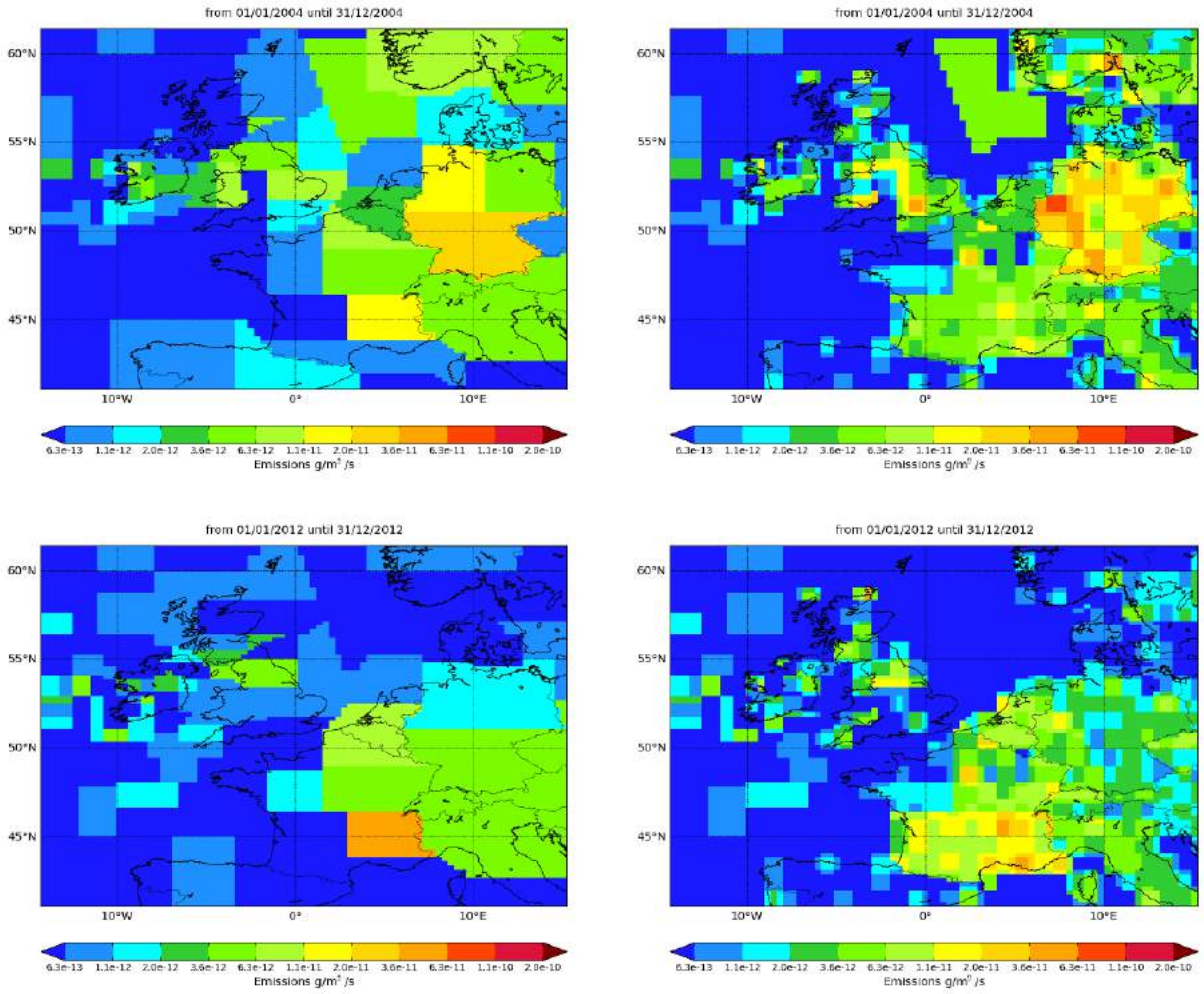

Figure 58: NAME-inversion emission estimates for 2004 (upper) and 2012 (lower). On the right hand side the emissions per grid box have been re-distributed based on population.

The significant uncertainties in the InTEM results entirely overlap with the inventory estimates although the median results are consistently higher. The statistical match between the model time-series and the observations is weak in 2004 and negligible in 2012.

Year	RMSE (ppt)	Correlation	Max obs. above baseline (ppt)	% obs. above baseline noise	Mean obs. above baseline (ppt)
2004	0.14	0.35	1.50	22	0.13
2012	0.1	0.05	0.45	19	0.07

Table 24: Comparison between modelled and observed time-series.

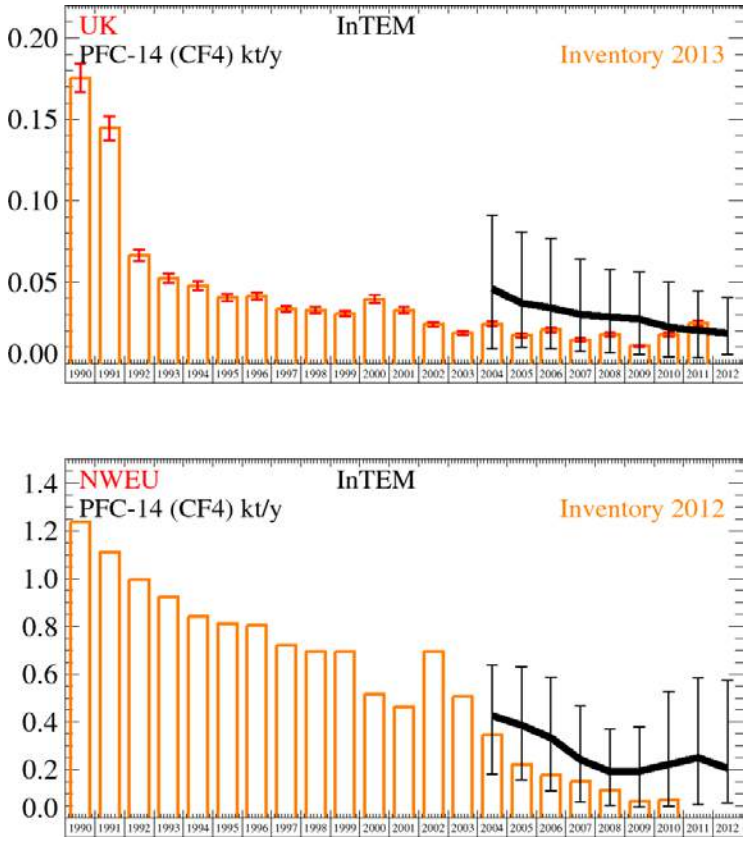

Figure 59: Emission (kt/y) estimates for UK and NWEU. The uncertainty bars represent the 5th and 95th percentiles.

Unit	Year	UK	(5th-95th)	NWEU	(5th-95th)
t/y	2004	46	(8.9- 91.)	430	(182.- 639.)
t/y	2005	37	(9.8- 81.)	390	(159.- 630.)
t/y	2006	34	(8.9- 77.)	330	(111.- 586.)
t/y	2007	30	(7.6- 64.)	240	(65.- 468.)
t/y	2008	29	(6.6- 58.)	192	(50.- 370.)
t/y	2009	27	(5.5- 56.)	194	(45.- 381.)
t/y	2010	22	(4.0- 50.)	220	(48.- 526.)
t/y	2011	20	(3.4- 44.)	250	(55.- 584.)
t/y	2012	18.6	(5.5- 41.)	210	(61.- 575.)

Table 25: Emission (t/y) estimates for UK and NWEU with uncertainty (5th – 95th %ile).

5.10 PFC-116

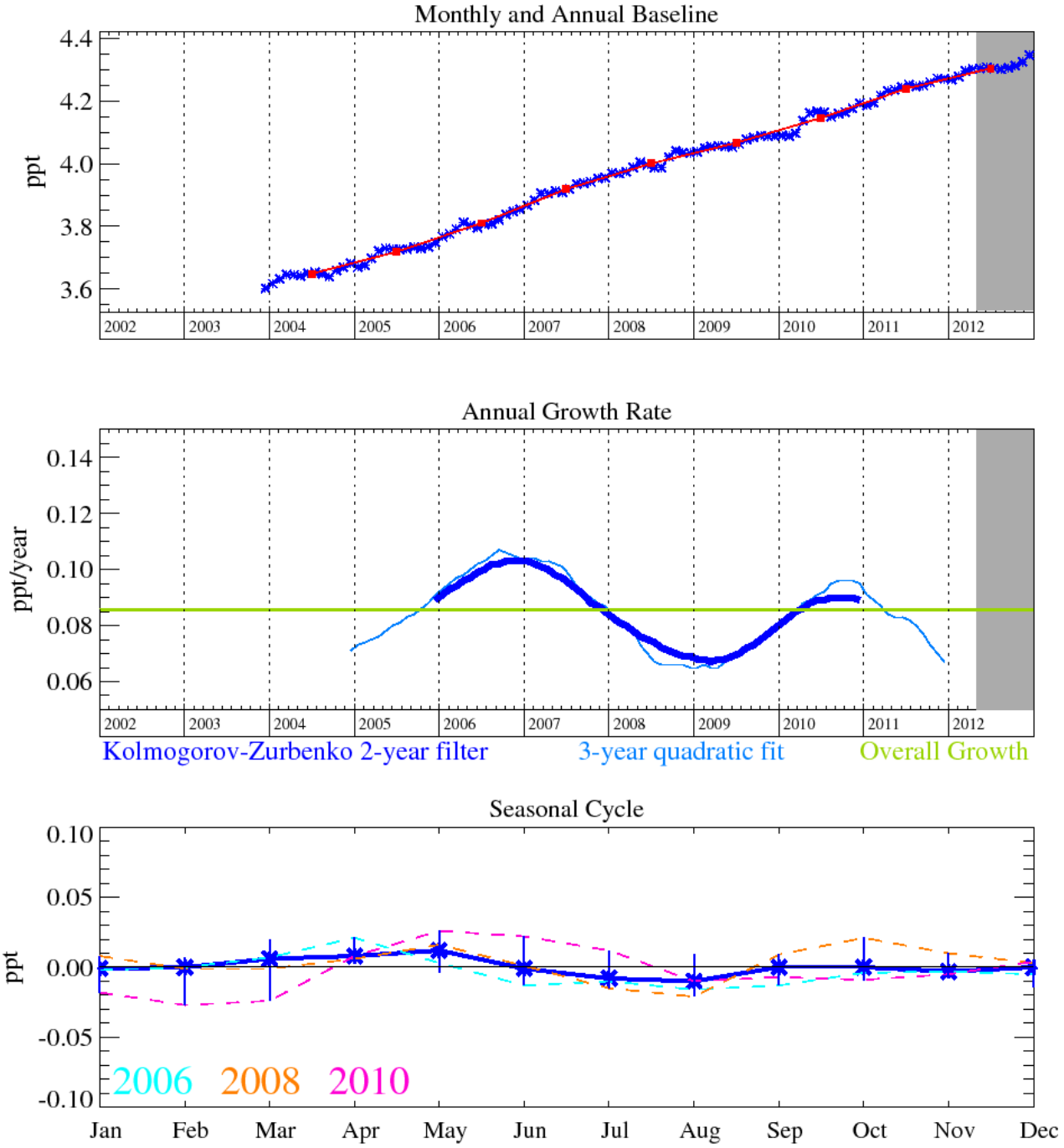

Figure 60: PFC-116 (C_2F_6): Monthly (blue) and annual (red) baseline concentrations (top plot). Annual (blue) and overall average growth rate (green) (middle plot). Seasonal cycle (de-trended) with year-to-year variability (lower plot). Grey area covers un-ratified and therefore provisional data.

PFC-116 (C_2F_6) is also a potent greenhouse gas with an atmospheric lifetime of >10,000 years. It has common sources to CF_4, this serves to help explain why all of the CF_4 above-baseline (pollution) events are usually correlated with those of C_2F_6. However, we note that there are many more frequent and greater magnitude emissions of C_2F_6 relative to CF_4. This is due to the dominant source of C_2F_6 being from semiconductor industries (plasma etching).

The current growth rate of atmospheric C_2F_6 is 0.08 ppt/yr. This compound will continue to accumulate in the atmosphere due to its very long atmospheric lifetimes. In December 2012 the mixing ratio of C_2F_6 was 4.3 ppt.

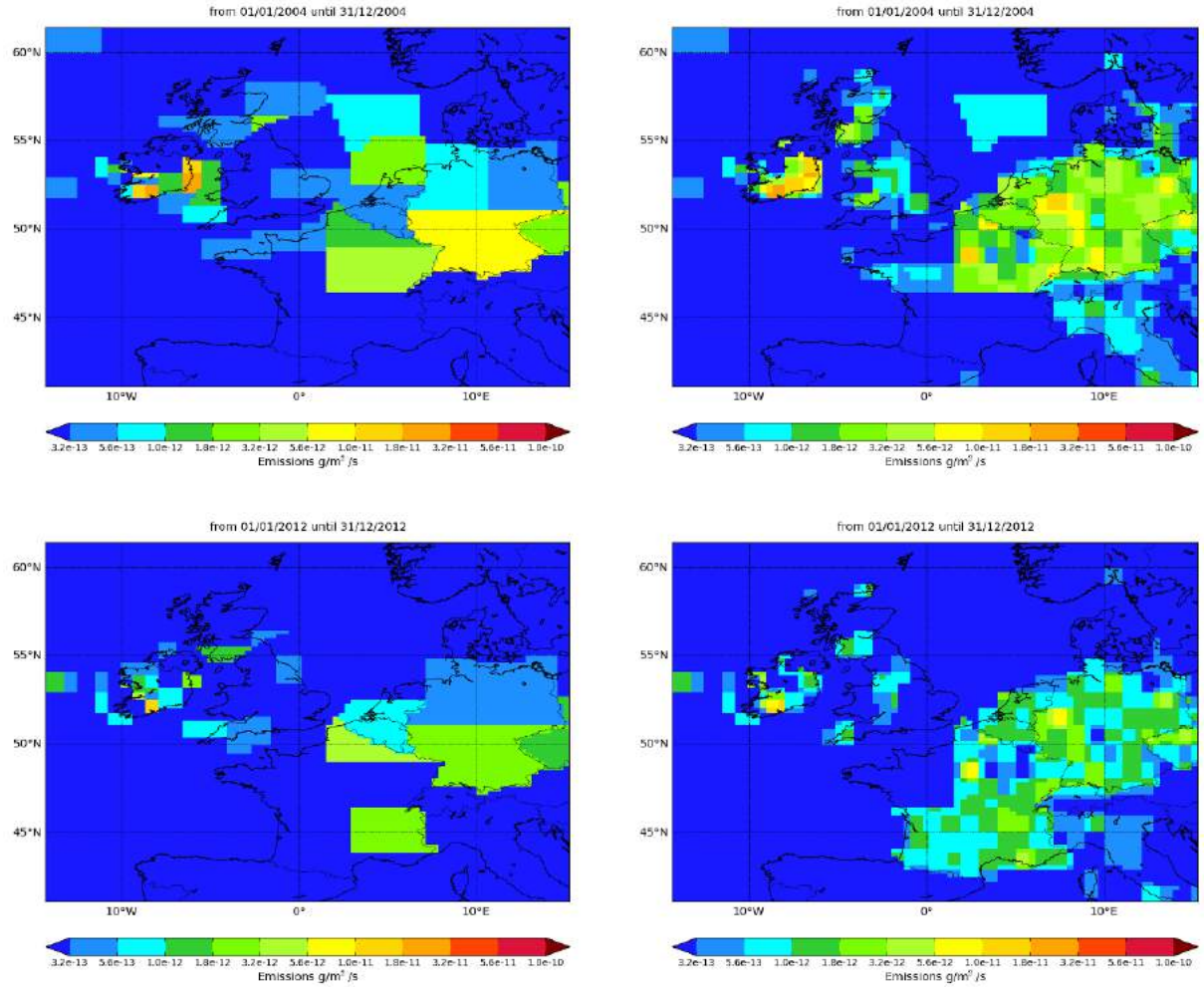

Figure 61: NAME-inversion emission estimates for 2004 (upper) and 2012 (lower). On the right hand side the emissions per grid box have been re-distributed based on population.

The InTEM uncertainty ranges for the regional emissions consistently overlap the inventory estimates. The statistical match between the estimated model time-series and the observations is fair to weak.

Year	RMSE (ppt)	Correlation	Max obs. above baseline (ppt)	% obs. above baseline noise	Mean obs. above baseline (ppt)
2004	0.06	0.43	1.14	22	0.043
2012	0.04	0.22	0.59	20	0.027

Table 26: Comparison between modelled and observed time-series.

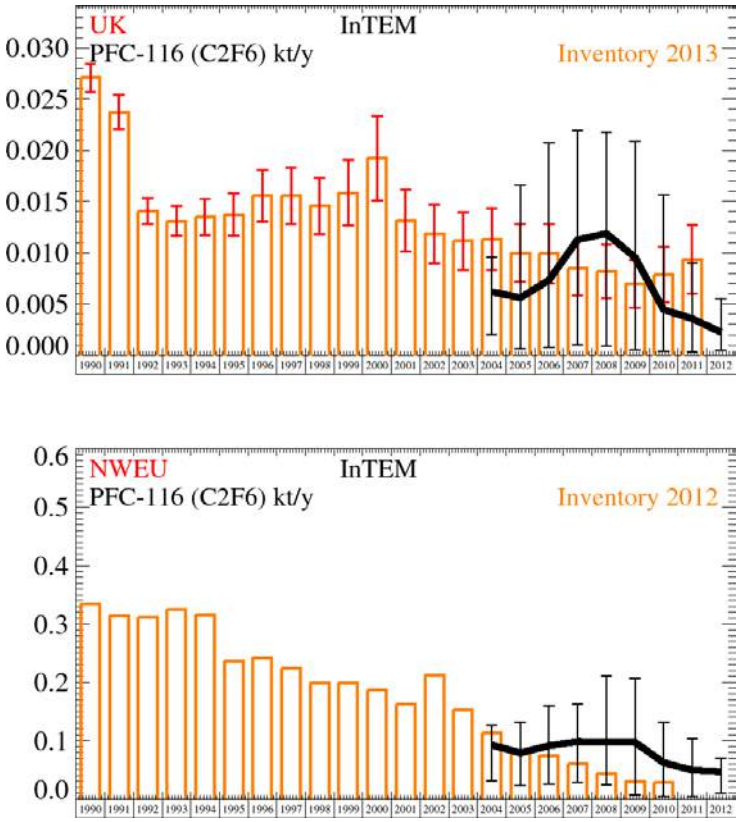

Figure 62: Emission (kt/y) estimates for UK and NWEU. The uncertainty bars represent the 5th and 95th percentiles.

Unit	Year	UK	(5th-95th)	NWEU	(5th-95th)
t/y	2004	6.2	(2.0- 10.)	93	(31.- 126.)
t/y	2005	5.6	(0.6- 17.)	79	(23.- 132.)
t/y	2006	7.3	(0.8- 21.)	91	(25.- 160.)
t/y	2007	11.3	(1.0- 22.)	98	(28.- 163.)
t/y	2008	11.9	(0.9- 22.)	97	(24.- 211.)
t/y	2009	9.6	(0.6- 21.)	97	(6.- 207.)
t/y	2010	4.4	(0.4- 16.)	62	(4.- 132.)
t/y	2011	3.6	(0.4- 9.)	49	(4.- 104.)
t/y	2012	2.2	(0.4- 6.)	47	(10.- 70.)

Table 27: Emission (t/y) estimates for UK and NWEU with uncertainty (5th – 95th %ile).

5.11 PFC-218

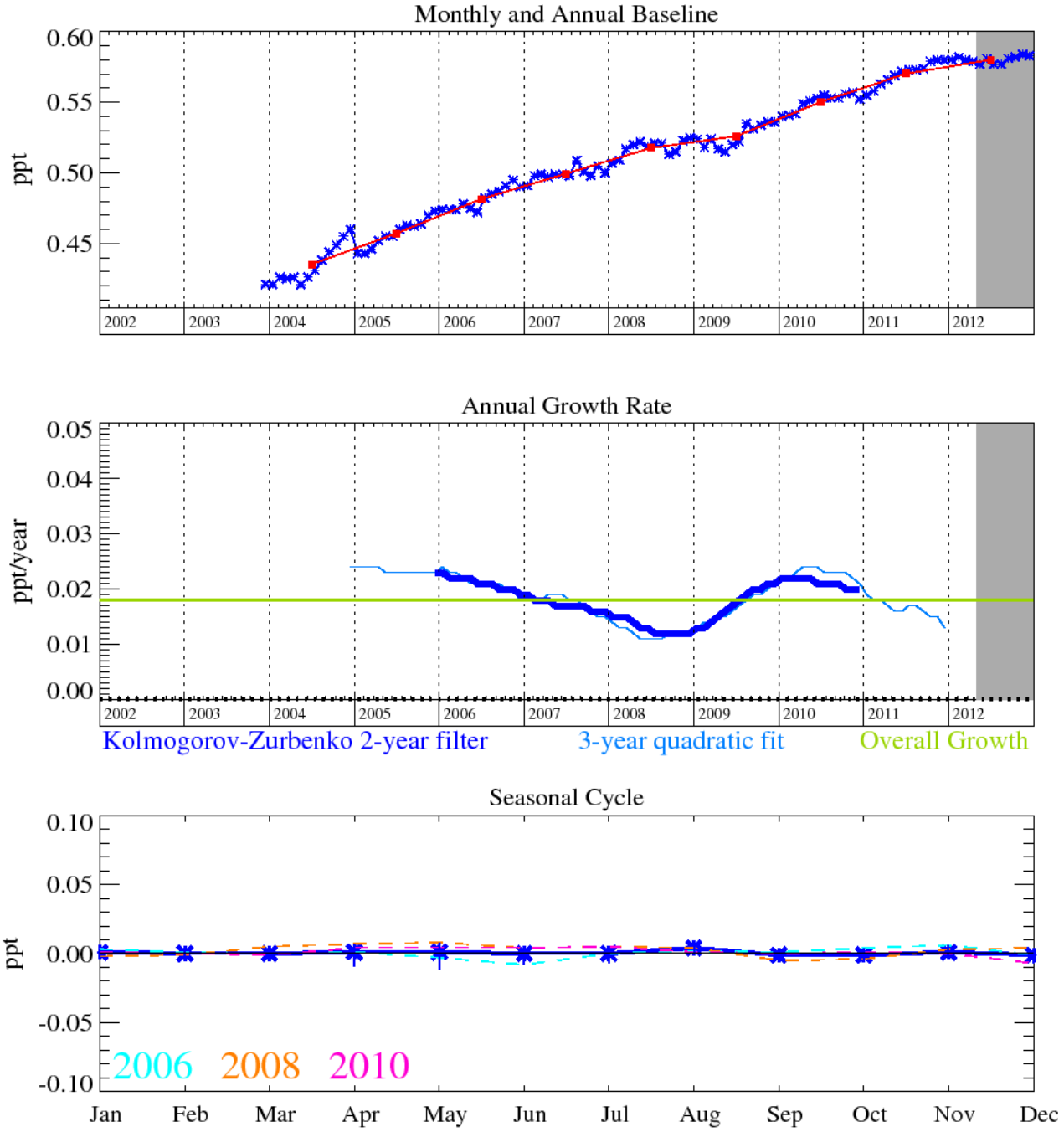

Figure 63: PFC-218 (C_3F_8): Monthly (blue) and annual (red) baseline concentrations (top plot). Annual (blue) and overall average growth rate (green) (middle plot). Seasonal cycle (de-trended) with year-to-year variability (lower plot). Grey area covers un-ratified and therefore provisional data.

PFC-218 (C_3F_8) has an atmospheric lifetime of 2600 years and a GWP_{100} of 8690, it is also used in semiconductor manufacturing, but to a lesser extent than C_2F_6. It also has a very small contribution from aluminium smelting and has an increasing contribution from refrigeration use. Observations of above-baseline C_3F_8 emissions are less frequent than those of C_2F_6 but are of a higher relative magnitude.

The current growth rate of atmospheric C_3F_8 is 0.02 ppt/yr. This compound will tend to accumulate in the atmosphere due to its very long atmospheric lifetime. In December 2012 the mixing ratio of C_3F_8 was 0.6 ppt.

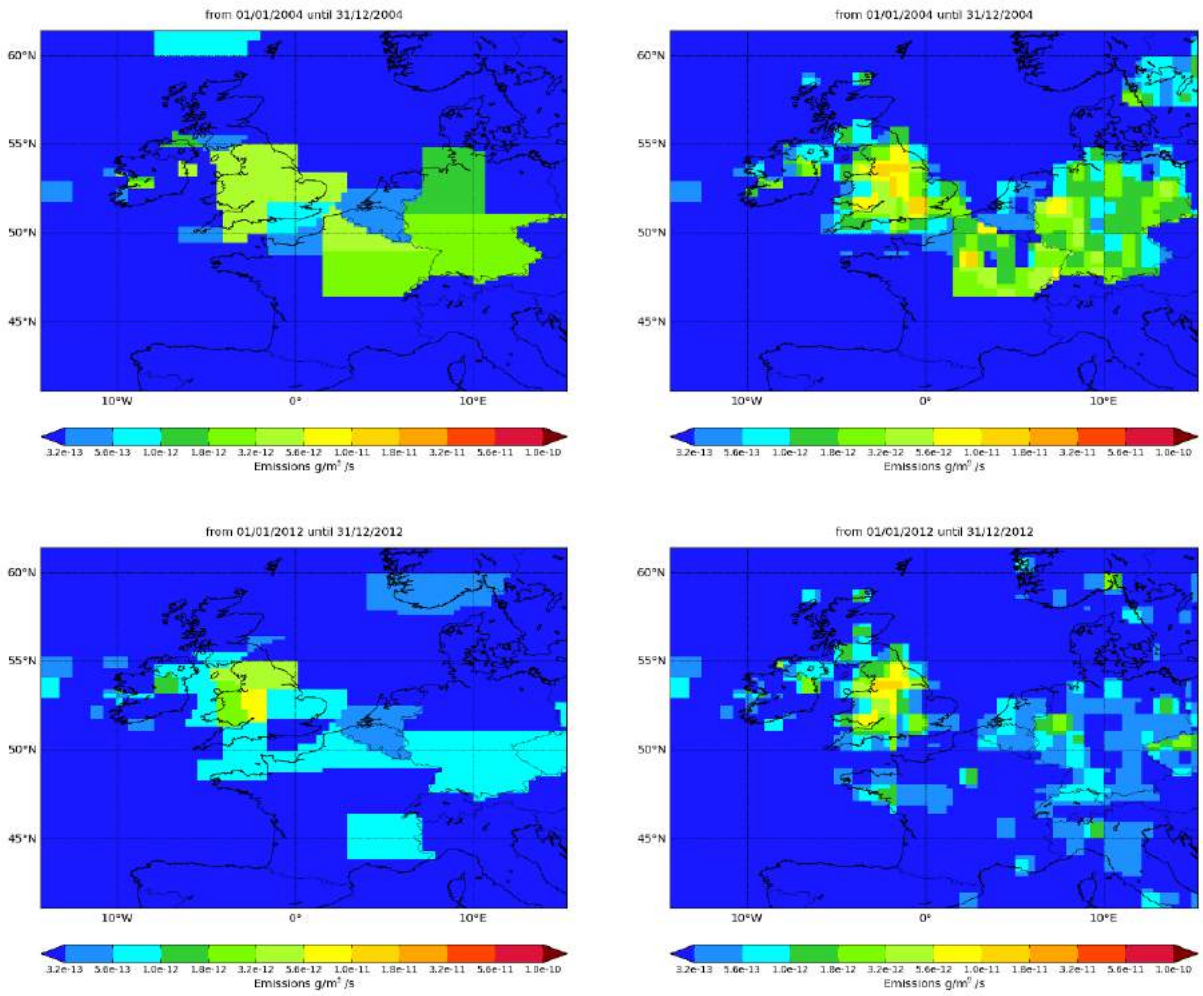

Figure 64: NAME-inversion emission estimates for 2004 (upper) and 2012 (lower). On the right hand side the emissions per grid box have been re-distributed based on population.

Even with the relatively large uncertainty in the InTEM emission estimates they are still consistently elevated (by a factor of ~2) compared to the inventory both in the UK and in NWEU. The statistical match between the model time-series and the observations is fair.

Year	RMSE (ppt)	Correlation	Max obs. above baseline (ppt)	% obs. above baseline noise	Mean obs. above baseline (ppt)
2004	0.03	0.40	0.75	26	0.02
2012	0.02	0.40	0.23	23	0.01

Table 28: Comparison between modelled and observed time-series.

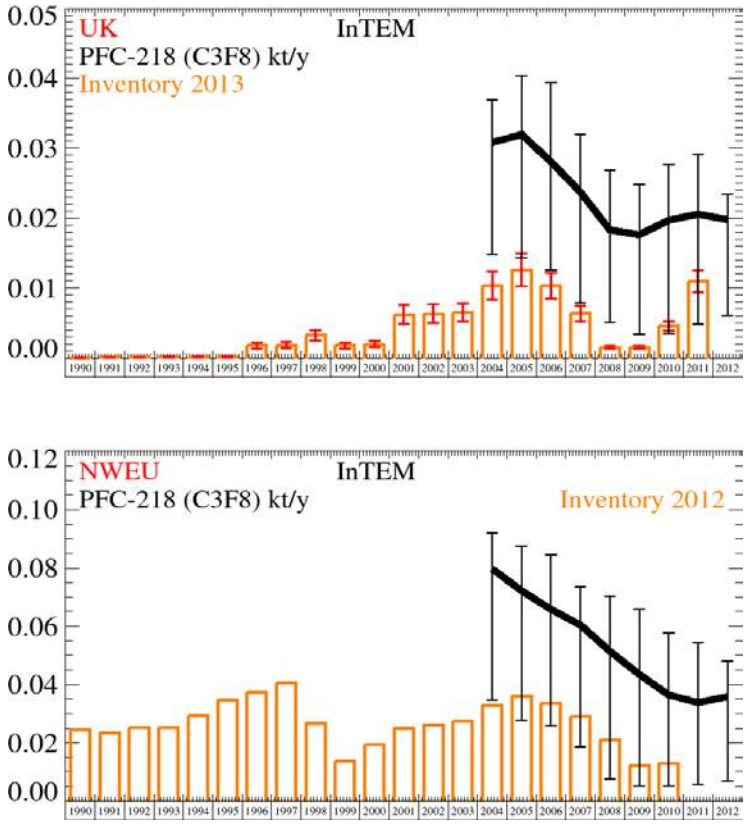

Figure 65: Emission (kt/y) estimates for UK and NWEU. The uncertainty bars represent the 5th and 95th percentiles.

Unit	Year	UK	(5th-95th)	NWEU	(5th-95th)
t/y	2004	31	(15.- 37.)	80	(35.- 92.)
t/y	2005	32	(14.- 40.)	72	(28.- 88.)
t/y	2006	28	(13.- 39.)	66	(26.- 84.)
t/y	2007	24	(8.- 32.)	60	(19.- 74.)
t/y	2008	18.3	(5.- 27.)	51	(8.- 70.)
t/y	2009	17.6	(3.- 25.)	43	(5.- 66.)
t/y	2010	19.7	(3.- 28.)	36	(5.- 58.)
t/y	2011	21	(5.- 29.)	34	(6.- 54.)
t/y	2012	19.8	(6.- 23.)	36	(7.- 48.)

Table 29: Emission (t/y) estimates for UK and NWEU with uncertainty (5th – 95th %ile).

5.12 PFC-318

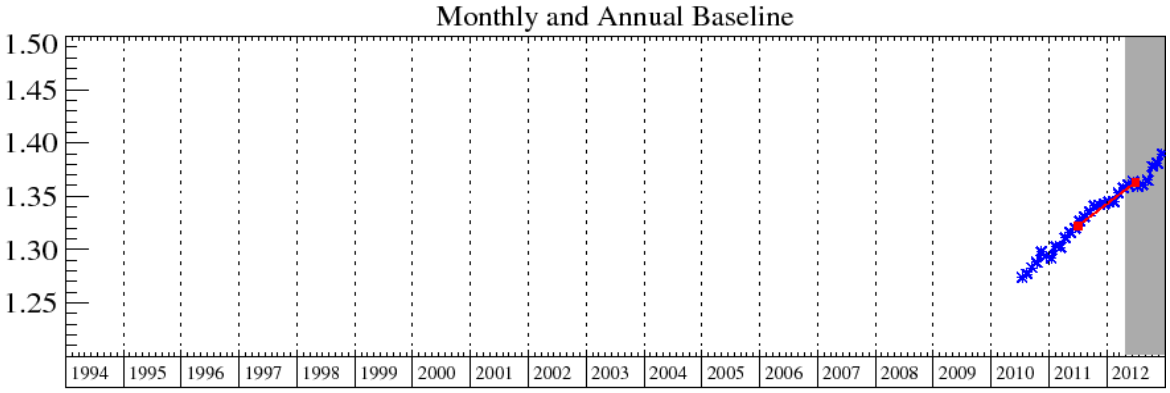

Figure 66: PFC-318 (C_4F_8): Monthly (blue) and annual (red) baseline concentrations.

This gas is increasingly used in the semiconductor and electronics industries for cleaning, plasma etching and deposition gas, also it has more minor use in aerolyzed foods, retinal detachment surgery, size estimation of natural gas and oil reservoirs, specialist military applications, tracer experiments and may also replace SF_6 as an electrically insulating gas. It has an atmospheric lifetime of 3,200 years, a GWP_{100} of 10,300 and a radiative efficiency of 0.32 W m^{-2} ppb^{-1}.

As yet it is too early to calculate growth rates for this gas, but this information will be included once 3 years of data have been acquired.

5.13 SF_6

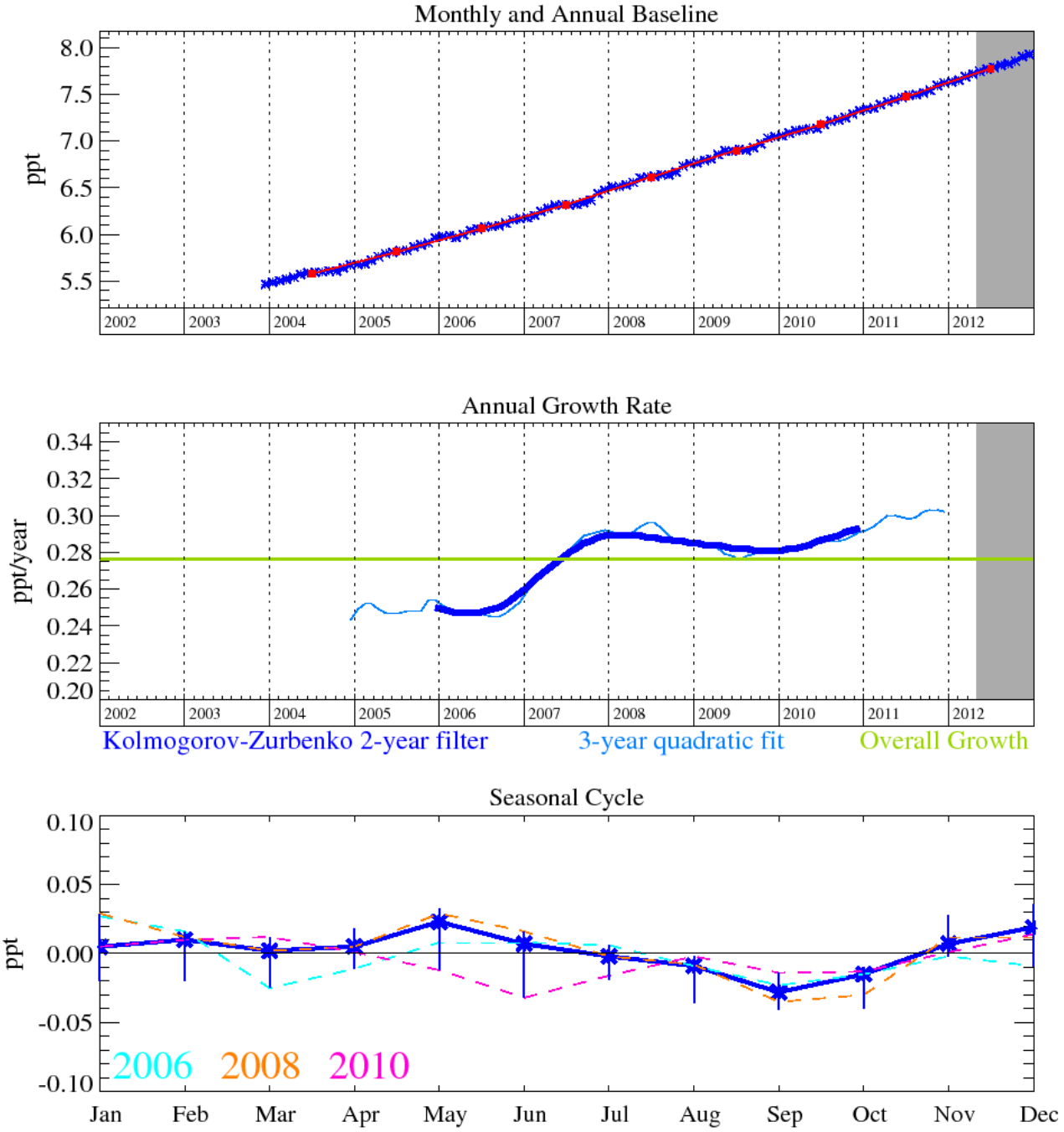

Figure 67: SF_6: Monthly (blue) and annual (red) baseline concentrations (top plot). Annual (blue) and overall average growth rate (green) (middle plot). Seasonal cycle (de-trended) with year-to-year variability (lower plot). Grey area covers un-ratified and therefore provisional data.

SF_6 is an important greenhouse gas since it has a long atmospheric lifetime of 3,200 years and a high radiative efficiency; giving rise to a GWP_{100} of 22800. It has an average atmospheric trend of 0.28 ppt/yr and reached a mixing ratio of 7.9 ppt by December 2012. Although having minor usage in the semiconductor industry, it is predominantly used in electrical circuit breakers, heavy-duty gas-insulated switchgear (GIS) for systems with voltages from 5,000-38,000 volts, and other switchgear used in the electrical transmission systems to manage high voltages (>38 kV). The electrical power industry uses roughly 80% of all SF_6 produced worldwide. Although the units themselves are hermetically sealed and pressurised, aging equipment, breakdown and disposal, alongside leakage from wear-and-tear will cause this sector to emit SF_6. A minor use of this gas is also reported in its use as a blanketing (i.e. oxygen inhibiting inert gas) agent during magnesium

production. Hence SF_6 will have many, and more diffuse, sources relative to the other perfluorinated species. Its atmospheric trend has been predicted to rise at a rate faster than linear, as older electrical switchgear is switched to higher efficiency units.

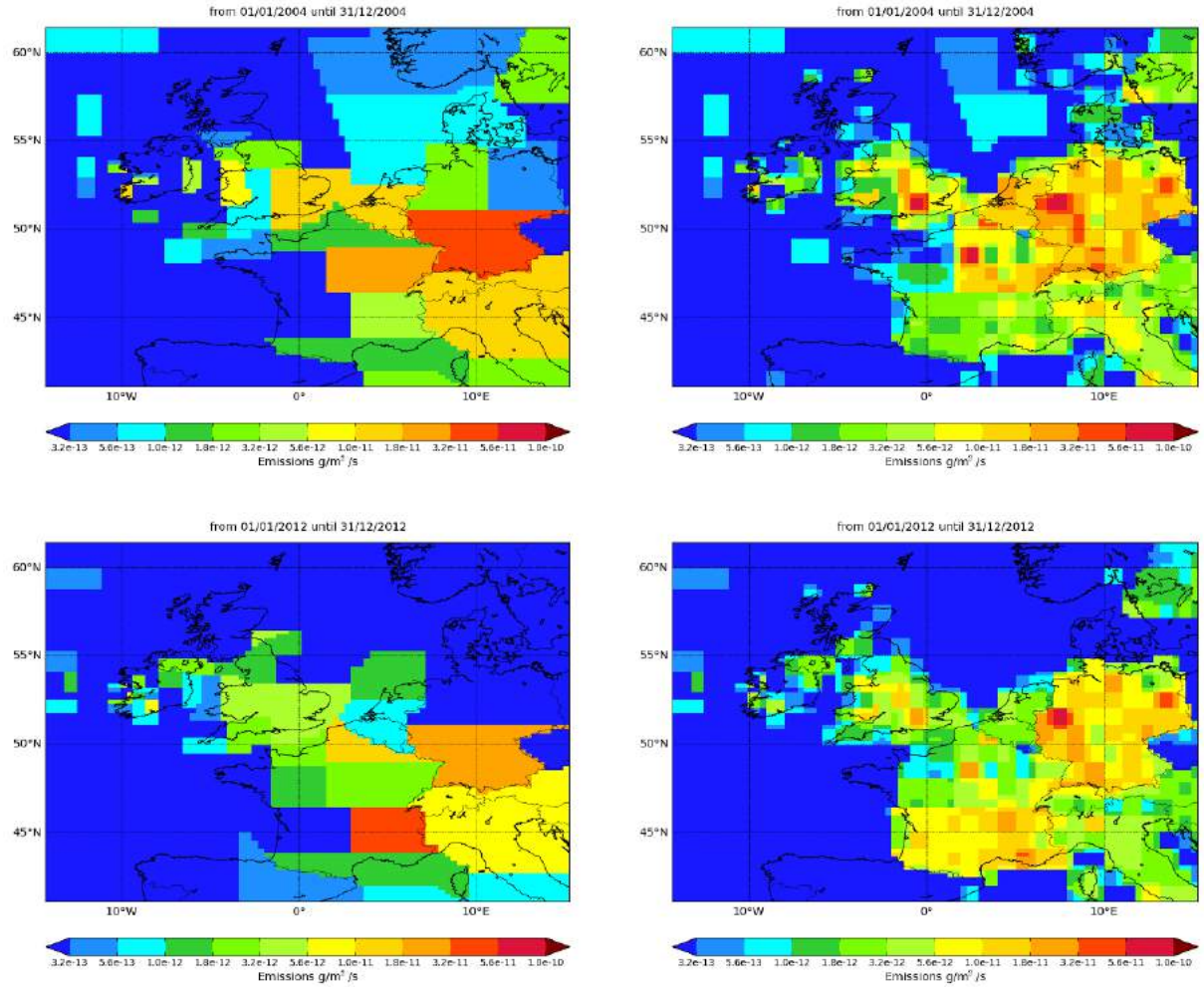

Figure 68: NAME-inversion emission estimates for 2004 (upper) and 2012 (lower). On the right hand side the emissions per grid box have been re-distributed based on population.

The InTEM estimates are consistently elevated compared to the inventory, however, for the UK at least, the InTEM uncertainty ranges do encompass the inventory estimates. The statistical match between the model time-series and the observations is fair.

Year	RMSE (ppt)	Correlation	Max obs. above baseline (ppt)	% obs. above baseline noise	Mean obs. above baseline (ppt)
2004	0.07	0.53	0.82	23	0.07
2012	0.04	0.28	0.35	29	0.04

Table 30: Comparison between modelled and observed time-series.

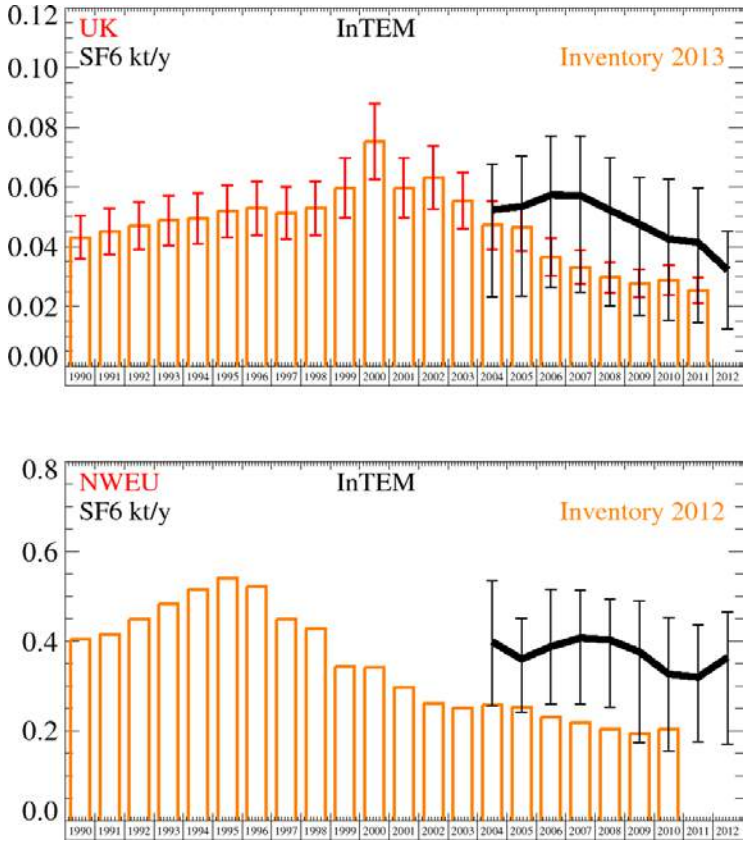

Figure 69: Emission (kt/y) estimates for UK and NWEU. The uncertainty bars represent the 5th and 95th percentiles.

Unit	Year	UK	(5th-95th)	NWEU	(5th-95th)
t/y	2004	52	(23.- 68.)	400	(255.- 535.)
t/y	2005	53	(23.- 70.)	360	(242.- 451.)
t/y	2006	57	(26.- 77.)	390	(260.- 516.)
t/y	2007	57	(25.- 77.)	410	(260.- 514.)
t/y	2008	52	(20.- 70.)	400	(252.- 494.)
t/y	2009	48	(17.- 63.)	380	(174.- 490.)
t/y	2010	43	(15.- 62.)	330	(153.- 452.)
t/y	2011	41	(15.- 60.)	320	(176.- 437.)
t/y	2012	32	(12.- 45.)	360	(170.- 465.)

Table 31: Emission (t/y) estimates for UK and NWEU with uncertainty (5th – 95th %ile).

5.13.1 SF_6 emissions estimated using the extended UK DECC network

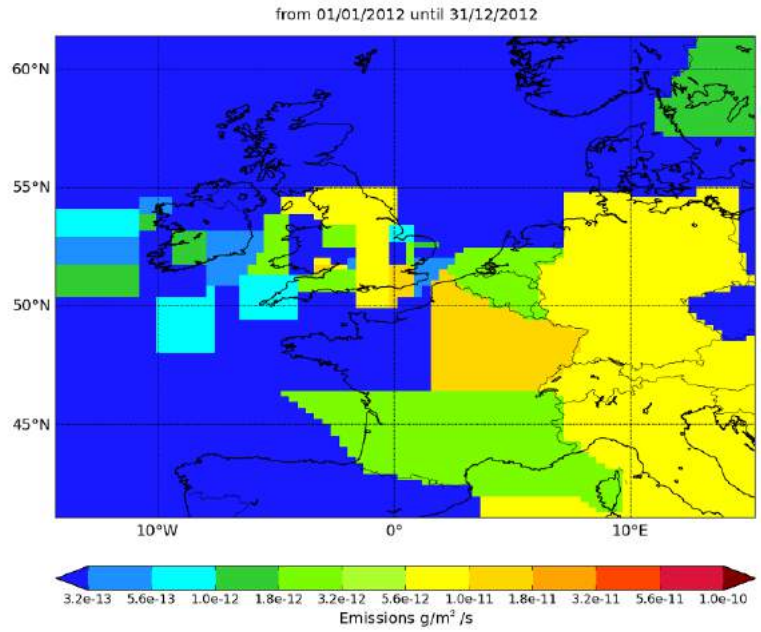

Figure 70: InTEM distribution of SF_6 emissions in 2012 using 3 sites.

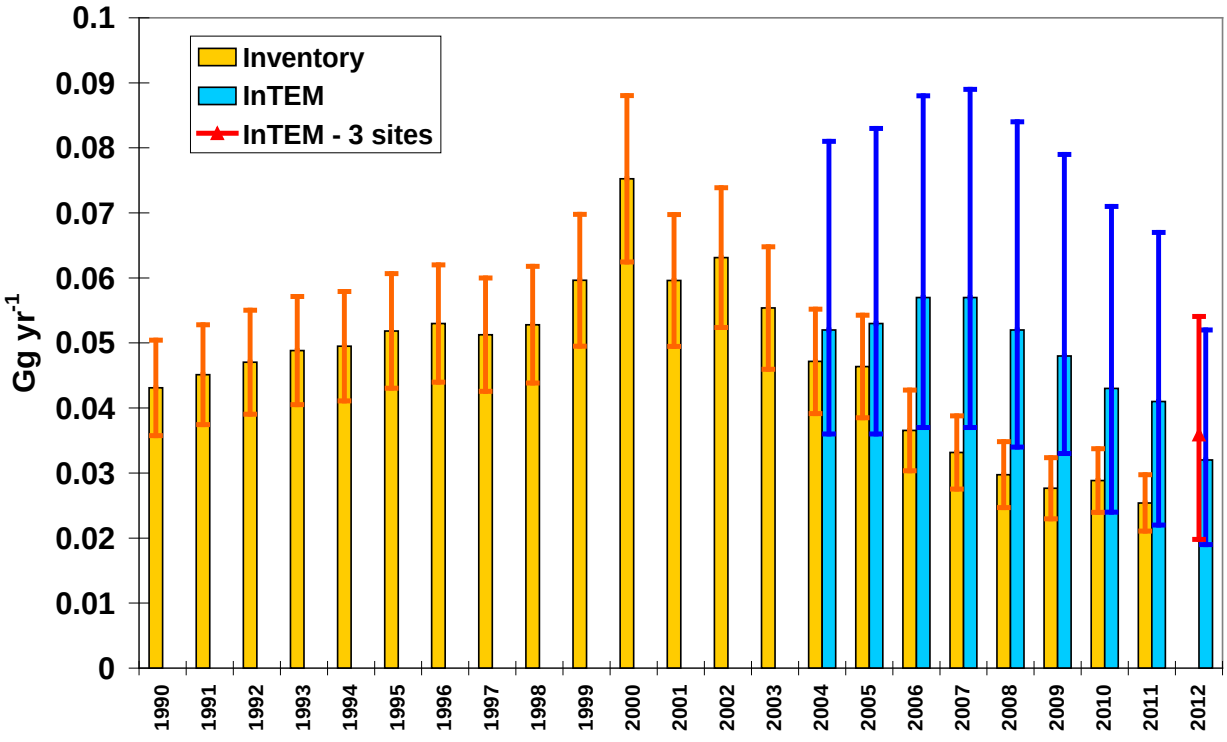

Figure 71: Comparison of 3-site InTEM results (Gg/yr = kt/yr) for the UK with the Mace Head (MHD) only results and UK Greenhouse Gas Inventory (GHGI) for SF_6.

As SF_6 is predominately released from electrical switchgear it is reasonable to assume that there is little seasonal variability in the emissions. The comparison between the 1-site (over 3 years) and 3-site InTEM results are very encouraging given that the 2 new UK sites do not have a complete year of data.

5.14 Methane (CH_4)

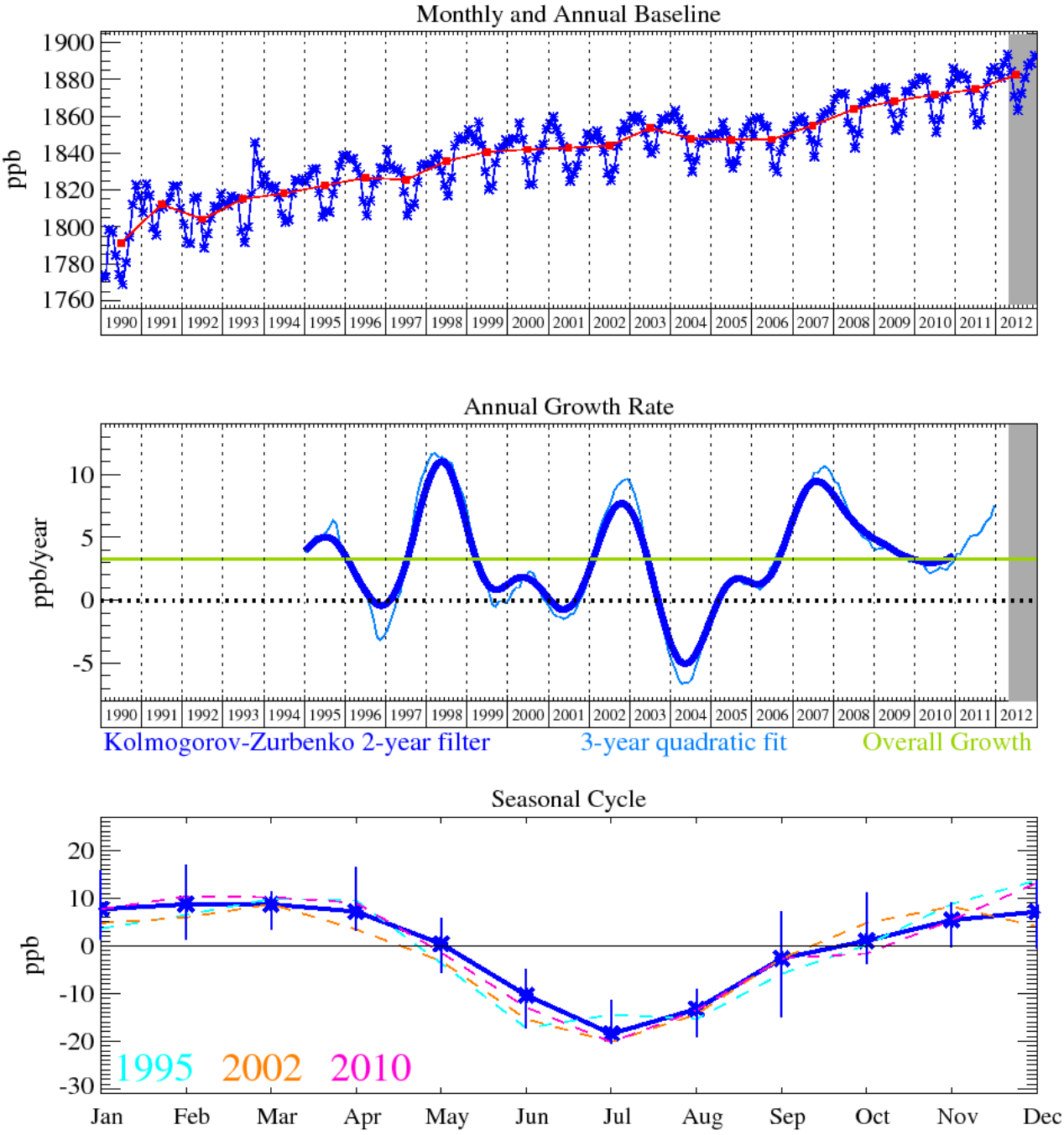

Figure 72: Methane: Monthly (blue) and annual (red) baseline concentrations (top plot). Annual (blue) and overall average growth rate (green) (middle plot). Seasonal cycle (de-trended) with year-to-year variability (lower plot). Grey area covers un-ratified and therefore provisional data.

The long term trend for CH_4, shown in Figure 72, is of particular interest with a steep rise up to about 2000 followed by a flat period with almost no growth and then most recently a steep rise of up to 9 ppb/yr over the period 2007-2008. Recent growth is estimated to be 5.3 ppb/yr with a mixing ratio of 1893 ppb in December 2012. The growth rate anomaly in 2007-2008 is unusual in that it occurred almost simultaneously in both hemispheres.

In our annual report in 2009 we discussed how the mole fraction of CH_4 in the atmosphere had been rising considerably faster than its long-term average growth rate. Several theories were postulated:

(1) Increased emissions from the high latitudes in the Northern hemisphere related to wetlands and reduced permafrost/snow cover.
(2) Increased emissions in the tropics due to increased emissions from wetlands/rice production or biomass burning due to El Niňo conditions.
(3) Reduced levels of OH in the atmosphere. OH is the major sink for atmospheric CH_4.

However each of these theories in isolation does not seem to completely fit the evidence gathered so far. For example, there is no evidence for any link to large scale biomass burning (i.e. no concomitant increase in carbon monoxide), as was the case in 1998 - driven by the largest ever El Nino drought.

The inferences drawn from the observations were that the CH_4 increase is driven by wetland emissions in the boreal region (driven by a temperature anomaly) and in the tropics (possibly driven by a precipitation anomaly) with a small role for OH changes a possibility in the tropics but not statistically significant. Satellite observations have also detected an increase in global mixing ratios in recent years [Bloom *et al*., 2010] and identified increased wetland emissions as a potential cause, consistent with *in situ* measurements. The mole fraction of CH_4 reported from Mace Head (and other AGAGE stations) in 2009 indicate that the rapid rise in CH_4 mole fractions has slowed (as shown in Figure 72). Future trends of CH_4 are uncertain but very important as CH_4 has a strong influence on radiative forcing and stratospheric ozone depletion.

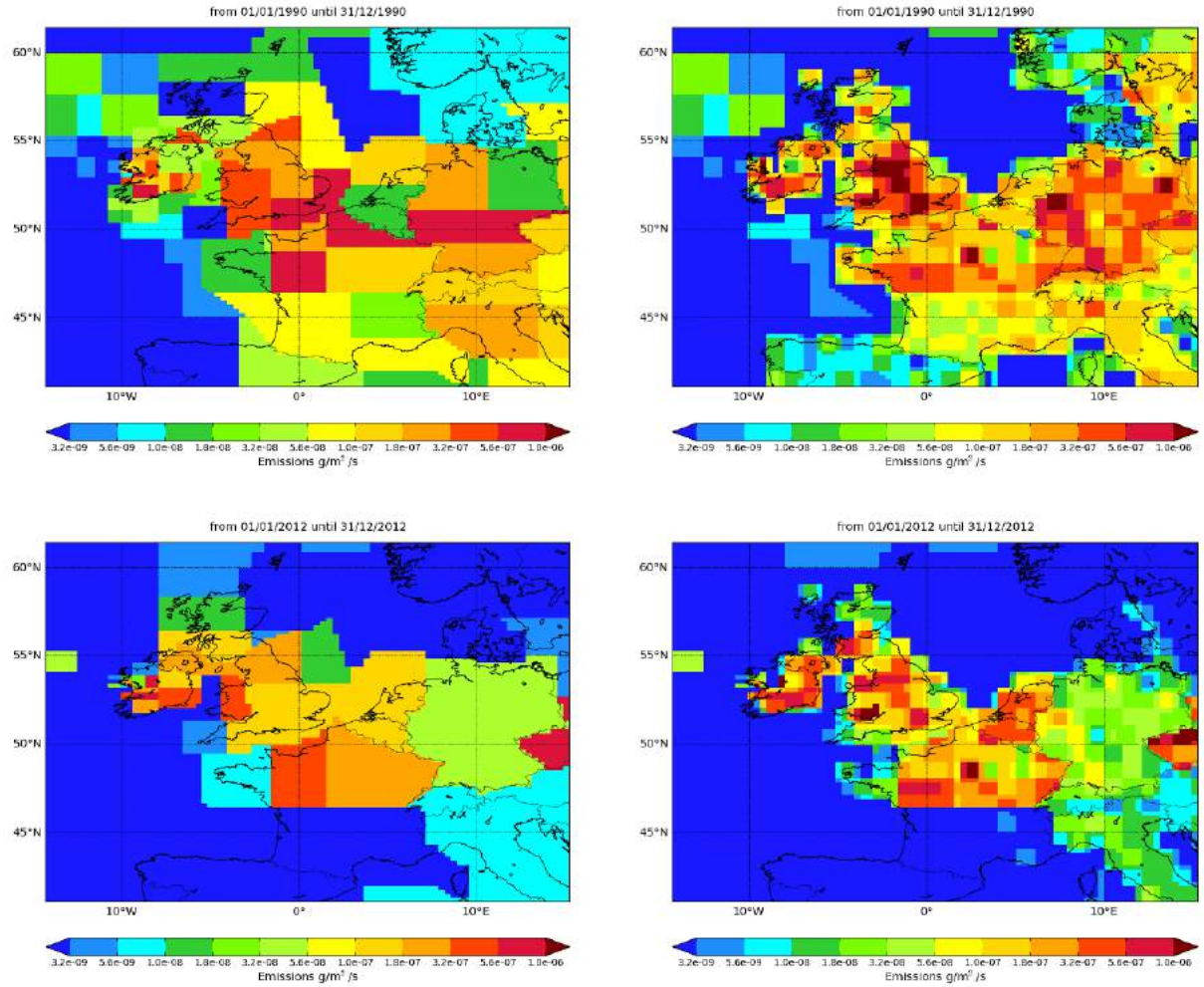

Figure 73: NAME-inversion emission estimates for 1990 (upper) and 2012 (lower). On the right hand side the emissions per grid box have been re-distributed based on population.

The inventory and InTEM emission estimates for the UK are similar from 2000 onwards, with the median InTEM estimates consistently above. In the early to mid 1990s the InTEM estimates for the UK were markedly lower than the inventory values, however throughout the entire period the uncertainty ranges from the two methods largely overlap. A similar but less pronounced picture is seen in the results for NWEU. The pollution events seen at Mace Head are regular and strong and the statistical match between the modelled time-series and the observations is good.

Year	RMSE (ppb)	Correlation	Max obs. above baseline (ppb)	% obs. above baseline noise	Mean obs. above baseline (ppb)
1990	18.7	0.65	252	32	26
2012	13.7	0.84	183	39	26

Table 32: Comparison between modelled and observed time-series.

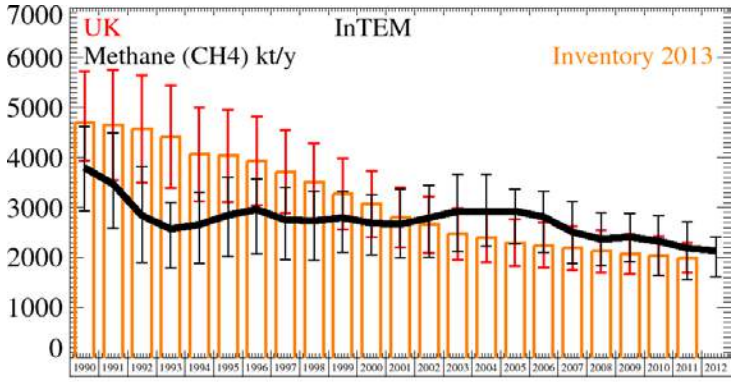

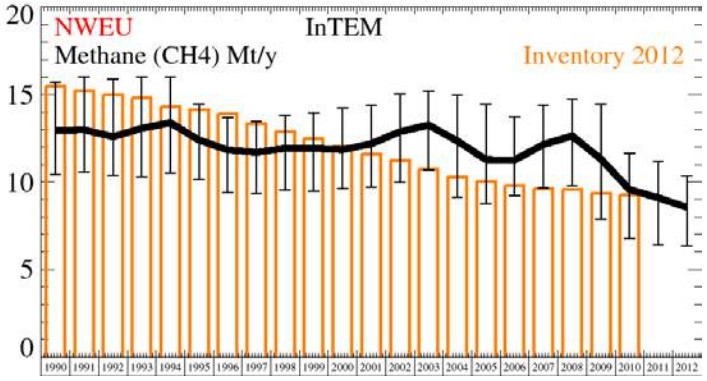

Figure 74: Emission (kt/y) estimates for UK and NWEU. The uncertainty bars represent the 5th and 95th percentiles.

Unit	Year	UK	(5th-95th)	NWEU	(5th-95th)
Mt/y	1990	3.8	(2.9- 4.6)	12.9	(10.- 16.)
Mt/y	1991	3.5	(2.6- 4.5)	13	(11.- 16.)
Mt/y	1992	2.8	(1.9- 3.8)	12.6	(10.- 16.)
Mt/y	1993	2.6	(1.8- 3.1)	13.1	(10.- 16.)
Mt/y	1994	2.7	(1.9- 3.3)	13.4	(11.- 16.)
Mt/y	1995	2.8	(2.0- 3.6)	12.4	(10.- 14.)
Mt/y	1996	3	(2.1- 3.6)	11.8	(9.- 14.)
Mt/y	1997	2.8	(2.0- 3.4)	11.7	(9.- 13.)
Mt/y	1998	2.7	(2.0- 3.3)	11.9	(10.- 14.)
Mt/y	1999	2.8	(2.1- 3.3)	11.9	(9.- 14.)
Mt/y	2000	2.7	(2.0- 3.3)	11.9	(10.- 14.)
Mt/y	2001	2.7	(2.0- 3.4)	12.2	(10.- 14.)
Mt/y	2002	2.8	(2.0- 3.4)	12.9	(10.- 15.)
Mt/y	2003	2.9	(2.1- 3.7)	13.3	(11.- 15.)
Mt/y	2004	2.9	(2.2- 3.7)	12.4	(9.- 15.)
Mt/y	2005	2.9	(2.3- 3.4)	11.3	(9.- 14.)
Mt/y	2006	2.8	(2.1- 3.3)	11.3	(9.- 14.)
Mt/y	2007	2.5	(1.9- 3.1)	12.1	(10.- 14.)
Mt/y	2008	2.4	(1.8- 2.9)	12.6	(10.- 15.)
Mt/y	2009	2.4	(1.9- 2.9)	11.3	(8.- 14.)
Mt/y	2010	2.3	(1.7- 2.8)	9.6	(7.- 12.)
Mt/y	2011	2.2	(1.6- 2.7)	9.1	(6.- 11.)
Mt/y	2012	2.1	(1.6- 2.4)	8.6	(6.- 10.)

Table 33: Emission (Mt/y) estimates for UK and NWEU with uncertainty (5th – 95th %ile).

5.14.1 CH_4 emissions estimated using the extended UK DECC network

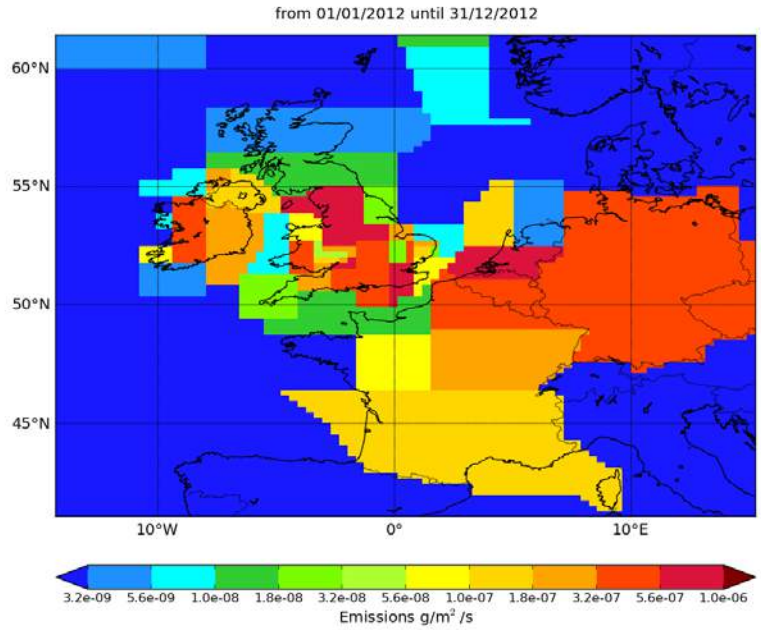

Figure 75: InTEM distribution of CH_4 emissions in 2012 using 3 sites.

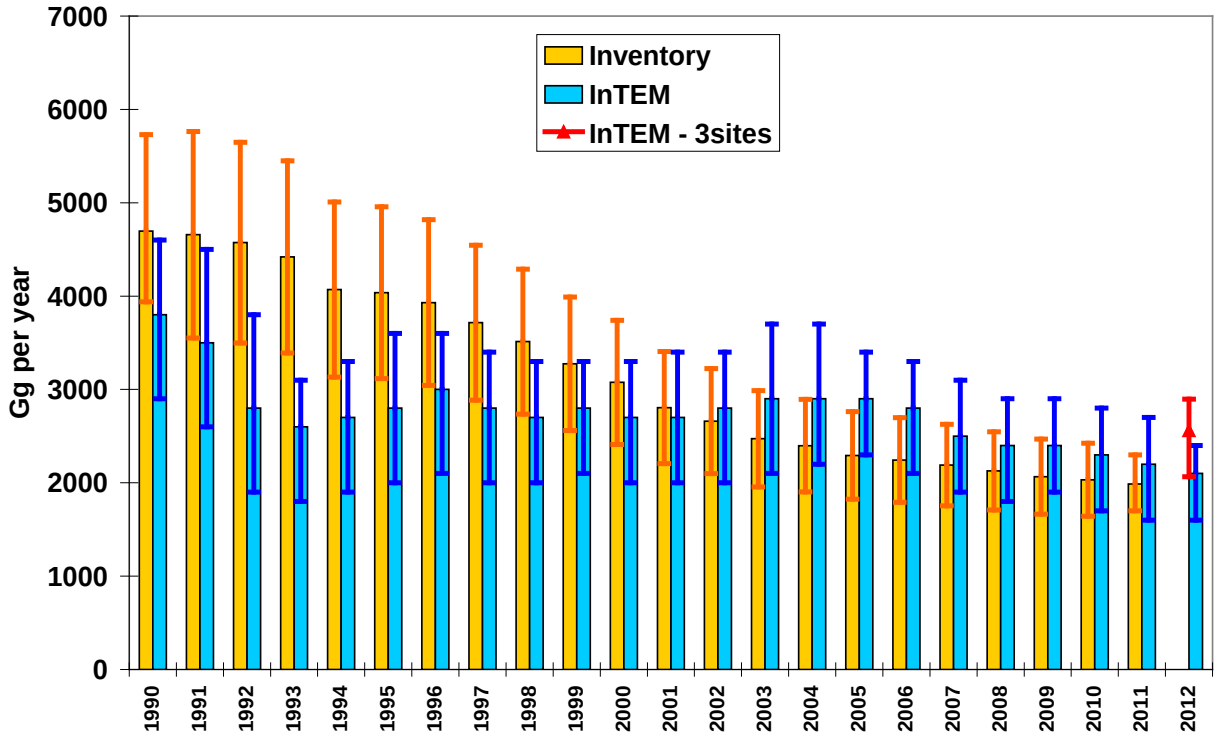

Figure 76: Comparison of 3-site InTEM results (Gg/yr = kt/yr) for the UK with the MHD-only results and UK GHGI for CH_4.

The uncertainty in the 3-site InTEM results for CH_4 overlap to a good degree with the 1-site InTEM results. However, it is tempting to infer that the emissions in the UK in the latter part of 2012 were elevated compared to the full year (NB. based on data spanning 3-years). However caution needs to be stressed. A complete year of observations will be needed to fully understand whether this is indeed the case. Inversion studies from each separate station and combined in different station combinations will be needed to fully explore the benefit of the data from the new stations and to understand the uncertainty in the inversion results.

5.15 Nitrous oxide (N_2O)

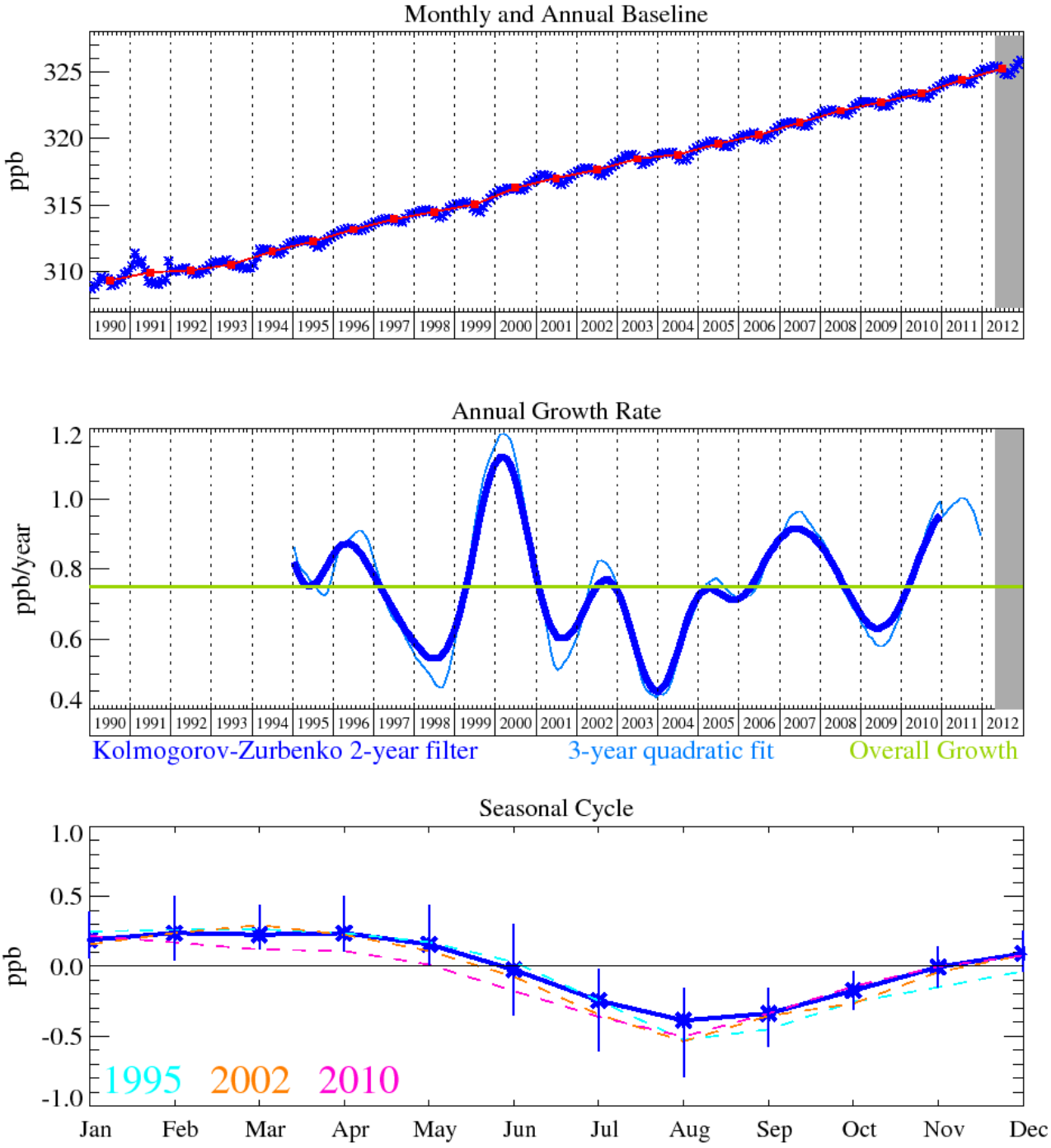

Figure 77: Nitrous oxide: Monthly (blue) and annual (red) baseline concentrations (top). Annual (blue) and overall growth rate (green) (middle). Seasonal cycle (de-trended) with year-to-year variability (lower plot). Grey area covers un-ratified and therefore provisional data.

Figure 77 shows the baseline monthly means and trend for N_2O with an almost linear upwards average trend of 0.72 ppb/yr. The most recent growth rate is estimated to be 0.97 ppb/yr. The mixing ratio in December 2012 was 325.8 ppb at Mace Head. The N_2O increase is attributable to human activities, such as fertilizer use and fossil fuel burning, although it is also emitted through natural processes occurring in soils and oceans. There are large uncertainties associated with the quantifying the sources of this gas. The global growth anomaly in N_2O is of particular interest with a very substantial increase in 2010-2011. At Mace Head the average historical growth rate of about 0.7 ppb/year has increased to over 0.8 ppb/year. Similarly in the Southern Hemisphere at Cape Grim, Tasmania the growth rate has increased from about 0.6 ppb/year in 2003 to about 1

ppb/year in 2011. Increases in N_2O emissions also may be linked to the tropics where 'wet and warm' microbes in soil can produce bursts in N_2O production, although this is contrary to reports where very saturated soils can decrease N_2O emissions, However, as noted by Dr R. Weiss of Scripps Institution of Oceanography, there may be different spatial distributions of "wetness" with increased N_2O emissions in some regions and decreases in others. Interestingly, hydrogen has also exhibited a growth spurt in 2011. Here wet soils tend to reduce the normal H_2 deposition velocities due to a reduction in diffusivity. At this stage more global sites need to be carefully assessed to confirm these increases in the N_2O growth rate. We expect AGAGE, in collaboration with NOAA, to address these issues in a forthcoming paper.

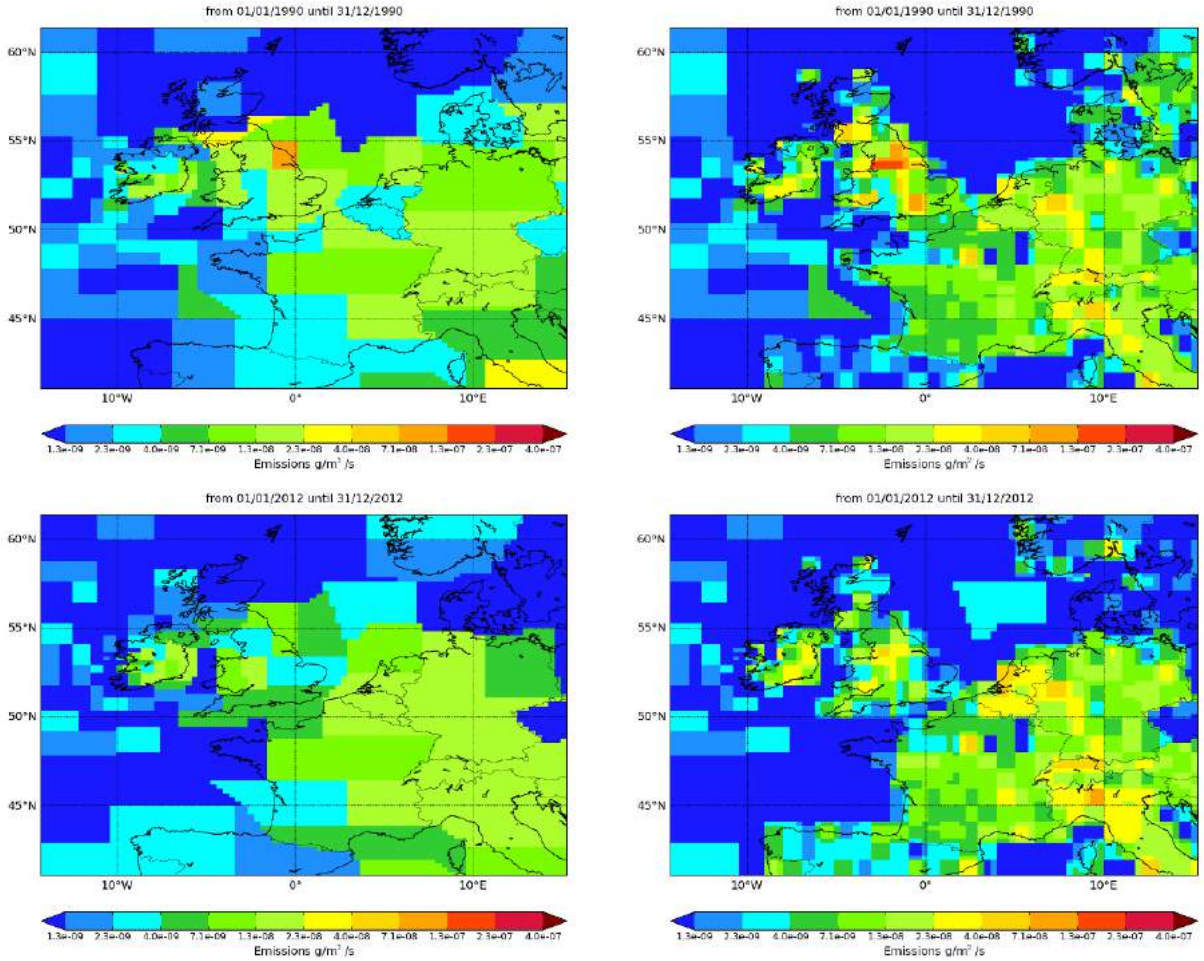

Figure 78: NAME-inversion emission estimates for 1990 (upper) and 2012 (lower). On the right hand side the emissions per grid box have been re-distributed based on population.

Year	RMSE (ppb)	Correlation	Max obs. above baseline (ppb)	% obs. above baseline noise	Mean obs. above baseline (ppb)
1990	0.62	0.48	4.6	25	0.64
2012	0.25	0.68	3.4	33	0.35

Table 34: Comparison between modelled and observed time-series.

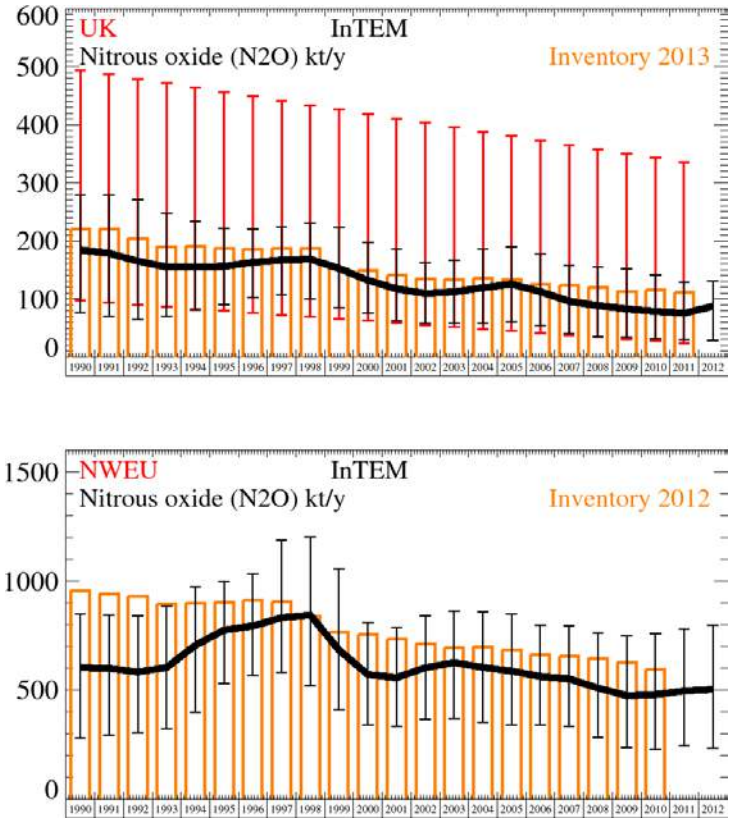

Figure 79: Emission (kt/y) estimates for UK and NWEU. The uncertainty bars represent the 5th and 95th percentiles.

Unit	Year	UK	(5th-95th)	NWEU	(5th-95th)
kt/y	1990	184	(77.- 279.)	600	(280.- 850.)
kt/y	1991	179	(70.- 279.)	600	(293.- 844.)
kt/y	1992	165	(65.- 271.)	580	(303.- 843.)
kt/y	1993	155	(70.- 247.)	600	(323.- 883.)
kt/y	1994	155	(81.- 234.)	710	(399.- 973.)
kt/y	1995	156	(90.- 222.)	780	(529.- 999.)
kt/y	1996	163	(102.- 221.)	790	(566.-1033.)
kt/y	1997	167	(107.- 224.)	830	(579.-1189.)
kt/y	1998	169	(100.- 231.)	840	(519.-1203.)
kt/y	1999	153	(84.- 223.)	680	(409.-1058.)
kt/y	2000	132	(75.- 198.)	570	(342.- 810.)
kt/y	2001	118	(62.- 185.)	560	(334.- 788.)
kt/y	2002	109	(58.- 163.)	600	(367.- 843.)
kt/y	2003	112	(58.- 167.)	630	(370.- 862.)
kt/y	2004	119	(59.- 186.)	600	(350.- 859.)
kt/y	2005	125	(60.- 190.)	590	(342.- 849.)
kt/y	2006	113	(55.- 177.)	560	(339.- 797.)
kt/y	2007	96	(40.- 157.)	550	(333.- 794.)
kt/y	2008	89	(35.- 155.)	510	(282.- 763.)
kt/y	2009	83	(35.- 152.)	470	(235.- 750.)
kt/y	2010	79	(31.- 142.)	480	(231.- 758.)
kt/y	2011	76	(29.- 129.)	500	(246.- 782.)
kt/y	2012	87	(29.- 130.)	500	(232.- 797.)

Table 35: Emission (kt/y) estimates for UK and NWEU with uncertainty (5th – 95th %ile).

5.15.1 N_2O emissions estimated using the extended UK DECC network

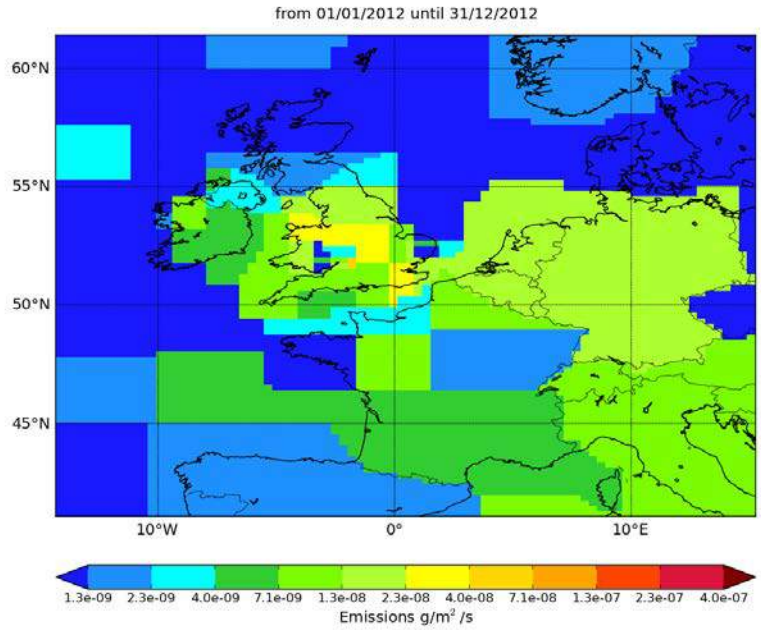

Figure 80: InTEM distribution of N_2O emissions in 2012 using 3 sites

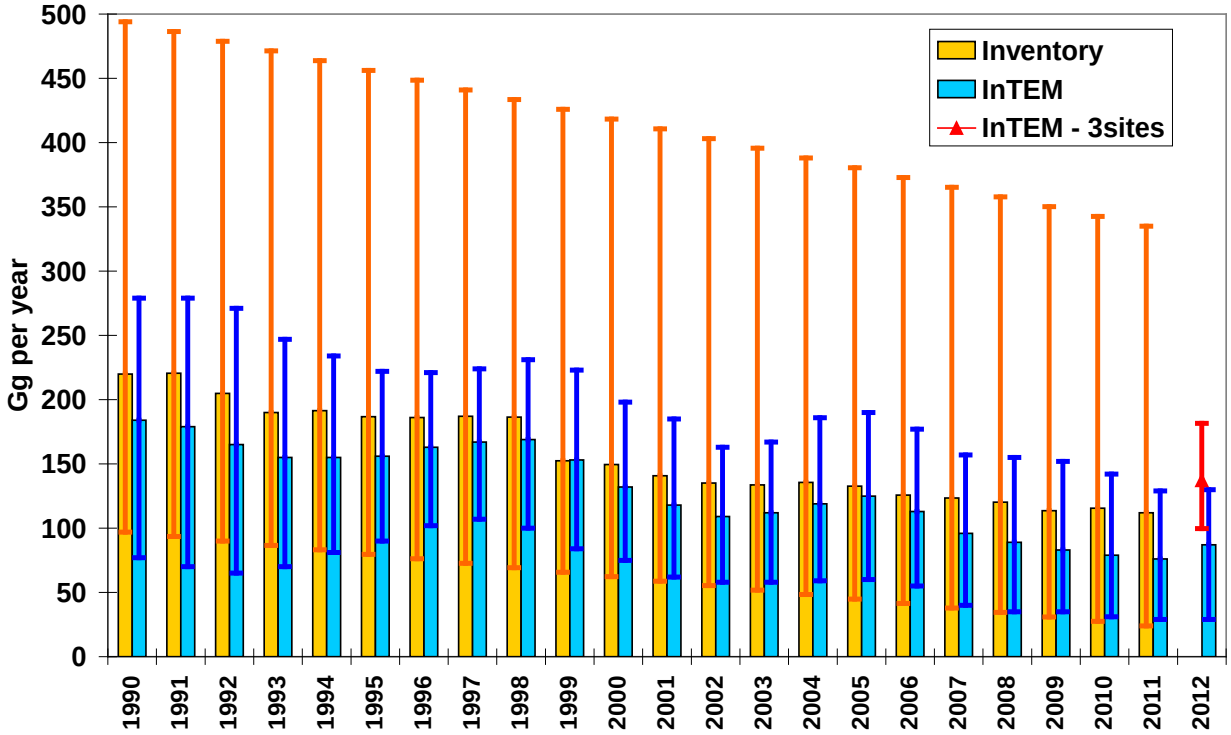

Figure 81: Comparison of 3-site InTEM results (Gg/yr = kt/yr) for the UK with the MHD-only results and UK GHGI for N_2O.

Although the uncertainty in the 3-site InTEM results for N_2O overlap to some degree, it is tempting to infer that the emissions in the UK in the latter part of 2012 were elevated compared to the full year (NB. based on data spanning 3-years). However caution needs to be stressed. A complete year of observations will be needed to fully understand whether this is indeed the case. Inversion studies from each separate station and using different station combinations will be needed to fully explore the benefit of the data from the new stations and to understand the uncertainty in the inversion results.

5.16 Carbon dioxide (CO_2)

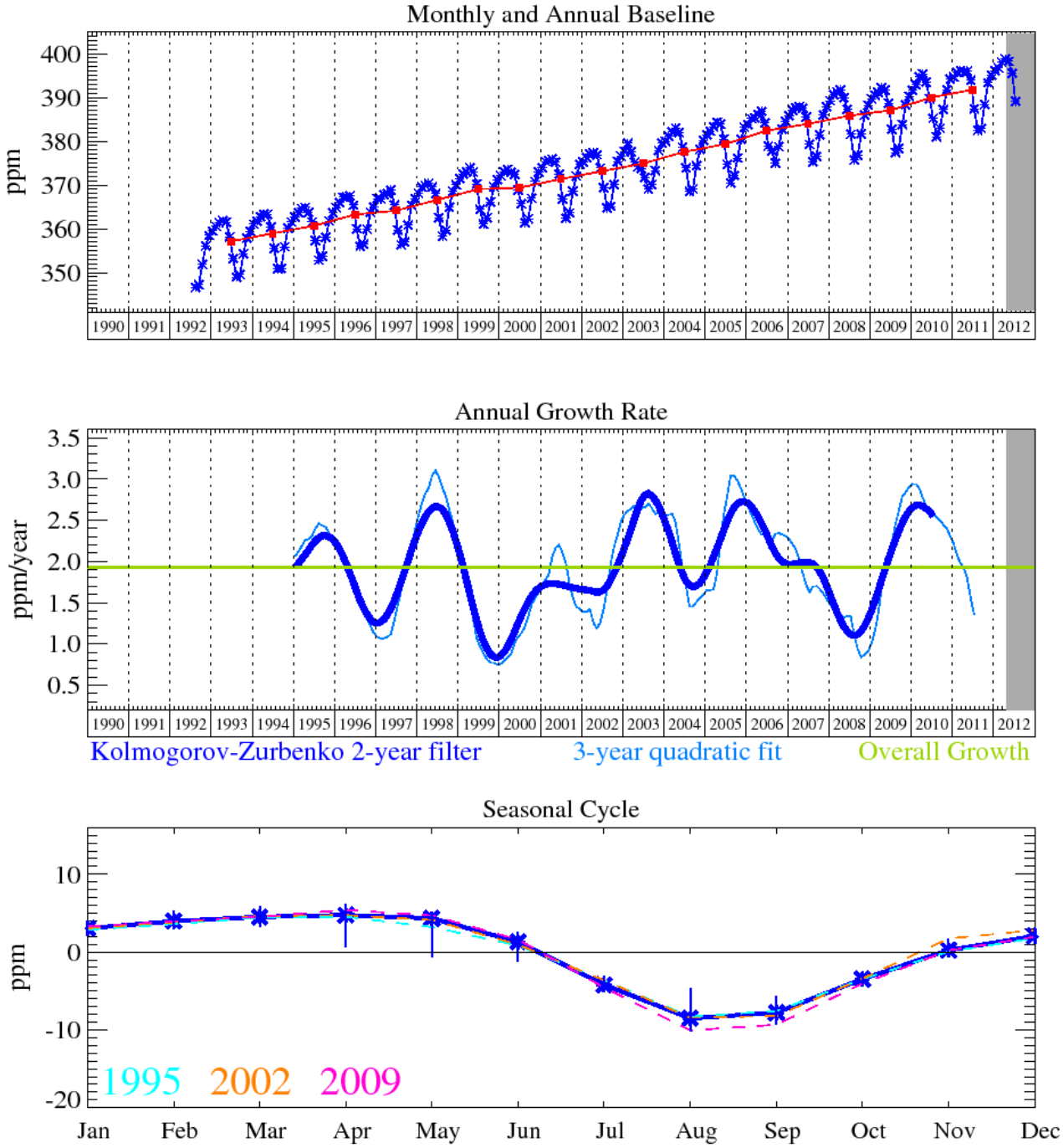

Figure 82: Carbon dioxide (CO_2): Monthly (blue) and annual (red) baseline concentrations (top plot). Annual (blue) and overall average growth rate (green) (middle plot). Seasonal cycle (de-trended) with year-to-year variability (lower plot). Grey area covers un-ratified and therefore provisional data.

CO_2 (Figure 82) is the most important greenhouse gas, and has steadily grown at an annual average rate of 1.9 ppm/yr, calculated from the baseline-selected monthly means. The most recent growth rate is estimated to be 2.1 ppm/yr. It has now reached a mixing ratio of 399 ppm (April 2012) which is the highest yet recorded at Mace Head, Ireland, and has shown significant growth rate anomalies in 1998/99 and 2002/03, which we suggest are a result of the global biomass burning events in those years.

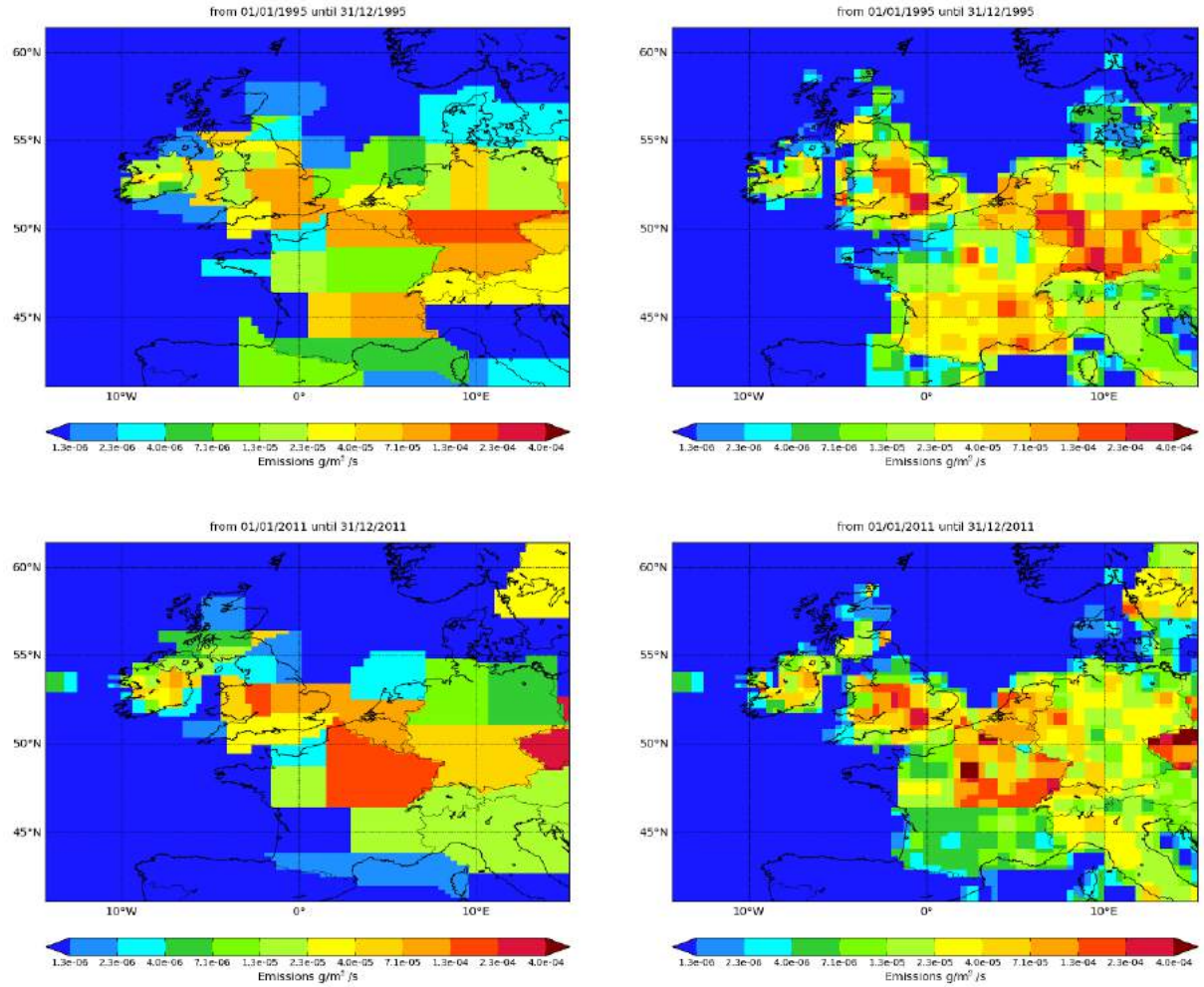

Figure 83: NAME-inversion emission estimates for 1995 (upper) and 2011 (lower). On the right hand side the emissions per grid box have been re-distributed based on population.

In the table below only the January and December CO_2 observations from Mace Head have been used. It is assumed that during these cold and dark months the biogenic emissions and removals are negligible.

Year	RMSE (ppm)	Correlation	Max obs. above baseline (ppm)	% obs. above baseline noise	Mean obs. above baseline (ppm)
1995	4.3	0.81	22	64	7.2
2011	1.3	0.66	8	37	1.6

Table 36: Comparison between modelled and observed time-series.

Plants both respire CO_2 and absorb it through photosynthesis. Therefore the CO_2 flux from vegetation has a diurnal and seasonal cycle and switches from positive to negative on a daily basis. This unknown natural (biogenic) component of the observed CO_2 is significant when compared to the anthropogenic (man-made) component and cannot be assumed negligible (except during the winter months). From the CO_2 mole fractions it is impossible to distinguish between biogenic and anthropogenic CO_2. Therefore it is difficult to use the CO_2 mole fractions directly in an inversion to estimate anthropogenic emissions because the diurnally varying biogenic CO_2 flux is contrary to the inversion method assumption of temporally invariant emissions. Methods are under development to attempt to over-come these challenges, such as the use of isotopic observations, through ratios with respect to anthropogenic CO and through the use of just the winter-time observations. The uncertainties associated with each of these methods are predicted to be significant.

The preliminary results for UK and NWEU emissions of CO_2 using the InTEM inversion results for CO are presented. The InTEM CO emission maps have been scaled by the annually varying UK inventory ratio of CO_2:CO emissions. The InTEM uncertainties has been arbitrarily increased by 50% to reflect the fact that the CO_2:CO ratio is variable across applications across the UK. The estimated uncertainties in the UK inventory are also presented. It can be noted that the uncertainties in the InTEM results are considerably larger than the inventory uncertainties.

The method described here is under review. It is certainly one plausible way forward but other ways are actively being researched. Further work will continue to best use the CO_2 observations to enable better comparisons with the CO_2 inventory estimates.

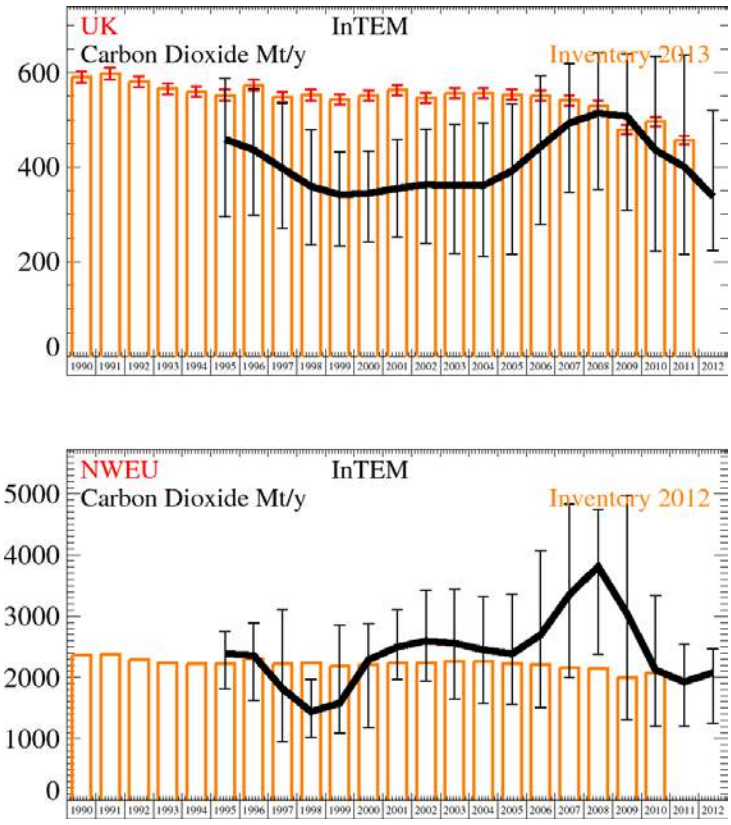

Figure 84: Emission (Mt/y) estimates for UK and NWEU. The uncertainty bars represent the 5th and 95th percentiles.

Unit	Year	UK	(5th-95th)	NWEU	(5th-95th)
Mt/y	1995	460	(350.- 545.)	2400	(2011.-2627.)
Mt/y	1996	440	(345.- 524.)	2400	(1871.-2709.)
Mt/y	1997	400	(312.- 489.)	1820	(1236.-2678.)
Mt/y	1998	360	(277.- 439.)	1440	(1165.-1791.)
Mt/y	1999	340	(270.- 402.)	1580	(1254.-2428.)
Mt/y	2000	340	(276.- 404.)	2300	(1551.-2683.)
Mt/y	2001	360	(286.- 424.)	2500	(2148.-2908.)
Mt/y	2002	360	(280.- 441.)	2600	(2159.-3152.)
Mt/y	2003	360	(265.- 447.)	2600	(1951.-3147.)
Mt/y	2004	360	(260.- 449.)	2500	(1865.-3035.)
Mt/y	2005	390	(275.- 487.)	2400	(1840.-3035.)
Mt/y	2006	440	(333.- 543.)	2700	(1908.-3608.)
Mt/y	2007	490	(395.- 578.)	3400	(2448.-4342.)
Mt/y	2008	510	(407.- 600.)	3800	(2853.-4428.)
Mt/y	2009	510	(374.- 596.)	3100	(1887.-4329.)
Mt/y	2010	440	(293.- 568.)	2100	(1510.-2935.)
Mt/y	2011	400	(277.- 559.)	1930	(1449.-2339.)
Mt/y	2012	340	(262.- 460.)	2100	(1533.-2337.)

Table 37: Emission (Mt/y) estimates for UK and NWEU with uncertainty (5^{th} – 95^{th} %ile).

6 Results and analysis of additional gases

6.1 Introduction

This section discusses the atmospheric trends and regional emissions of the other gases that are measured at Mace Head. The table below describes, if applicable, the principle uses of each of the gases, their radiative efficiency, atmospheric lifetime, global warming potential in a 100-year framework (GWP_{100}) and ozone depleting potential (ODP). In the following sections each of these gases are discussed. The amount of detail provided per gas is dependant on their relative importance as a greenhouse gas (GHG) or ozone-depleting substance.

Gas	Primary use	Radiative Efficiency (W m^{-2} ppb^{-1})	Atmospheric Lifetime (years)	GWP_{100}	ODP
CFC-11	Widespread – discontinued	0.25	45	4,750	1
CFC-12	Refrigerant	0.32	100	10,900	0.82
CFC-113	Coolant, electronics	0.30	85	6,130	0.85
CFC-115	Refrigerant	0.18	1,020	7,230	0.57
HCFC-124	Refrigerant, fire suppression	0.22	5.9	619	0.02
HCFC-141b	Foam blowing	0.14	9.2	717	0.12
HCFC-142b	Chemical synthesis, foam blowing	0.20	17.2	2,220	0.06
HCFC-22	Propellant, air conditioning	0.2	11.9	1,790	0.04
HFC-236fa	Fire extinguisher	0.28	242	9,820	
HFC-245fa	Foam blowing	0.28	7.6	1,020	
HFC-365mfc	Foam blowing	0.22	8.7	842	
HFC-4310mee	Electronics industry	0.40	15.9	1,640	
SO_2F_2	Fumigant		36		
CH_3Cl	Natural, refrigerant	0.01	1	13	0.02
CH_2Cl_2	Foam plastic, solvent, natural		144 days		
$CHCl_3$	Bi-product, natural		149 days		
CCl_4	Fire suppression, precursor	0.13	26	1,400	0.82
CH_3CCl_3	Solvent	0.06	5	146	0.16
$CHClCCl_2$	Degreasing solvent		5 days	5	
CCl_2CCl_2	Solvent, dry cleaning		90 days	15	
CH_3Br	Natural (seaweed), fumigant		0.8		
CH_2Br_2	Natural (seaweed)		123 days		
$CHBr_3$	Natural (seaweed)		24 days		0.66
$CBrClF_2$	Fire suppression (military)	0.3	16	1,890	7.9
$CBrF_3$	Fire suppression	0.32	65	7,140	15.9
$C_2Br_2F_4$	Fire suppression	0.33	20	1,640	13.0
CH_3I	Natural (seaweed)		7 days		
C_2H_6	Combustion, gas leakage				
CO	Combustion		30-90 days		
O_3	Reactions in atmosphere				
H_2	Combustion, photolysis				

Table 38: The principle uses of the gases observed at Mace Head, their radiative efficiency, atmospheric lifetime, global warming potential in a 100 year framework (GWP_{100}) and ozone depleting potential (ODP). The gases listed in red are specifically covered by the Montreal Protocol. All of the gases with a GWP are GHGs but not all GHGs are covered by the Kyoto Protocol.

6.2 CFC-11

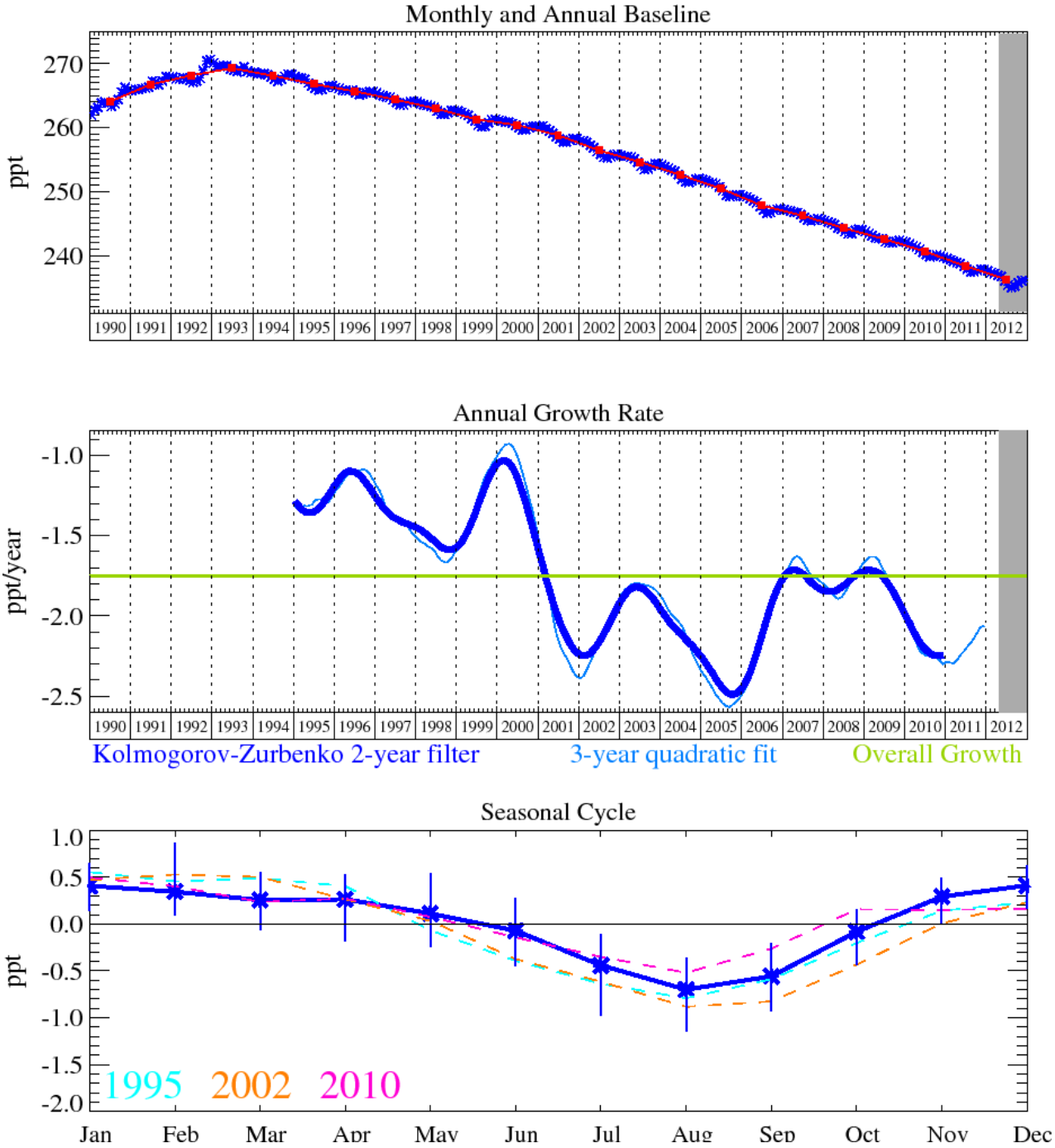

Figure 85: CFC-11 (CCl_3F): Monthly (blue) and annual (red) baseline (top plot). Annual (blue) and overall average growth rate (green) (middle plot). Seasonal cycle (de-trended) with year-to-year variability (lower plot). The grey area covers un-ratified and therefore provisional data.

The time series of mid-latitude northern hemisphere baseline (i.e. pollution, local and southerly events removed) monthly means for atmospheric CFC-11 is shown in Figure 85.

The emissions of all of the CFC compounds have decreased substantially in response to the Montreal Protocol on Substances that Deplete the Ozone Layer, the rate of removal of these compounds by their sinks is limited by their long atmospheric lifetimes.

CFC-11 (45 year lifetime) has declined from its peak year in 1993. Its current rate of decline is 2.2 ppt/yr and by December 2012 its mixing ratio at Mace Head was 236.1 ppt (Figure 85).

It was reported in the 2010 WMO Ozone Assessment, that the decline of CFC-11 and CFC-12 has been smaller than projected. This is most likely due to releases of these compounds from banks being fairly constant over time rather than declining over time as was originally expected. It is also possible that the atmospheric lifetimes of these compounds are potentially longer than reported; this aspect is currently being explored in the forthcoming SPARC lifetimes assessment, and is dealt with in a publication by Rigby *et al.* [2013].

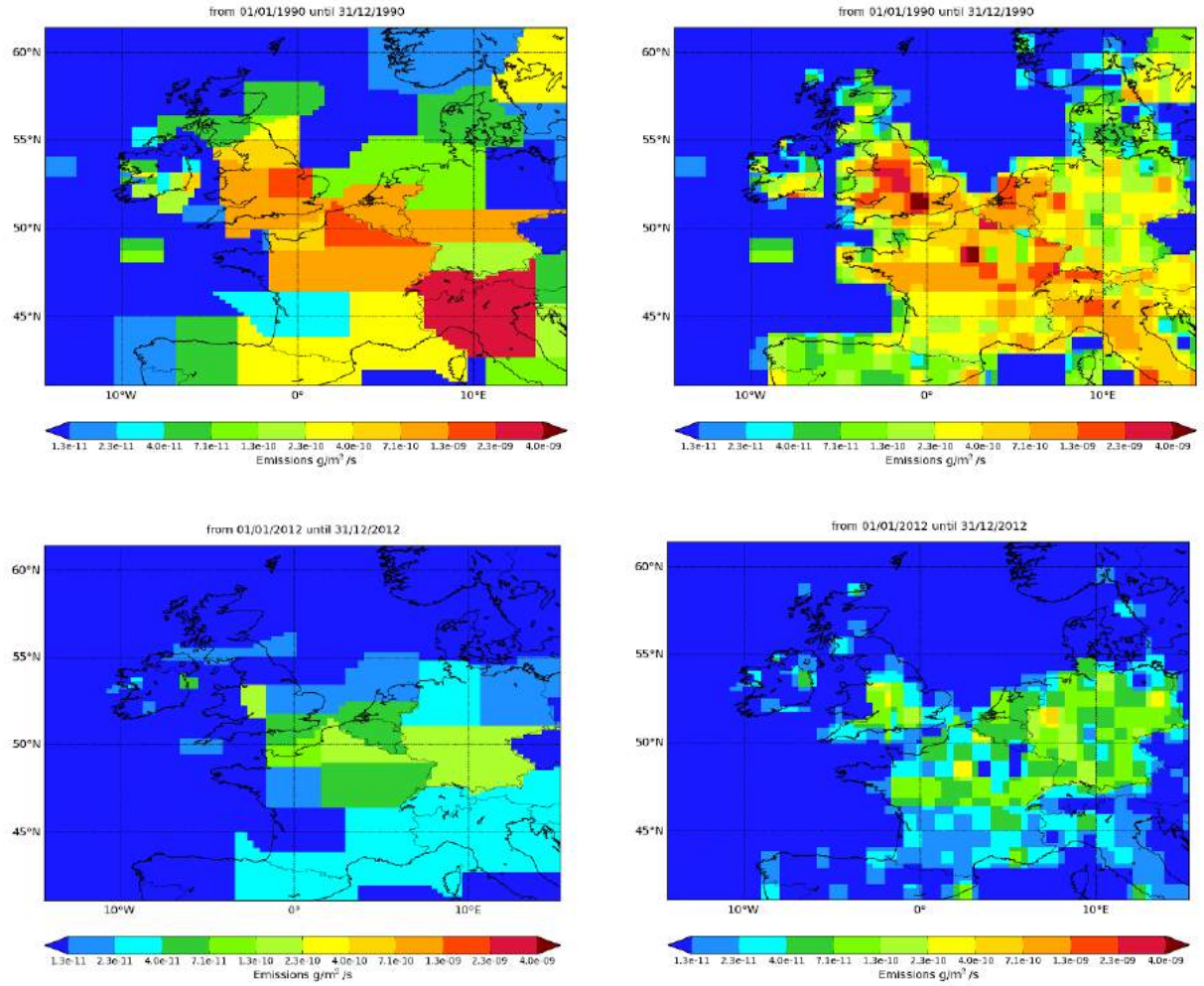

Figure 86: NAME-inversion emission estimates for 1990 (upper) and 2012 (lower). On the right hand side the emissions per grid box have been re-distributed based on population.

The emissions of CFC-11 in both the UK and NWEU as a whole fell very significantly between 1990 and the late 1990s. This clearly shows the impact of the Montreal Protocol, which banned the use of this gas in developed countries from 1995 onwards. The residual emissions reflect the leakage from old appliances e.g. fridges.

Year	RMSE (ppt)	Correlation	Max obs. above baseline (ppt)	% obs. above baseline noise	Mean obs. above baseline (ppt)
1990	4.2	0.78	87.4	34	4.5
2012	0.3	0.31	3.4	20	0.34

Table 39: Comparison between modelled and observed time-series.

In 1990 there were significant pollution events, some events reaching more than 80 ppt above baseline, by 2012 they were barely discernible above baseline. This explains the difference between the RMSE and correlation results in the two years.

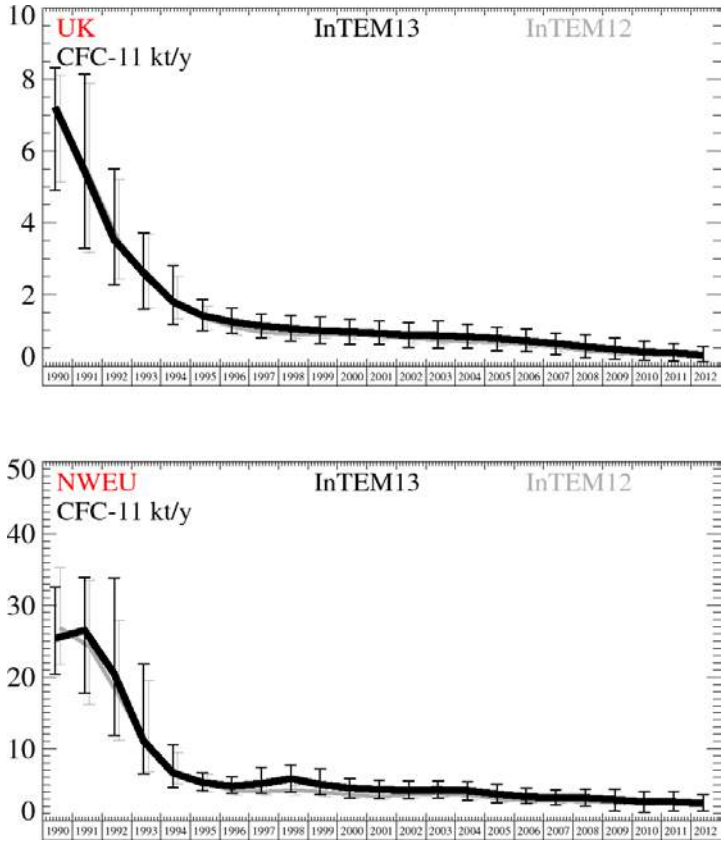

Figure 87: Emission estimates for UK and NWEU. The uncertainty bars represent the 5th and 95th percentiles. Grey line represents the emission estimates presented in last year's report.

Unit	Year	UK	(5th-95th)	NWEU	(5th-95th)
kt/y	1990	7.2	(4.9- 8.3)	25	(20.- 33.)
kt/y	1991	5.4	(3.3- 8.1)	27	(18.- 34.)
kt/y	1992	3.5	(2.3- 5.5)	21	(12.- 34.)
kt/y	1993	2.6	(1.6- 3.7)	11.1	(7.- 22.)
kt/y	1994	1.8	(1.2- 2.8)	6.6	(5.- 11.)
kt/y	1995	1.41	(1.0- 1.9)	5.3	(4.- 7.)
kt/y	1996	1.24	(0.9- 1.6)	4.8	(4.- 6.)
kt/y	1997	1.12	(0.8- 1.5)	5.1	(4.- 7.)
kt/y	1998	1.05	(0.7- 1.4)	5.8	(4.- 8.)
kt/y	1999	0.99	(0.6- 1.4)	5	(4.- 7.)
kt/y	2000	0.96	(0.6- 1.3)	4.5	(3.- 6.)
kt/y	2001	0.91	(0.6- 1.3)	4.3	(3.- 6.)
kt/y	2002	0.86	(0.5- 1.2)	4.2	(3.- 5.)
kt/y	2003	0.85	(0.5- 1.2)	4.3	(3.- 6.)
kt/y	2004	0.82	(0.5- 1.2)	4.2	(3.- 5.)
kt/y	2005	0.78	(0.4- 1.1)	3.7	(2.- 5.)
kt/y	2006	0.7	(0.4- 1.0)	3.3	(2.- 5.)
kt/y	2007	0.63	(0.3- 0.9)	3.2	(2.- 4.)
kt/y	2008	0.55	(0.2- 0.9)	3.2	(2.- 4.)
kt/y	2009	0.47	(0.2- 0.8)	2.9	(1.- 4.)
kt/y	2010	0.39	(0.2- 0.7)	2.6	(1.- 4.)
kt/y	2011	0.37	(0.1- 0.6)	2.6	(1.- 4.)
kt/y	2012	0.31	(0.1- 0.5)	2.4	(1.- 4.)

Table 40: Emission estimates for UK and NWEU with uncertainty (5th – 95th %ile).

6.3 CFC-12

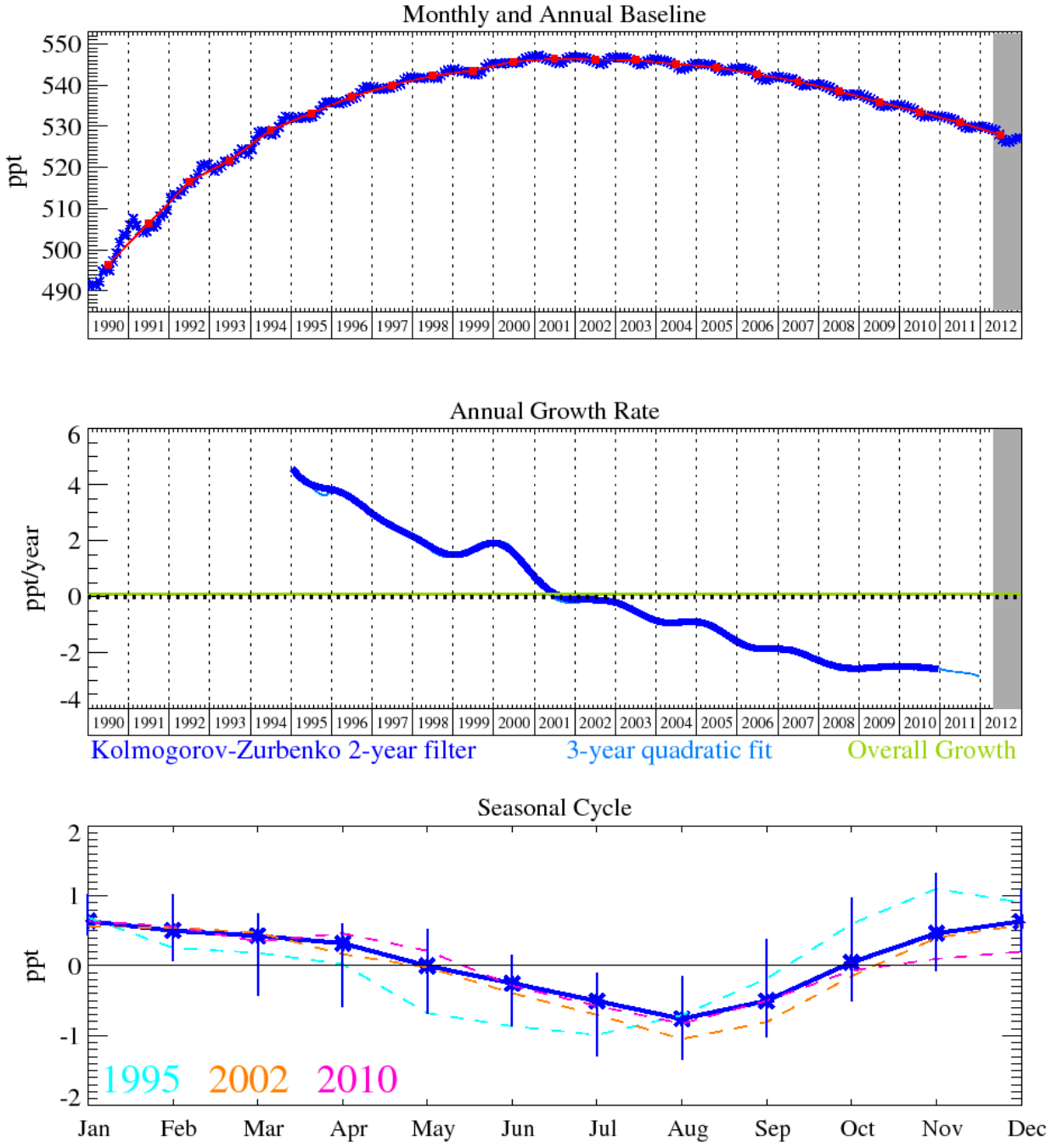

Figure 88: CFC-12: Monthly (blue) and annual (red) baseline (top plot). Annual (blue) and overall average growth rate (green) (middle plot). Seasonal cycle (de-trended) with year-to-year variability (lower plot). The grey area covers un-ratified and therefore provisional data.

CFC-12, which has a 100-year lifetime, is currently declining at a rate of 2.7 ppt/yr reaching a mixing ratio in December 2012 of 527.2 ppt (Figure 88).

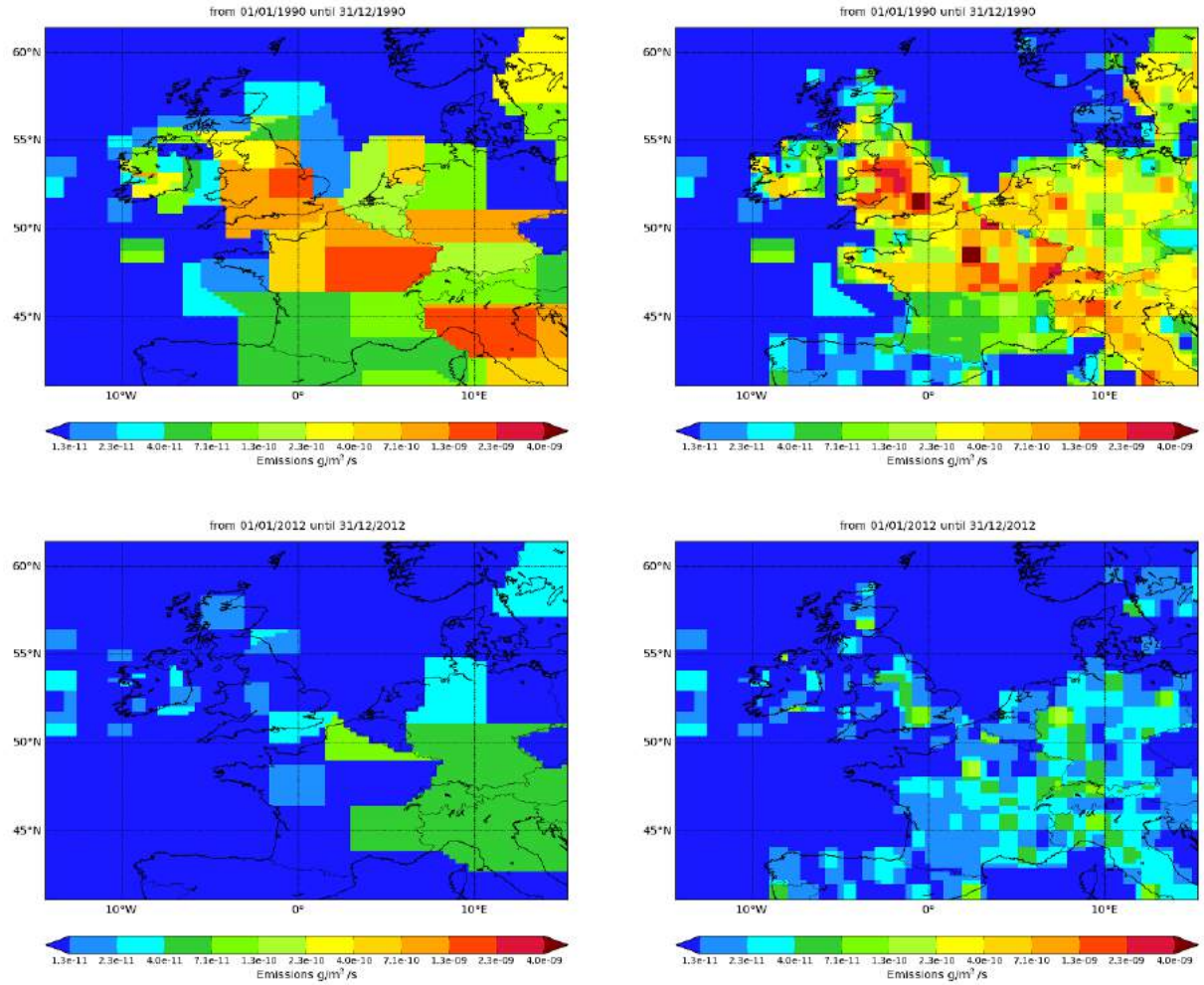

Figure 89: NAME-inversion emission estimates for 1990 (upper) and 2012 (lower). On the right hand side the emissions per grid box have been re-distributed based on population.

The emissions of CFC-12 in both the UK and NWEU as a whole fell very significantly between 1990 and the late 1990s. This clearly shows the impact of the Montreal Protocol, which banned the use of this gas in developed countries from 1995 onwards. The residual emissions reflect the leakage from old appliances.

Year	RMSE (ppt)	Correlation	Max obs. above baseline (ppt)	% obs. above baseline noise	Mean obs. above baseline (ppt)
1990	4.9	0.62	79.2	33	5.33
2012	0.4	0.09	2.7	15	0.28

Table 41: Comparison between modelled and observed time-series.

In 1990 there were significant pollution events, but by 2012 they were barely discernible above baseline. This explains the difference between the RMSE and correlation results in the two years.

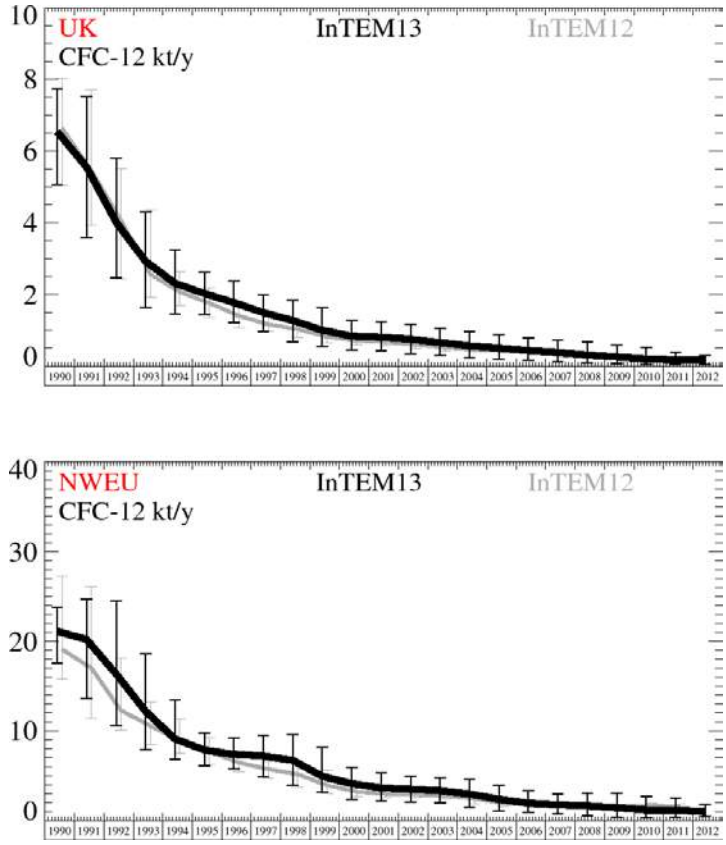

Figure 90: Emission estimates for UK and NWEU. The uncertainty bars represent the 5th and 95th percentiles. Grey line represents the emission estimates presented in last year's report.

Unit	Year	UK	(5th-95th)	NWEU	(5th-95th)
kt/y	1990	6.5	(5.1- 7.7)	21	(18.- 24.)
kt/y	1991	5.6	(3.6- 7.5)	20	(14.- 25.)
kt/y	1992	4	(2.5- 5.8)	16.4	(11.- 25.)
kt/y	1993	2.9	(1.6- 4.3)	12.2	(8.- 19.)
kt/y	1994	2.3	(1.5- 3.2)	9.1	(7.- 13.)
kt/y	1995	2	(1.4- 2.6)	7.9	(6.- 10.)
kt/y	1996	1.77	(1.2- 2.4)	7.4	(6.- 9.)
kt/y	1997	1.49	(1.0- 2.0)	7.2	(5.- 9.)
kt/y	1998	1.27	(0.7- 1.8)	6.7	(4.- 10.)
kt/y	1999	1	(0.5- 1.6)	4.9	(3.- 8.)
kt/y	2000	0.84	(0.5- 1.3)	4.1	(2.- 6.)
kt/y	2001	0.81	(0.4- 1.2)	3.6	(2.- 5.)
kt/y	2002	0.75	(0.4- 1.2)	3.5	(2.- 5.)
kt/y	2003	0.65	(0.3- 1.1)	3.3	(2.- 5.)
kt/y	2004	0.56	(0.2- 1.0)	2.9	(1.- 5.)
kt/y	2005	0.5	(0.2- 0.9)	2.4	(1.- 4.)
kt/y	2006	0.43	(0.2- 0.8)	1.93	(1.- 3.)
kt/y	2007	0.38	(0.1- 0.7)	1.75	(1.- 3.)
kt/y	2008	0.31	(0.1- 0.7)	1.64	(1.- 3.)
kt/y	2009	0.25	(0.1- 0.6)	1.43	(0.- 3.)
kt/y	2010	0.2	(0.0- 0.5)	1.16	(0.- 3.)
kt/y	2011	0.18	(0.0- 0.4)	1.17	(0.- 3.)
kt/y	2012	0.17	(0.1- 0.3)	0.99	(0.- 2.)

Table 42: Emission estimates for UK and NWEU with uncertainty (5th – 95th %ile).

6.4 CFC-113

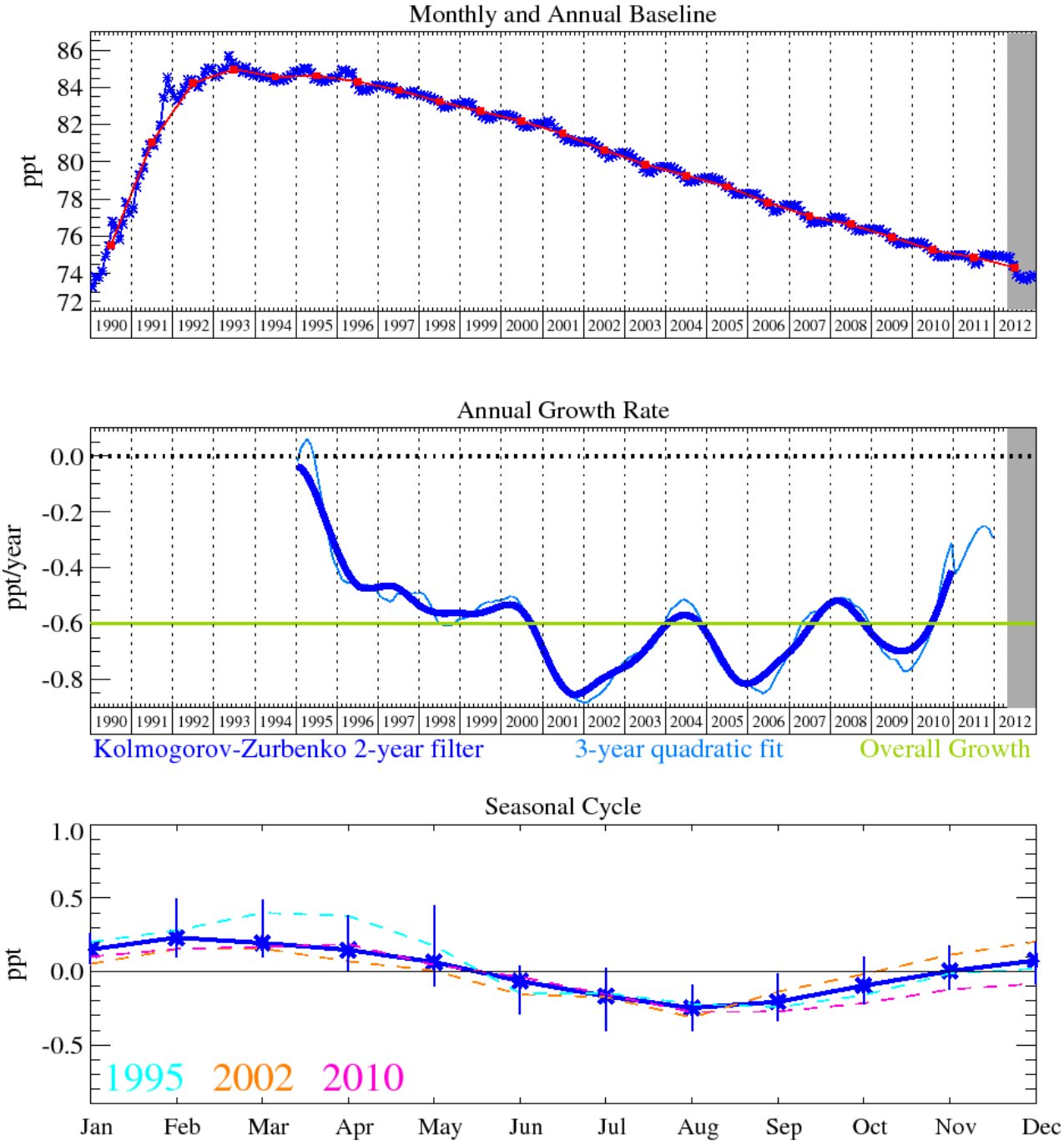

Figure 91: CFC-113 ($C_2Cl_3F_3$): Monthly (blue) and annual (red) baseline concentrations (top plot). Annual (blue) and overall average growth rate (green) (middle plot). Seasonal cycle (de-trended) with year-to-year variability (lower plot). The grey area covers un-ratified and therefore provisional data.

As shown in Figure 91, CFC-113 (85 year lifetime) is currently declining at a rate of 0.6 ppt/yr, by December 2012 it had fallen to 73.9 ppt. Again the decline is less than had been projected and is most likely due to the potential presence of small residual emissions.

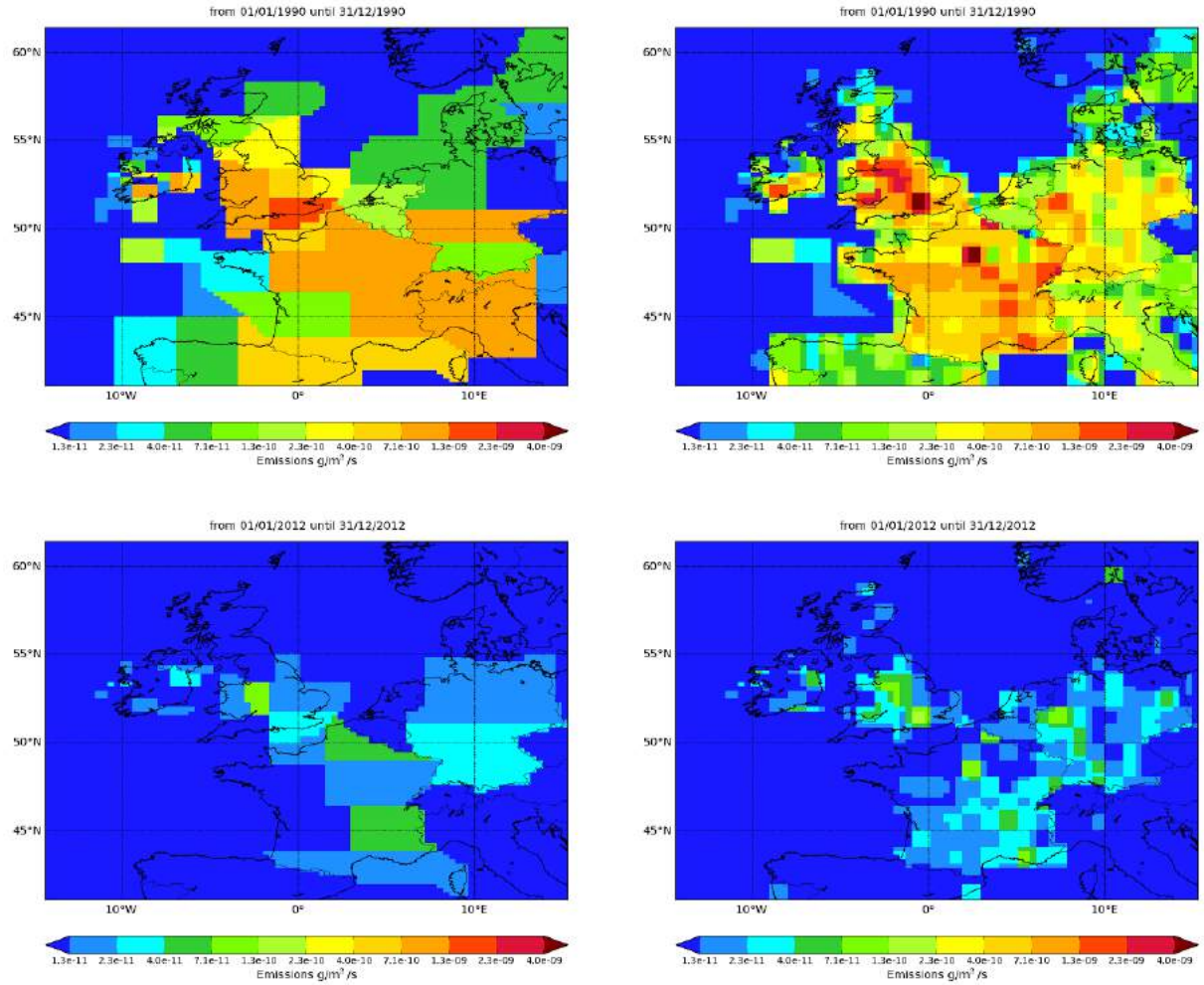

Figure 92: NAME-inversion emission estimates for 1990 (upper) and 2012 (lower). On the right hand side the emissions per grid box have been re-distributed based on population.

The emissions of CFC-113 in both the UK and NWEU as a whole fell very significantly between 1990 and the late 1990s. This again shows the impact of the Montreal Protocol which banned the use of this gas in developed countries from 1995 onwards with residual emissions a result of leakage from old appliances e.g. fridges.

Year	RMSE (ppt)	Correlation	Max obs. above baseline (ppt)	% obs. above baseline noise	Mean obs. above baseline (ppt)
1990	5.3	0.64	62.4	32	3.21
2012	0.2	0.20	1.7	18	0.20

Table 43: Comparison between modelled and observed time-series.

In 1990 there were significant pollution events, by 2012 they were barely discernible above baseline. This explains the difference between the RMSE and correlation results in the two years.

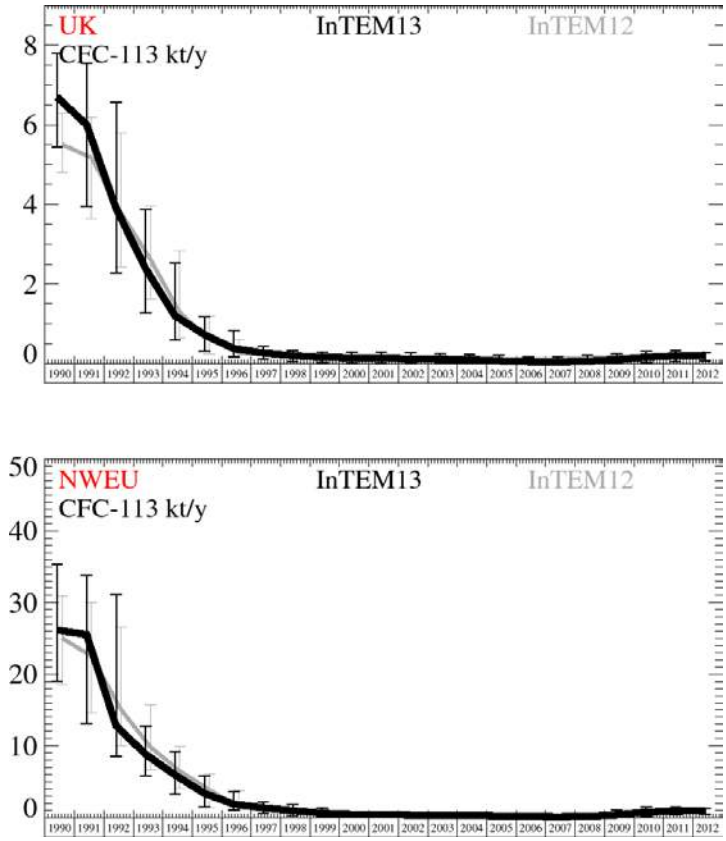

Figure 93: Emission estimates for UK and NWEU. The uncertainty bars represent the 5th and 95th percentiles. Grey line represents the emission estimates presented in last year's report.

Unit	Year	UK	(5th-95th)	NWEU	(5th-95th)
kt/y	1990	6.7	(5.4- 7.8)	26	(19.- 35.)
kt/y	1991	6	(4.0- 7.6)	26	(13.- 34.)
kt/y	1992	3.9	(2.3- 6.6)	12.8	(8.- 31.)
kt/y	1993	2.4	(1.3- 3.9)	8.8	(6.- 13.)
kt/y	1994	1.2	(0.6- 2.5)	5.9	(3.- 9.)
kt/y	1995	0.73	(0.3- 1.2)	3.4	(1.- 6.)
kt/y	1996	0.37	(0.2- 0.8)	1.86	(1.- 4.)
kt/y	1997	0.27	(0.1- 0.4)	1.37	(1.- 2.)
kt/y	1998	0.2	(0.0- 0.3)	0.97	(0.- 2.)
kt/y	1999	0.16	(0.0- 0.3)	0.61	(0.- 1.)
kt/y	2000	0.14	(0.0- 0.3)	0.45	(0.- 1.)
kt/y	2001	0.14	(0.0- 0.3)	0.4	(0.- 1.)
kt/y	2002	0.12	(0.0- 0.3)	0.35	(0.- 1.)
kt/y	2003	0.11	(0.0- 0.3)	0.34	(0.- 1.)
kt/y	2004	0.09	(0.0- 0.2)	0.3	(0.- 1.)
kt/y	2005	0.07	(0.0- 0.2)	0.22	(0.- 1.)
kt/y	2006	0.05	(0.0- 0.2)	0.15	(0.- 0.)
kt/y	2007	0.04	(0.0- 0.2)	0.12	(0.- 0.)
kt/y	2008	0.06	(0.0- 0.2)	0.16	(0.- 1.)
kt/y	2009	0.1	(0.0- 0.2)	0.36	(0.- 1.)
kt/y	2010	0.16	(0.0- 0.3)	0.76	(0.- 1.)
kt/y	2011	0.19	(0.0- 0.3)	0.88	(0.- 2.)
kt/y	2012	0.21	(0.1- 0.3)	1.02	(0.- 1.)

Table 44: Emission estimates for UK and NWEU with uncertainty (5th – 95th %ile).

6.5 CFC-115

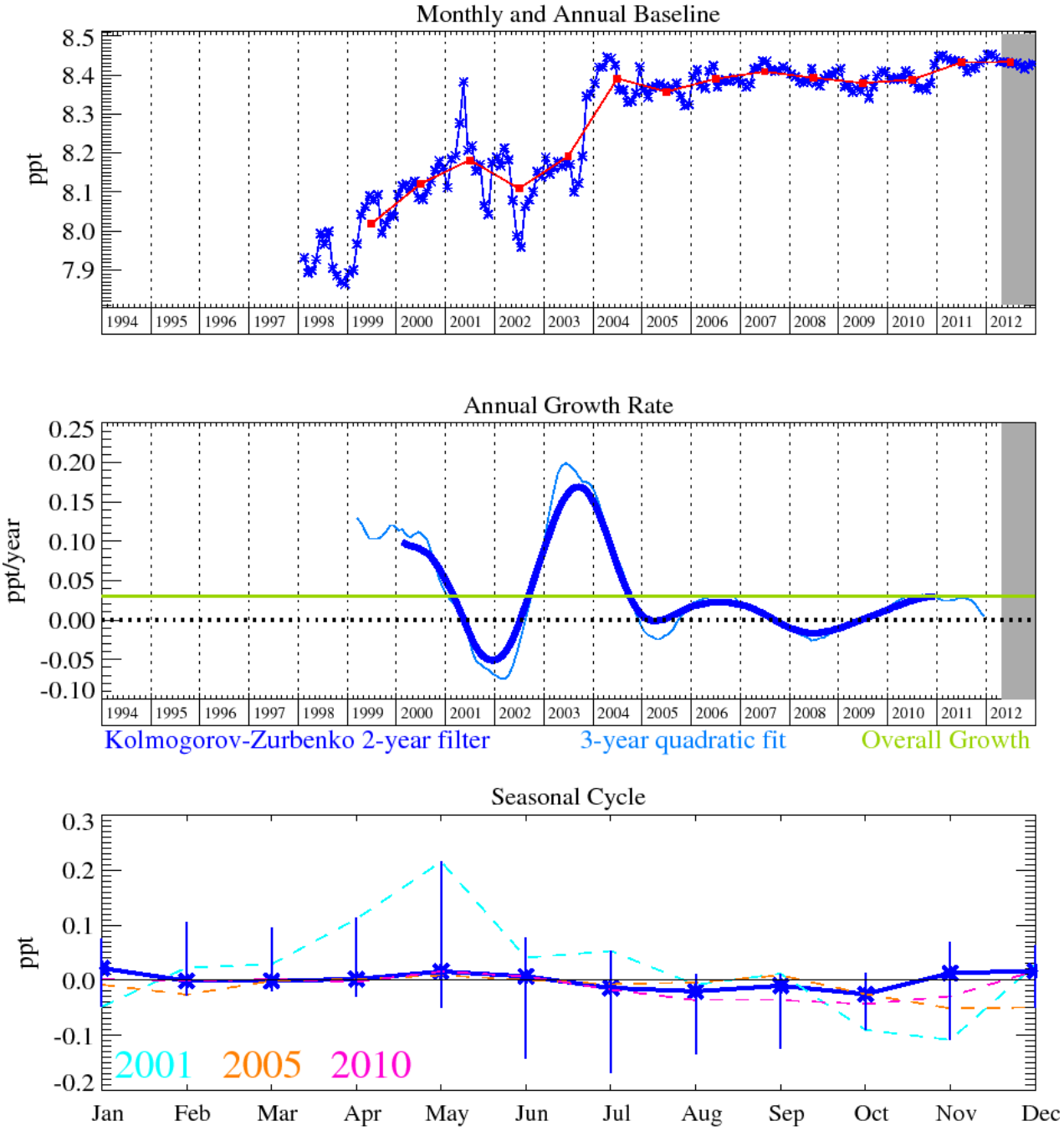

Figure 94: CFC-115 (C_2ClF_5): Monthly (blue) and annual (red) baseline concentrations (top plot). Annual (blue) and overall average growth rate (green) (middle plot). Seasonal cycle (de-trended) with year-to-year variability (lower plot). The grey area covers un-ratified and therefore provisional data.

The mixing ratios of the substantially less abundant CFC-115, has not changed appreciably since 2006. Its atmospheric abundance and current growth rate is 8.4 ppt and +0.02 ppt/yr respectively.

6.6 HCFC-124

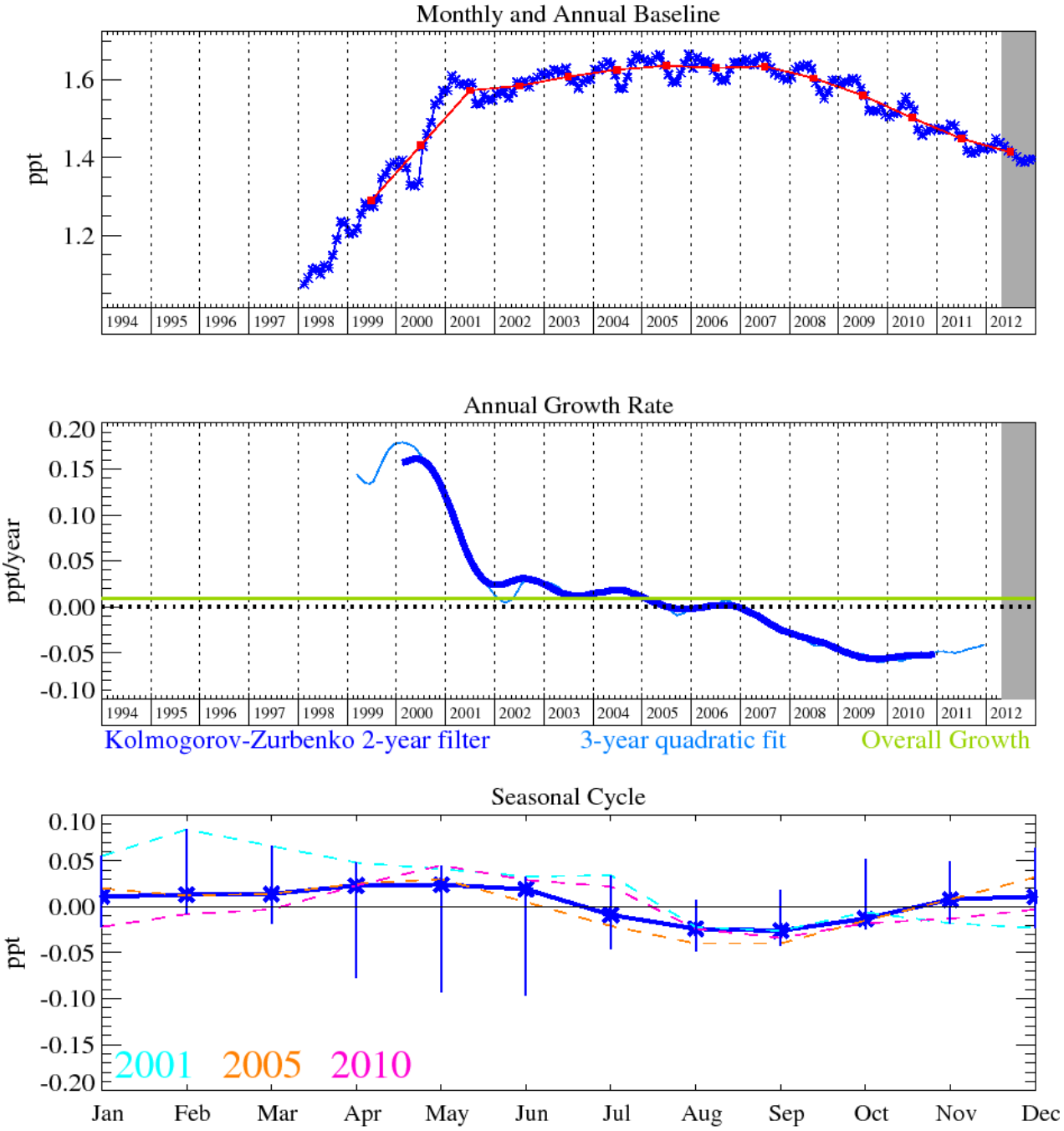

Figure 95: HCFC-124 (C_2HClF_4): Monthly (blue) and annual (red) baseline concentrations (top plot). Annual (blue) and overall average growth rate (green) (middle plot). Seasonal cycle (de-trended) with year-to-year variability (lower plot). The grey area covers un-ratified and therefore provisional data.

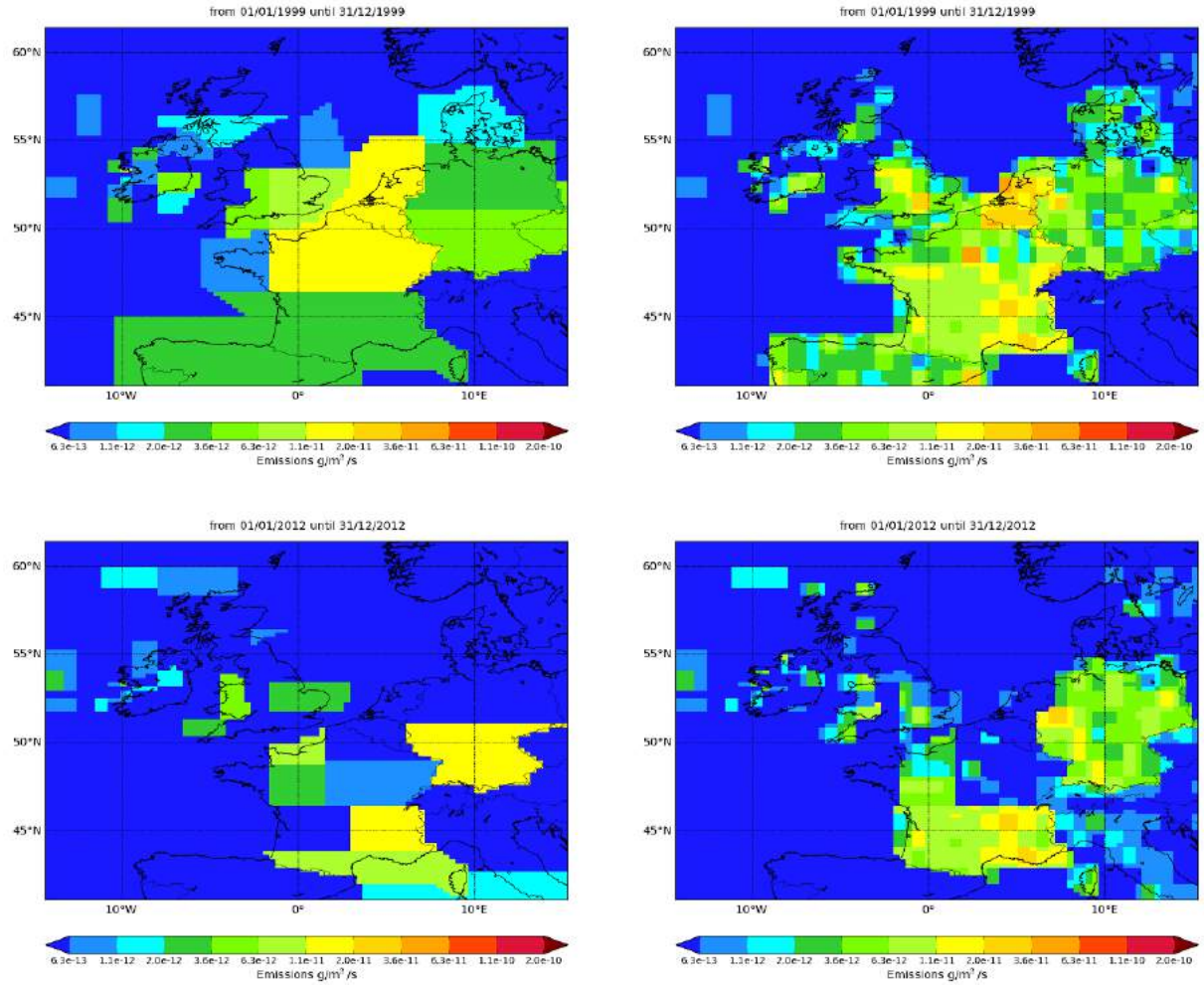

Figure 96: NAME-inversion emission estimates for 1999 (upper) and 2012 (lower). On the right hand side the emissions per grid box have been re-distributed based on population.

The measured pollution events for HCFC-124 have always been small and have slowly declined since 1999. The estimated regional emissions are therefore small and have significant uncertainty.

Year	RMSE (ppt)	Correlation	Max obs. above baseline (ppt)	% obs. above baseline noise	Mean obs. above baseline (ppt)
1999	0.07	0.55	1.1	29	0.07
2012	0.05	0.27	0.6	21	0.04

Table 45: Comparison between modelled and observed time-series.

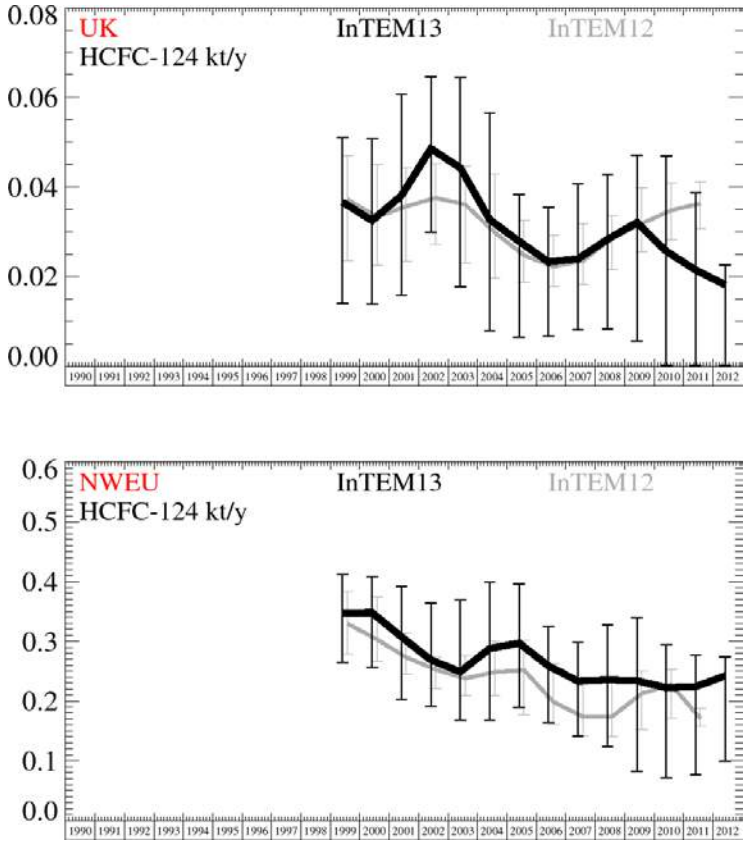

Figure 97: Emission estimates for UK and NWEU. The uncertainty bars represent the 5th and 95th percentiles. Grey line represents the emission estimates presented in last year's report.

Unit	Year	UK	(5th-95th)	NWEU	(5th-95th)
t/y	1999	37	(14.- 51.)	350	(265.- 412.)
t/y	2000	32	(14.- 51.)	350	(257.- 408.)
t/y	2001	38	(16.- 61.)	310	(202.- 392.)
t/y	2002	49	(30.- 65.)	270	(191.- 364.)
t/y	2003	44	(18.- 64.)	250	(168.- 369.)
t/y	2004	33	(8.- 57.)	290	(168.- 399.)
t/y	2005	28	(7.- 38.)	300	(190.- 396.)
t/y	2006	23	(7.- 35.)	260	(164.- 325.)
t/y	2007	24	(8.- 41.)	230	(141.- 298.)
t/y	2008	28	(8.- 43.)	240	(123.- 328.)
t/y	2009	32	(6.- 47.)	230	(83.- 340.)
t/y	2010	26	(0.- 47.)	220	(71.- 295.)
t/y	2011	21	(0.- 39.)	220	(77.- 277.)
t/y	2012	18.2	(0.- 23.)	240	(99.- 274.)

Table 46: Emission estimates for UK and NWEU with uncertainty (5th – 95th %ile).

6.7 HCFC-141b

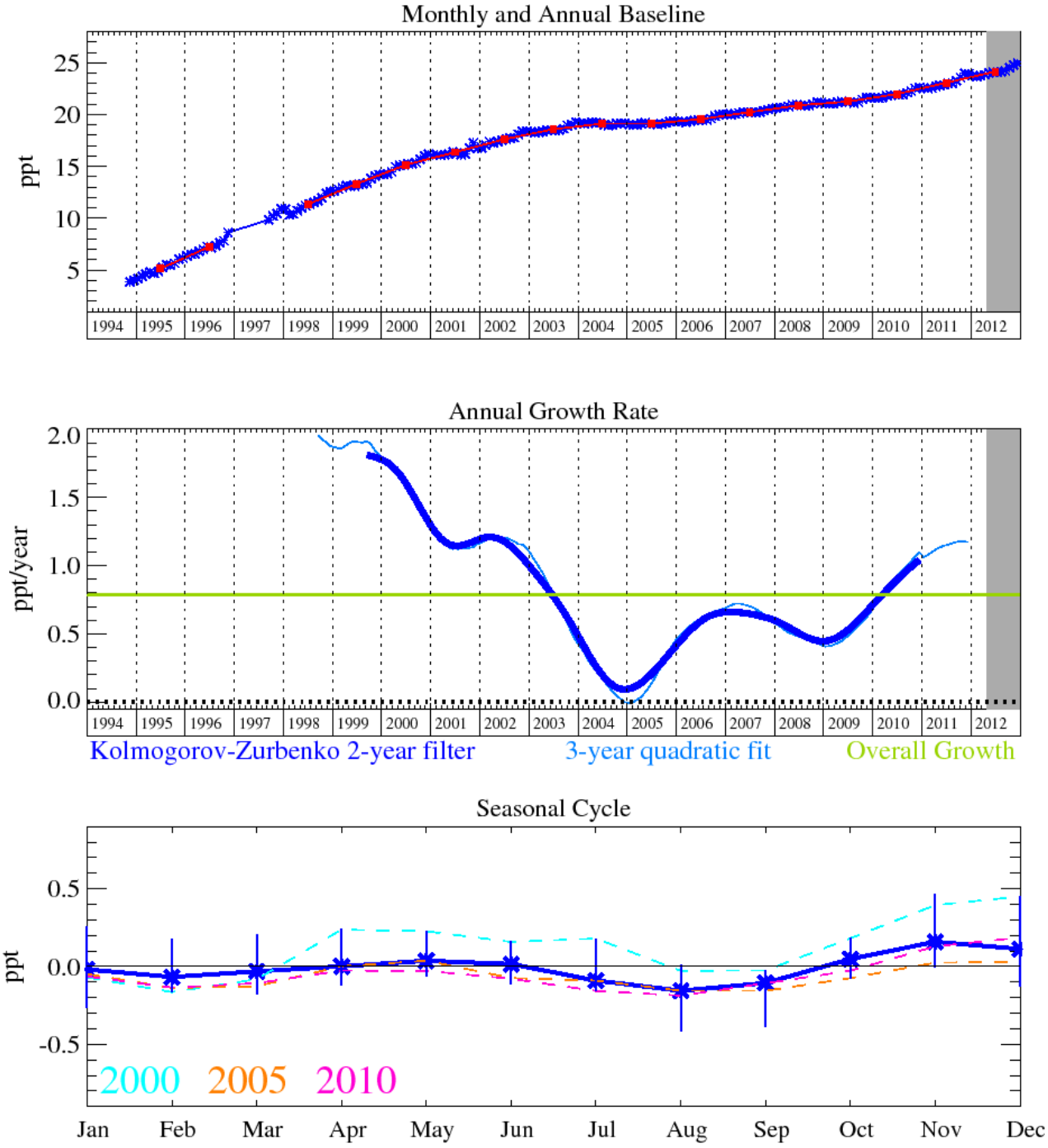

Figure 98: HCFC-141b ($C_2H_3Cl_2F$): Monthly (blue) and annual (red) baseline concentrations (top). Annual (blue) and overall average growth rate (green) (middle plot). Seasonal cycle (de-trended) with year-to-year variability (lower plot). The grey area covers un-ratified and therefore provisional data.

HCFC-142b, HCFC-141b and HCFC-22 have continued to grow in the atmosphere at increased rates since 2005. The rate of growths for all three gases peaked in 2007/08, but, unlike the other two, the growth rate for HCFC-141b is increasing once again. Prior to 2005 HCFC-142b and HFCF-141b showed reduced growth in the atmosphere in line with their expected phase-out (90% phase-out of production and consumption by 2015 for Article 2 parties and 10% phase-out by Article 5 parties). Analysis of the HCFC content of regionally-polluted air arriving at Mace Head from the European continent shows that European emissions reached a peak during 2000-2001 and have subsequently declined following the phase-out in their usage. The reductions are consistent with the phase-out of HCFC production and use from the year 2001 onwards mandated

by European regulations designed to exceed the requirements of the Montreal Protocol. In the US implementation of HCFC phase-out through the Clean Air Act Regulations, 2004 resulted in no production or importation of HCFC-141b since 2003, these restrictions did not apply to HCFC-142b until 2010. Increasing evidence indicates that increased emissions of these compounds from Asia, in particular China are now offsetting the phase-out in developed countries. The current growth rates of HCFC-141b and 142b are 1.1 and 0.6 ppt/yr respectively. The growth rates of these compounds, calculated from the baseline mean mixing ratios shown in Figures 98 and 101, are also presented in Table 1c.

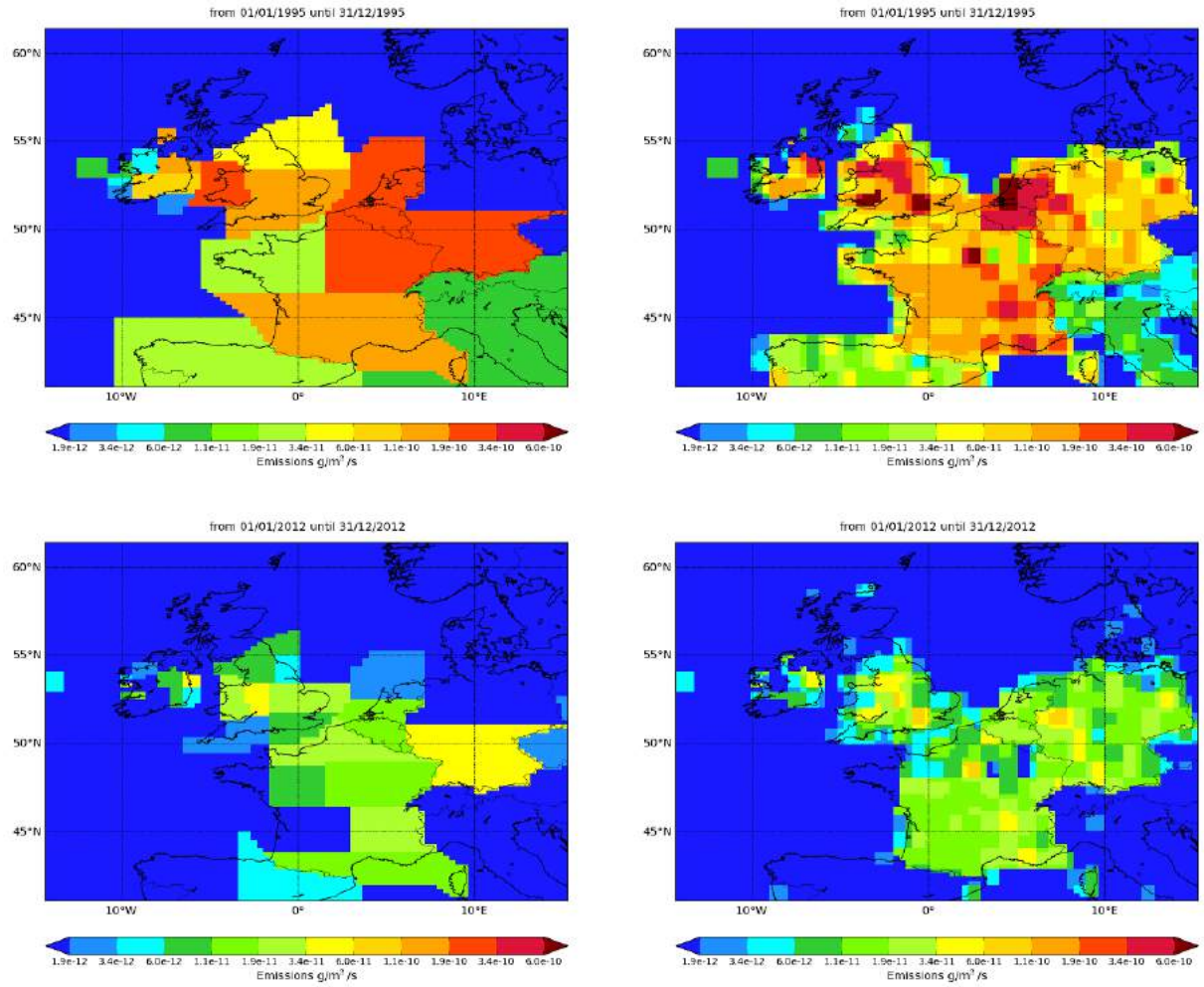

Figure 99: NAME-inversion emission estimates for 1995 (upper) and 2012 (lower). On the right hand side the emissions per grid box have been re-distributed based on population.

The emissions of HCFC-141b in both the UK and NWEU as a whole fell very significantly between 2003 and 2005. This clearly shows the impact of the Montreal Protocol, which banned the use of this gas in developed countries from 2005 onwards. Before 2005 there were significant pollution events, by 2012 they had considerably reduced in magnitude. This explains the difference between the RMSE and correlation results in the two years.

Year	RMSE (ppt)	Correlation	Max obs. above baseline (ppt)	% obs. above baseline noise	Mean obs. above baseline (ppt)
1995	0.89	0.69	14.4	40	0.90
2012	0.15	0.28	1.7	29	0.15

Table 47: Comparison between modelled and observed time-series.

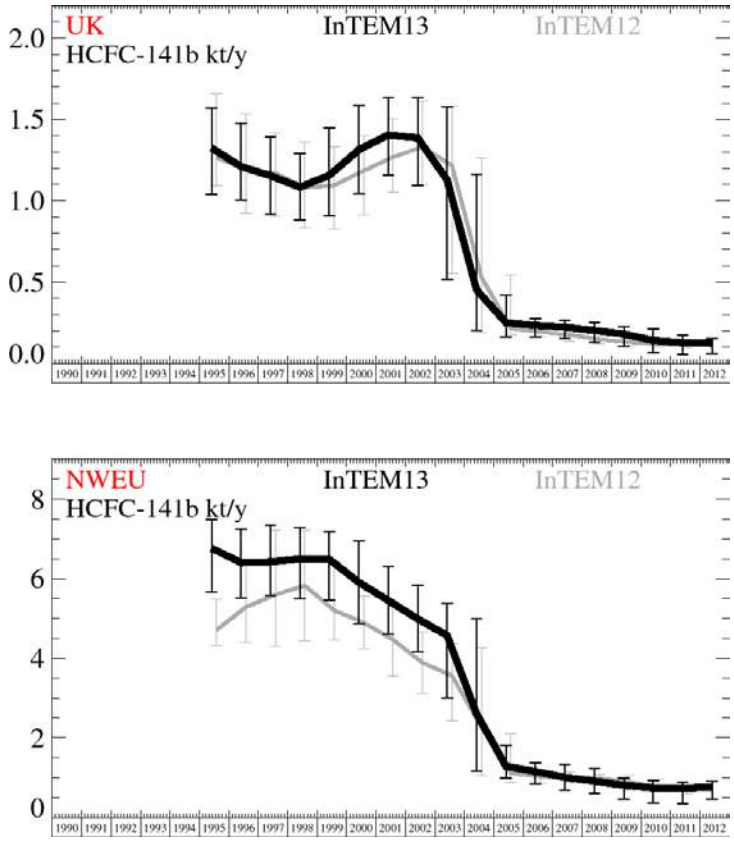

Figure 100: Emission estimates for UK and NWEU. The uncertainty bars represent the 5th and 95th percentiles. Grey line represents the emission estimates presented in last year's report.

Unit	Year	UK	(5th-95th)	NWEU	(5th-95th)
t/y	1995	1320	(1037.-1569.)	6800	(5656.-7483.)
t/y	1996	1210	(1002.-1477.)	6400	(5518.-7250.)
t/y	1997	1150	(916.-1394.)	6400	(5579.-7354.)
t/y	1998	1080	(881.-1288.)	6500	(5500.-7294.)
t/y	1999	1160	(906.-1447.)	6500	(5451.-7198.)
t/y	2000	1310	(1042.-1587.)	5900	(4875.-6950.)
t/y	2001	1400	(1157.-1634.)	5500	(4614.-6295.)
t/y	2002	1390	(1095.-1634.)	5000	(4173.-5846.)
t/y	2003	1130	(516.-1576.)	4600	(3003.-5376.)
t/y	2004	450	(203.-1164.)	2600	(1165.-4999.)
t/y	2005	250	(166.- 417.)	1290	(999.-1805.)
t/y	2006	230	(163.- 275.)	1160	(847.-1379.)
t/y	2007	220	(154.- 267.)	1010	(688.-1337.)
t/y	2008	200	(129.- 250.)	910	(612.-1233.)
t/y	2009	181	(102.- 228.)	810	(459.- 999.)
t/y	2010	141	(67.- 211.)	740	(366.- 929.)
t/y	2011	128	(57.- 175.)	730	(351.- 897.)
t/y	2012	124	(62.- 152.)	770	(471.- 913.)

Table 48: Emission estimates for UK and NWEU with uncertainty (5th – 95th %ile).

6.8 HCFC-142b

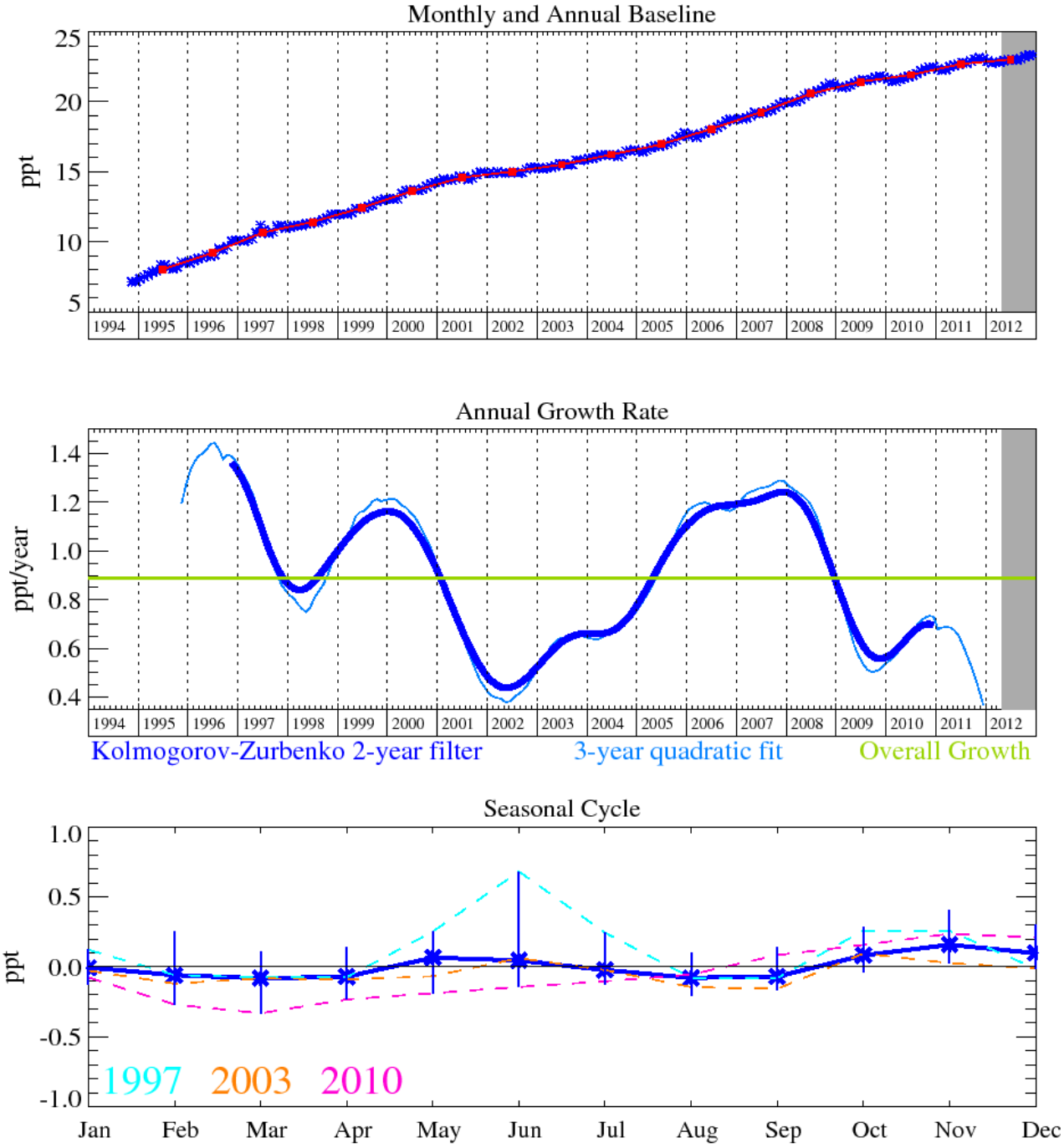

Figure 101: HCFC-142b ($C_2H_3ClF_2$): Monthly (blue) and annual (red) baseline concentrations (top). Annual (blue) and overall average growth rate (green) (middle plot). Seasonal cycle (de-trended) with year-to-year variability (lower plot). The grey area covers un-ratified and therefore provisional data.

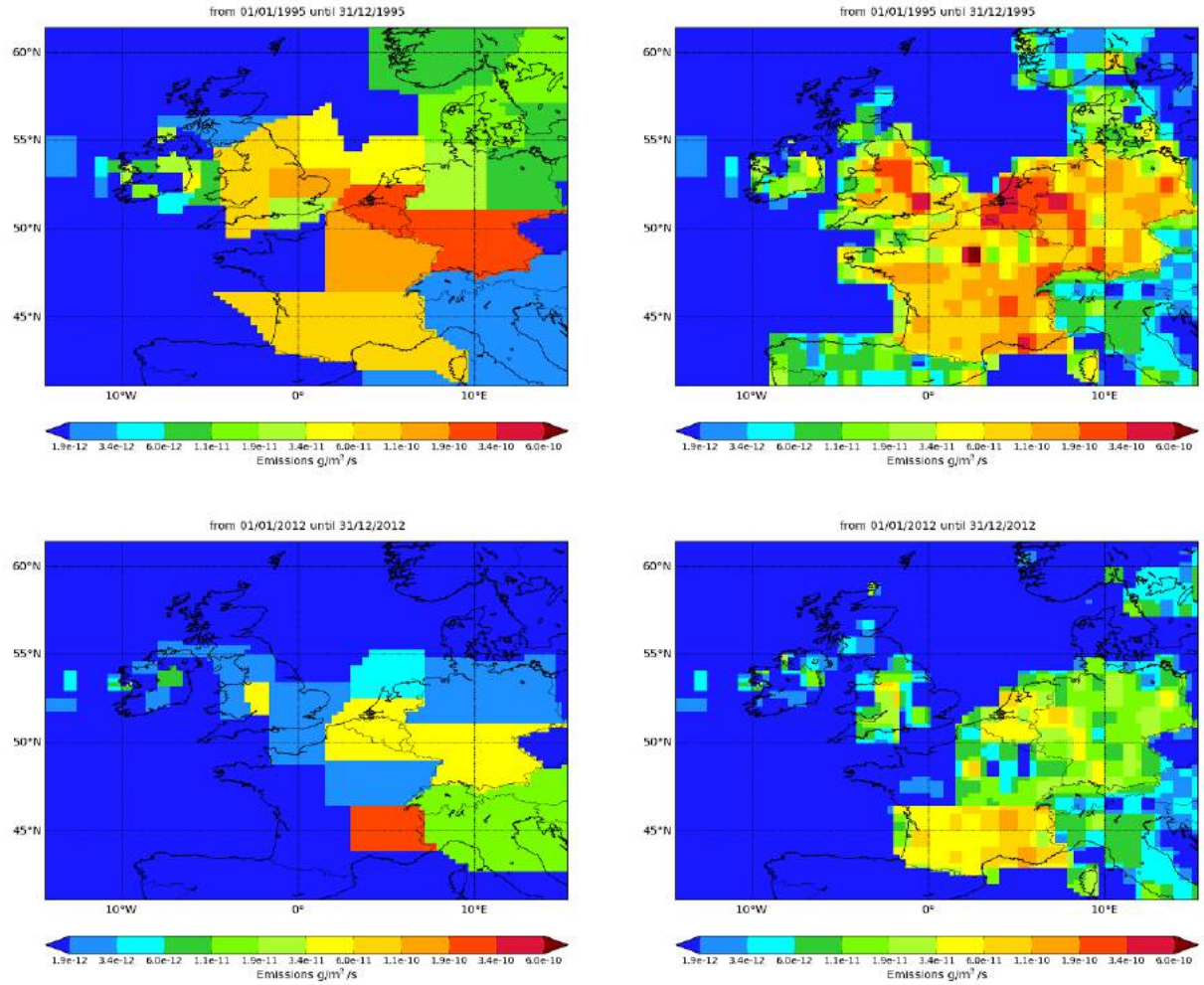

Figure 102: NAME-inversion emission estimates for 1990 (upper) and 2012 (lower). On the right hand side the emissions per grid box have been re-distributed based on population.

The emissions of HCFC-142b in both the UK and NWEU as a whole fell very significantly between 2000 and 2005. Like HCFC-141b, this clearly shows the impact of the Montreal Protocol, which banned the use of this gas in developed countries from 2005 onwards. Before 2002 there were significant pollution events, by 2012 they had considerably reduced in magnitude. This explains the difference between the RMSE and correlation results in the two years.

Year	RMSE (ppt)	Correlation	Max obs. above baseline (ppt)	% obs. above baseline noise	Mean obs. above baseline (ppt)
1995	0.62	0.72	8.9	41	0.65
2012	0.15	0.37	3.0	28	0.13

Table 49: Comparison between modelled and observed time-series

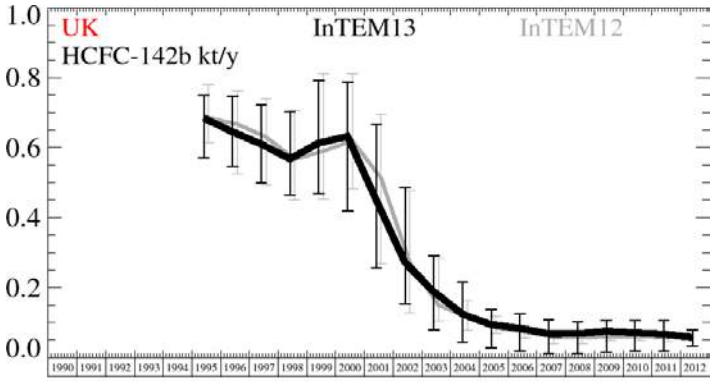

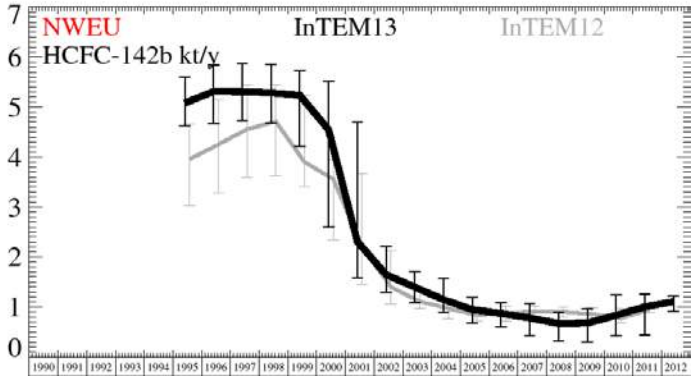

Figure 103: Emission estimates for UK and NWEU. The uncertainty bars represent the 5th and 95th percentiles. Grey line represents the emission estimates presented in last year's report.

Unit	Year	UK	(5th-95th)	NWEU	(5th-95th)
t/y	1995	680	(572.- 750.)	5100	(4625.-5604.)
t/y	1996	650	(545.- 748.)	5300	(4664.-5834.)
t/y	1997	610	(498.- 724.)	5300	(4735.-5875.)
t/y	1998	570	(462.- 703.)	5300	(4690.-5857.)
t/y	1999	610	(468.- 792.)	5200	(4219.-5726.)
t/y	2000	630	(420.- 787.)	4500	(2602.-5515.)
t/y	2001	450	(255.- 666.)	2300	(1587.-4700.)
t/y	2002	270	(152.- 485.)	1650	(1283.-2212.)
t/y	2003	188	(79.- 291.)	1400	(1090.-1704.)
t/y	2004	124	(44.- 216.)	1150	(891.-1561.)
t/y	2005	94	(28.- 138.)	950	(679.-1185.)
t/y	2006	84	(19.- 126.)	870	(601.-1087.)
t/y	2007	68	(12.- 109.)	780	(431.-1075.)
t/y	2008	68	(12.- 102.)	670	(314.- 897.)
t/y	2009	75	(17.- 106.)	680	(305.- 952.)
t/y	2010	71	(18.- 105.)	830	(427.-1242.)
t/y	2011	67	(18.- 106.)	1000	(440.-1262.)
t/y	2012	58	(32.- 80.)	1110	(917.-1221.)

Table 50: Emission estimates for UK and NWEU with uncertainty (5th – 95th %ile).

6.9 HCFC-22

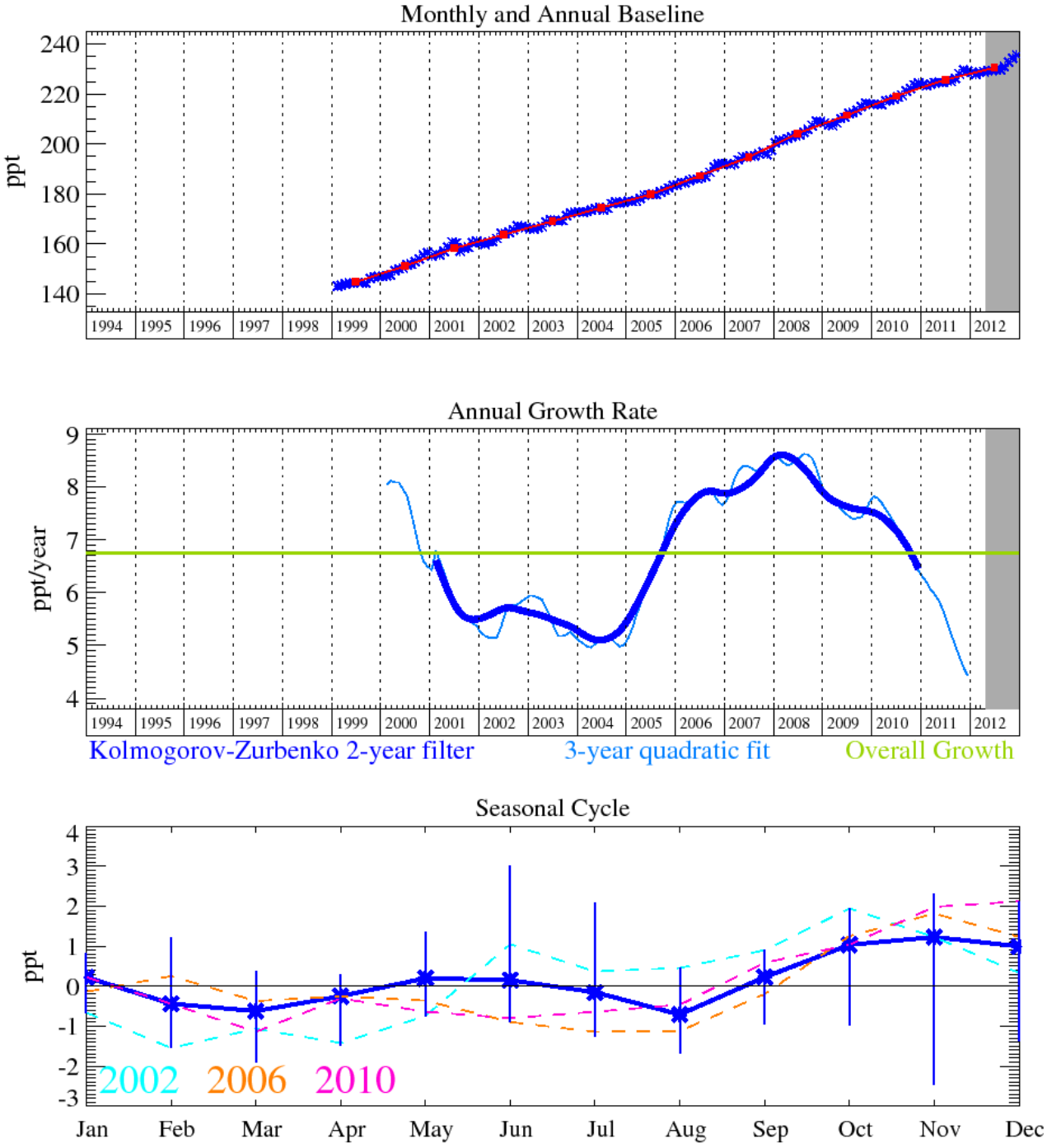

Figure 104: HCFC-22 ($CHClF_2$): Monthly (blue) and annual (red) baseline concentrations (top plot). Annual (blue) and overall average growth rate (green) (middle plot). Seasonal cycle (de-trended) with year-to-year variability (lower plot). Grey area covers un-ratified and therefore provisional data.

Over the past 12-months HCFC-22, the dominant globally produced HCFC compound, was growing at a rate of 5.5 ppt/yr and, by December 2012, had reached a level at Mace Head of approximately 235.6 ppt. This rate of growth has steadily slowed from its maximum in 2008.

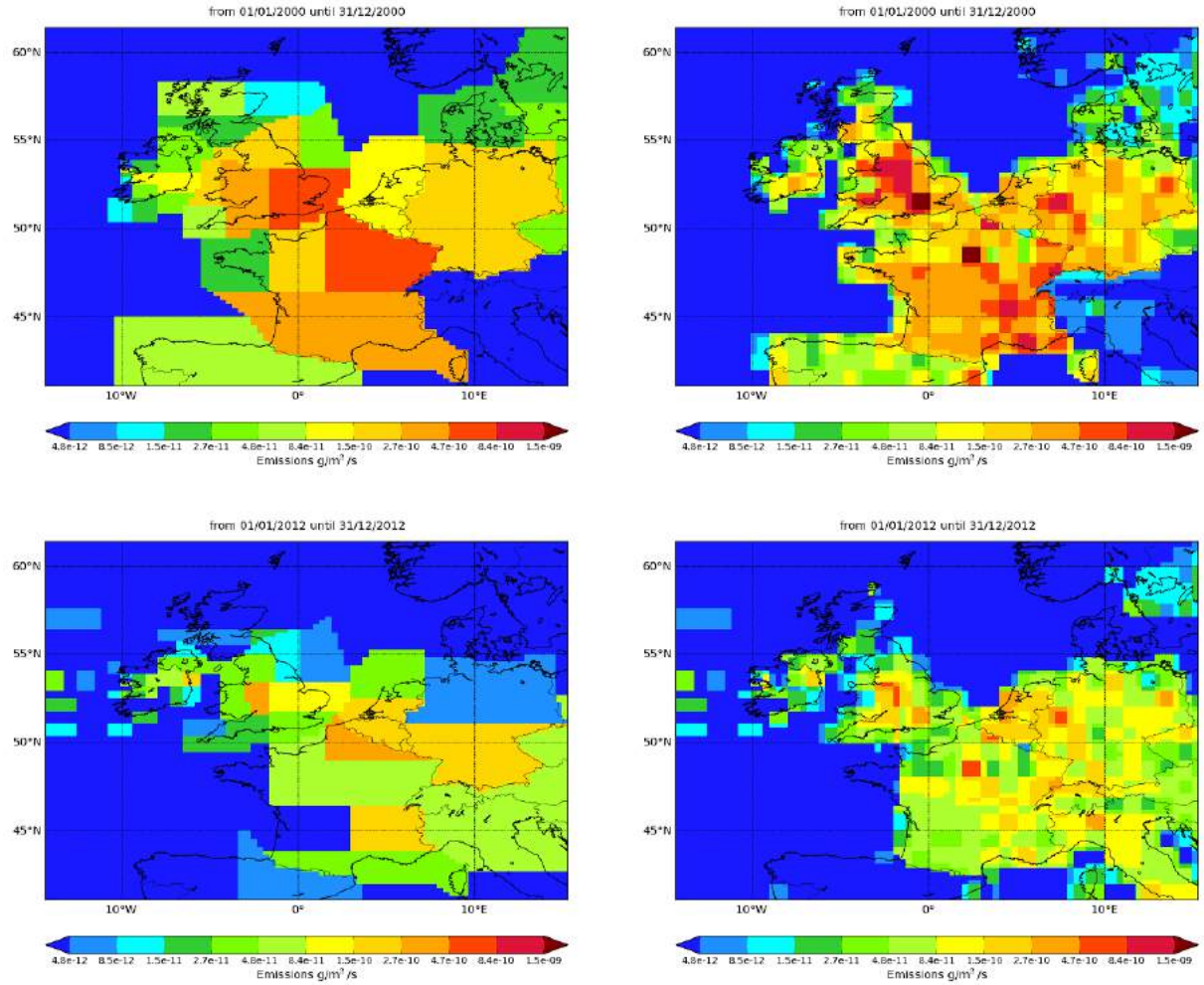

Figure 105: NAME-inversion emission estimates for 2000 (upper) and 2012 (lower). On the right hand side the emissions per grid box have been re-distributed based on population.

The emissions of HCFC-22 have decreased steadily over the 13 years from 2000. The magnitude of the pollution events have similarly declined.

Year	RMSE (ppt)	Correlation	Max obs. above baseline (ppt)	% obs. above baseline noise	Mean obs. above baseline (ppt)
1995	2.2	0.68	39	30	2.69
2012	1.2	0.26	22	27	1.06

Table: Comparison between modelled and observed time-series.

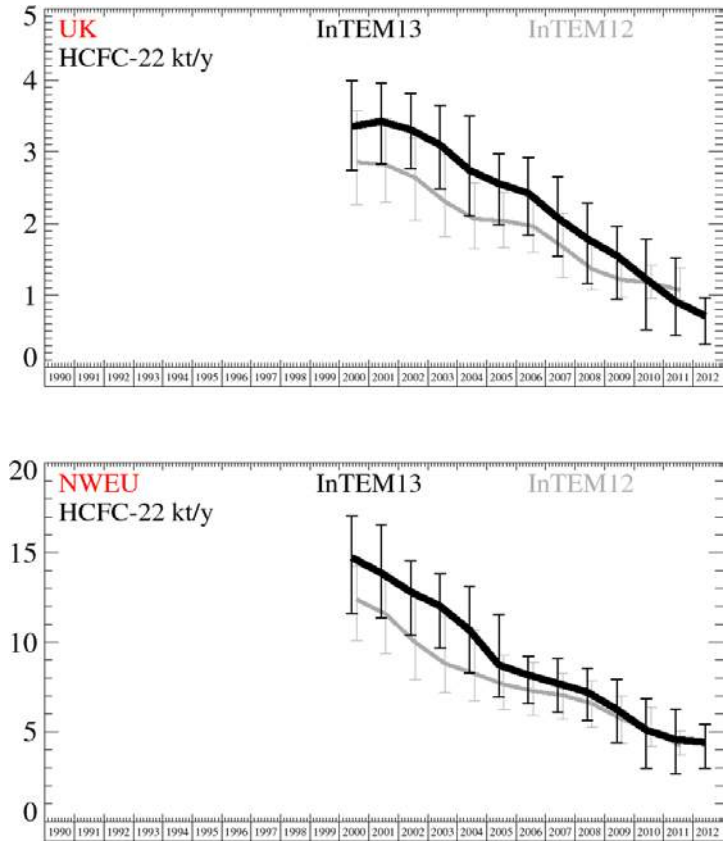

Figure 106: Emission estimates for UK and NWEU. The uncertainty bars represent the 5th and 95th percentiles. Grey line represents the emission estimates presented in last year's report.

Unit	Year	UK	(5th-95th)	NWEU	(5th-95th)
kt/y	2000	3.4	(2.7- 4.0)	14.7	(12.- 17.)
kt/y	2001	3.4	(2.8- 4.0)	13.9	(11.- 17.)
kt/y	2002	3.3	(2.8- 3.8)	12.8	(10.- 15.)
kt/y	2003	3.1	(2.5- 3.6)	12	(10.- 14.)
kt/y	2004	2.7	(2.1- 3.5)	10.7	(8.- 13.)
kt/y	2005	2.6	(2.0- 3.0)	8.7	(7.- 12.)
kt/y	2006	2.4	(1.8- 2.9)	8.2	(7.- 9.)
kt/y	2007	2.1	(1.5- 2.7)	7.7	(6.- 9.)
kt/y	2008	1.79	(1.2- 2.3)	7.2	(6.- 9.)
kt/y	2009	1.55	(0.9- 2.0)	6.3	(4.- 8.)
kt/y	2010	1.23	(0.5- 1.8)	5.1	(3.- 7.)
kt/y	2011	0.91	(0.4- 1.5)	4.6	(3.- 6.)
kt/y	2012	0.71	(0.3- 1.0)	4.4	(3.- 5.)

Table 51: Emission estimates for UK and NWEU with uncertainty (5th – 95th %ile).

6.10 HFC-236fa

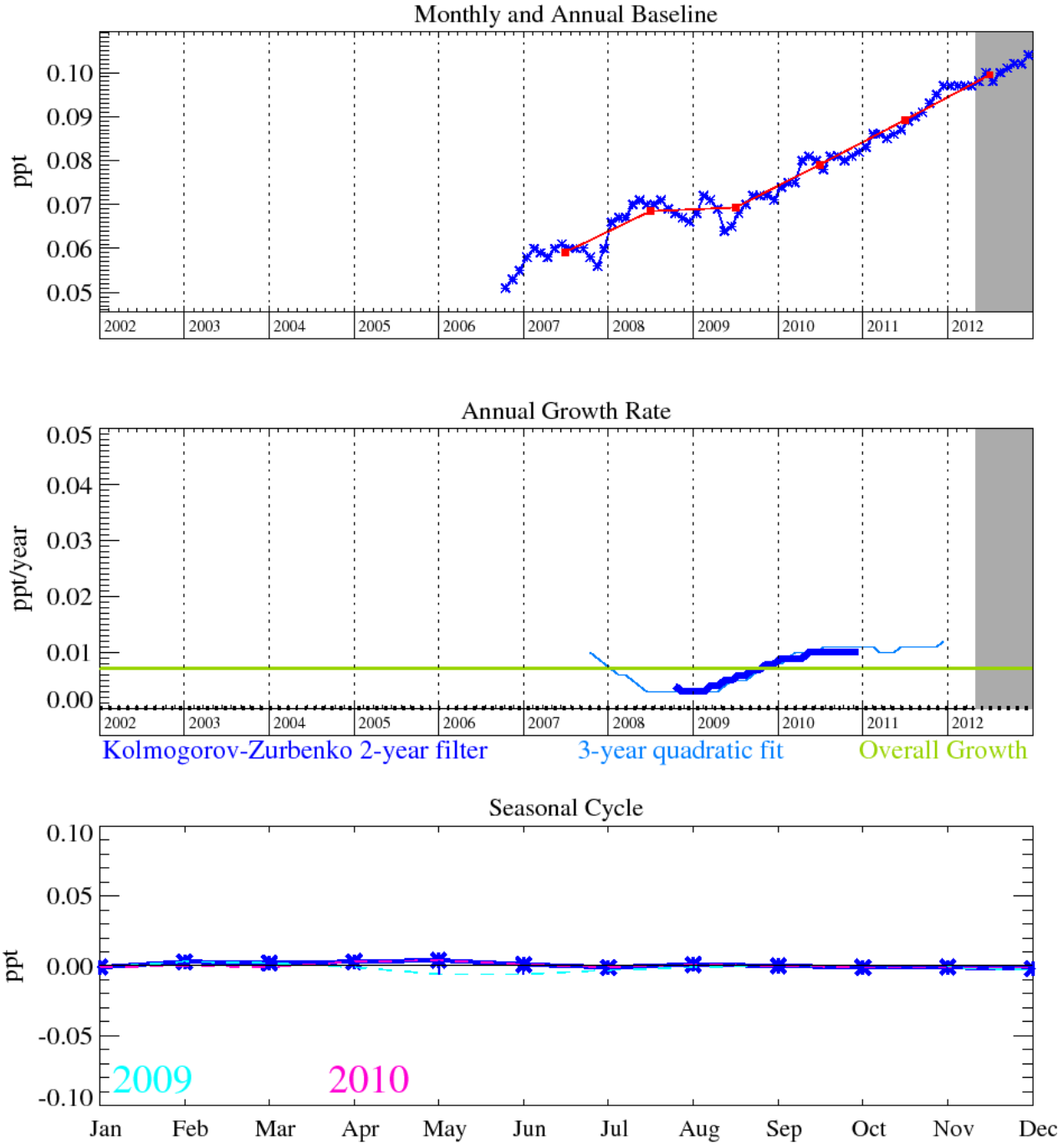

Figure 107: HFC-236fa ($C_3H_2F_6$): Monthly (blue) and annual (red) baseline concentrations (top plot). Annual (blue) and overall average growth rate (green) (middle plot). Seasonal cycle (de-trended) with year-to-year variability (lower plot). Grey area covers un-ratified and therefore provisional data.

HFC-236fa is used as a fire-fighting agent (atmospheric lifetime 240 years and GWP_{100} of 9500) and has reached a mixing ratio of 0.10 ppt and is growing at a rate of 0.01 ppt/yr.

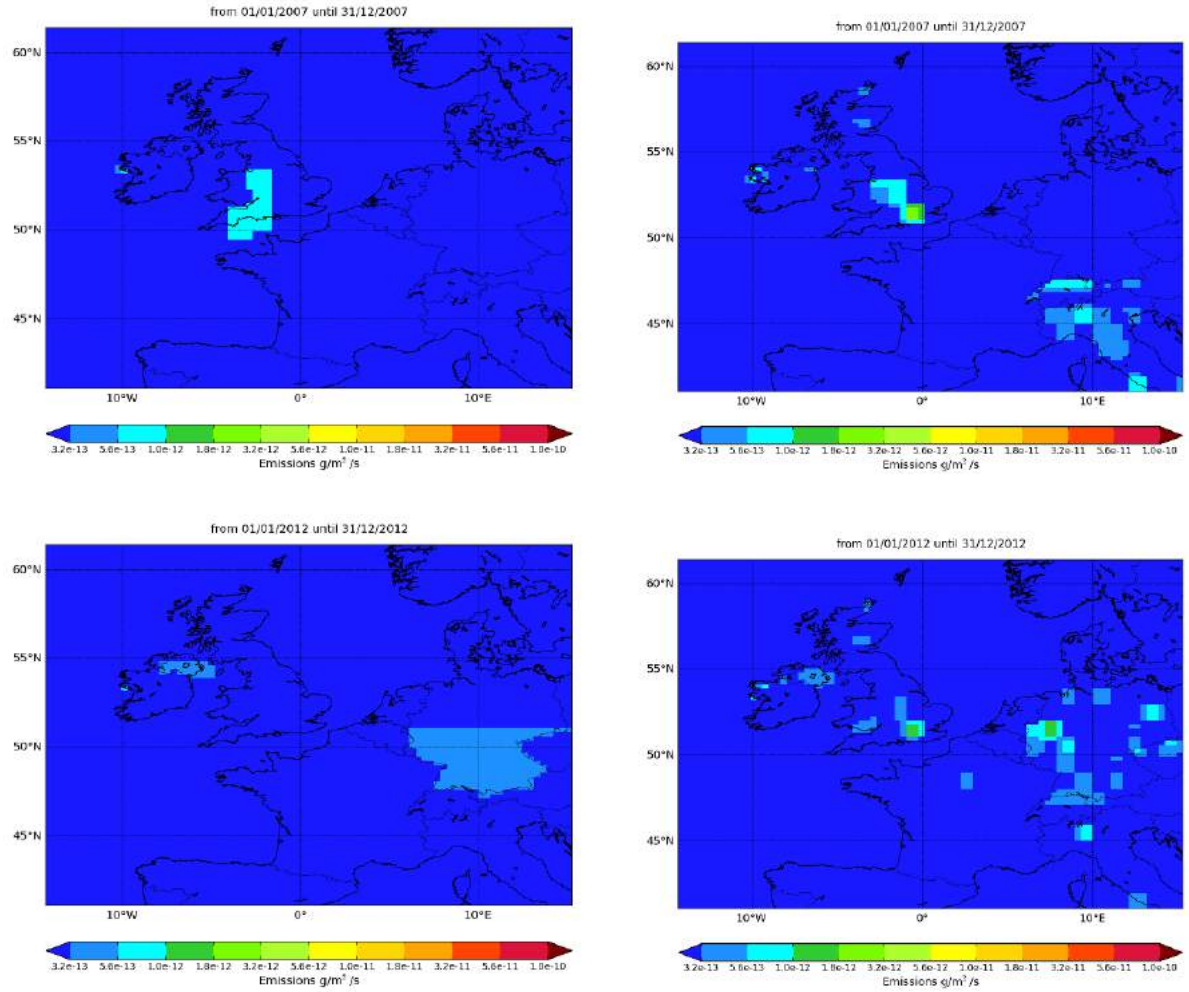

Figure 108: NAME-inversion emission estimates for 2007 (upper) and 2012 (lower). On the right hand side the emissions per grid box have been re-distributed based on population.

Year	RMSE (ppt)	Correlation	Max obs. above baseline (ppt)	% obs. above baseline noise	Mean obs. above baseline (ppt)
2007	0.01	0.09	0.09	19	0.006
2012	0.01	0.10	0.03	21	0.006

Table 52: Comparison between modelled and observed time-series.

It is clear that there are only very limited emissions of this gas across Europe. The magnitude of the pollution events are very low compared to the noise in the baseline and therefore the uncertainty in the InTEM results are significant.

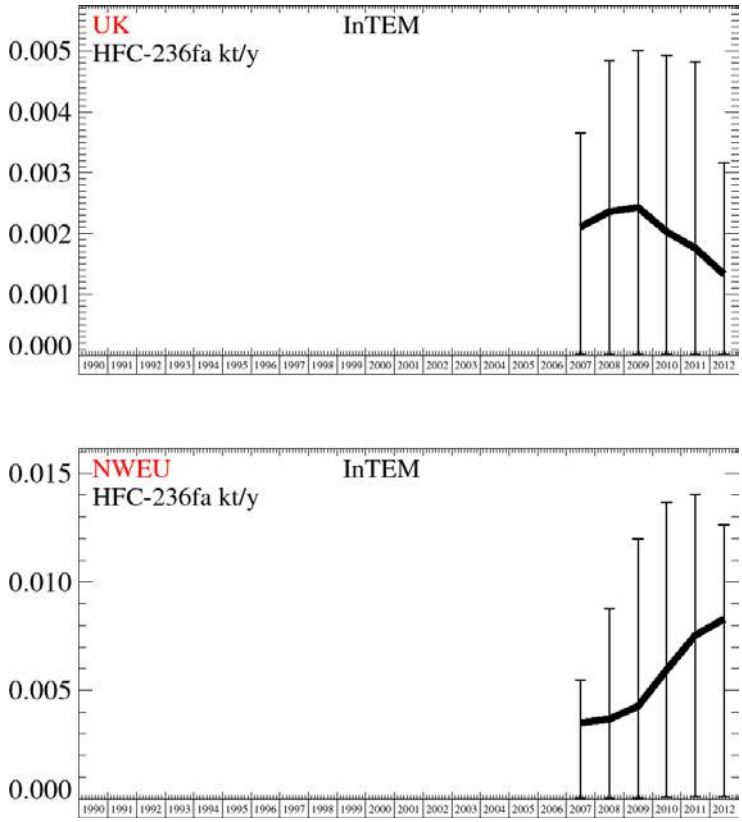

Figure 109: Emission estimates for UK and NWEU. The uncertainty bars represent the 5th and 95th percentiles.

Unit	Year	UK	(5th-95th)	NWEU	(5th-95th)
t/y	2007	2.1	(0.0- 3.7)	3.5	(0.06- 5.)
t/y	2008	2.4	(0.0- 4.8)	3.7	(0.06- 9.)
t/y	2009	2.4	(0.0- 5.0)	4.3	(0.06- 12.)
t/y	2010	2	(0.0- 4.9)	5.9	(0.07- 14.)
t/y	2011	1.76	(0.0- 4.8)	7.5	(0.10- 14.)
t/y	2012	1.33	(0.0- 3.2)	8.3	(0.10- 13.)

Table 53: Emission estimates for UK and NWEU with uncertainty (5th – 95th %ile).

6.11 HFC-245fa

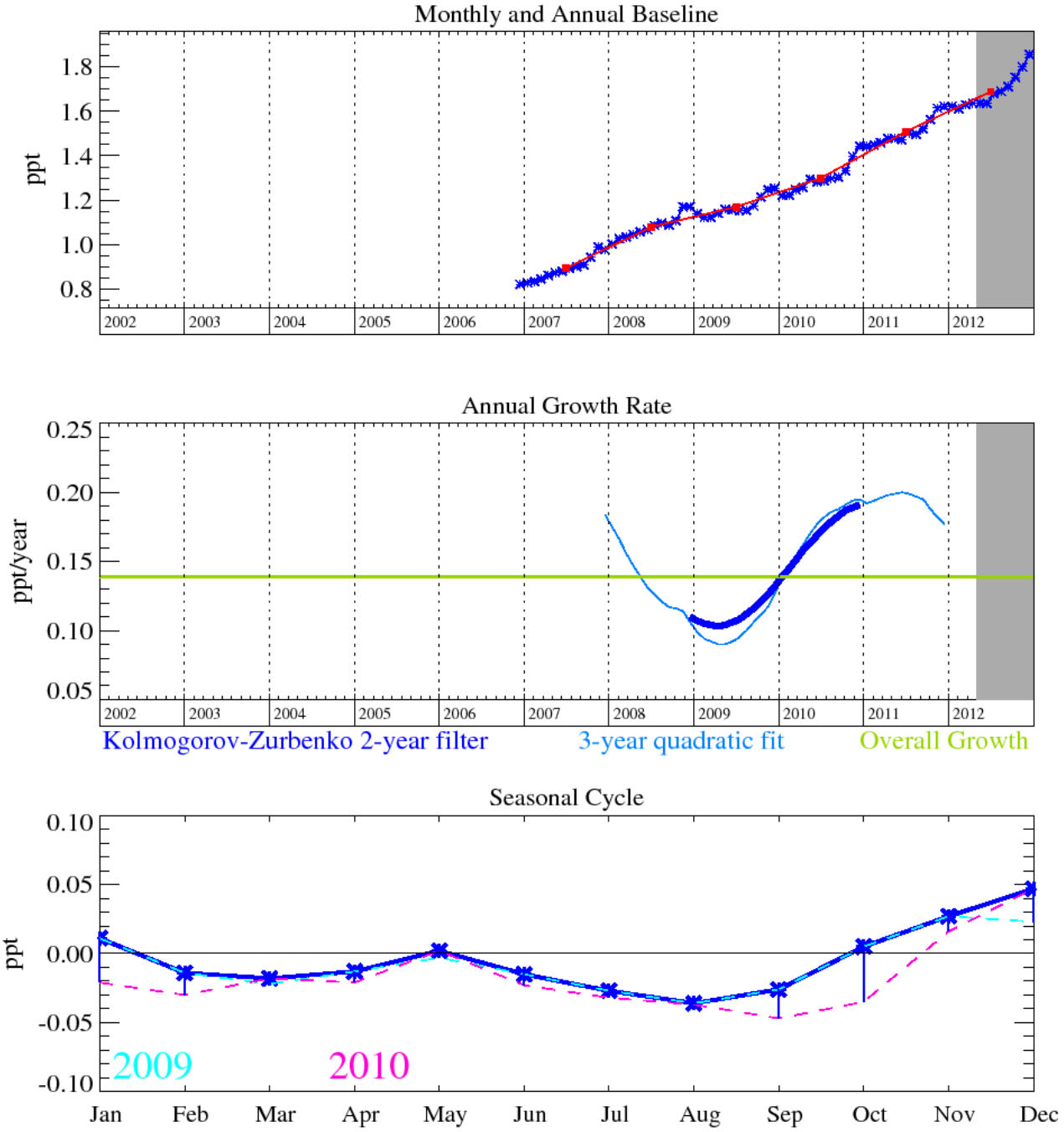

Figure 110: HFC-245fa ($C_3H_3F_5$): Monthly (blue) and annual (red) baseline concentrations (top plot). Annual (blue) and overall average growth rate (green) (middle plot). Seasonal cycle (de-trended) with year-to-year variability (lower plot). Grey area covers un-ratified and therefore provisional data.

HFC-245fa is used as a foam-blowing agent for polyurethane (PUR) foams. It has an atmospheric lifetime 7.6 years and GWP_{100} of 1020. In December 2012 its atmospheric mole fraction was 1.9 ppt and it is growing at a rate of 0.19 ppt/yr.

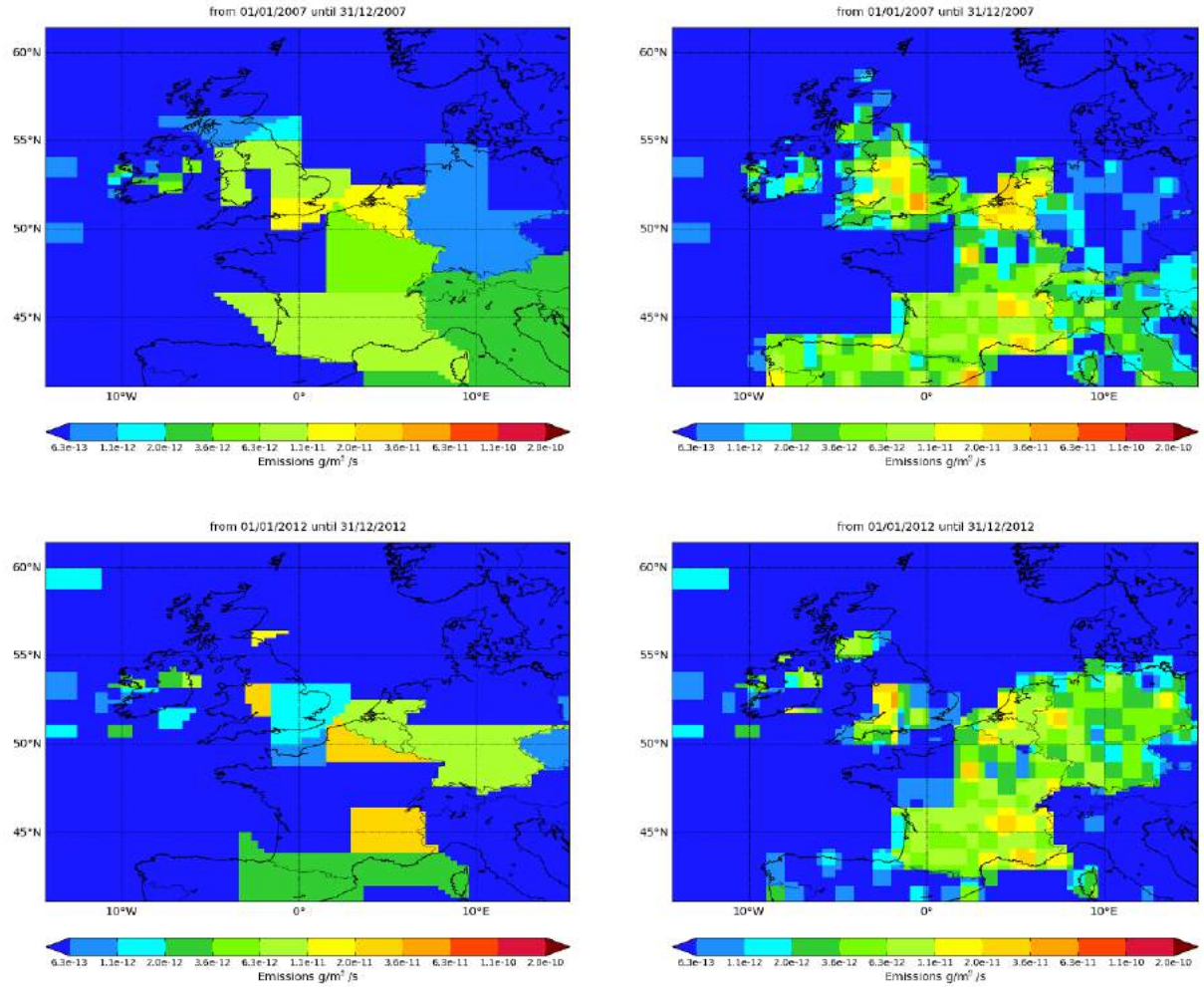

Figure 111: NAME-inversion emission estimates for 2007 (upper) and 2012 (lower). On the right hand side the emissions per grid box have been re-distributed based on population.

Year	RMSE (ppt)	Correlation	Max obs. above baseline (ppt)	% obs. above baseline noise	Mean obs. above baseline (ppt)
2007	0.07	0.39	1.13	29	0.06
2012	0.05	0.27	0.48	27	0.05

Table 54: Comparison between modelled and observed time-series.

The statistical match between the modelled and observed time-series is not strong giving rise to significant uncertainty in the UK emission estimates. However the overall decline in UK emissions is a robust signal, one that is not observed in NWEU as a whole.

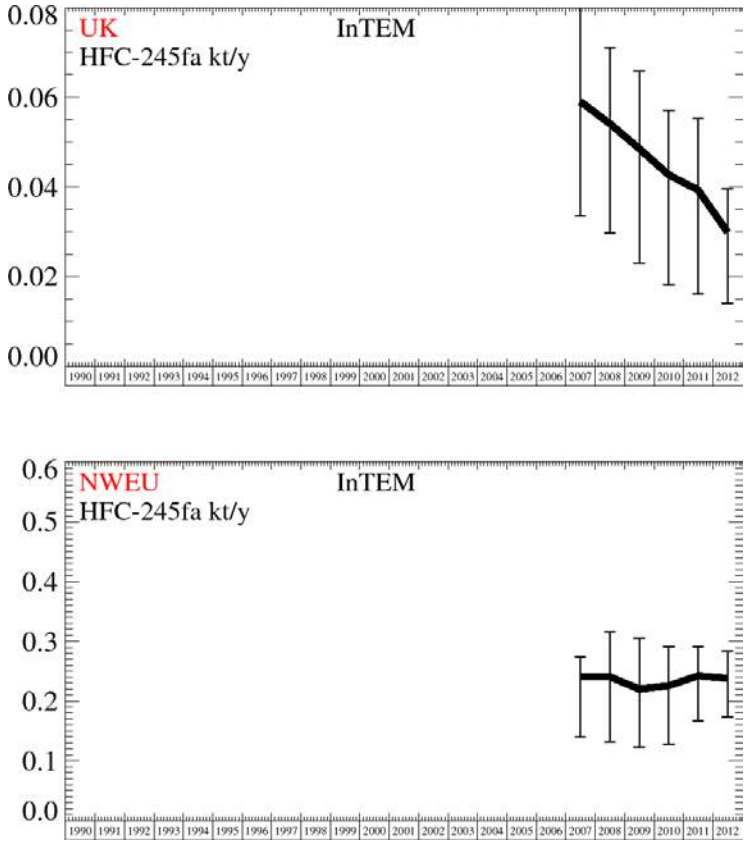

Figure 112: Emission estimates for UK and NWEU. The uncertainty bars represent the 5th and 95th percentiles.

Unit	Year	UK	(5th-95th)	NWEU	(5th-95th)
t/y	2007	59	(34.- 81.)	240	(140.- 274.)
t/y	2008	54	(30.- 71.)	240	(132.- 316.)
t/y	2009	49	(23.- 66.)	220	(122.- 305.)
t/y	2010	43	(18.- 57.)	230	(127.- 291.)
t/y	2011	39	(16.- 55.)	240	(166.- 291.)
t/y	2012	30	(14.- 40.)	240	(173.- 283.)

Table 55: Emission estimates for UK and NWEU with uncertainty (5th – 95th %ile).

6.12 HFC-365mfc

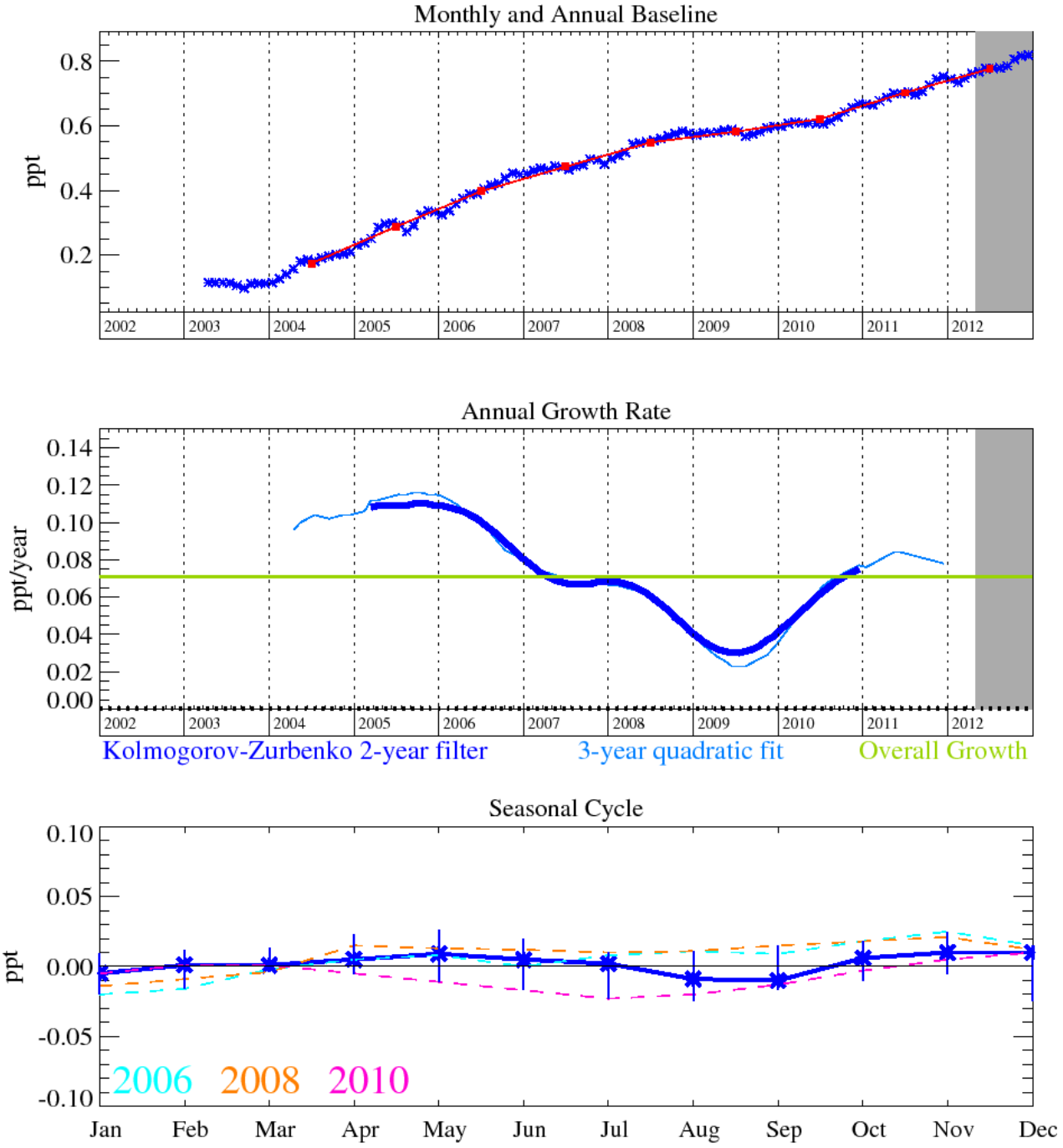

Figure 113: HFC-365mfc ($C_4H_5F_5$): Monthly (blue) and annual (red) baseline concentrations (top plot). Annual (blue) and overall average growth rate (green) (middle plot). Seasonal cycle (de-trended) with year-to-year variability (lower plot). Grey area covers un-ratified and therefore provisional data.

HFC-365mfc is used mainly for polyurethane structural foam blowing as a replacement for HCFC-141b, and to a minor extent as a blend component for solvents. It has an atmospheric lifetime of 8.6 years and a GWP estimated at 790-997 (100-year time horizon). It is currently growing in the atmosphere at a rate of 0.08 ppt/yr and reached a mole fraction of 0.8 ppt in 2012.

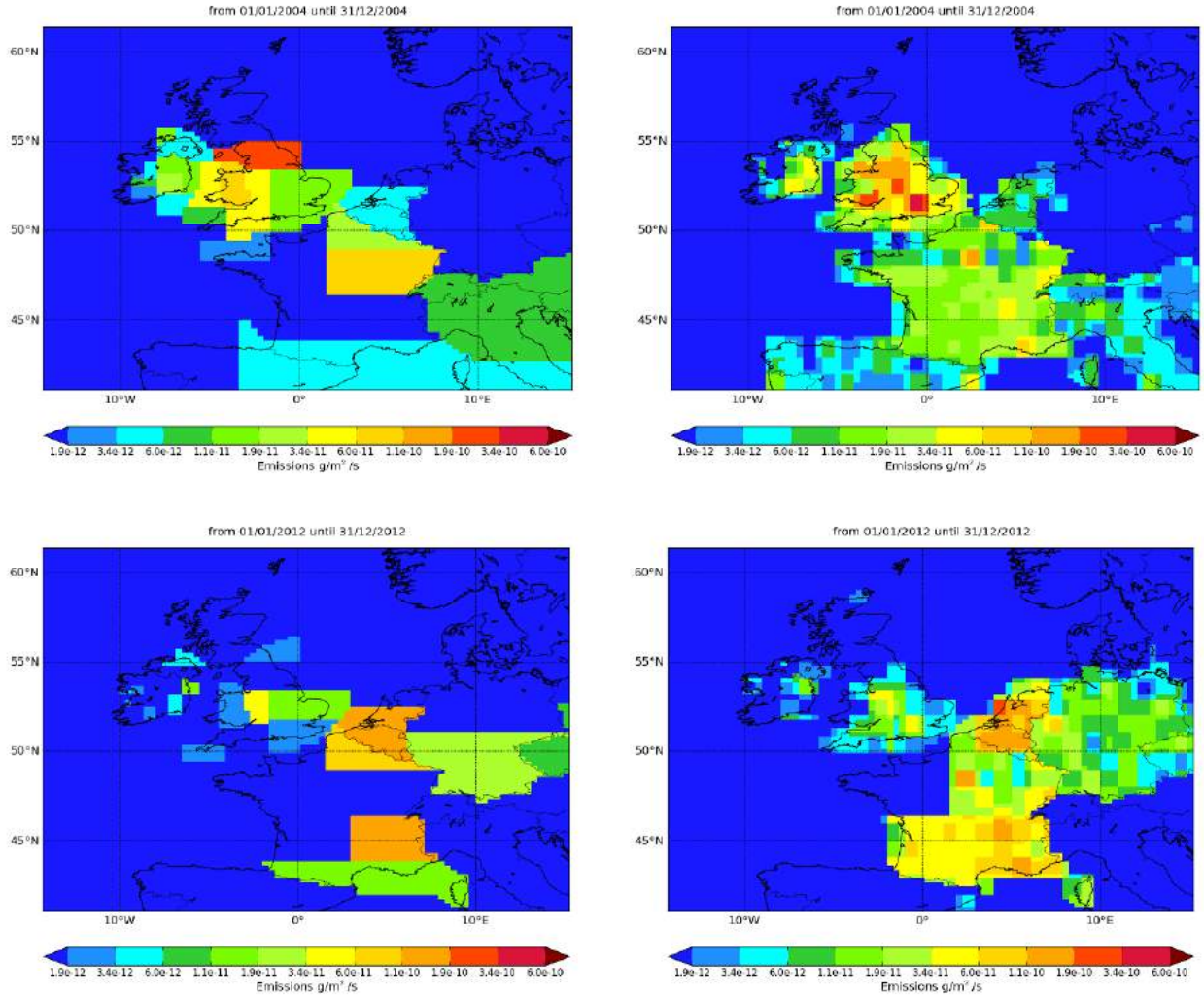

Figure 114: NAME-inversion emission estimates for 2004 (upper) and 2012 (lower). On the right hand side the emissions per grid box have been re-distributed based on population.

Year	RMSE (ppt)	Correlation	Max obs. above baseline (ppt)	% obs. above baseline noise	Mean obs. above baseline (ppt)
2004	0.14	0.63	2.8	39	0.10
2012	0.09	0.75	2.3	39	0.08

Table 56: Comparison between modelled and observed time-series.

The statistical match between the modelled and observed time-series is good. The emissions in the UK have decreased significantly whereas those in NWEU have remained somewhat static with the continental emissions taking up the reduction in emissions over the UK.

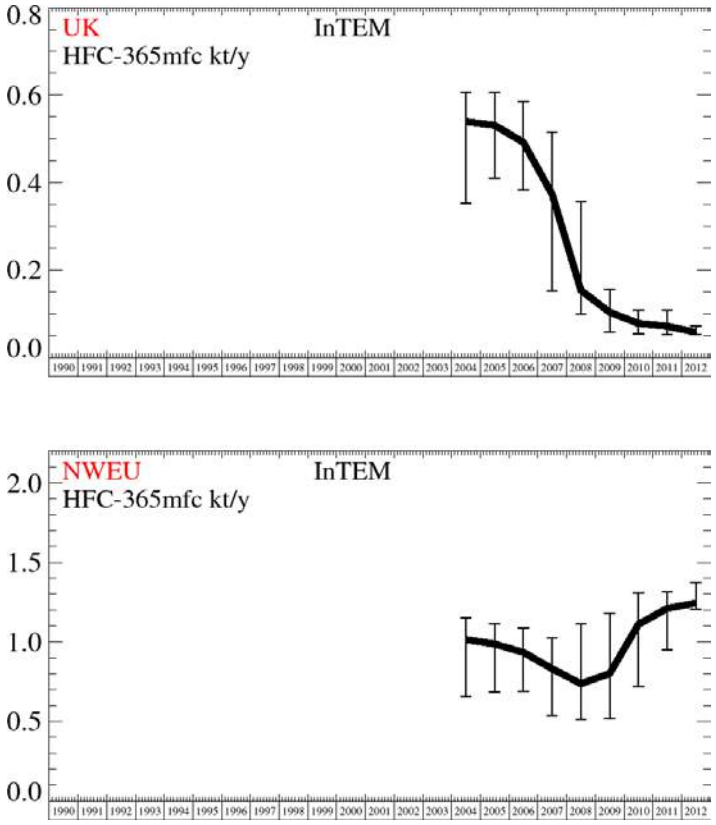

Figure 115: Emission estimates for UK and NWEU. The uncertainty bars represent the 5th and 95th percentiles.

Unit	Year	UK	(5th-95th)	NWEU	(5th-95th)
t/y	2004	540	(352.- 606.)	1020	(653.-1154.)
t/y	2005	530	(409.- 607.)	990	(685.-1114.)
t/y	2006	490	(384.- 586.)	930	(688.-1088.)
t/y	2007	370	(153.- 516.)	830	(538.-1023.)
t/y	2008	154	(99.- 357.)	740	(512.-1112.)
t/y	2009	104	(57.- 156.)	800	(519.-1179.)
t/y	2010	78	(54.- 108.)	1110	(718.-1309.)
t/y	2011	71	(52.- 108.)	1210	(951.-1316.)
t/y	2012	58	(52.- 72.)	1240	(1205.-1372.)

Table 57: Emission estimates for UK and NWEU with uncertainty (5th – 95th %ile).

6.13 HFC-4310mee

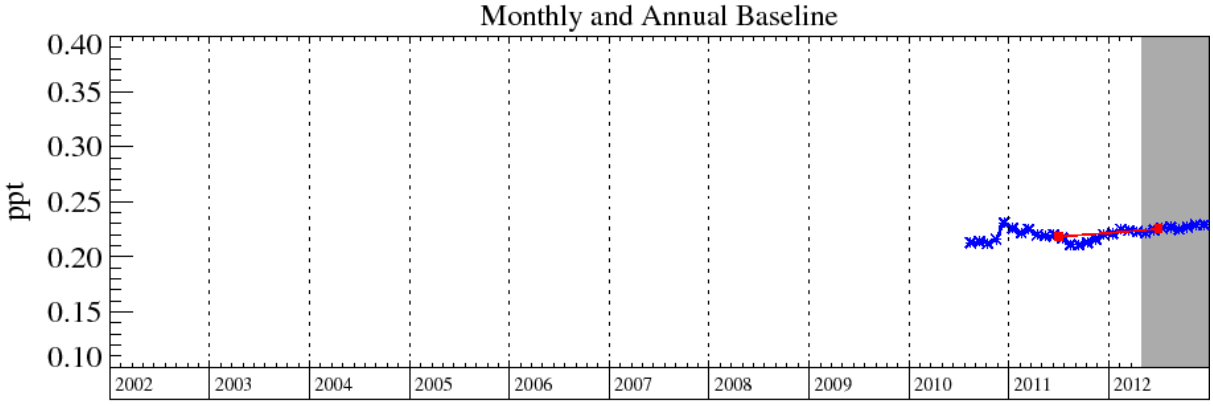

Figure 116: HFC-4310mee: Monthly (blue) and annual (red) baseline concentrations.

HFC-43-10mee: Introduced in the mid 1990s as a replacement for CFC-113. It meets many requirements in the electronics industries and replaces PFCs in some uses such as a carrier fluid for lubricants applied to computer hard disks. It has an atmospheric lifetime of 15.9 years, a GWP_{100} of 1,640 and a radiative efficiency of 0.4 W m^{-2} ppb^{-1}.

As yet it is too early to calculate growth rates for this gas, but this information will be included once 3 years of data have been acquired.

6.14 SO_2F_2

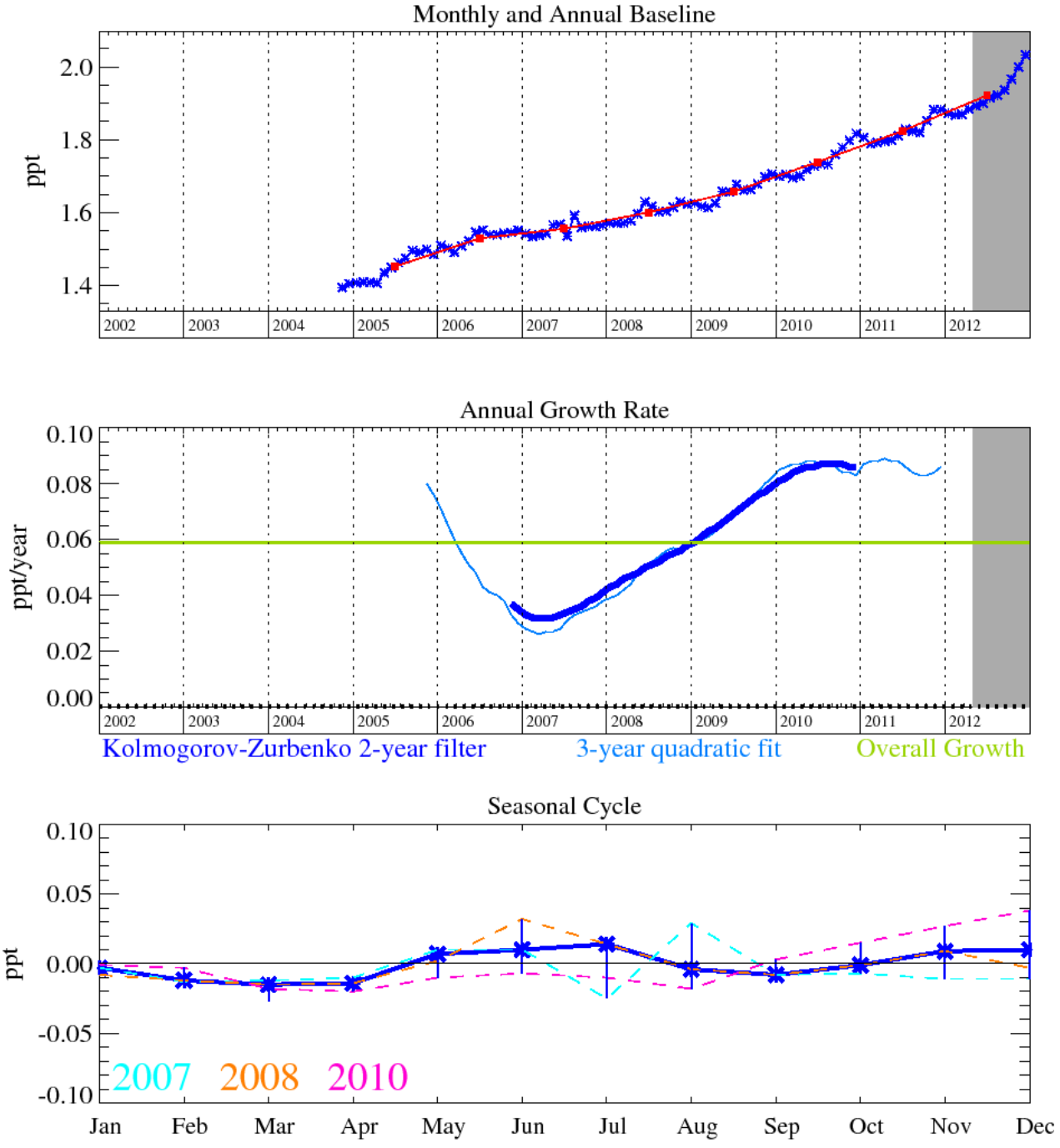

Figure 117: SO_2F_2: Monthly (blue) and annual (red) baseline concentrations (top plot). Annual (blue) and overall average growth rate (green) (middle plot). Seasonal cycle (de-trended) with year-to-year variability (lower plot). Grey area covers un-ratified and therefore provisional data.

6.15 CH_3Cl

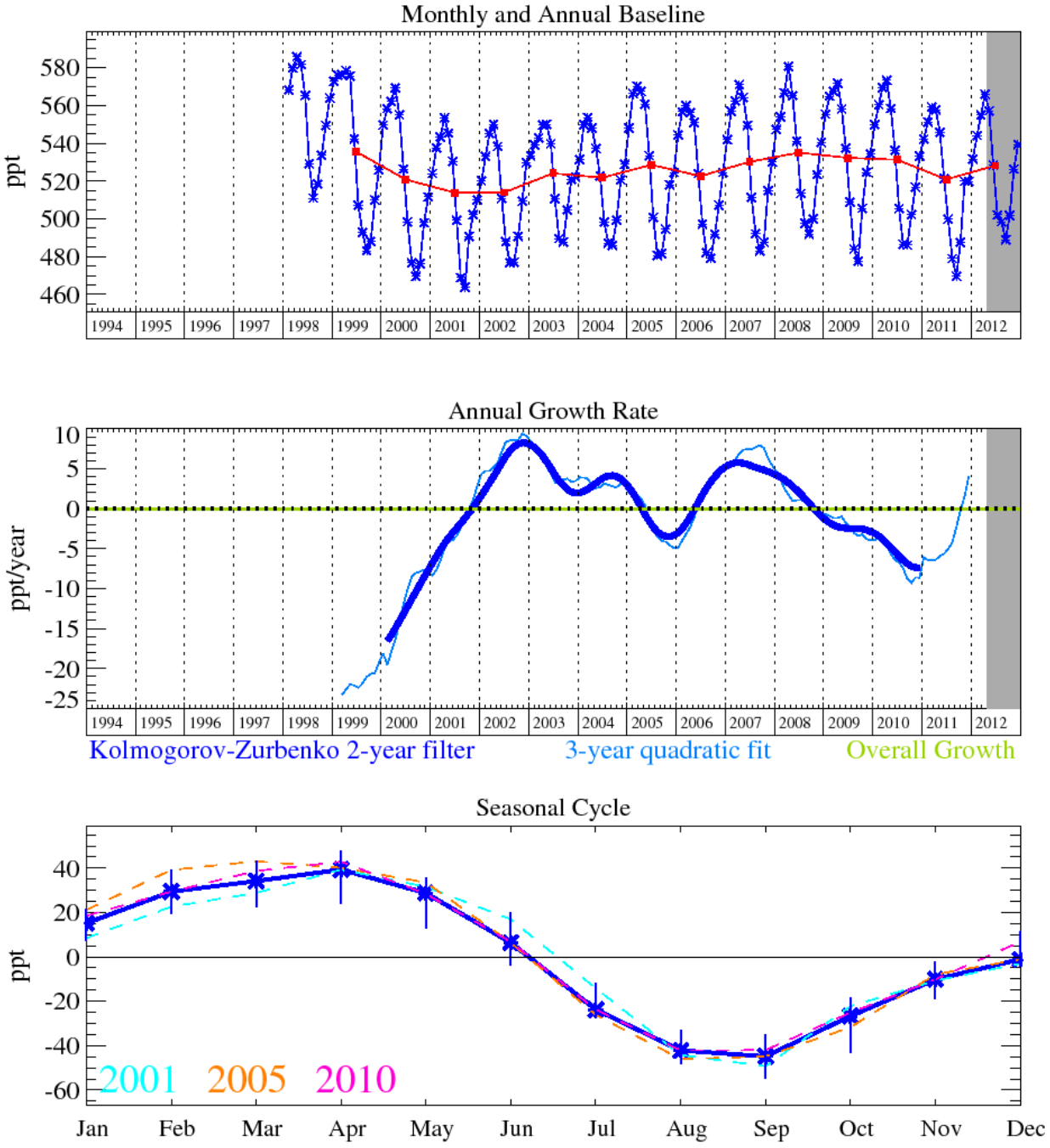

Figure 118: CH_3Cl: Monthly (blue) and annual (red) baseline concentrations (top plot). Annual (blue) and overall growth rate (green) (middle). Seasonal cycle (de-trended) with year-to-year variability (lower plot). Grey area covers un-ratified and therefore provisional data.

A number of long lived and very short lived substances (VSLS) halocarbons are measured by the Medusa GC-MS. Previously we reported the recovery of CH_3Cl growth in the atmosphere, this growth abated in 2010 and the trend now shows a decline of 3.6 ppt/yr to 528 ppt in 2012 (Figure 118). Methyl chloride (CH_3Cl) is not a controlled substance and is emitted from a range of biogenic and anthropogenic sources globally. It is estimated that ~55% of CH_3Cl emissions arise from terrestrial tropical areas with emission rates dependent on global temperature changes. Other major sources are biomass burning, anthropogenic activities and oceans. The atmospheric lifetime of CH_3Cl is 1 year [*Montzka et al.*, 2011] and it has a GWP_{100} of 13 [*Forster et al.*, 2007]. CH_3Cl contributes 16% of the total chlorine loading to the troposphere for long-lived species and is thus the most abundant chlorine containing compound in the atmosphere.

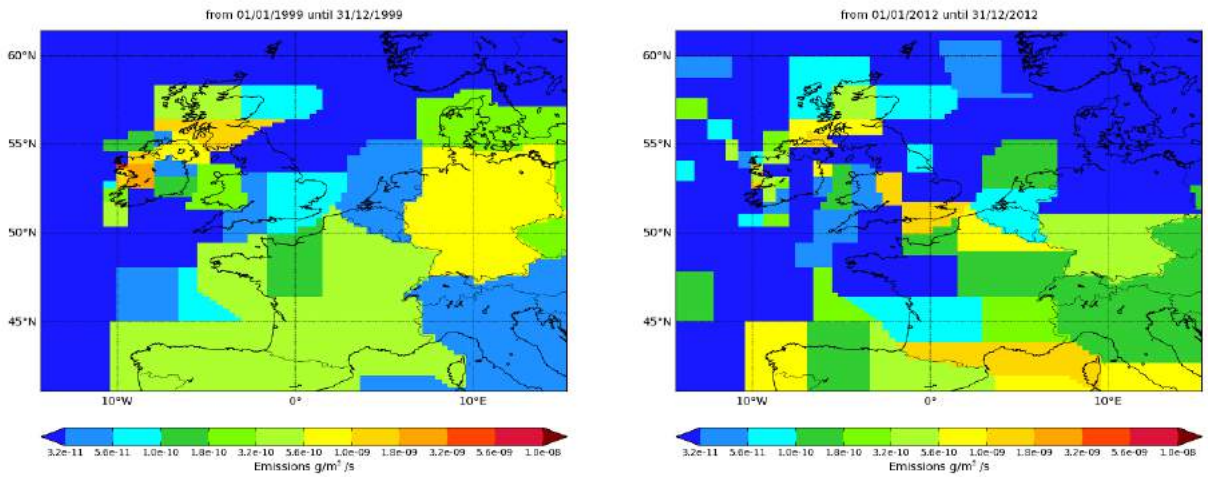

Figure 119: NAME-inversion emission estimates for 1999 (upper) and 2012 (lower).

For this gas the emissions have not been re-distributed based on population because given its natural releases its emissions are not well correlated with population.

Year	RMSE (ppt)	Correlation	Max obs. above baseline (ppt)	% obs. above baseline noise	Mean obs. above baseline (ppt)
1999	44.4	0.45	1318	37	32
2012	16.8	0.49	193	39	23

Table 58: Comparison between modelled and observed time-series.

The statistical match between the observations and model time-series is reasonable but there is significant uncertainty in the InTEM emission estimates. The emissions over the UK and NWEU as a whole have remained broadly constant over the length of the record.

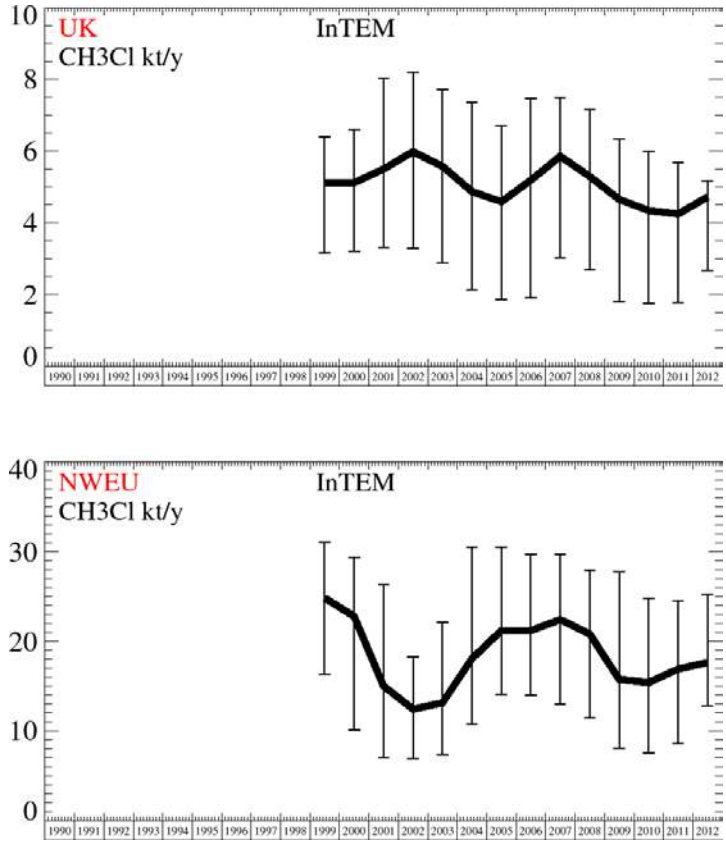

Figure 120: Emission estimates for UK and NWEU. The uncertainty bars represent the 5th and 95th percentiles.

Unit	Year	UK	(5th-95th)	NWEU	(5th-95th)
kt/y	1999	5.1	(3.2- 6.4)	25	(16.- 31.)
kt/y	2000	5.1	(3.2- 6.6)	23	(10.- 29.)
kt/y	2001	5.5	(3.3- 8.0)	15	(7.- 26.)
kt/y	2002	6	(3.3- 8.2)	12.4	(7.- 18.)
kt/y	2003	5.6	(2.9- 7.7)	13.1	(7.- 22.)
kt/y	2004	4.9	(2.1- 7.4)	18.1	(11.- 30.)
kt/y	2005	4.6	(1.9- 6.7)	21	(14.- 30.)
kt/y	2006	5.2	(1.9- 7.5)	21	(14.- 30.)
kt/y	2007	5.9	(3.0- 7.5)	22	(13.- 30.)
kt/y	2008	5.3	(2.7- 7.2)	21	(11.- 28.)
kt/y	2009	4.7	(1.8- 6.3)	15.7	(8.- 28.)
kt/y	2010	4.3	(1.7- 6.0)	15.4	(8.- 25.)
kt/y	2011	4.2	(1.8- 5.7)	16.9	(9.- 25.)
kt/y	2012	4.7	(2.7- 5.2)	17.6	(13.- 25.)

Table 59: Emission estimates for UK and NWEU with uncertainty (5th – 95th %ile).

6.16 CH_2Cl_2

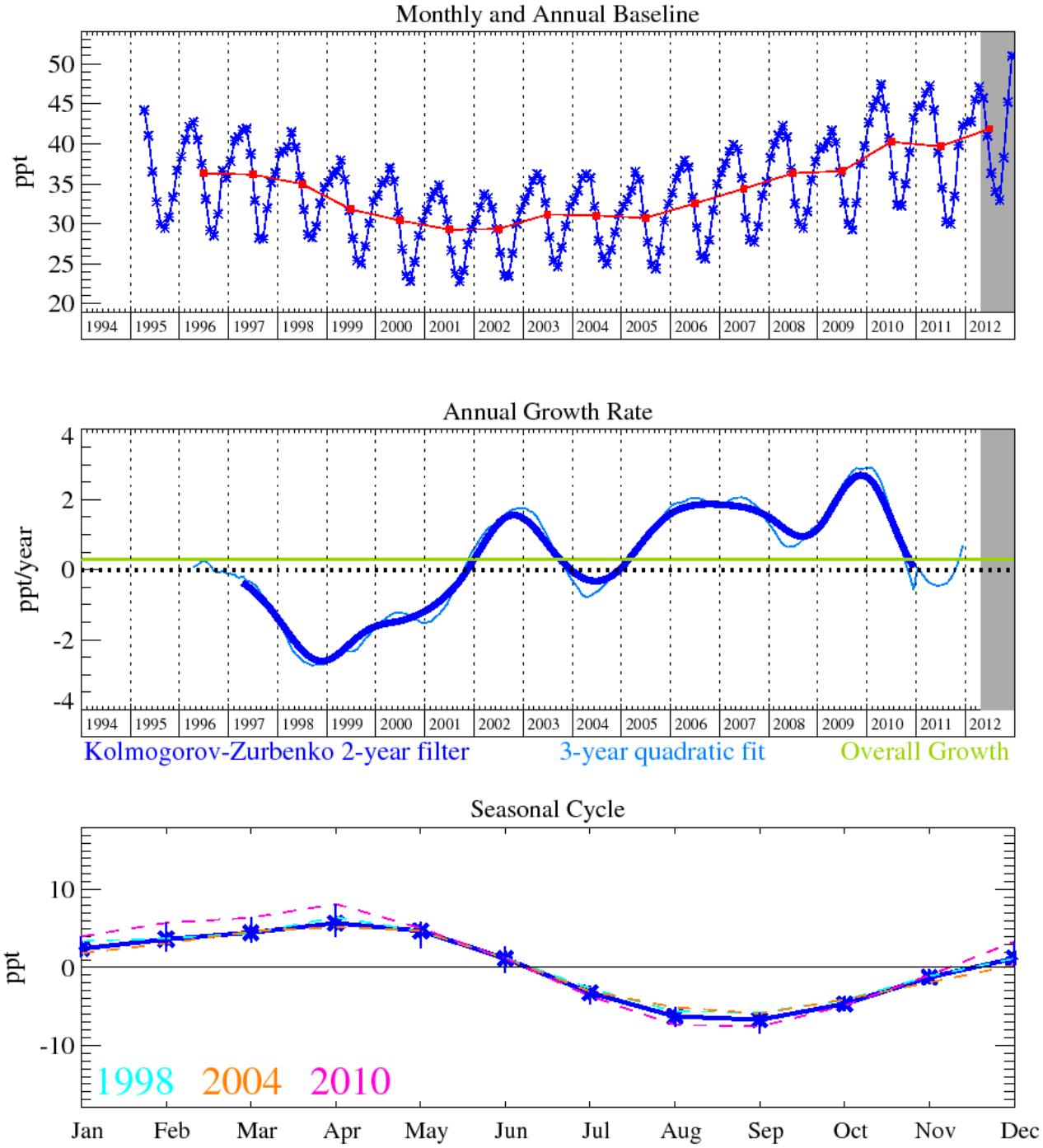

Figure 121: CH_2Cl_2: Monthly (blue) and annual (red) baseline concentrations (top plot). Annual (blue) and overall average growth rate (green) (middle plot). Seasonal cycle (de-trended) with year-to-year variability (lower plot). Grey area covers un-ratified and therefore provisional data.

Dichloromethane (CH_2Cl_2) global sources are thought to be 70% or greater of anthropogenic origin [*Keene et al.*, 1999; *Cox et al.*, 2003]. It is predominantly used as a paint stripper, degreaser, foam-blowing agent and in pharmaceutical production methods. Its use as a paint stripper has been banned since 2010 in the EU. CH_2Cl_2 also showed a decline in line with a reduction in the many solvent applications for this compound, however, between 2002 and 2010, measurements at Mace Head have shown it to be generally accumulating in the atmosphere as shown in Figure 121. Its recent growth rate is close to zero. Its average mixing ratio in 2012 was 41.9 ppt. Emission totals derived using the NAME model and the industry derived inventory suggest that emissions from the NW Europe (and the UK) are decreasing, which implies a source of CH_2Cl_2 to the atmosphere

from locations outside of Europe. CH_2Cl_2 has a lifetime of 144 days [*Montzka et al.*, 2011] and a GWP_{100} of 8.7 [*Forster et al.*, 2007].

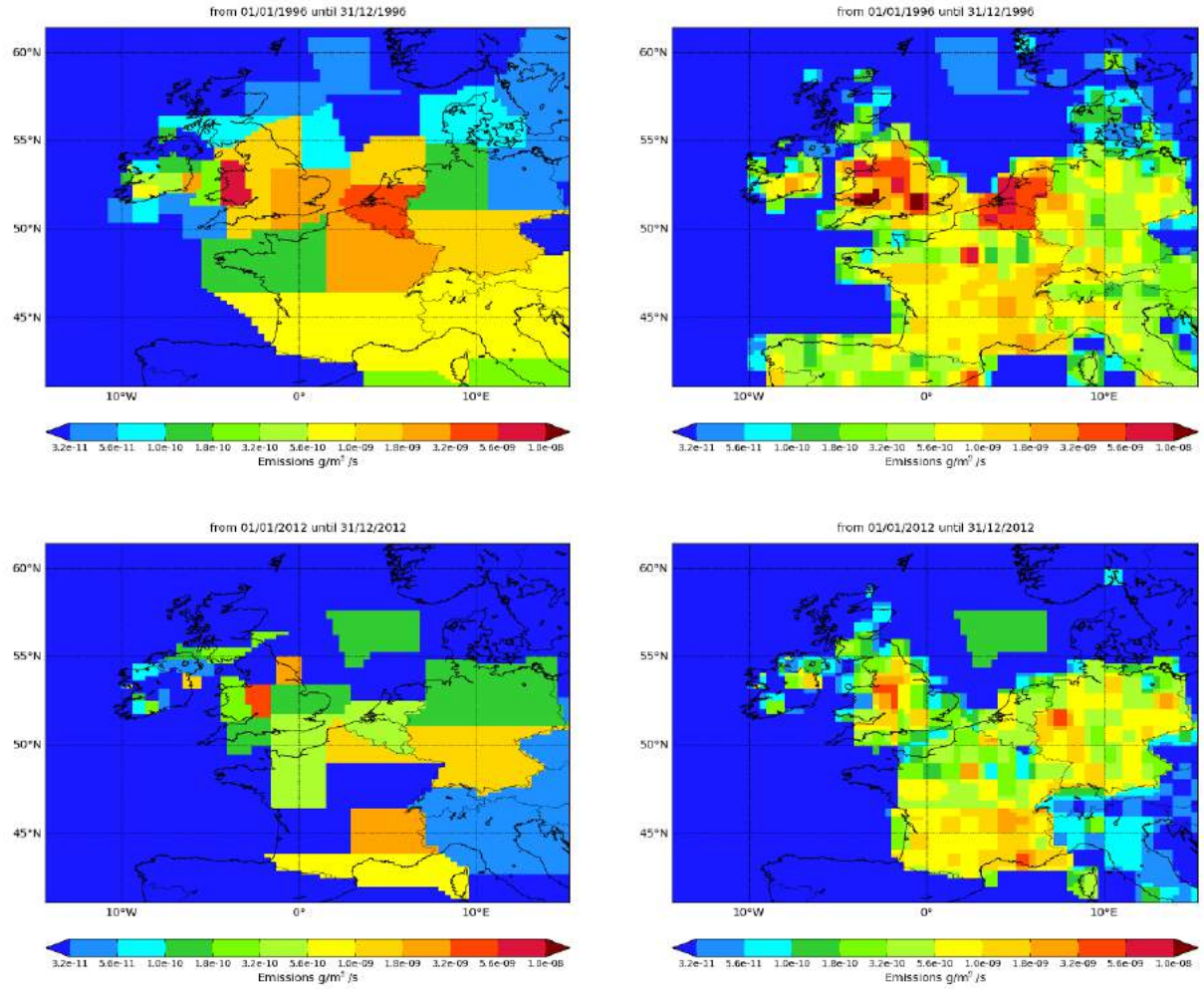

Figure 122: NAME-inversion emission estimates for 2004 (upper) and 2012 (lower). On the right hand side the emissions per grid box have been re-distributed based on population.

Year	RMSE (ppt)	Correlation	Max obs. above baseline (ppt)	% obs. above baseline noise	Mean obs. above baseline (ppt)
1996	22.5	0.83	310	55	26
2012	5.0	0.55	105	38	5

Table 60: Comparison between modelled and observed time-series.

There is strong evidence across all of the metrics that UK and NWEU emissions have declined significantly over the past 17 years although there are still relatively strong discernible pollution events. The statistical match between the modelled and observed time-series is good.

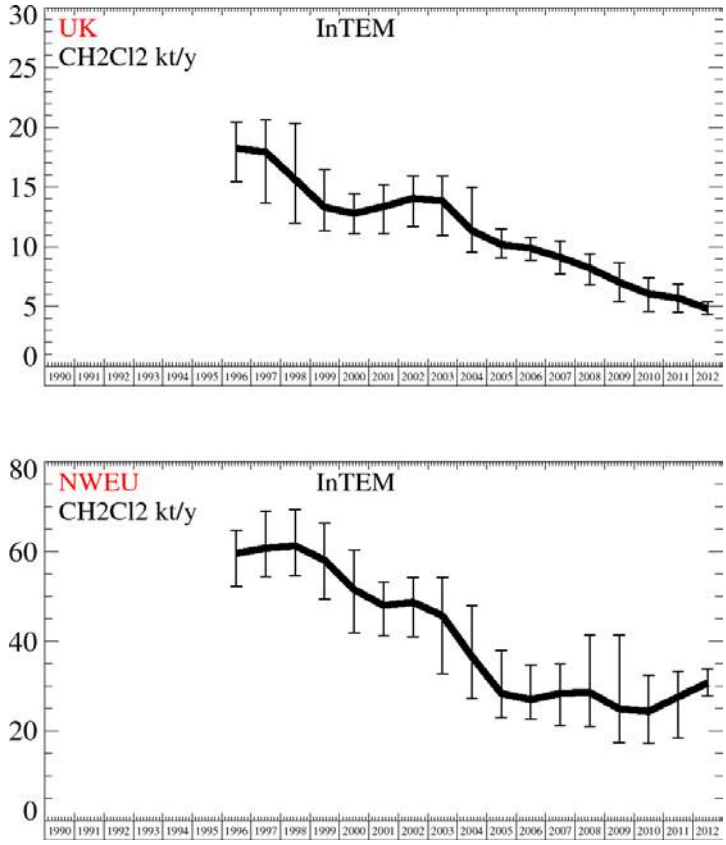

Figure 123: Emission estimates for UK and NWEU. The uncertainty bars represent the 5th and 95th percentiles.

Unit	Year	UK	(5th-95th)	NWEU	(5th-95th)
kt/y	1996	18.2	(15.- 20.)	60	(52.- 65.)
kt/y	1997	17.9	(14.- 21.)	61	(54.- 69.)
kt/y	1998	15.6	(12.- 20.)	61	(55.- 69.)
kt/y	1999	13.3	(11.- 16.)	58	(49.- 66.)
kt/y	2000	12.8	(11.- 14.)	52	(42.- 60.)
kt/y	2001	13.3	(11.- 15.)	48	(41.- 53.)
kt/y	2002	14.1	(12.- 16.)	49	(41.- 54.)
kt/y	2003	13.8	(11.- 16.)	46	(33.- 54.)
kt/y	2004	11.4	(10.- 15.)	37	(27.- 48.)
kt/y	2005	10.2	(9.- 12.)	28	(23.- 38.)
kt/y	2006	9.9	(9.- 11.)	27	(23.- 35.)
kt/y	2007	9.1	(8.- 11.)	28	(21.- 35.)
kt/y	2008	8.2	(7.- 9.)	29	(21.- 41.)
kt/y	2009	7	(5.- 9.)	25	(17.- 41.)
kt/y	2010	6.1	(5.- 7.)	24	(17.- 32.)
kt/y	2011	5.7	(5.- 7.)	28	(18.- 33.)
kt/y	2012	4.8	(4.- 5.)	31	(28.- 34.)

Table 61: Emission estimates for UK and NWEU with uncertainty (5th – 95th %ile).

6.17 $CHCl_3$ (chloroform)

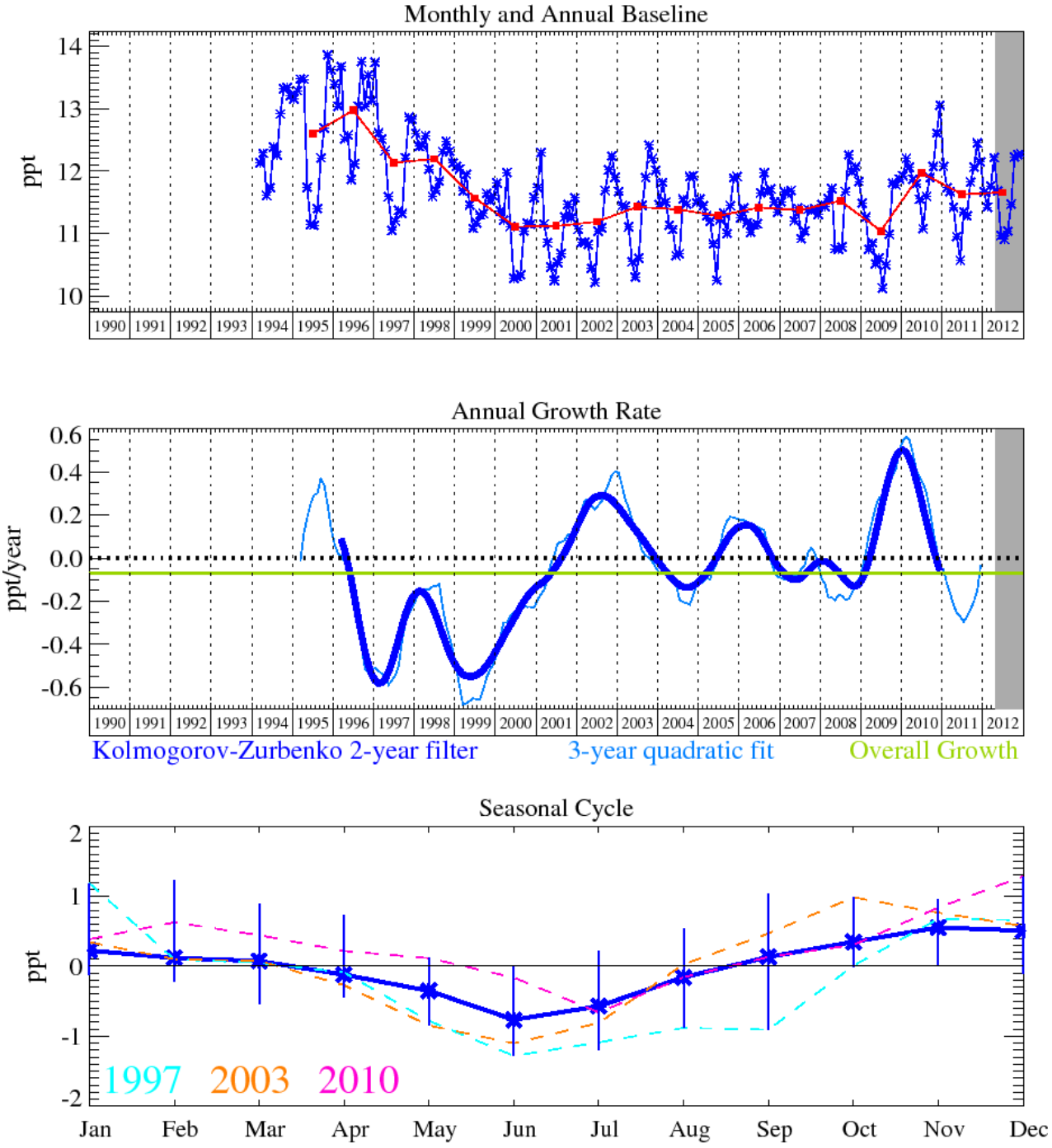

Figure 124: $CHCl_3$: Monthly (blue) and annual (red) baseline concentrations (top plot). Annual (blue) and overall average growth rate (green) (middle plot). Seasonal cycle (de-trended) with year-to-year variability (lower plot). Grey area covers un-ratified and therefore provisional data.

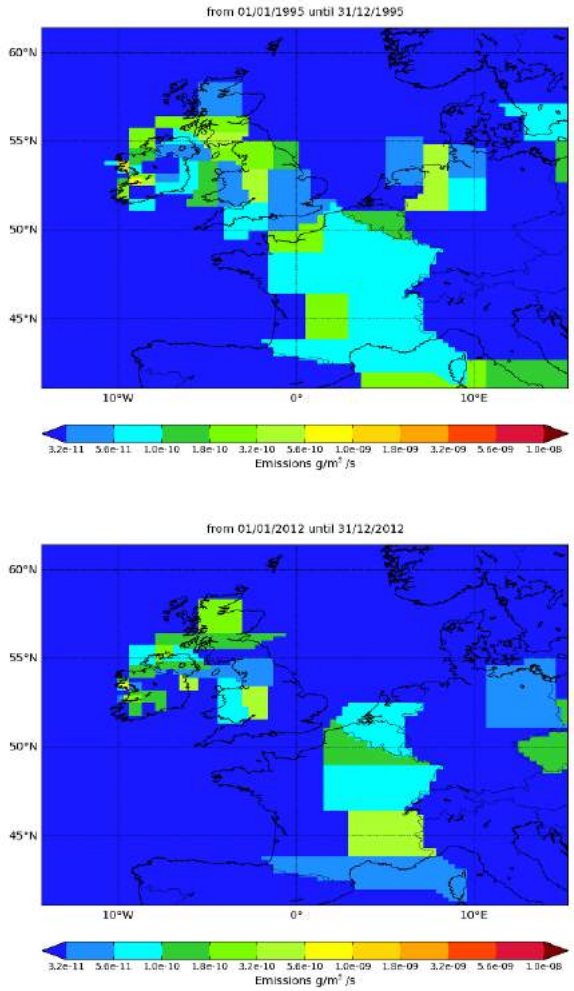

Figure 125: NAME-inversion emission estimates for 1995 (upper) and 2012 (lower). On the right hand side the emissions per grid box have been re-distributed based on population.

Year	RMSE (ppt)	Correlation	Max obs. above baseline (ppt)	% obs. above baseline noise	Mean obs. above baseline (ppt)
1995	3.2	0.71	46	40	3.6
2012	1.7	0.78	25	41	2.4

Table 62: Comparison between modelled and observed time-series.

The statistical match between the modelled and observed time-series is consistently good. There has been a modest decline in emissions in both the UK and NWEU in line with the reduction in the magnitude of the average and maximum pollution event.

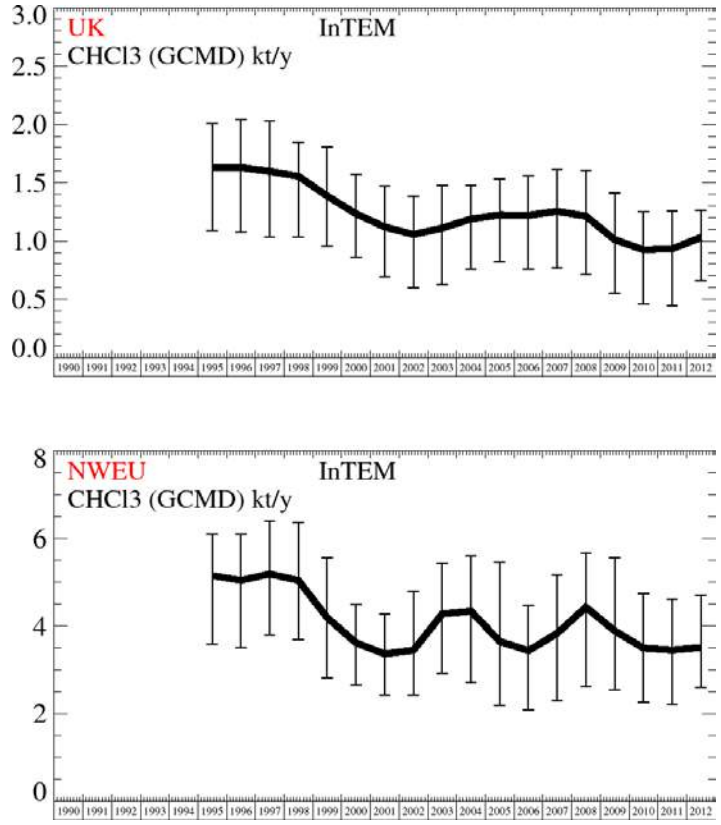

Figure 126: Emission estimates for UK and NWEU. The uncertainty bars represent the 5th and 95th percentiles.

Unit	Year	UK	(5th-95th)	NWEU	(5th-95th)
t/y	1995	1630	(1087.-2006.)	5200	(3584.-6106.)
t/y	1996	1630	(1076.-2043.)	5000	(3517.-6095.)
t/y	1997	1600	(1034.-2026.)	5200	(3788.-6404.)
t/y	1998	1550	(1036.-1845.)	5000	(3695.-6369.)
t/y	1999	1390	(953.-1809.)	4200	(2813.-5566.)
t/y	2000	1230	(859.-1574.)	3600	(2643.-4498.)
t/y	2001	1120	(691.-1471.)	3400	(2410.-4282.)
t/y	2002	1050	(599.-1386.)	3400	(2417.-4793.)
t/y	2003	1110	(622.-1480.)	4300	(2910.-5436.)
t/y	2004	1190	(763.-1479.)	4300	(2701.-5599.)
t/y	2005	1220	(820.-1528.)	3600	(2187.-5463.)
t/y	2006	1220	(757.-1556.)	3400	(2084.-4483.)
t/y	2007	1250	(765.-1610.)	3800	(2295.-5173.)
t/y	2008	1210	(714.-1602.)	4400	(2615.-5672.)
t/y	2009	1010	(554.-1407.)	3900	(2549.-5567.)
t/y	2010	920	(459.-1251.)	3500	(2254.-4736.)
t/y	2011	930	(447.-1258.)	3400	(2206.-4614.)
t/y	2012	1030	(660.-1261.)	3500	(2603.-4707.)

Table 63: Emission estimates for UK and NWEU with uncertainty (5th – 95th %ile).

6.18 CCl_4 (carbon tetrachloride)

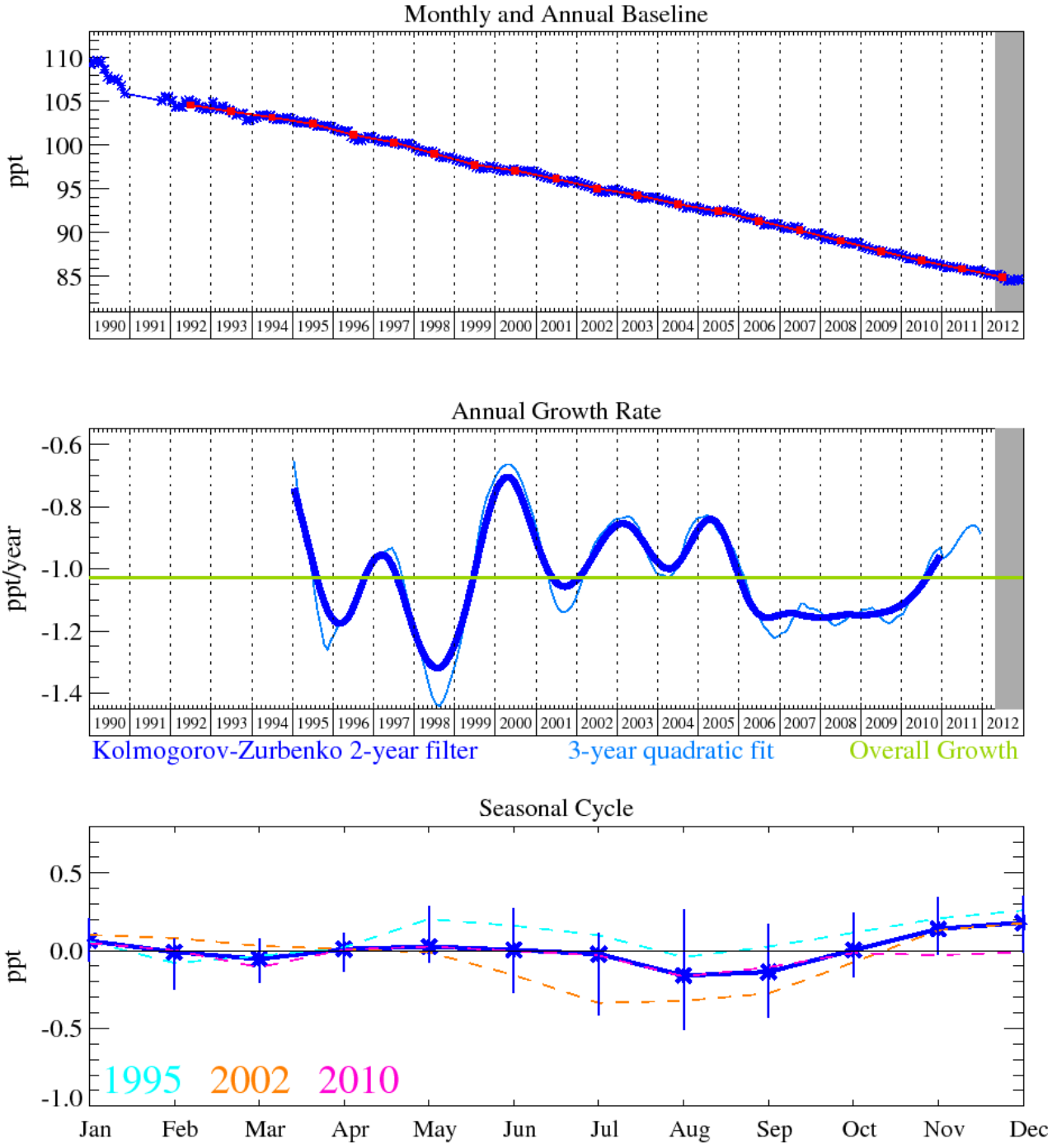

Figure 127: CCl_4: Monthly (blue) and annual (red) baseline concentrations (top plot). Annual (blue) and overall average growth rate (green) (middle plot). Seasonal cycle (de-trended) with year-to-year variability (lower plot). Grey area covers un-ratified and therefore provisional data.

Figure 127 illustrates the steady downward trend of CCl_4 (26 year lifetime [*Montzka et al.*, 2011]), currently 0.9 ppt/yr, making this compound the second most rapidly decreasing chlorocarbon after CH_3CCl_3. The level of CCl_4 at Mace Head in December 2012 was 84.6 ppt. Its major use was as a feedstock for CFC manufacturing and unlike CH_3CCl_3 a significant inter-hemispheric CCl_4 gradient still exists, resulting from a persistence of significant northern hemisphere (NH) emissions. It is interesting that atmospheric observations for this compound are decreasing less rapidly than projected in the A1 scenario of the Ozone Assessment [Daniel and Velders *et al.*, 2007]. CCl_4 emissions derived from atmospheric observations (top-down) suggest substantially smaller emissions than emissions derived from bottom-up techniques using reported production, feedstock

and destruction data. The reason for this discrepancy is the subject of study for the forthcoming WMO SPARC report.

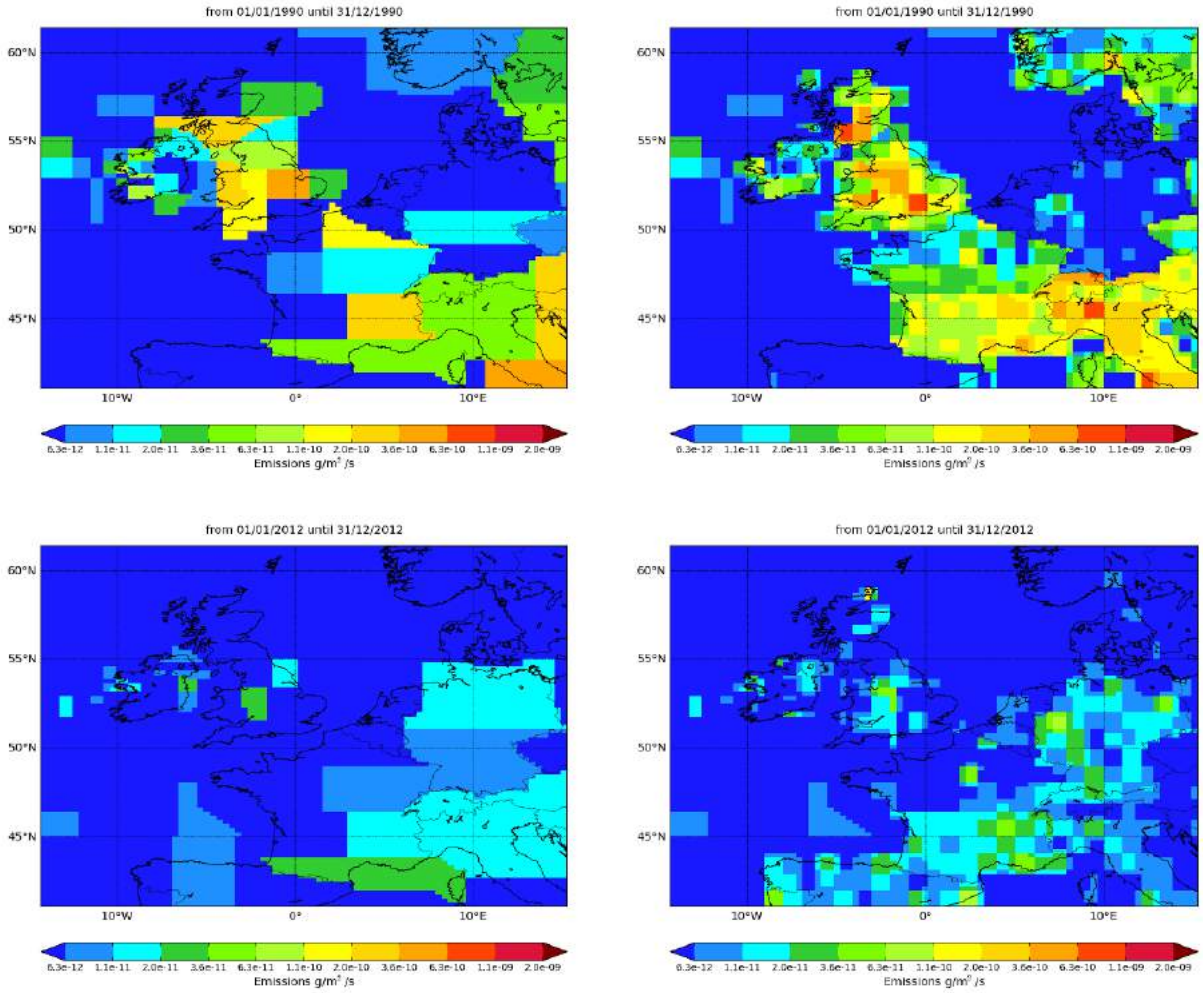

Figure 128: NAME-inversion emission estimates for 1990 (upper) and 2012 (lower). On the right hand side the emissions per grid box have been re-distributed based on population.

Year	RMSE (ppt)	Correlation	Max obs. above baseline (ppt)	% obs. above baseline noise	Mean obs. above baseline (ppt)
1990	1.5	0.46	18.1	25	1.3
2012	0.2	0.09	1.7	9	0.2

Table 64: Comparison between modelled and observed time-series.

The magnitude of the pollution events reaching Mace Head have fallen very significantly from 1990 reflecting the impact of the Montreal Protocol and the strong decline in emissions across NWEU. The pollution events are now poorly resolved against the uncertainty in the baseline leading to a poor correlation between the model time-series and the observations in the latter years.

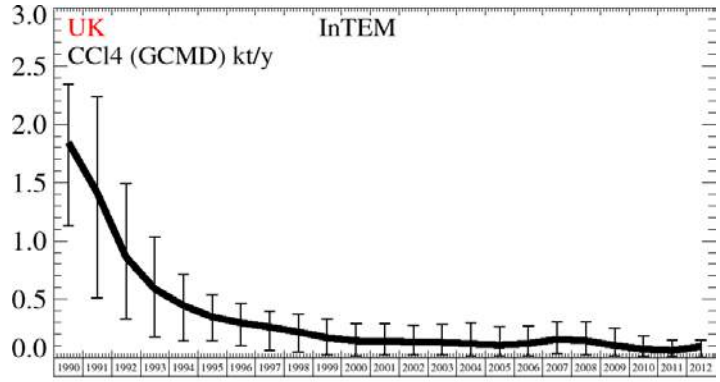

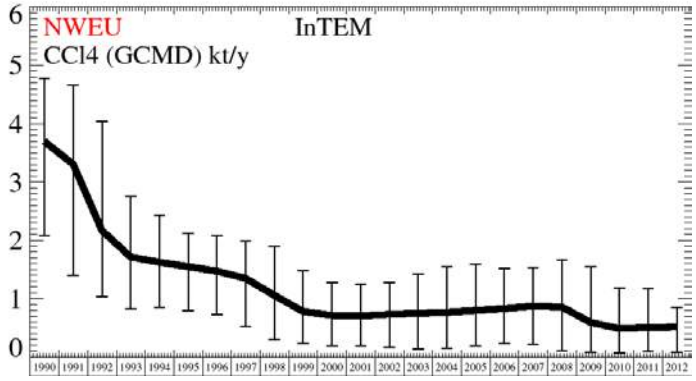

Figure 129: Emission estimates for UK and NWEU. The uncertainty bars represent the 5th and 95th percentiles.

Unit	Year	UK	(5th-95th)	NWEU	(5th-95th)
t/y	1990	1840	(1130.-2340.)	3700	(2082.-4776.)
t/y	1991	1410	(510.-2238.)	3300	(1392.-4656.)
t/y	1992	860	(333.-1493.)	2200	(1038.-4040.)
t/y	1993	590	(179.-1035.)	1710	(820.-2753.)
t/y	1994	450	(144.- 711.)	1620	(843.-2425.)
t/y	1995	350	(139.- 541.)	1550	(795.-2123.)
t/y	1996	300	(101.- 462.)	1470	(721.-2086.)
t/y	1997	260	(62.- 395.)	1350	(525.-1990.)
t/y	1998	220	(47.- 367.)	1060	(303.-1899.)
t/y	1999	170	(21.- 333.)	780	(237.-1483.)
t/y	2000	143	(18.- 292.)	710	(194.-1273.)
t/y	2001	139	(19.- 289.)	700	(184.-1255.)
t/y	2002	134	(20.- 274.)	730	(159.-1283.)
t/y	2003	129	(19.- 281.)	750	(132.-1426.)
t/y	2004	118	(15.- 296.)	760	(144.-1551.)
t/y	2005	107	(13.- 261.)	800	(191.-1586.)
t/y	2006	120	(15.- 272.)	830	(224.-1516.)
t/y	2007	155	(33.- 302.)	870	(221.-1537.)
t/y	2008	143	(24.- 303.)	850	(110.-1671.)
t/y	2009	104	(13.- 251.)	590	(79.-1541.)
t/y	2010	72	(8.- 185.)	490	(74.-1179.)
t/y	2011	61	(6.- 146.)	510	(93.-1174.)
t/y	2012	94	(5.- 147.)	510	(88.- 848.)

Table 65: Emission estimates for UK and NWEU with uncertainty (5th – 95th %ile).

6.19 CH_3CCl_3 (methyl chloroform)

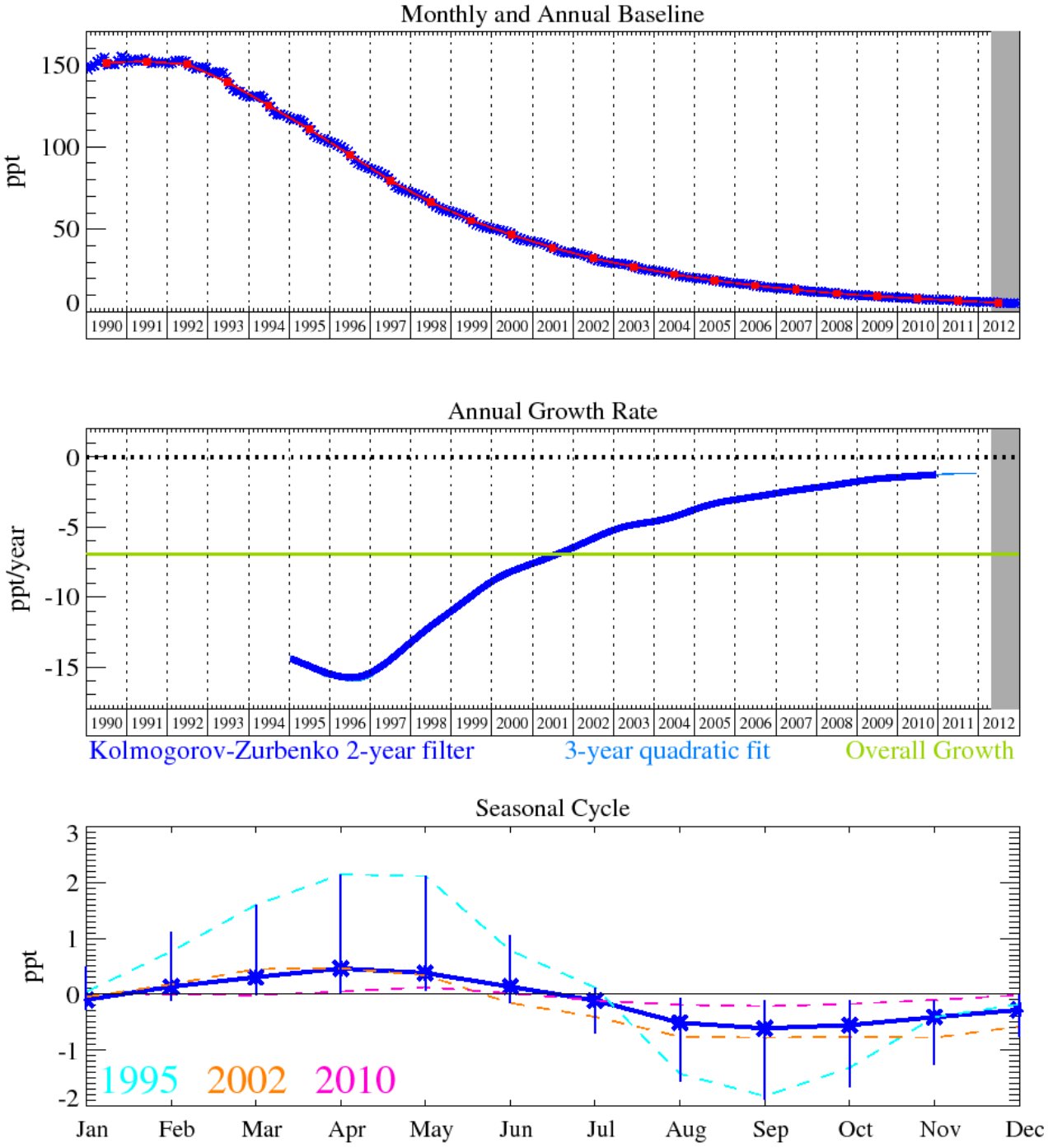

Figure 130: CH_3CCl_3: Monthly (blue) and annual (red) baseline concentrations (top plot). Annual (blue) and overall average growth rate (green) (middle plot). Seasonal cycle (de-trended) with year-to-year variability (lower plot). Grey area covers un-ratified and therefore provisional data.

The major solvent methyl chloroform (CH_3CCl_3) is an important compound because of its use to estimate concentrations of the hydroxyl radical (OH), which is the major sink species for CH_4, HFCs and HCFCs. The global atmospheric CH_3CCl_3 concentration peaked in 1992 (Prinn *et al.*, 2000) then declined in accordance with its short atmospheric lifetime (5.0 years [*Forster et al.*, 2007]) and phase out under the terms of the Montreal protocol. The baseline mixing ratio of CH_3CCl_3 at Mace Head (Figure 130) is currently decreasing by 1.2 ppt/yr and reached a mixing ratio of 4.9 ppt in December 2012. The GWP_{100} of methyl chloroform is 146.

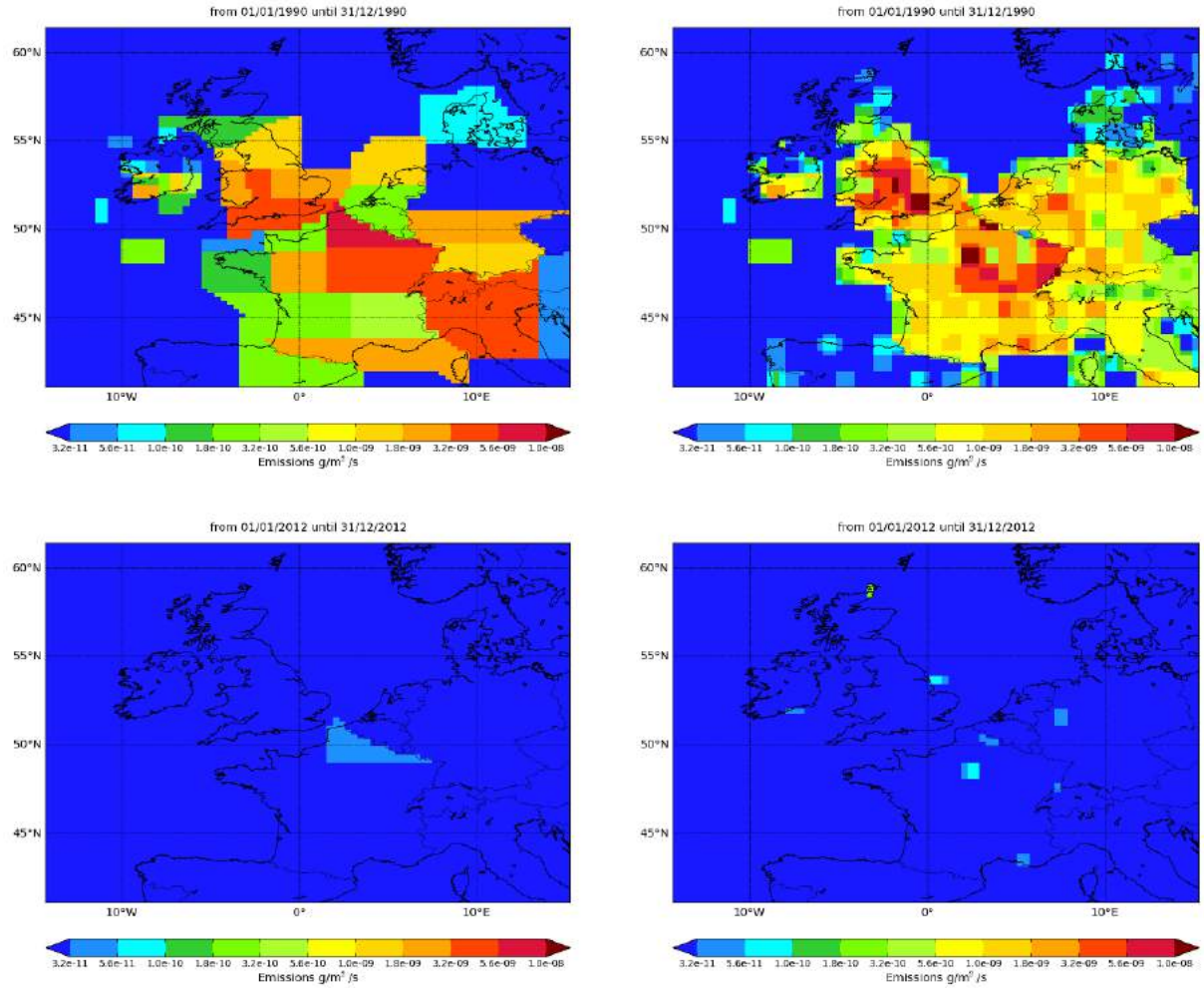

Figure 131: NAME-inversion emission estimates for 1990 (upper) and 2012 (lower). On the right hand side the emissions per grid box have been re-distributed based on population.

Year	RMSE (ppt)	Correlation	Max obs. above baseline (ppt)	% obs. above baseline	Mean obs. above baseline (ppt)
1990	10.4	0.83	174	37	11.9
2012	0.2	0.06	1.2	10	0.1

Table 66: Comparison between modelled and observed time-series.

Like carbon tetrachloride, the magnitude of the pollution events reaching Mace Head have fallen very significantly from 1990 reflecting the impact of the Montreal Protocol and the strong decline in emissions across NWEU. The pollution events are now poorly resolved against the uncertainty in the baseline leading to a poor correlation between the model time-series and the observations in the latter years.

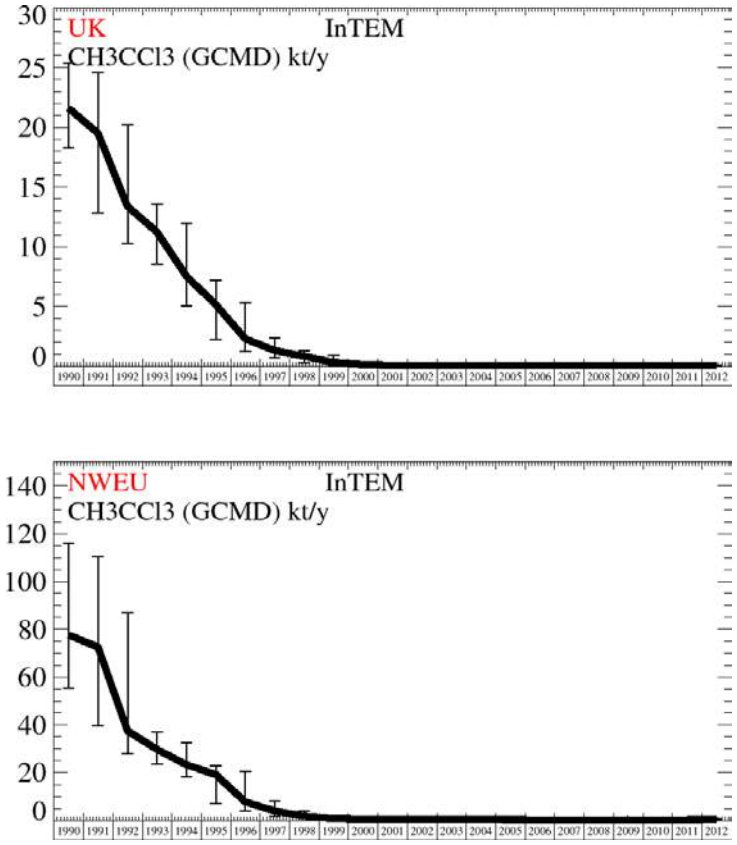

Figure 132: Emission estimates for UK and NWEU. The uncertainty bars represent the 5th and 95th percentiles.

Unit	Year	UK	(5th-95th)	NWEU	(5th-95th)
kt/y	1990	22	(18.- 25.)	78	(56.- 116.)
kt/y	1991	19.5	(13.- 25.)	73	(40.- 110.)
kt/y	1992	13.4	(10.- 20.)	38	(28.- 87.)
kt/y	1993	11.2	(9.- 14.)	30	(24.- 37.)
kt/y	1994	7.5	(5.- 12.)	23	(18.- 33.)
kt/y	1995	5.1	(2.- 7.)	19.2	(7.- 23.)
kt/y	1996	2.3	(1.- 5.)	7.8	(4.- 20.)
kt/y	1997	1.3	(1.- 2.)	4	(2.- 8.)
kt/y	1998	0.82	(0.- 1.)	1.8	(1.- 4.)
kt/y	1999	0.31	(0.- 1.)	0.86	(0.- 2.)
kt/y	2000	0.12	(0.- 0.)	0.6	(0.- 1.)
kt/y	2001	0.06	(0.- 0.)	0.5	(0.- 1.)
kt/y	2002	0.05	(0.- 0.)	0.46	(0.- 1.)
kt/y	2003	0.06	(0.- 0.)	0.42	(0.- 1.)
kt/y	2004	0.06	(0.- 0.)	0.44	(0.- 1.)
kt/y	2005	0.04	(0.- 0.)	0.4	(0.- 1.)
kt/y	2006	0.04	(0.- 0.)	0.35	(0.- 1.)
kt/y	2007	0.05	(0.- 0.)	0.34	(0.- 1.)
kt/y	2008	0.04	(0.- 0.)	0.32	(0.- 1.)
kt/y	2009	0.03	(0.- 0.)	0.37	(0.- 1.)
kt/y	2010	0.03	(0.- 0.)	0.38	(0.- 1.)
kt/y	2011	0.03	(0.- 0.)	0.37	(0.- 1.)
kt/y	2012	0.04	(0.- 0.)	0.43	(0.- 1.)

Table 67: Emission estimates for UK and NWEU with uncertainty (5th – 95th %ile).

6.20 $CHClCCl_2$

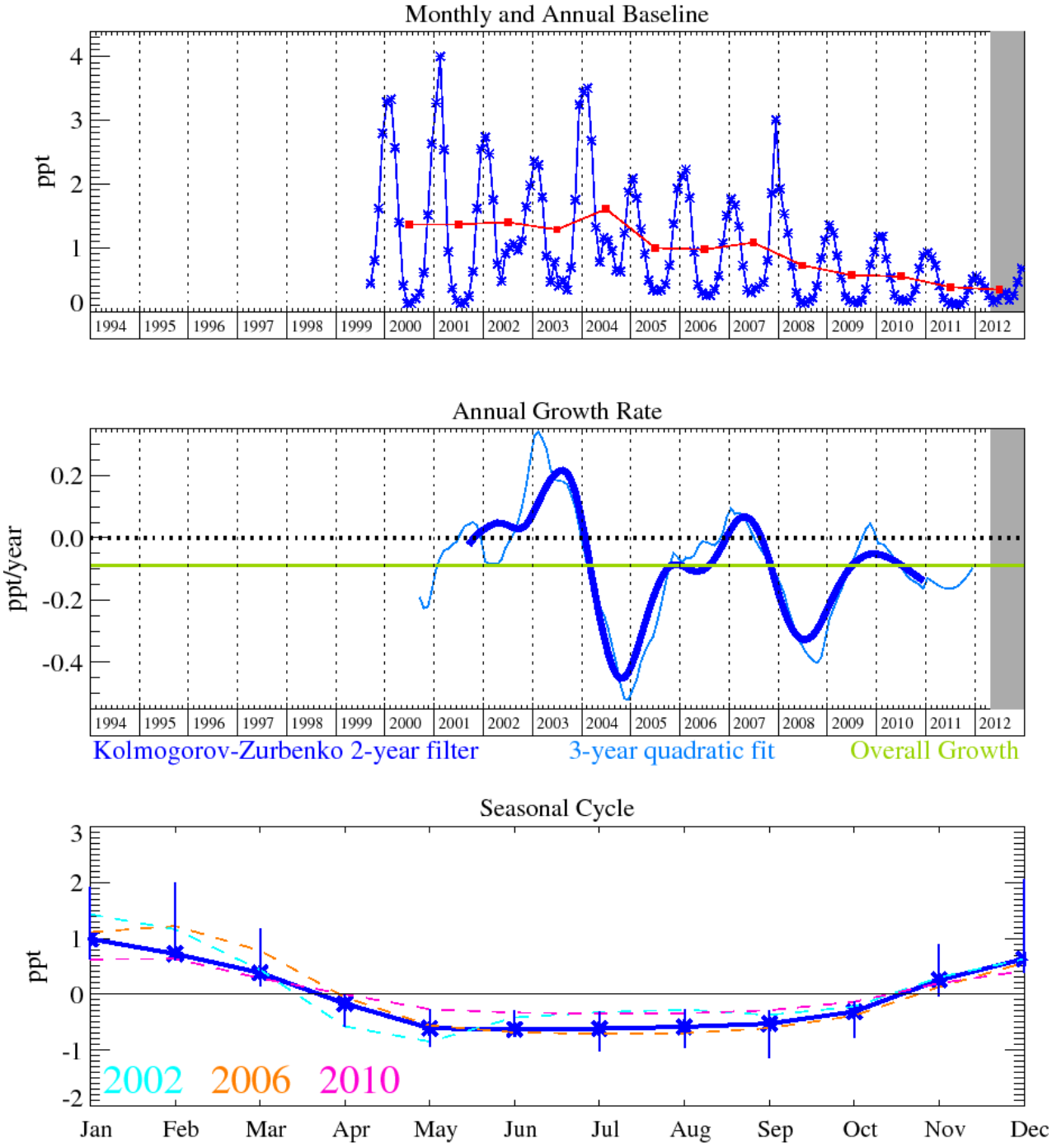

Figure 133: $CHClCCl_2$: Monthly (blue) and annual (red) baseline concentrations (top plot). Annual (blue) and overall average growth rate (green) (middle plot). Seasonal cycle (de-trended) with year-to-year variability (lower plot). Grey area covers un-ratified and therefore provisional data.

The major source of trichloroethylene (C_2HCl_3) is from industrial usage as a degreasing agent. In 2012 its average mole fraction at Mace Head was 0.3 ppt, but is decreasing in the atmosphere at a rate of 0.14 ppt/yr (Figure 133). All but about 2% of the sales are in the NH. The main removal process is with OH. It has an atmospheric lifetime of 4.9 days [*Montzka et al.*, 2011] with this lifetime resulting in a low GWP_{100} of approximately 5 [*UNEP (United Nations Environment Program)*, 2003]. C_2HCl_3 can also undergo reductive de-chlorination to 1,2-dichloroethylene through the activity of soil microbes. Natural sources of C_2HCl_3 are from the oceans and seawater algae. It has been reported that salt lakes are also a natural source of C_2HCl_3 due to the microbial activity of halobacteria [*Weissflog et al.*, 2005].

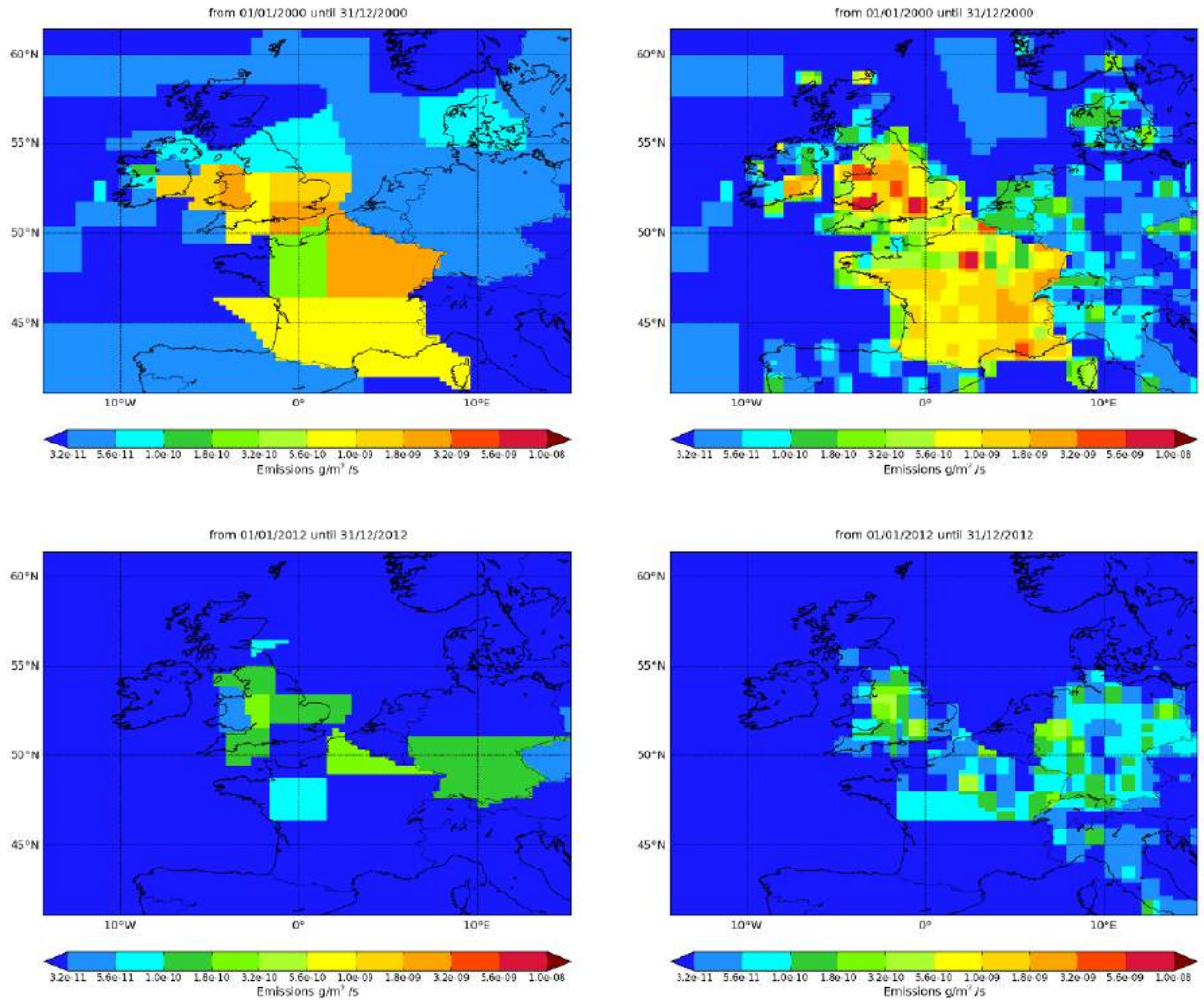

Figure 134: NAME-inversion emission estimates for 2000 (upper) and 2012 (lower). On the right hand side the emissions per grid box have been re-distributed based on population.

Year	RMSE (ppt)	Correlation	Max obs. above baseline (ppt)	% obs. above baseline	Mean obs. above baseline (ppt)
2000	6.35	0.73	62.4	41	4.54
2012	0.40	0.48	3.3	37	0.19

Table 68: Comparison between modelled and observed time-series.

The magnitude of the pollution events reaching Mace Head have declined sharply since records began in 1999 with emissions estimated through InTEM similarly declining. The statistical match between the model time-series and observations is good.

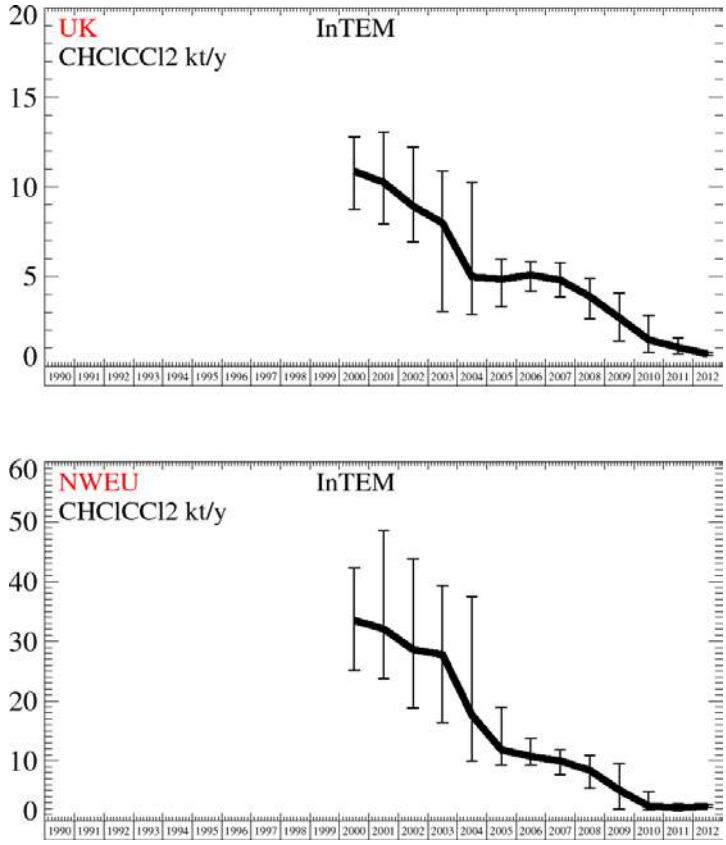

Figure 135: Emission estimates for UK and NWEU. The uncertainty bars represent the 5th and 95th percentiles. Grey line represents the emission estimates presented in last year's report.

Unit	Year	UK	(5th-95th)	NWEU	(5th-95th)
kt/y	2000	10.9	(8.7- 13.)	33	(25. -42.)
kt/y	2001	10.3	(7.9- 13.)	32	(24. -49.)
kt/y	2002	8.9	(7.0- 12.)	29	(19. -44.)
kt/y	2003	8	(3.0- 11.)	28	(16. -39.)
kt/y	2004	5	(2.9- 10.)	17.6	(10. -37.)
kt/y	2005	4.9	(3.3- 6.)	11.8	(9. -19.)
kt/y	2006	5.1	(4.2- 6.)	10.7	(9. -14.)
kt/y	2007	4.8	(3.9- 6.)	10	(8. -12.)
kt/y	2008	3.9	(2.7- 5.)	8.4	(5. -11.)
kt/y	2009	2.7	(1.4- 4.)	5.1	(2. -10.)
kt/y	2010	1.47	(0.8- 3.)	2.4	(2. - 5.)
kt/y	2011	1.05	(0.7- 2.)	2.2	(2. - 3.)
kt/y	2012	0.67	(0.6- 1.)	2.4	(2. - 3.)

Table 69: Emission estimates for UK and NWEU with uncertainty (5th – 95th %ile).

6.21 CCl_2CCl_2

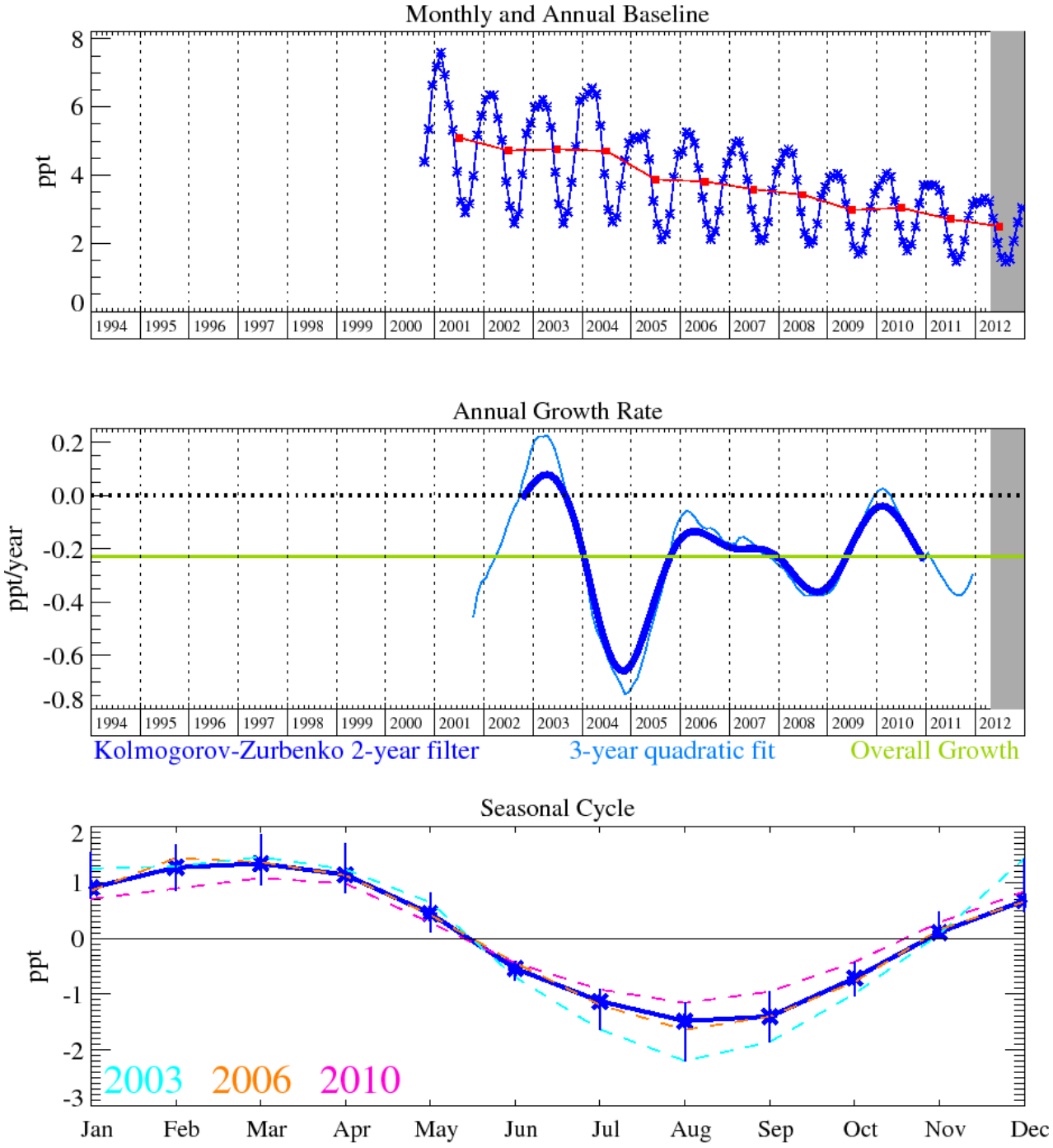

Figure 136: CCl_2CCl_2: Monthly (blue) and annual (red) baseline concentrations (top plot). Annual (blue) and overall average growth rate (green) (middle plot). Seasonal cycle (de-trended) with year-to-year variability (lower plot). Grey area covers un-ratified and therefore provisional data.

Perchloroethylene (C_2Cl_4) is mainly used for dry cleaning and as a metal degreasing solvent. Small but significant quantities of C_2Cl_4 are emitted in the flue gas from coal-fired power plants. The atmospheric lifetime of C_2Cl_4 is 90 days [*Montzka et al.*, 2011] and its primary atmospheric sink is reaction with OH. Its December 2012 atmospheric mole fraction was 3.0 with a trend currently decreasing at the rate of 0.3 ppt/yr (Figure 136). The short lifetime of perchloroethylene results in a GWP_{100} of approximately 12 [*UNEP (United Nations Environment Program)*, 2003].

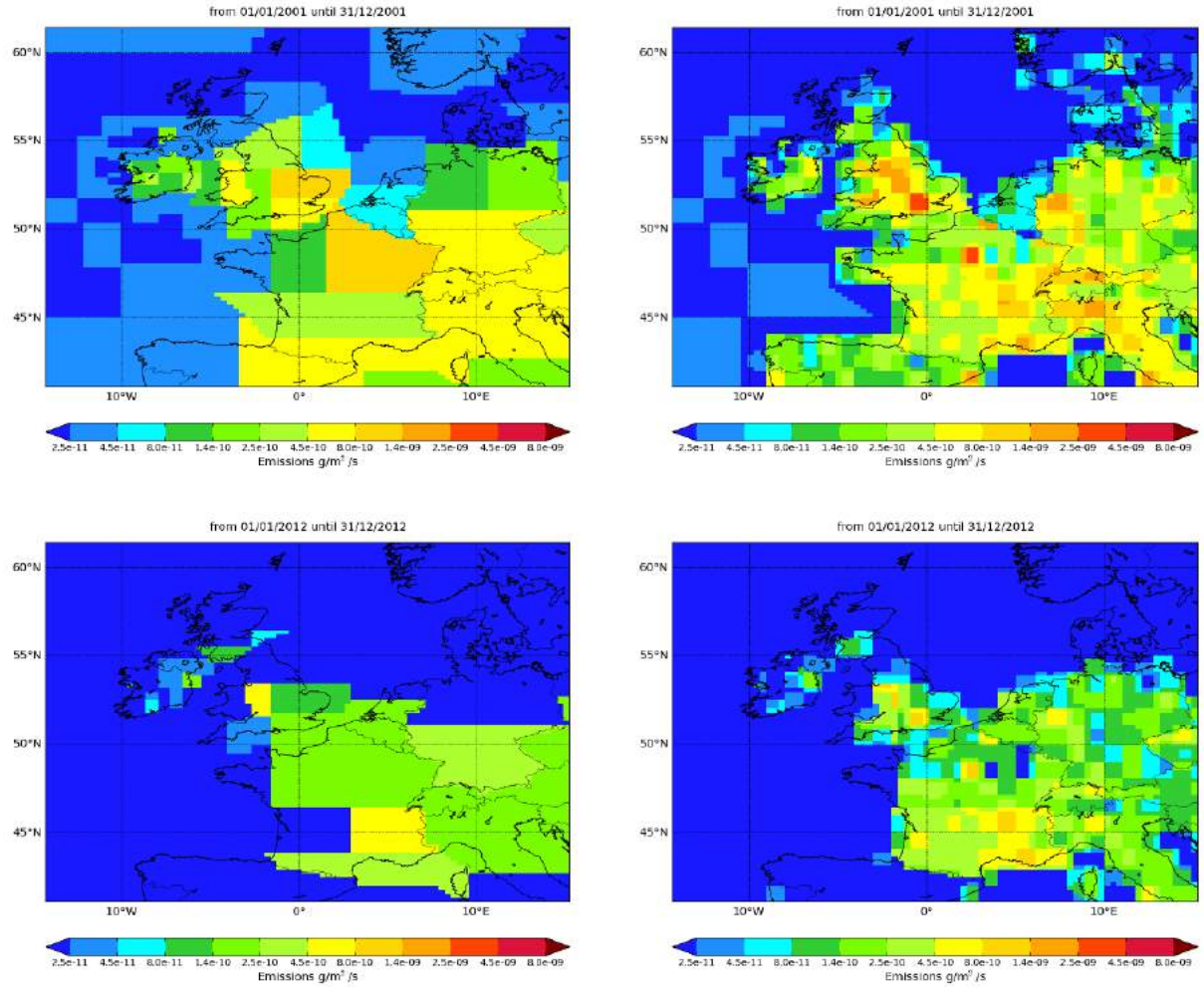

Figure 137: NAME-inversion emission estimates for 2001 (upper) and 2012 (lower). On the right hand side the emissions per grid box have been re-distributed based on population.

Year	RMSE (ppt)	Correlation	Max obs. above baseline (ppt)	% obs. above baseline noise	Mean obs. above baseline (ppt)
2001	3.4	0.73	62	49	3.3
2012	0.6	0.61	7.4	40	0.6

Table 70: Comparison between modelled and observed time-series.

The statistical match between the model time-series and the observations is good. The magnitude of the pollution events has declined steeply since 2001, a trend matched in the UK and NWEU estimated emissions.

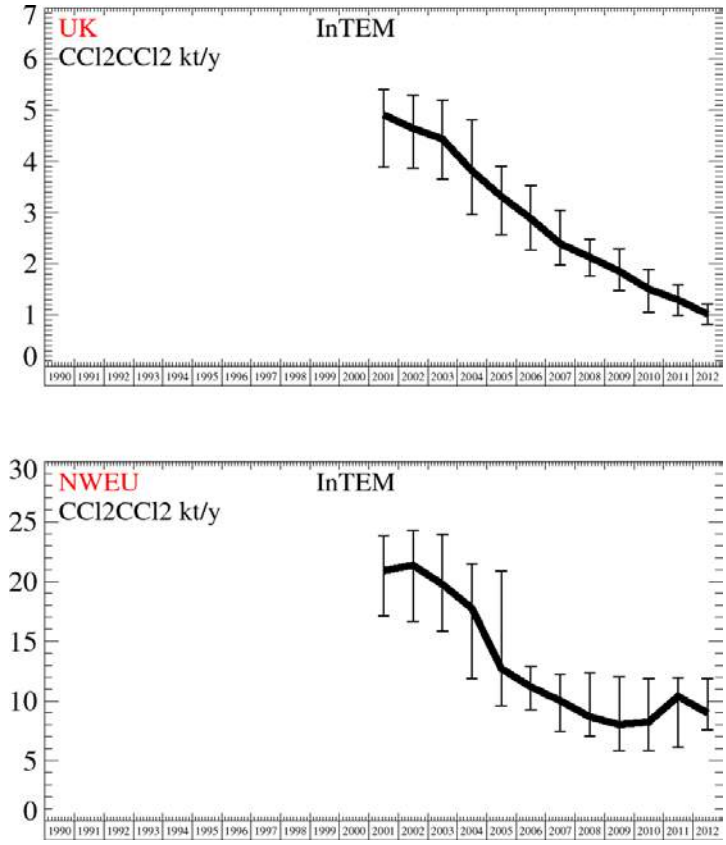

Figure 138: Emission estimates for UK and NWEU. The uncertainty bars represent the 5th and 95th percentiles.

Unit	Year	UK	(5th-95th)	NWEU	(5th-95th)
kt/y	2001	4.9	(3.9- 5.4)	21	(17.- 24.)
kt/y	2002	4.6	(3.9- 5.3)	21	(17.- 24.)
kt/y	2003	4.4	(3.7- 5.2)	19.8	(16.- 24.)
kt/y	2004	3.8	(3.0- 4.8)	17.7	(12.- 22.)
kt/y	2005	3.3	(2.6- 3.9)	12.7	(10.- 21.)
kt/y	2006	2.9	(2.3- 3.5)	11.2	(9.- 13.)
kt/y	2007	2.4	(2.0- 3.0)	10	(7.- 12.)
kt/y	2008	2.1	(1.8- 2.5)	8.7	(7.- 12.)
kt/y	2009	1.86	(1.5- 2.3)	8	(6.- 12.)
kt/y	2010	1.51	(1.1- 1.9)	8.2	(6.- 12.)
kt/y	2011	1.3	(1.0- 1.6)	10.4	(6.- 12.)
kt/y	2012	1.02	(0.8- 1.2)	9	(8.- 12.)

Table 71: Emission estimates for UK and NWEU with uncertainty (5th – 95th %ile).

6.22 Methyl bromide (CH_3Br)

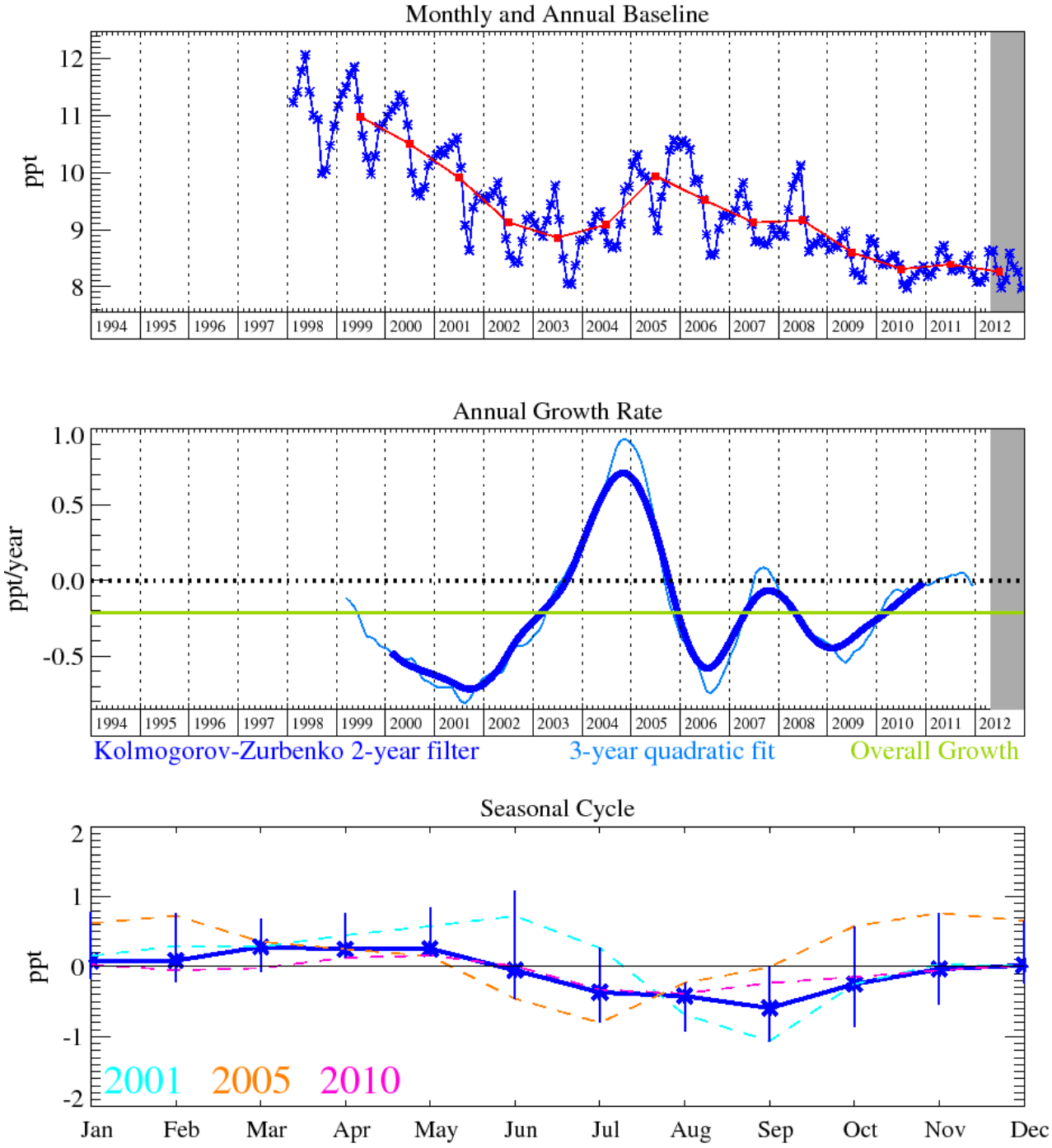

Figure 139: Methyl bromide: Monthly (blue) and annual (red) baseline concentrations (top plot). Annual (blue) and overall average growth rate (green) (middle plot). Seasonal cycle (de-trended) with year-to-year variability (lower plot). Grey area covers un-ratified and therefore provisional data.

The instrument change in 2005 to the Medusa system produced a discontinuity in the methyl bromide record and should be discounted (Figure 139).

6.23 CH_2Br_2

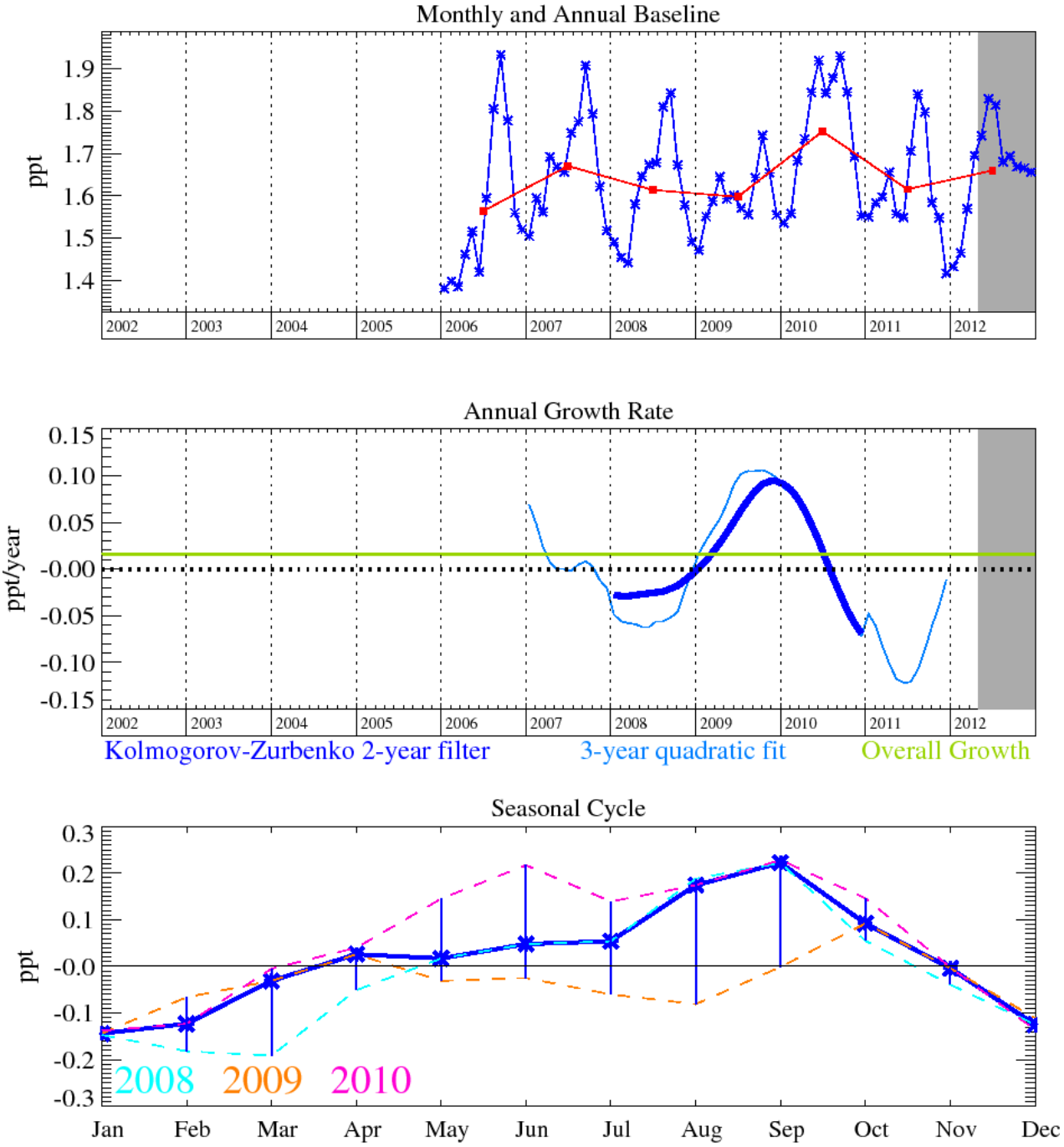

Figure 140: Dibromomethane (CH_2Br_2): Monthly (blue) and annual (red) baseline concentrations (top plot). Annual (blue) and overall average growth rate (green) (middle plot). Seasonal cycle (de-trended) with year-to-year variability (lower plot). Grey area covers un-ratified and therefore provisional data.

6.24 Bromoform ($CHBr_3$)

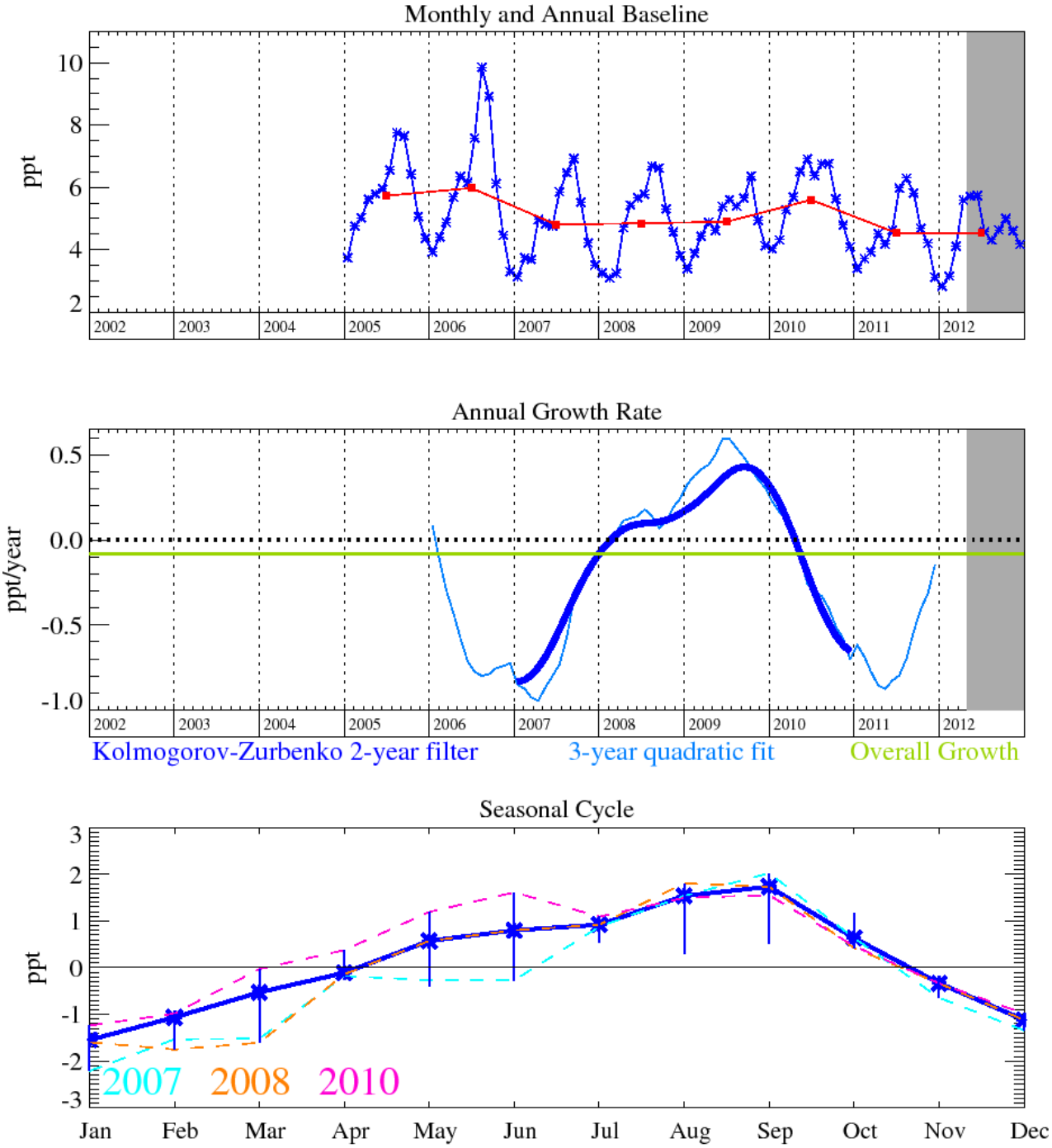

Figure 141: Bromoform ($CHBr_3$): Monthly (blue) and annual (red) baseline concentrations (top plot). Annual (blue) and overall average growth rate (green) (middle plot). Seasonal cycle (de-trended) with year-to-year variability (lower plot). Grey area covers un-ratified and therefore provisional data.

6.25 Halon-1211

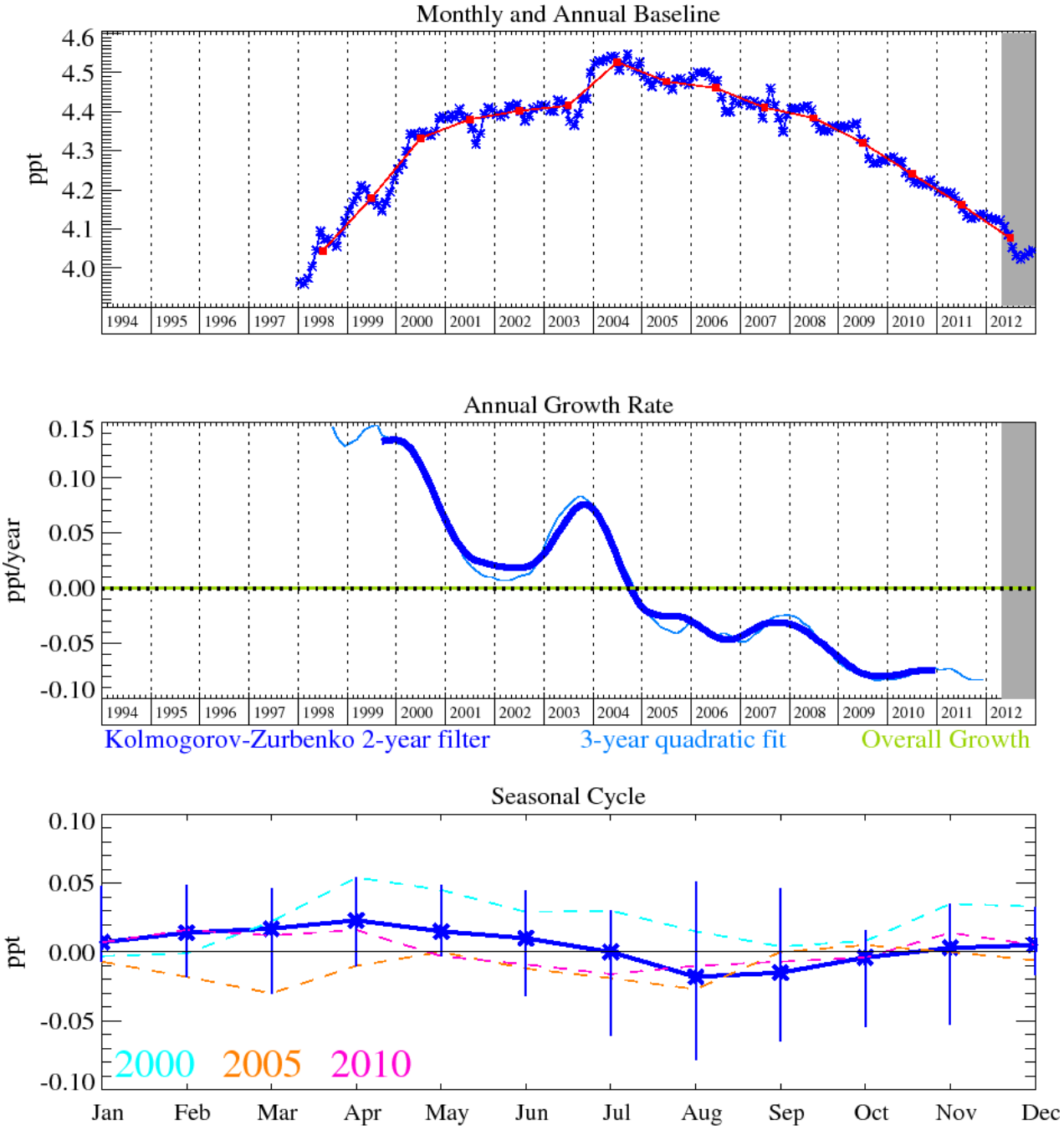

Figure 142: Halon-1211 ($CBrClF_2$): Monthly (blue) and annual (red) baseline concentrations (top plot). Annual (blue) and overall average growth rate (green) (middle plot). Seasonal cycle (de-trended) with year-to-year variability (lower plot). Grey area covers un-ratified and therefore provisional data.

Halon-1211 (Figure 142) continues to show a slight reduction of 0.08 ppt/yr due to limits imposed on halon production in developed nations. Levels at Mace Head are 4.05 ppt for halon-1211 at the end of December 2012. Halon-1211 has an atmospheric lifetime of 16 years,

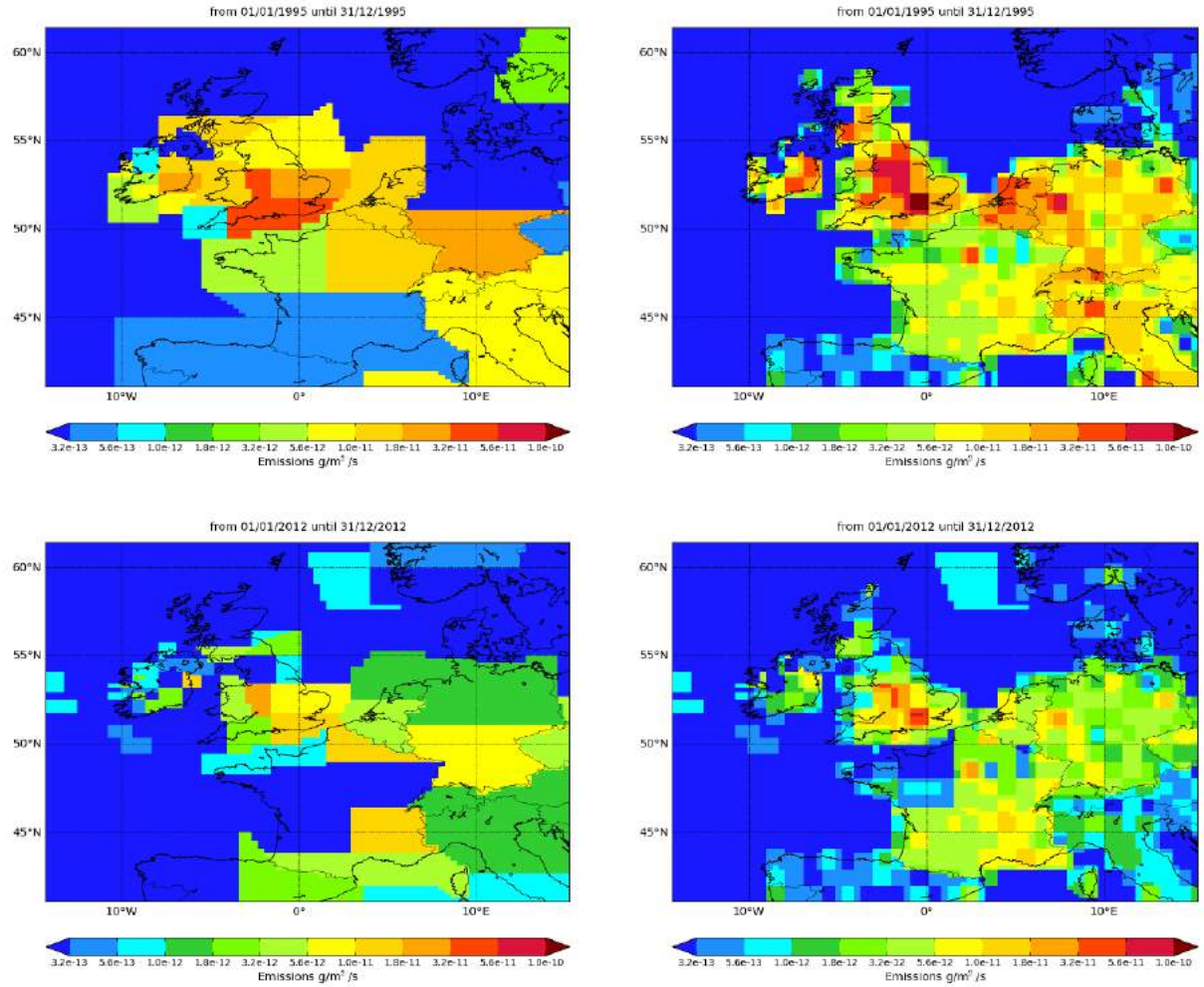

Figure 143: NAME-inversion emission estimates for 1995 (upper) and 2012 (lower). On the right hand side the emissions per grid box have been re-distributed based on population.

Year	RMSE (ppt)	Correlation	Max obs. above baseline (ppt)	% obs. above baseline noise	Mean obs. above baseline (ppt)
1995	0.14	0.55	1.3	29	0.15
2012	0.03	0.46	0.5	31	0.03

Table 72: Comparison between modelled and observed time-series.

The UK and NWEU estimated emissions of halon-1211 have declined steadily since 1995, a trend seen in the magnitude of the pollution events seen at Mace Head.

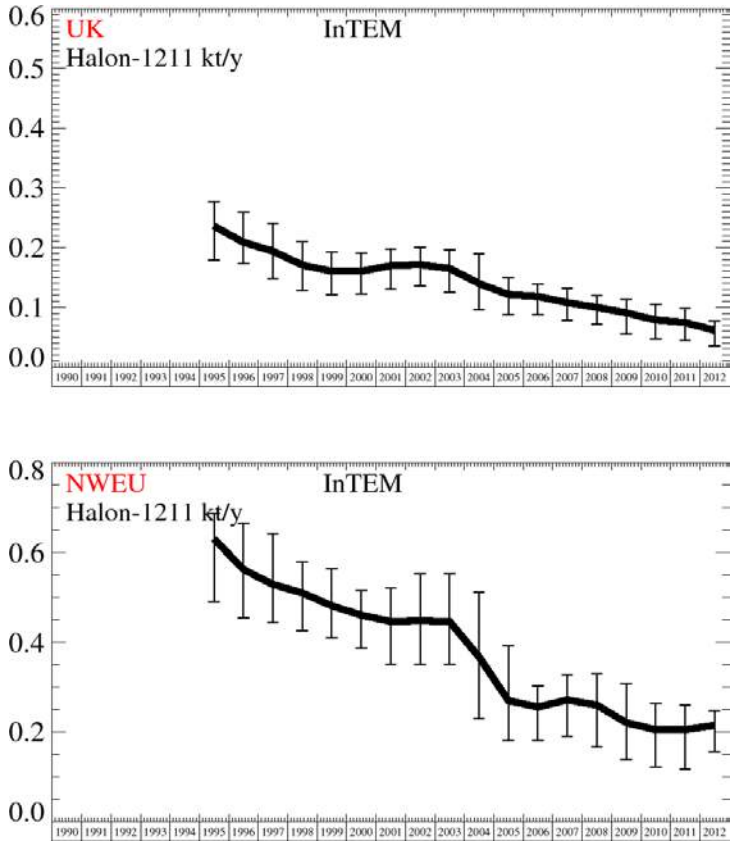

Figure 144: Emission estimates for UK and NWEU. The uncertainty bars represent the 5th and 95th percentiles.

Unit	Year	UK	(5th-95th)	NWEU	(5th-95th)
t/y	1995	240	(178.- 277.)	630	(491.- 687.)
t/y	1996	210	(174.- 259.)	560	(454.- 666.)
t/y	1997	194	(147.- 241.)	530	(443.- 642.)
t/y	1998	171	(127.- 210.)	510	(426.- 581.)
t/y	1999	160	(121.- 192.)	480	(410.- 563.)
t/y	2000	160	(123.- 191.)	460	(387.- 515.)
t/y	2001	170	(130.- 198.)	450	(351.- 521.)
t/y	2002	171	(136.- 200.)	450	(351.- 553.)
t/y	2003	165	(125.- 196.)	450	(351.- 553.)
t/y	2004	140	(95.- 190.)	370	(230.- 512.)
t/y	2005	121	(87.- 149.)	270	(181.- 392.)
t/y	2006	118	(87.- 139.)	260	(181.- 303.)
t/y	2007	108	(78.- 132.)	270	(189.- 328.)
t/y	2008	100	(72.- 120.)	260	(167.- 330.)
t/y	2009	91	(55.- 113.)	220	(138.- 308.)
t/y	2010	79	(47.- 105.)	200	(121.- 264.)
t/y	2011	74	(45.- 98.)	200	(117.- 259.)
t/y	2012	61	(35.- 77.)	210	(157.- 247.)

Table 73: Emission estimates for UK and NWEU with uncertainty (5th – 95th %ile).

6.26 Halon-1301

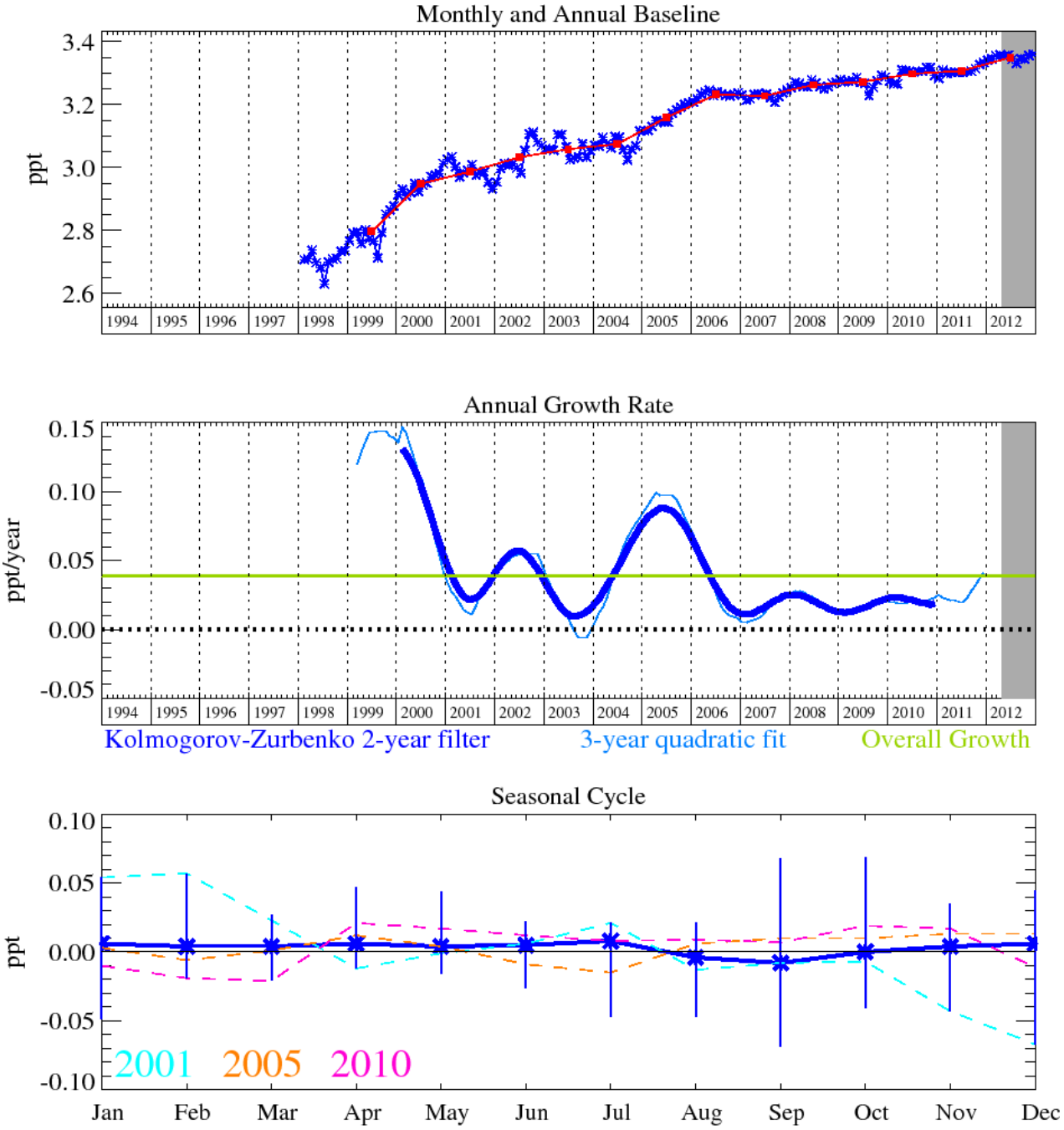

Figure 145: Halon-1301 ($CBrF_3$): Monthly (blue) and annual (red) baseline concentrations (top plot). Annual (blue) and overall average growth rate (green) (middle plot). Seasonal cycle (de-trended) with year-to-year variability (lower plot). Grey area covers un-ratified and therefore provisional data.

The halon-1301 mole fraction shown in Figure 145 is very slightly growing and by December 2012 had reached 3.36 ppt in the background atmosphere at Mace Head. Halon-1301 has an atmospheric lifetime of 65 years. The main source of halon emissions are from stockpiles and banks, where bank related emissions are thought to account for a large majority of the current halon emissions.

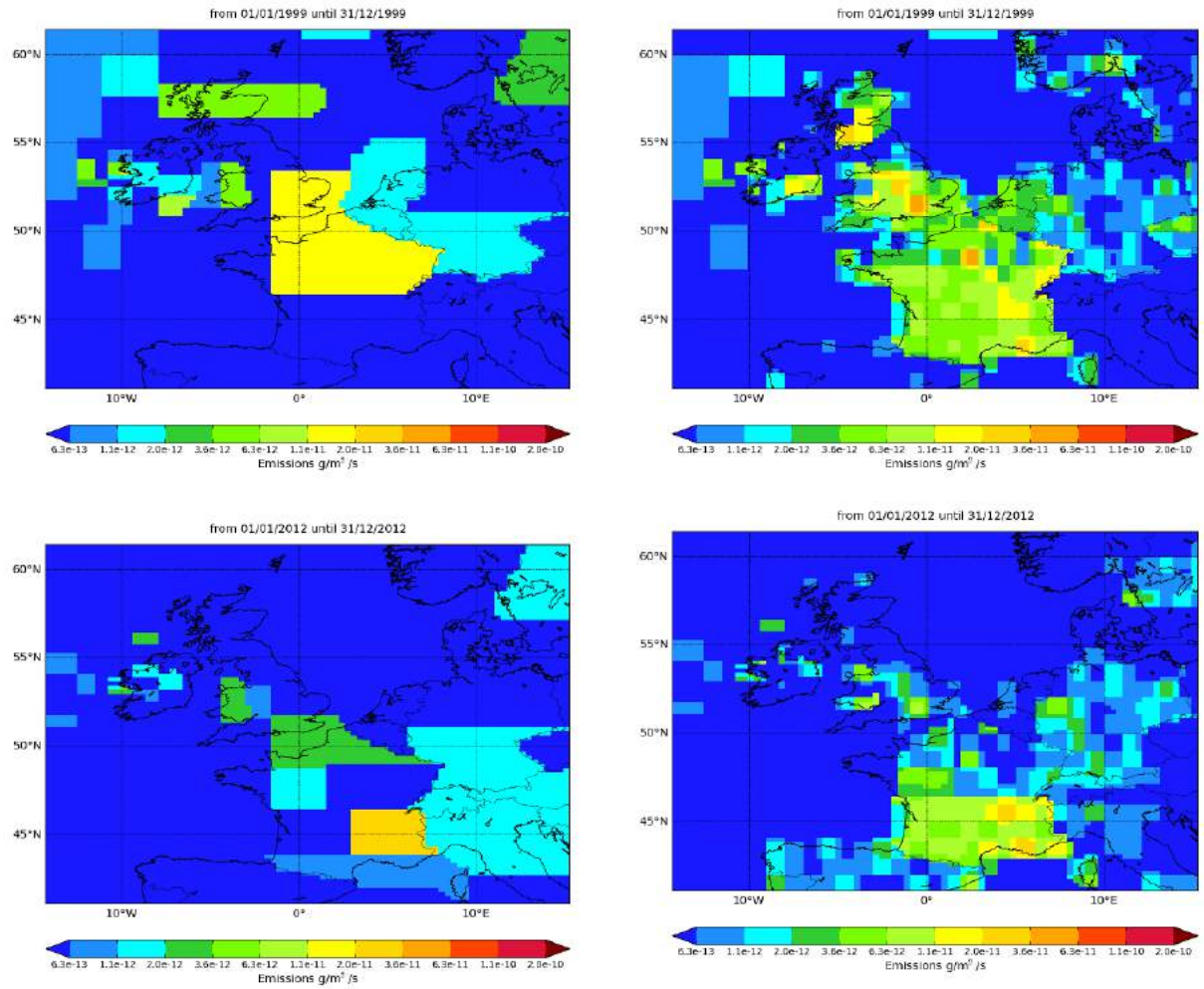

Figure 146: NAME-inversion emission estimates for 1999 (upper) and 2012 (lower). On the right hand side the emissions per grid box have been re-distributed based on population.

Year	RMSE (ppt)	Correlation	Max obs. above baseline (ppt)	% obs. above baseline noise	Mean obs. above baseline (ppt)
1999	0.13	0.38	0.9	23	0.11
2012	0.04	0.18	0.2	20	0.04

Table 74: Comparison between modelled and observed time-series.

The magnitude of the pollution events relative to the estimated noise in the baseline is small and so the uncertainty in the emission estimates is very significant. The data suggests there has been a decline in emissions over NWEU, certainly the magnitude of the pollution events are smaller now than a decade ago.

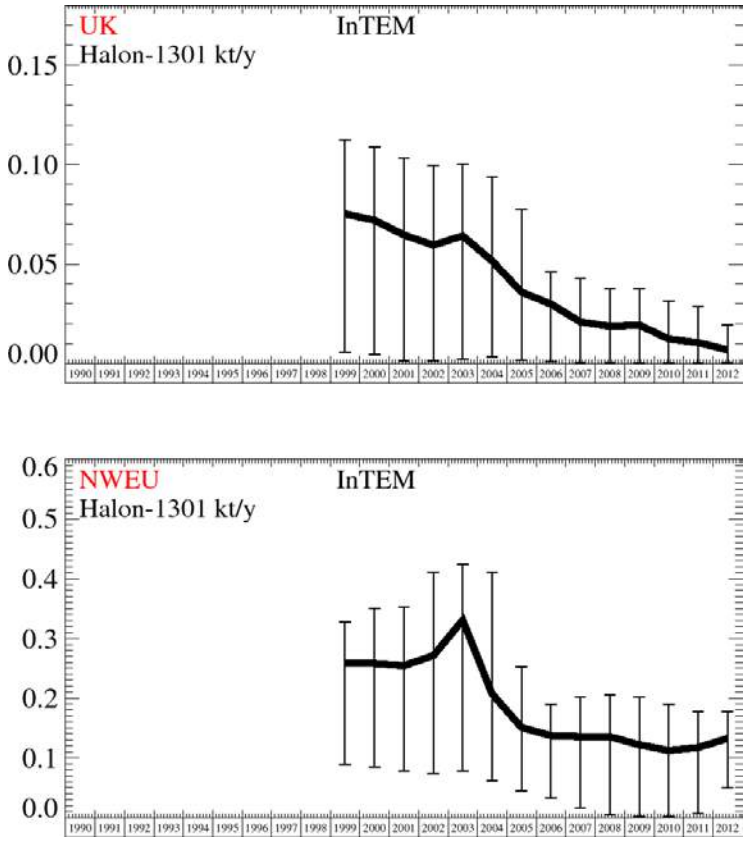

Figure 147: Emission estimates for UK and NWEU. The uncertainty bars represent the 5th and 95th percentiles.

Unit	Year	UK	(5th-95th)	NWEU	(5th-95th)
t/y	1999	75	(5.9- 113.)	260	(89.- 328.)
t/y	2000	72	(4.3- 109.)	260	(85.- 351.)
t/y	2001	65	(1.4- 103.)	250	(78.- 354.)
t/y	2002	59	(1.4- 99.)	270	(75.- 411.)
t/y	2003	64	(2.3- 100.)	330	(78.- 425.)
t/y	2004	51	(3.1- 94.)	210	(62.- 411.)
t/y	2005	36	(1.6- 77.)	151	(45.- 252.)
t/y	2006	30	(0.9- 46.)	137	(33.- 189.)
t/y	2007	21	(0.6- 43.)	135	(17.- 201.)
t/y	2008	18.7	(0.4- 38.)	135	(4.- 206.)
t/y	2009	19.3	(0.2- 38.)	122	(1.- 202.)
t/y	2010	12.4	(0.2- 31.)	112	(2.- 189.)
t/y	2011	10.5	(0.3- 29.)	117	(7.- 178.)
t/y	2012	6.9	(0.5- 20.)	132	(50.- 178.)

Table 75: Emission estimates for UK and NWEU with uncertainty (5th – 95th %ile).

6.27 Halon-2402

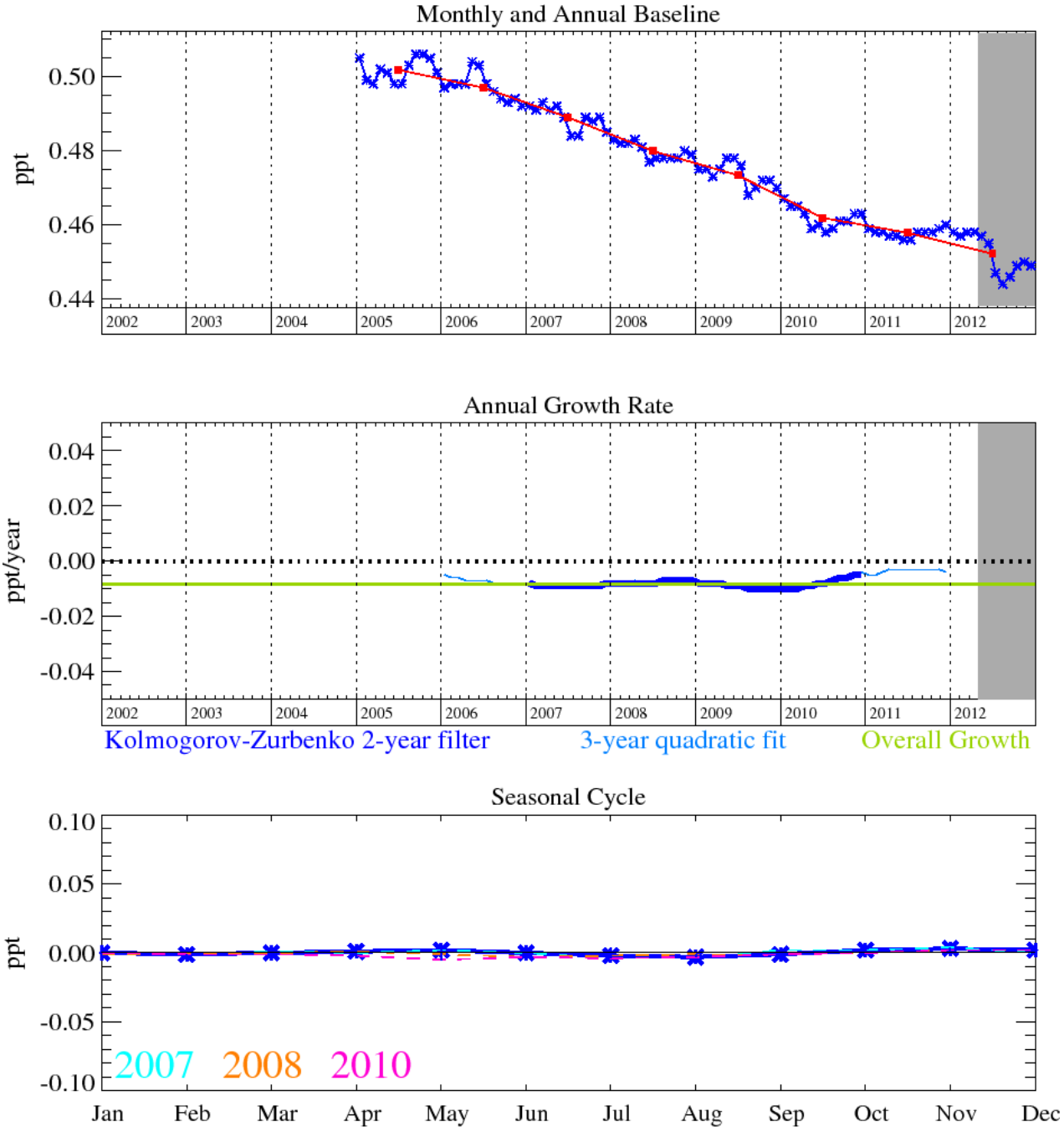

Figure 148: Halon-2402 ($C_2Br_2F_4$): Monthly (blue) and annual (red) baseline concentrations (top plot). Annual (blue) and overall average growth rate (green) (middle plot). Seasonal cycle (de-trended) with year-to-year variability (lower plot). Grey area covers un-ratified and therefore provisional data.

We continue to report trends for the minor halon-2402 (20 year lifetime). This compound was used predominantly in the former Soviet Union. No information on the production of halon-2402 before 1986 has been found. Fraser *et al*., (1999) developed emission projections for halon-2402 based on atmospheric measurements. They reported that the emissions grew steadily in the 1970s and 1980s, peaking in the 1988-91 timeframe at 1.7 Gg/yr and found these results to be qualitatively consistent with the peak production of 28,000 ODP tonnes reported by the Russian Federation under Article VII of the Montreal Protocol (or assuming all production was halon-2402 and an ODP of 6, a peak production of approximately 4.650 Gg/yr). Measurements at Mace Head indicate that the levels of halon-2402 are very slowly falling in the atmosphere. The baseline level in December 2012 was estimated to be 0.45 ppt, however the error bars associated with the measurement are

large. This magnitude of reduction is consistent with declines in global surface mixing ratios reported in the 2010 WMO Ozone Assessment.

6.28 CH_3I

Methyl Iodide (CH3I) is a short-lived species with a lifetime of only 7 days [Montzka *et al*., 2011] and has an insignificant GWP as a result. In common with the majority of iodated gases it is predominantly of biogenic origin with the majority of worldwide emissions occurring from sea/air exchange in open ocean locations [Yokouchi *et al.*, 2001]. Due to the close proximity of Mace Head to the Atlantic Ocean a significant variability can be seen in both the baseline measurements and annual growth rates. There are also significant macroalgae sources on the shoreline of the coastal bays to the south and east of Mace Head which tend to dominate the above baseline measurements.

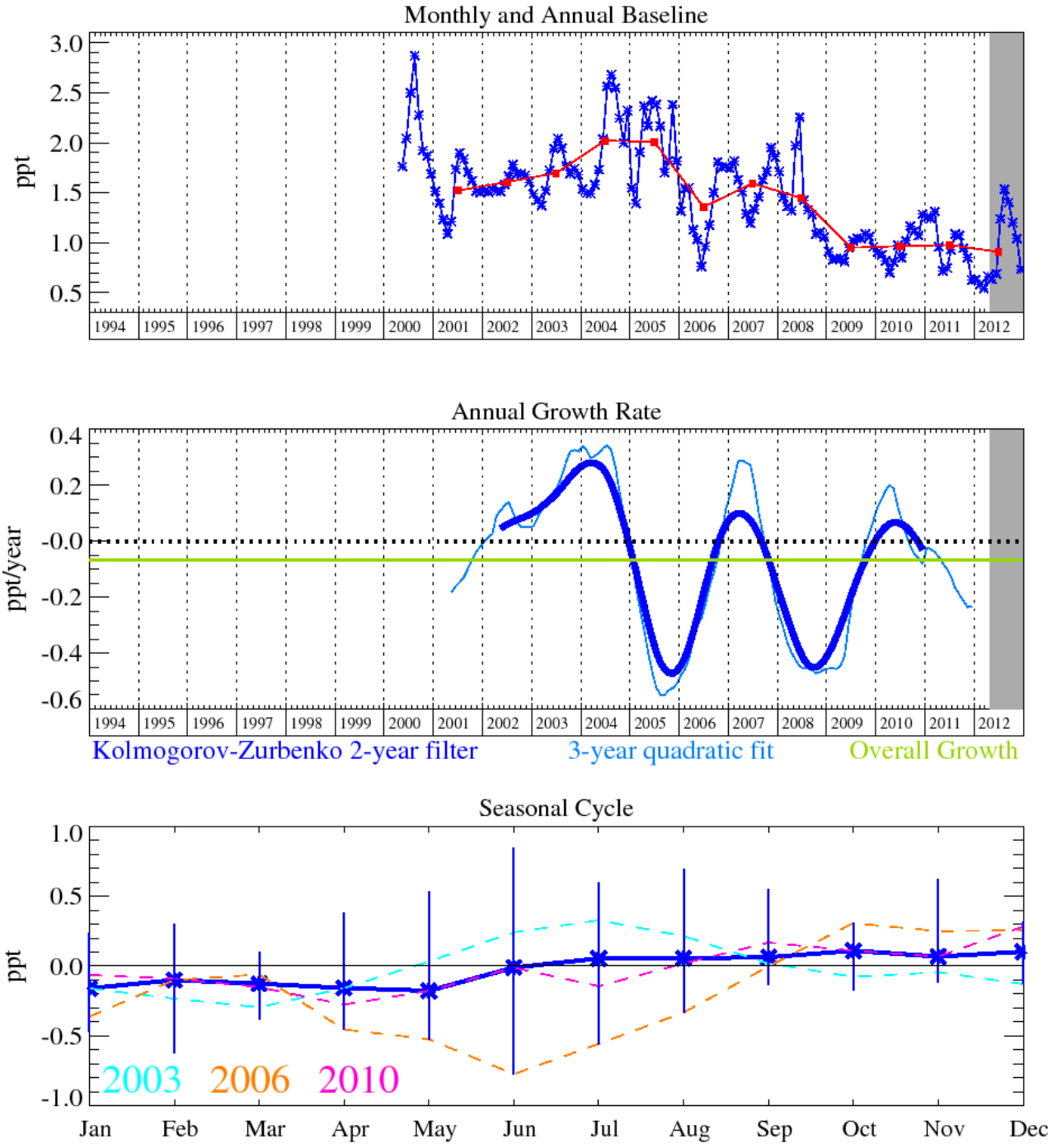

Figure 149: CH_3I: Monthly (blue) and annual (red) baseline concentrations (top plot). Annual (blue) and overall average growth rate (green) (middle plot). Seasonal cycle (de-trended) with year-to-year variability (lower plot). Grey area covers un-ratified and therefore provisional data.

6.29 Ethane (C_2H_6)

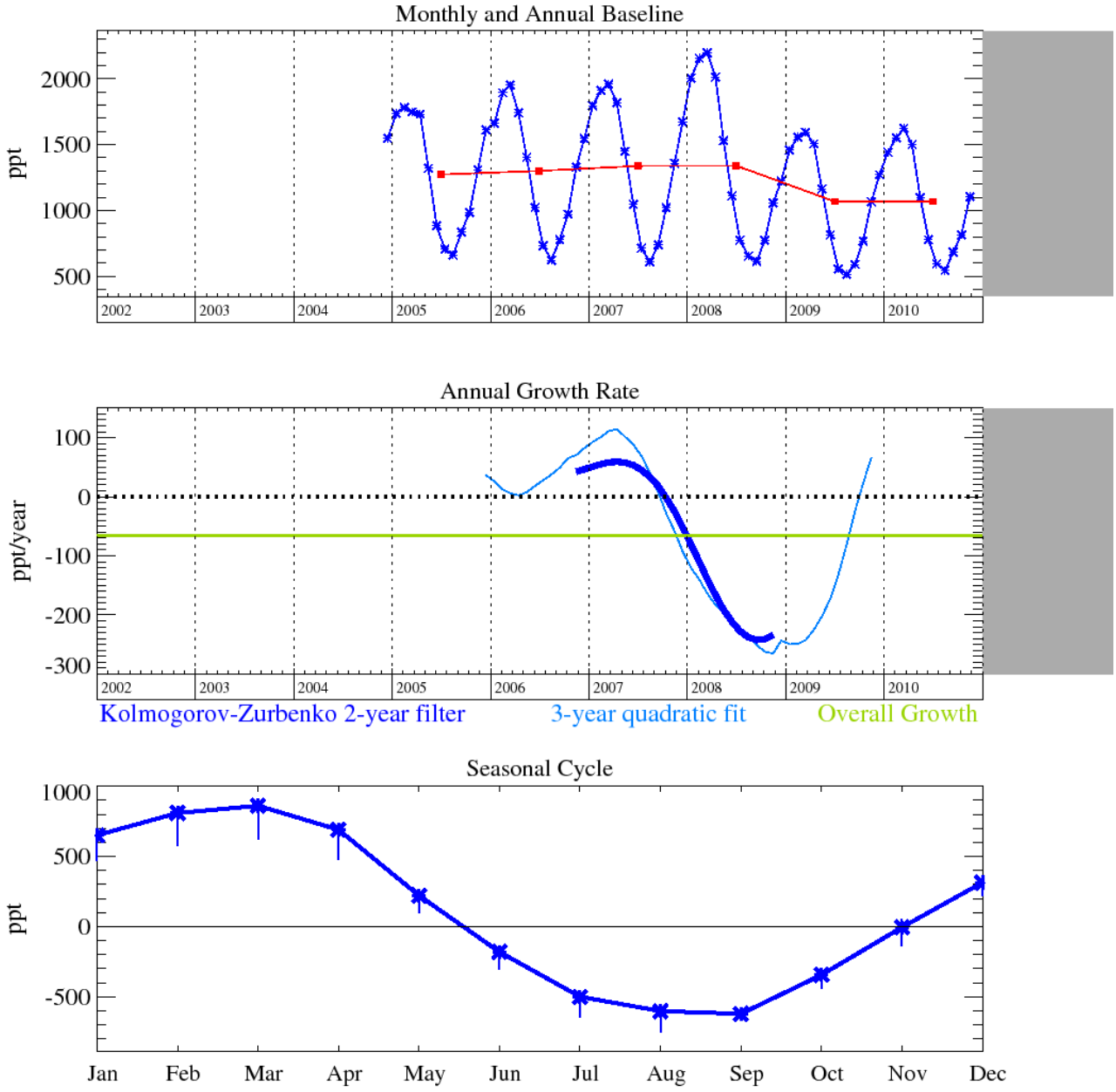

Figure 150: Ethane (C_2H_6): Monthly (blue) and annual (red) baseline concentrations (top plot). Annual (blue) and overall average growth rate (green) (middle plot). Seasonal cycle (de-trended) with year-to-year variability (lower plot). Grey area covers un-ratified and therefore provisional data.

6.30 Carbon monoxide (CO)

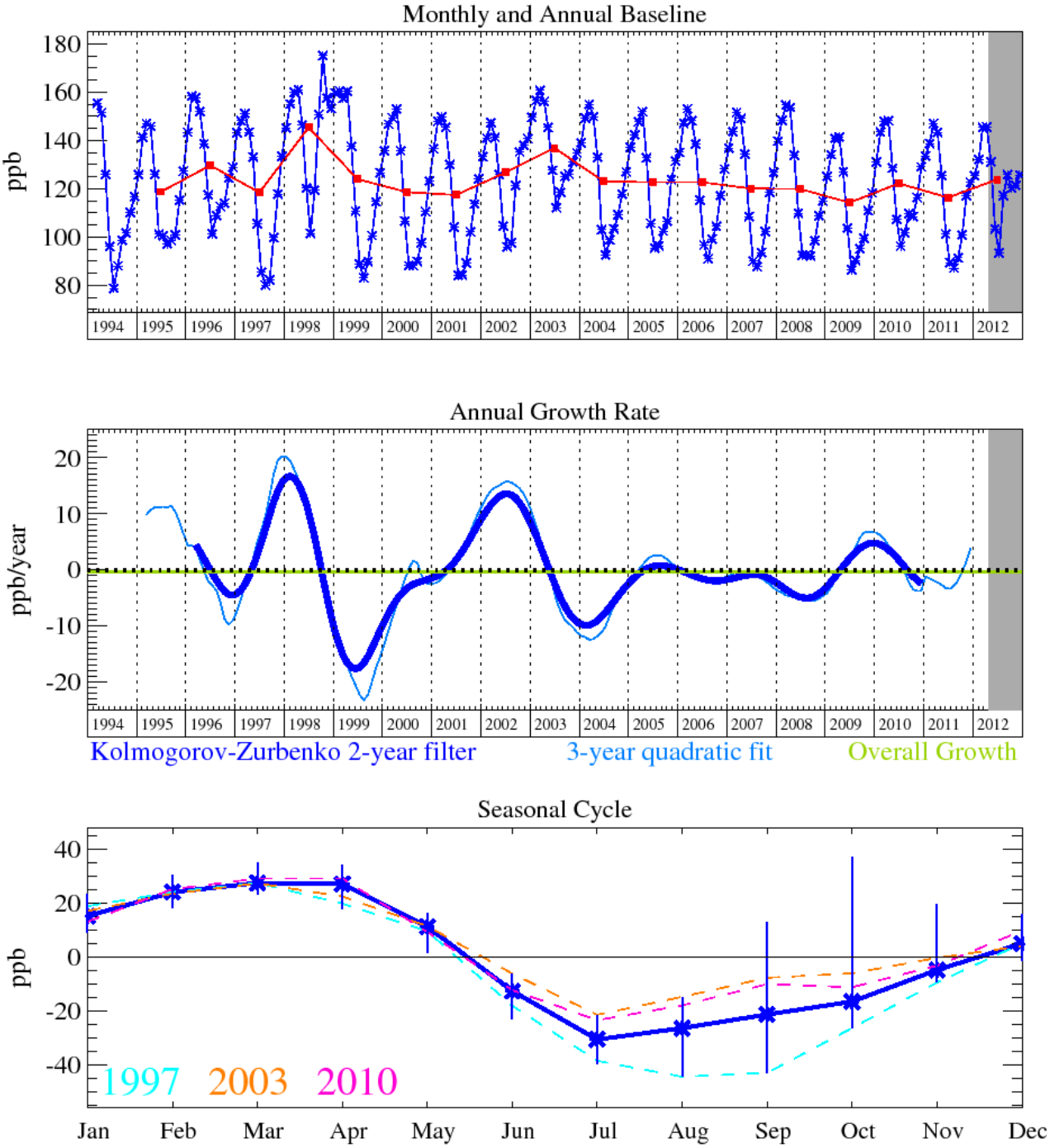

Figure 151: CO: Monthly (blue) and annual (red) baseline concentrations (top plot). Annual (blue) and overall average growth rate (green) (middle plot). Seasonal cycle (de-trended) with year-to-year variability (lower plot). Grey area covers un-ratified and therefore provisional data.

Annual mean baseline CO levels in 2012 have remained largely unchanged since 2005. Levels in 2010 showed a small step up relative to those in 2009 and 2011, which is attributed to the forest fires in the Russian Federation (WDCGG, 2012). The average baseline mole fraction in 2012 was 124 ppb, which is significantly lower than its peak annual values of 145 ppb in 1998 and 137 ppb in 2003.

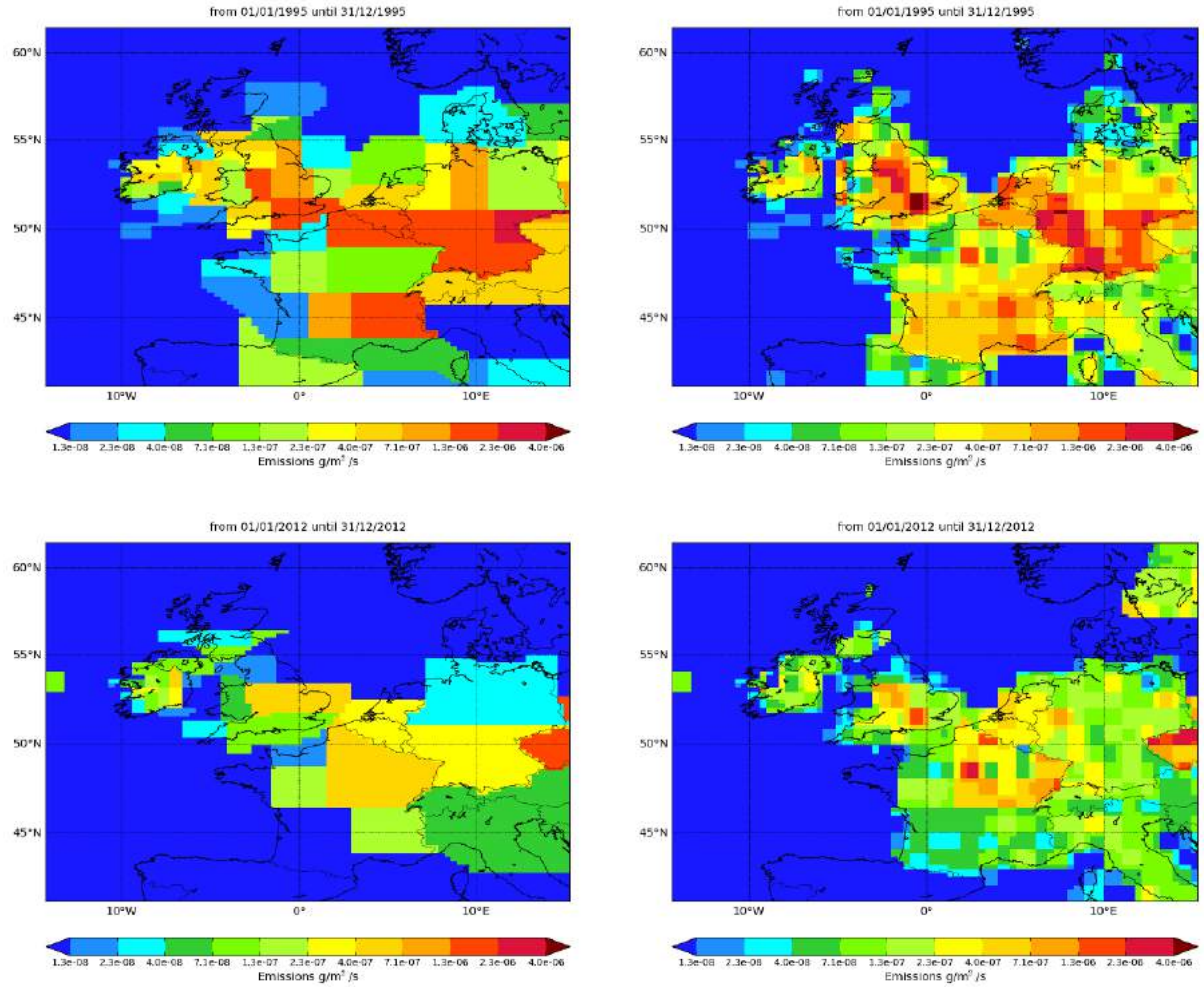

Figure 152: NAME-inversion emission estimates for 1995 (upper) and 2012 (lower). On the right hand side the emissions per grid box have been re-distributed based on population.

Year	RMSE (ppt)	Correlation	Max obs. above baseline (ppt)	% obs. above baseline noise	Mean obs. above baseline (ppt)
1995	24	0.76	391	45	32
2012	9	0.60	221	33	10

Table 76: Comparison between modelled and observed time-series.

The estimated emissions of CO in the UK have declined steadily in both the inventory and the InTEM emission estimates. The latter are, before 2007, approximately 30% smaller than the reported inventory. The magnitude of the pollution events seen at Mace Head have significantly declined since 1995 and the statistical match between the model time-series and observations is good.

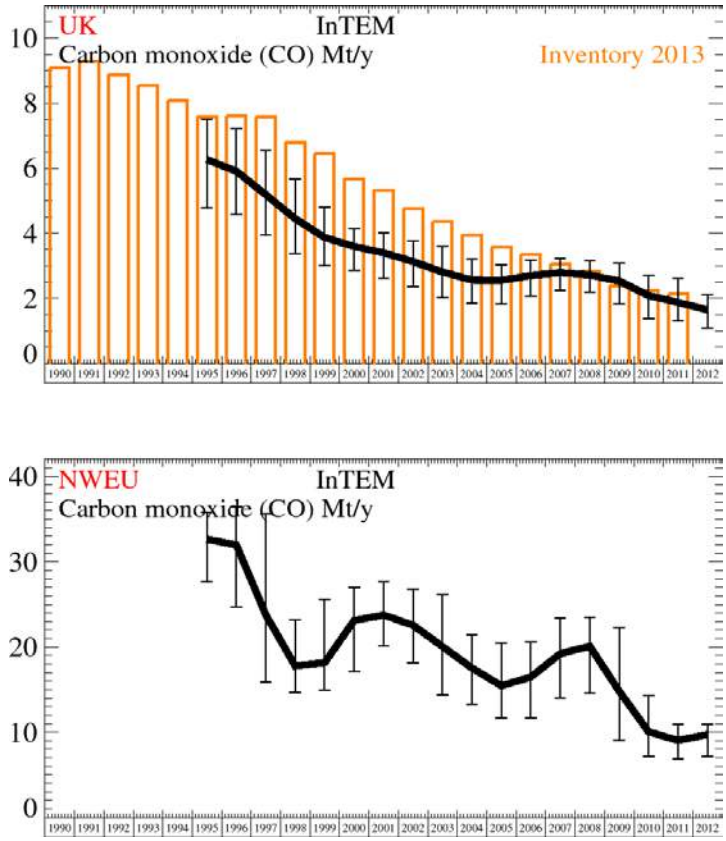

Figure 153: Emission estimates for UK and NWEU. The uncertainty bars represent the 5th and 95th percentiles.

Unit	Year	UK	(5th-95th)	NWEU	(5th-95th)
Mt/y	1995	6.3	(4.8- 7.5)	33	(28.- 36.)
Mt/y	1996	5.9	(4.6- 7.2)	32	(25.- 37.)
Mt/y	1997	5.2	(3.9- 6.6)	24	(16.- 36.)
Mt/y	1998	4.4	(3.4- 5.7)	17.8	(15.- 23.)
Mt/y	1999	3.9	(3.0- 4.8)	18.2	(15.- 26.)
Mt/y	2000	3.6	(2.9- 4.2)	23	(17.- 27.)
Mt/y	2001	3.4	(2.6- 4.0)	24	(20.- 28.)
Mt/y	2002	3.1	(2.4- 3.8)	23	(18.- 27.)
Mt/y	2003	2.8	(2.0- 3.6)	20	(14.- 26.)
Mt/y	2004	2.6	(1.8- 3.2)	17.5	(13.- 21.)
Mt/y	2005	2.6	(1.8- 3.0)	15.5	(12.- 20.)
Mt/y	2006	2.7	(2.1- 3.2)	16.5	(12.- 21.)
Mt/y	2007	2.8	(2.2- 3.2)	19.2	(14.- 23.)
Mt/y	2008	2.7	(2.2- 3.2)	20	(15.- 23.)
Mt/y	2009	2.5	(1.8- 3.1)	14.8	(9.- 22.)
Mt/y	2010	2.1	(1.4- 2.7)	10	(7.- 14.)
Mt/y	2011	1.88	(1.3- 2.6)	9	(7.- 11.)
Mt/y	2012	1.65	(1.1- 2.1)	9.7	(7.- 11.)

Table 77: Emission estimates for UK and NWEU with uncertainty (5th – 95th %ile).

6.31 Ozone (O_3)

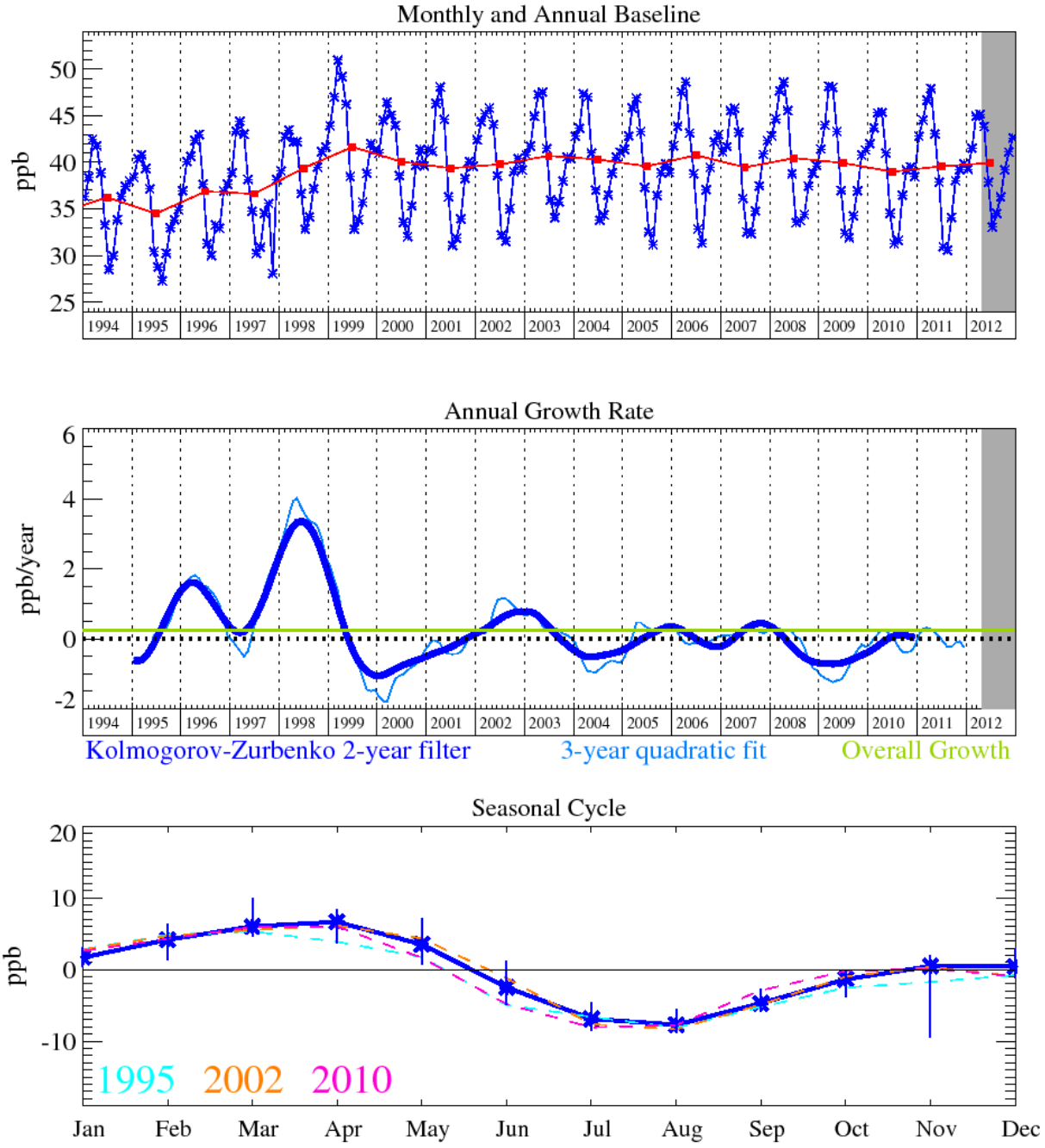

Figure 154: Ozone (O_3): Monthly (blue) and annual (red) baseline concentrations (top plot). Annual (blue) and overall average growth rate (green) (middle plot). Seasonal cycle (de-trended) with year-to-year variability (lower plot). Grey area covers un-ratified and therefore provisional data.

Tropospheric O_3 measurements first started at Mace Head in 1987 and the trends derived from the baseline-selected monthly means, the growth rate and seasonal cycles are shown in Figure 154. The Mace Head O_3 measurements exhibited a positive trend (~0.49 ppb) up to about 2003. However, since then there has been no significant growth in ozone and the most recent growth rate is estimated to be 0.02 ppb/yr. Its average mole fraction in 2012 at Mace Head was 39.9. Assessment of the long-term trends in tropospheric ozone is difficult due to the scarcity of representative observing sites with long records. The records that do exist vary both in terms of sign and magnitude (Forster *et al.,* 2007). However, the behaviour seen at Mace Head, Ireland is entirely consistent with that reported at two other European baseline stations: Arkona-Zingst and Jungfraujoch (Parrish *et al.*, 2012).

6.31.1 Analysis of Mace Head ozone data 1987 - 2012

A member of the team joined an international cooperation exercise to establish which of the tropospheric ozone records are of the highest quality and then to use them to establish long-term trends in tropospheric ozone.

In the first study, Logan *et al*., (2012), problems were found with the ozone-sondes from Asia and North America which meant that they are not suitable for long-term trend analysis. A combination of European ozone-sondes, regular aircraft flights, alpine surface sites and Mace Head data were used to build a self-consistent analysis of robust changes in the time evolution of tropospheric ozone above 2 km in altitude over Europe. These data sets were most consistent after 1998, with each showing similar interannual variability and downward trends of -0.15 ppb per year. Ozone levels increased by 6.5 – 10 ppb during 1978 – 1989 and by 2.5 – 4.5 ppb in the 1990s. It is difficult to reconcile these observed changes with trends in the emissions of ozone precursors and ozone behaviour in the lowermost stratosphere as shown by current chemistry-transport models.

In the second study, Parrish *et al*., (2012), eleven mid-latitude northern hemisphere surface records, including Mace Head, were selected for analysis. The data sets selected for analysis represent the longest, highest quality measurement records available from sites that represent baseline conditions. The chosen highest quality data sets included ten ground-based and one airborne. The ground-based sites comprised, six European beginning in the 1950s and before, two North American beginning 1984 and two Asian beginning in 1991. Altogether a consistent picture of tropospheric ozone at the surface of the northern hemisphere mid-latitudes over six decades was assembled. Ozone levels have doubled over the period from 1950 to 2000 in all seasons and at all sites. At most sites, the rate of increase has slowed over the last decade to the extent that, at present, ozone is decreasing at some sites in some seasons, particularly in summer. This study has presented a summary of long-term changes in lower tropospheric baseline ozone levels with the goal of providing benchmarks to which retrospective model calculations of the global ozone distribution can be compared. Such comparisons should include the long-term ozone increase in each season over 1950 – 2000 and the more recent slowing of that increase over Europe. Currently, chemistry-transport models are unable to reproduce quantitatively these long-term changes.

In the third study, Parrish *et al*., (2013) report another manifestation of changes in the abundance of tropospheric ozone, namely a shift in the seasonal cycle in northern hemispheric mid-latitudes. This study analysed five data sets with the longest, continuous high quality data records with the best year round coverage. The selected sites included two alpine sites, a mid-continental site and Mace Head from Europe and one North American site. All five sites show a marked seasonal cycle in ozone with highest levels in the spring and lowest levels during the summer or winter. There is substantial evidence that these seasonal cycles have shifted earlier in the year when comparing the 1980s with the 2000s. These shifts are such as to bring the ozone peaks earlier in the year than was observed in previous decades. This rate of shift has been about 3 to 6 days per decade since the 1970s. Various possible reasons have been brought together to explain these shifts and the suggestion is that it may be due to changes in atmospheric transport patterns combined with spatial and temporal changes in emissions. Detailed modelling is required to test these hypotheses and in so doing will provide a stringent test for global chemistry-climate models.

These three studies have pointed out the importance and uniqueness of the Mace Head ozone record in terms of its location, unrivalled data capture and accuracy over its 25 years of operation.

6.32 Hydrogen

Hydrogen (Figure 155) is an oxidation product of methane and isoprene whose main sink is surface uptake mainly in the northern hemisphere. Annual mean baseline levels have remained roughly constant (within measurement uncertainty) for much of the Mace Head record. It shows an average mole fraction in 2012 of 505 ppb. There is evidence of anomalous growth in 2010-2011 through the influence of the forest fires in the Russian Federation.

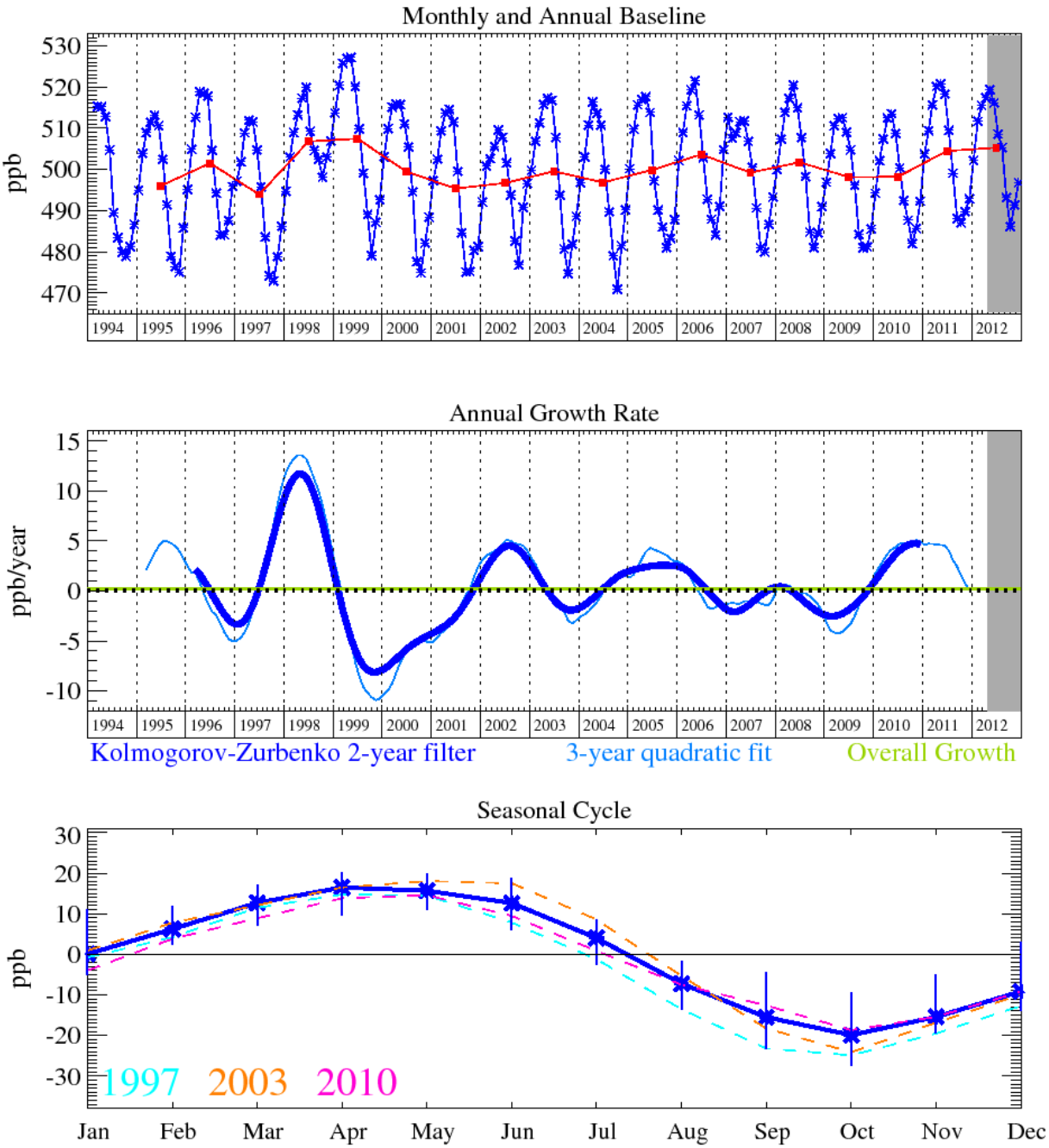

Figure 155: Hydrogen (H_2): Monthly (blue) and annual (red) baseline concentrations (top plot). Annual (blue) and overall average growth rate (green) (middle plot). Seasonal cycle (de-trended) with year-to-year variability (lower plot). Grey area covers un-ratified and therefore provisional data.

7 References

Arnold, T., C.M. Harth, J. Mühle, A.J. Manning, P.K. Salameh, J. Kim, D.J. Ivy, L.P. Steele, V.V. Petrenko, J.P. Severinghaus, D. Baggenstos, and R.F. Weiss, Nitrogen trifluoride global emissions estimated from updated atmospheric measurements, PNAS 2013 110 (6) 2029-2034, 2013, doi:10.1073/pnas.1212346110

Bergamaschi, P., M. Krol, F. Dentener, A. Vermeulen, F. Meinhardt, R. Graul, M. Ramonet, W. Peters, and E. J. Dlugokencky (2005), Inverse modeling of national and European CH4 emissions using the atmospheric zoom model TM5, Atmos. Chem. Phys., 5, 2431-2460.

Bloom, A.A, P.I. Palmer, A. Fraser, D.S. Reay, and C. Frankenberg, Large-scale controls of methanogenesis inferred from methane and gravity spaceborne data, Science, 327 (5963), 322-325, doi: 10.1126/science.1175176, 2010

Cox, M. L., G. A. Sturrock, P. J. Fraser, S. T. Siems, P. B. Krummel and S. O'Doherty, Regional sources of methyl chloride, chloroform and dichloromethane identified from AGAGE observations at Cape Grim, Tasmania, 1998-2000, J. Atmos. Chem., 45 (1): 79-99, 2003

Daniel, J.S., and G.J.M Velders (Lead Authors), A.R. Douglass, P.M.D. Forster, D.A. Hauglustaine, I.S.A. Isaksen, L.J.M. Kuijpers, A. McCulloch, and T.J. Wallington, Halocarbon scenarios, ozone depletion potentials, and global warming potentials, Chapter 8 in Scientific Assessment of Ozone Depletion: 2006, Global Ozone Research and Monitoring, Project—Report No. 50, 572 pp., World Meteorological Organization, Geneva, Switzerland, 2007.

Dlugokencky, E. J., R. C. Myers, P. M. Lang, K. A. Masarie, A. M. Crotwell, K. W. Thoning, B. D. Hall, J. W. Elkins, and L. P. Steele, Conversion of NOAA atmospheric dry air CH4 mole fractions to a gravimetrically prepared standard scale, Journal of Geophysical Research: Atmospheres, 110(D18), doi:10.1029/2005JD006035.

Forster, P., P. Ramaswamy, T. Artaxo, R. Berntsen, D. Betts, J. Fahey, J. Haywood, D. Lean, G. Lowe, J. Myhre, R. Nganga, R. Prinn, M. Raga R. Schulz & R. van Dorland (lead authors), Changes in Atmospheric Constituents and in Radiative Forcing, Chapter 2 in Climate Change 2007: the Physical Science Basis, contribution of Working Group I to the Fourth Assessment Report of the Intergovernmental Panel on Climate Change, Cambridge University Press, 129-234, 2007.

Fraser, P.J., D.E. Oram, C.E. Reeves, S.A. Penkett, and A. McCulloch, Southern Hemispheric halon trends (1978-1998) and global halon emissions, J. Geophys. Res., 104 (D13), 1598515999, 1999.

Hammer, S., D. W. T. Griffith, G. Konrad, S. Vardag, C. Caldow, and I. Levin, Assessment of a multi-species in-situ FTIR for precise atmospheric greenhouse gas observations, Atmos. Meas. Tech. Discuss., 5, 3645-3692, 2012 www.atmos-meas-tech-discuss.net/5/3645/2012/ doi:10.5194/amtd-5-3645-2012

Ivy, D. J., T. Arnold, C. M. Harth, L. P. Steele, J. Mühle, M. Rigby, P. K. Salameh, M. Leist, P. B. Krummel, P. J. Fraser, R. F. Weiss, and R. G. Prinn, Atmospheric histories and growth trends of C_4F_{10}, C_5F_{12}, C_6F_{14}, C_7F_{16} and C_8F_{18}, Atmos. Chem. Phys., 12(9), 4313–4325, doi:10.5194/acp-12-4313-2012, 2012a.

Ivy, D. J., M. Rigby, M. Baasandorj, J. B. Burkholder, and R. G. Prinn, Global emission estimates and radiative impact of C_4F_{10}, C_5F_{12}, C_6F_{14}, C_7F_{16} and C_8F_{18}, Atmos. Chem. Phys., 12(16), 7635–7645, doi:10.5194/acp-12-7635-2012, 2012b.

Keene, W.C., M.A.K. Khalil, D.J. Erickson, A. McCulloch, T.E. Graedel, J.M. Lobert, M.L. Aucott, S.L. Gong, D.B. Harper, G. Kleiman, P. Midgley, R.M. Moore, C. Seuzaret, W.T. Sturges, C.M. Benkovitz, V. Koropalov, L.A. Barrie, and Y.F. Li, Composite global emissions of reactive chlorine from anthropogenic and natural sources: Reactive Chlorine Emissions Inventory, J. Geophys. Res., 104 (D7), 8429-8440, doi: 10.1029/1998JD100084, 1999.

Lehman, S.J., Miller, J.B., Tans, P.P, Monzka, S.A., Sweeney, C., Andrews, A., Turnbull, J.C., and J. Southon (2012) $14CO_2$ Processing and Measurement Activities at CU-INSTAAR and NOAA/ESRL 16th WMO/IAEA Meeting on Carbon Dioxide, Other Greenhouse Gases, and Related Measurement Techniques (GGMT-2011), (Wellington, NZ, 25-28 Oct. 2011), World Meteorological Organization Global Atmosphere Watch Report No. 206, Geneva CH., p. 139-144.

Logan, J.A., Staehelin, J., Megretskaia, I.A., Cammas, J.-P, Thouret, V., Claude, H., De Backer, H., Steinbacher, M., Scheel, H.-E., Stubi, R.,Frohlich, M., and Derwent, R. Changes in ozone over Europe: Analysis ofozone measurements from sondes, regular aircraft (MOZAIC) and alpine surfacesites. Journal of Geophys.Res., 117,D09301,doi:10.1029/2011JD016952.

Miller, J.B.*, Lehman, S.J.*, Montzka, S.A., Sweeney,C., Miller, B.R., Karion, A., Wolak, C., Miller, L., Dlugokencky, E.J., Southon, J., Turnbull, J.C. and P. P. Tans (2012). Linking emissions of fossil fuel CO_2 and other anthropogenic trace gases using atmospheric $^{14}CO_2$. Journal of Geophysical Research 117,D08302, 23 pp., doi:10.1029/2011JD017048.

Montzka, S. A. and Reimann, S.: Ozone-depleting substances (ODSs) and related chemicals, in: Scientific Assessment of Ozone Depletion: 2010, Global Ozone Research and Monitoring Project, Rep. 52, World Meteorol. Org., Geneva, Switzerland, 1–108, 2011.

NASA (1994), Report on Concentrations, Lifetimes, and Trends of CFCs, Halons, and Related Species, J. A. Kaye, S. A. Penkett, F. M. Ormond (Eds.), NASA RP 1339.

O'Doherty, S., D. M. Cunnold, B. R. Miller, J. Mühle, A. McCulloch, P. G. Simmonds, A. J. Manning, S. Reimann, M. K. Vollmer, B. R. Greally, R. G. Prinn, P. J. Fraser, L. P. Steele, P. B. Krummel, B. L. Dunse, L. W. Porter, C. R. Lunder, N. Schmidbauer, O. Hermansen, P. K. Salameh, C. M. Harth, R. H. J. Wang, and R. F. Weiss, Global and regional emissions of HFC-125 (CHF2CF3) from in situ and air archive atmospheric observations at AGAGE and SOGE observatories, J. Geophys. Res., 114, D23304, doi:10.1029/2009 D012184, 2009.

Oram, D. E., Mani, F. S., Laube, J. C., Newland, M. J., Reeves, C. E., Sturges, W. T., Penkett, S. A., Brenninkmeijer, C. A. M., Rockmann, T., and Fraser, P. J.: Long-term tropospheric trend of octafluorocyclobutane (c-C_4F_8 or PFC-318), Atmos. Chem. Phys., 12, 261–269, doi:10.5194/acp-12-261-2012

Parrish, D.D., Law, K.S., Staehelin, J., Derwent, R., Cooper, O.R.,Tanimotot, H., Volz-Thomas, A., Gilge, S., Scheel, H.-E., Steinbacher, M.,and Chan, E. Long-term changes in lower tropospheric baseline ozone concentrations at northern mid-latitudes. Atmos. Chem. Phys., 12, 11485-11504, 2012.

Parrish, D.D., Law, K.S., Staehelin, J., Derwent, R., Cooper, O.R.,Tanimotot, H., Volz-Thomas, A., Gilge, S., Scheel, H.-E., Steinbacher, M.,and Chan, E. Lower tropospheric ozone at northern mid-latitudes: Changing seasonal cycle. Geophys. Res. Letters, 40, 1-6, 2013, DOI: 10.1002/grl.50303, 2013.

Prather, M.J, and J. Hsu, NF_3, the greenhouse gas missing from Kyoto, J. Geophys. Res. Letters, 35, L12810, doi:10.1029/2008GL034542, 2008.

Press, W. H., S. A. Teukolsky, W. T. Vetterling, and B. P. Flannery, Numerical Recipes in Fortran: The art of scientific computing, 2nd edition, Publ. Cambridge University Press, UK, 1992.

Prinn, R. G., and R. Zander (Lead Authors), D. M. Cunnold, J. W. Elkins, A. Engel, P. J. Fraser, M. R. Gunson, M. K. W. Ko, E. Mahieu, P. M. Midgley, J. M. Russell III, C. M. Volk, and R. F.Weiss, Long- lived ozone- related compounds, Chapter 1 in Scientific Assessment of Ozone Depletion: 1998, Global Ozone Research and Monitoring Project–Report No. 44, WorldMeteorological Organization, Geneva, Switzerland, 1999.
http://www.esrl.noaa.gov/csd/assessments/ozone/1998/

Prinn, R.G., R.F. Weiss, P.J. Fraser, P.G. Simmonds, D.M. Cunnold, F.N. Alyea, S. O'Doherty, P. Salameh, B.R. Miller, J. Huang, R.H.J. Wang, D.E. Hartley, C. Harth, L.P. Steele, G. Sturrock, P.M. Midgley, and A. McCulloch, A history of chemically and radiatively important gases in air deduced from ALE/GAGE/AGAGE, J. Geophys. Res., 115, 17751-17792, 2000.

Rigby, M., R. G. Prinn, S. O'Doherty, S. A. Montzka, A. McCulloch, C. M. Harth, J. Mühle, P. K. Salameh, R. F. Weiss, D. Young, P. G. Simmonds, B. D. Hall, G. S. Dutton, D. Nance, D. J. Mondeel, J. W. Elkins, P. B. Krummel, L. P. Steele, and P. J. Fraser, Re-evaluation of the lifetimes of the major CFCs and CH3CCl3 using atmospheric trends, Atmos. Chem. Phys., 13(5), 2691–2702, doi:10.5194/acp-13-2691-2013, 2013.

Rigby, M., A. J. Manning, and R. G. Prinn, The value of high-frequency, high-precision methane isotopologue measurements for source and sink estimation, Journal of Geophysical Research, 117(D12), D12312, doi:10.1029/2011JD017384, 2012.

Turnbull, J.C., Lehman, S.J., Miller, J.B., Tans, P., Sparks, R.J., and J. Southon. (2007). A new high-precision $^{14}CO_2$ time series for North American continental air. Journal of Geophysical Research doi:10.1029/2006JD008184, 10 pp.

Turnbull, J.C., Lehman, S.J., Morgan, S. and C. Wolak (2010). A new automated extraction system of ^{14}C measurement in atmospheric CO_2. Radiocarbon 52, 1261-9.

UNEP (United Nations Environment Program), 2002 Report of the Solvents, Coatings and Adhesives Technical Options Committee - 2002 Assessment (STOC 2002), edited by B. Ellis, UNEP Ozone Secretariat, Nairobi, Kenya. 2003.

Vaughn, B.H., Ferretti, D., Miller, J., James W. C. White, 2004: Stable isotope measurements of atmospheric CO_2 and CH_4. Handbook of Stable Isotope Analytical Techniques, volume 1, ch.14. Elsiever, 272-304

Velders, G. J. M., Fahey, D. M., Daniel, J. S., McFarland, M., Andersen, S. O.: The large contribution of projected HFC emissions to future climate forcing, PNAS, 106, 10949–10954, doi:10.1073/pnas.0902817106, 2009.

Weiss, R.F, Muhle, J, Salameh, P.K, Harth, C.M., Nitrogen trifluoride in the global atmosphere Geophys. Res. Lett., 35, (20), 2008, DOI: 10.1029/2008GL035913

Weissflog, L., C. A. Lange, et al. (2005). "Sediments of salt lakes as a new source of volatilehighly chlorinated C1/C2 hydrocarbons." *Geophysical Research Letters* 32(1) 32 (1): Art. No. L01401, Jan 4, 2005

Yokouchi, Y., K. Osada, M. Wada, F. Hasebe, M. Agama, R. Murakami, H. Mukai, Y. Nojiri, Y. Inuzuka, D. Toom-Sauntry, and P. Fraser, Global distribution and seasonal concentration change of methyl iodide in the atmosphere, J. Geophys. Res., 113, D18311, doi: 10.1029/2008JD009861, 2008.

8 Appendices

8.1 Instrumental

The map in Figure 156 shows the location of the three new sites, Angus, Ridge Hill and Tacolneston along with the original site at Mace Head, which has been operational since 1987. All new sites are operational. The site at Ridge Hill was set-up in February 2012 and Tacolneston began operating at the end of July 2012. Deployment at Tacolneston was delayed as planning permission was required to position the University of Bristol mobile lab (a custom built shipping container) at the site. Angus data has been collected since late 2005 and the University of Edinburgh have provided data from the beginning of March 2011. Problems with the GC-ECD at Angus from the beginning of the project contract have meant N_2O data for the whole of 2011 is unusable in calculating emission estimates using the inversion methodology InTEM (discussed in detail in the main report). Table 78 gives an overview of the gases which are measured at each of the sites and specifies which instrument each gas is measured on. Full details on all instrumentation can be found at the project website (www.metoffice.gov.uk/atmospheric-trends).

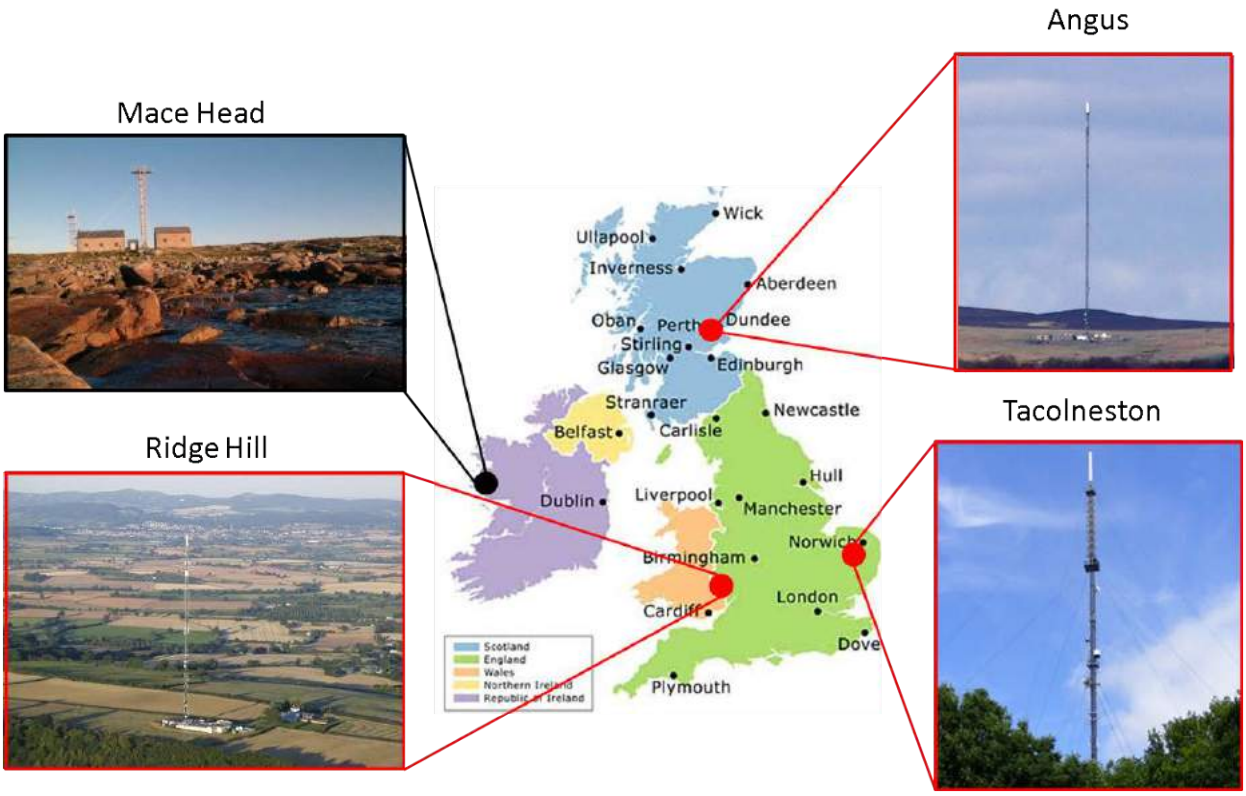

Figure 156: The location of Mace Head and the three new sites in the UK Deriving Emissions linked to Climate Change network (UK DECC Network).

Sites -> Species	Mace Head MHD	Tacolneston TAC	Ridge Hill RGL	Angus* TTA
CO_2	Picarro 2301*(1)*	Picarro 2301*(1)*	Picarro 2301*(1)*	LiCor 7000*(1)*
CH_4	Picarro 2301(1), GC-FID*(40)*	Picarro 2301*(1)*	Picarro 2301*(1)*	GC-FID*(40)*
N_2O	GC-ECD*(40)*	GC-ECD*(20)*	GC-ECD*(20)*	GC-ECD*(40)*
SF_6	Medusa*(120)*	GC-ECD*(20)*, Medusa*(120)*	GC-ECD*(20)*	GC-ECD*(40)*
H_2	GC-RGA*(40)*	GC-RGA*(20)*	-	-
CO	GC-RGA*(40)*	GC-RGA*(20)*	-	-
CF_4	Medusa*(120)*	Medusa*(120)*	-	-
C_2F_6	Medusa*(120)*	Medusa*(120)*	-	-
C_3F_8	Medusa*(120)*	Medusa*(120)*	-	-
c-C_4F_8	Medusa*(120)*	-	-	-
HFC-23	Medusa*(120)*	Medusa*(120)*	-	-
HFC-32	Medusa*(120)*	Medusa*(120)*	-	-
HFC-134a	Medusa*(120)*	Medusa*(120)*	-	-
HFC-152a	Medusa*(120)*	Medusa*(120)*	-	-
HFC-125	Medusa*(120)*	Medusa*(120)*	-	-
HFC-143a	Medusa*(120)*	Medusa*(120)*	-	-
HFC-227ea	Medusa*(120)*	Medusa*(120)*	-	-
HFC-236fa	Medusa*(120)*	Medusa*(120)*	-	-
HFC-43-10mee	Medusa*(120)*	-	-	-
HFC-365mfc	Medusa*(120)*	Medusa*(120)*	-	-
HFC-245fa	Medusa*(120)*	Medusa*(120)*	-	-
HCFC-22	Medusa*(120)*	Medusa*(120)*	-	-
HCFC-141b	Medusa*(120)*	Medusa*(120)*	-	-
HCFC-142b	Medusa*(120)*	Medusa*(120)*	-	-
HCFC-124	Medusa*(120)*	Medusa*(120)*	-	-
HCFC-123	-	Medusa*(120)*	-	-
CFC-11	Medusa*(120)*	Medusa*(120)*	-	-
CFC-12	Medusa*(120)*	Medusa*(120)*	-	-
CFC-13	Medusa*(120)*	Medusa*(120)*	-	-
CFC-113	Medusa*(120)*	Medusa*(120)*	-	-
CFC-114	Medusa*(120*	Medusa*(120)*	-	-
CFC-115	Medusa*(120)*	Medusa*(120)*	-	-
H-1211	Medusa*(120)*	Medusa*(120)*	-	-
H-1301	Medusa*(120)*	Medusa*(120)*	-	-
H-2402	Medusa*(120)*	Medusa*(120)*	-	-
CH_3Cl	Medusa*(120)*	Medusa*(120)*	-	-
CH_3Br	Medusa*(120)*	Medusa*(120)*	-	-
CH_3I	Medusa*(120)*	Medusa*(120)*	-	-
CH_2Cl_2	Medusa*(120)*	Medusa*(120)*	-	-
CH_2Br_2	Medusa*(120)*	Medusa*(120)*	-	-
$CHCl_3$	Medusa*(120)*	Medusa*(120)*	-	-
$CHBr_3$	Medusa*(120)*	Medusa*(120)*	-	-
CCl_4	Medusa*(120)*	Medusa*(120)*	-	-
CH_3CCl_3	Medusa*(120)*	Medusa*(120)*	-	-
$CHCl=CCl_2$	Medusa*(120)*	Medusa*(120)*	-	-
$CCl_2=CCl_2$	Medusa*(120)*	Medusa*(120)*	-	-

Table 78: Operational sites, instrumentation and observed species. Number in brackets indicates frequency of calibrated air measurement in minutes.

8.2 Sites

8.2.1 Mace Head

8.2.1.1 Medusa-GCMS

Overall, the Medusa performed well during the reporting period with no major issues. It was noted that GCWerks frequently exits on completing a data update. This does not affect the running of the instrument and only occurs for the Medusa version of the software.

A number of unexplained alarm shutdowns have occurred during the reporting period, presumed to be due to communications errors. On a number of occasions, the site manager was in the lab at the time and noted no obvious reason for the error.

The MEMS mass flow controller (MFC) was replaced with a Red-Y MFC on the 20th June 2012 during a site-visit.

A blockage of the Nafion purge flow was discovered on the 31st of July 2012. The zero air pressure was increased to compensate and generate normal purge flow. On the 22nd of August, the low flow/high flow solenoid and restrictor (needle valve) was bypassed – this resulted in the Nafion flow returning to normal at normal delivery pressure. The blockage was eventually identified as being a faulty solenoid valve. The solenoid remains bypassed as it is not necessary on the system at Mace Head.

The Medusa lab experienced some problems with leakage of refrigerants from the onsite air conditioners. Exceptionally high levels of HFC-32 and HFC-125 were observed in lab air samples on 15th August. An engineer leak checked all onsite units on 20th August using an ultrasonic leak checker. One definite small leak was found in the second shore lab building. A lab air run on the 23rd August still showed exceptionally high HFC-32/125 levels. Lab air runs were disabled. It seems clear that commercial ultrasonic leak detectors are not sensitive enough to pinpoint the leaks in the AC at the site. A possible solution is to switch to a water-cooled system which would have the refrigeration unit outside the lab i.e., no HFC's piped into the lab.

Co-incident air sampling with the MD was noted to be affecting pressure measurements on the 4th of September 2012. The same happens with co-incident tertiary measurements. Independent pressure regulation to both instruments would seem to be the only solution unless active control of the delivery pressure of samples can be achieved.

A GAW audit of VOC measurements was carried out between 18-19th September 2012. Audit tanks had been analysed prior to the audit itself.

8.2.1.2 GC-MD

The MD proved yet again to be a most reliable system and performed well for the reporting period. Most of the data loss resulted from ancillary equipment failure or late gas delivery.

Tertiary tank J-151 arrived at Mace Head later than hoped. Since the pressure in working tank, J-144 was low it was decided to stop use of J-144 and use G-055 as a temporary standard for 8 days between 14-22nd of June 2012.

In July, an audible leak from the TOC was found to come from a cracked O-ring on top of the first inlet filter bowl. A temporary repair was carried out using PTFE tape. The site manager has recommended the installation of a good quality, external filter/dryer upstream of the TOC so the leaky internal filter unit can be bypassed.

During October, contractors were onsite at various times in relation to compressed gas safety upgrade works. These works briefly consisted of installation of a cylinder storage cage, removal of electrical outlets close to the location of H_2 cylinders, installation of a stainless steel, outdoor

housing for flammable gases (H_2 and P5), installation of new panel mounted regulators and piping for outdoor gas cylinders.

On the 30th of October, the H_2 tank ran out due to late delivery. This resulted in loss of CH_4 data until 2nd of November 2012.

A Fourier Transform Infra Red spectrometer (FTIR) system measuring CO_2, CH_4, CO, N_2O, SF_6 and $\delta^{13}CO_2$ was installed onsite on 23rd February 2013, a comparison of calibration gases between the FTIR and GC-MD was carried out. The FTIR will measure ambient air at Mace Head for ~2 month. The results will then be compared to the *in situ* MD and Medusa measurements.

8.2.2 Ridge Hill

The site at Ridge Hill in Herefordshire has been operational since the 23rd of February 2012 (Figure 157). Sampling lines at 45 and 90 meters were installed in the first week of February and civil works were completed on the 12th of February. Equipment was transported from the research lab at the University of Bristol on the 22nd of February and installation of measurement equipment was completed on the 23rd of February.

8.2.2.1 CRDS

The Picarro 2301 Cavity Ring Down Spectrometer (CRDS) has been running well at Ridge Hill over the last 14 months. The CRDS samples air from the two tower heights of 45 m and 90 m, alternating every 30 minutes. The CRDS operates by measuring CO_2 and CH_4 in an evacuated cavity at very low pressure. During the last 14 months of operation the vacuum pump used to evacuate the cavity broke down three times causing 10 days of data loss overall. A more robust pump (Vacuubrand MD-1) was purchased and fitted on the 4th of February 2013 to prevent any future pump failures. Data from the CRDS is automatically transferred each day to the Integrated Carbon Observation System (ICOS) data server. This automated data transfer was updated at Ridge Hill on the 17th of January 2013 keeping in line with the new ICOS data processing server. As well as data being transferred daily to the ICOS server for processing, calibrated data is also returned daily to the data server held at University of Bristol.

8.2.2.2 GC-ECD

The gas chromatograph with electron capture detector (ECD), which measures N_2O, and SF_6 at Ridge Hill, ran well from February until the bad storms towards the end of November 2012.

During July 2012 significant improvements were made to instrumental precision by changing the air sample loop size from 3 to 8 ml and by improving insulation of the ECD. As the cabin at Ridge Hill which houses the instrumentation is not air conditioned it is subject to large temperature fluctuations which effects ECD instrument precision. By addition of extra insulation to the ECD this effect is minimised.

During heavy rain and strong winds on the 15th of November 2012 the water traps at the base of the tower overfilled and water was sucked into the instrument. The instrument was shut down and a site visit was made on the 20th of November to fix the problems which this caused and measurements restarted. On the 25th and 26th of November another bad storm crossed the west of England resulting in further instrumental failure. The air sampling setup inside the cabin was modified so that if the water traps become overfilled again in the future this will not compromise the equipment. Numerous attempts were made to fix the instrument but after various testing and liaison with Agilent, the GC manufacturers, at the end of December 2012 it was decided that the ECD had been badly damaged and needed replacement.

A contract was immediately set up for this process; however as the ECD contains a radioactive source its shipment is a lengthy process. The new ECD arrived at the University of Bristol on the 21st of January 2013. The heavy snowfall during this week meant that the site was inaccessible due to its elevation and narrow road access. The replacement ECD was installed by an Agilent engineer on the 4th of February. The instrument began operating well after the replacement.

Further instrumental improvements were made to column heating which improved separation of N_2O from SF_6 and also improved N_2O peak shape and data precision. In conclusion, N_2O and SF_6 measurements made at Ridge Hill are now the same precision as measurements of these gases made at Mace Head with daily precisions of 0.05% and 0.6% respectively.

In September 2012 a cover was made and fitted to the gas cylinder rack at Ridge Hill. Carrier gas cylinders at this site are housed in an external rack and this cover protects the cylinders and regulators from heat, wind, rain and ice damage. A large temperature range is experienced at the site from summer temperatures of above 30 ^oC and winter temperatures of -10 ^oC. The rack cover was made in white material with mesh squares at the bottom to aid ventilation. This cover will protect the expensive regulators from frost damage and prevent the (dark grey) carrier gas cylinders from getting too hot in the summer.

The site is currently operating without problems and fortnightly site visits are being made to ensure all instrumentation is running well and there are sufficient calibration and carrier gases.

Figure 157: The 166.4 metre Tall tower at Ridge Hill (right) with a view of the surrounding countryside (top centre). The grey cabin houses instrumentation and the images on the left show the first measurements of CO_2 and CH_4 taken from the new site at Ridge Hill.

8.2.3 Tacolneston

The site at Tacolneston in Norfolk has been operational since the 25th of July 2012. Sampling lines at 54, 100 and 185 meters were installed in November 2011. Figure 158 shows the top of the 100 m and 185 m sample lines attached to protective cups to prevent water ingress. Planning permission was required for the placement of the mobile lab (a custom built shipping container which houses all instrumentation) at the site, this was granted on the 28th of March 2012. Civil works were completed on the 24th of July and the mobile lab was craned into place.

During the period between January 2012 (when we were informed planning permission would be required) and July 2012 (when the mobile lab was craned into place at the site) all instrumentation was installed in the mobile lab at the University of Bristol. Instrumentation was optimised and set up for the measurement of air from the tower at the three inlet heights in Tacolneston. Training for technical staff from the University of East Anglia was carried out in the mobile lab whilst it was

operational in Bristol. The lead technician in charge of routine instrumentation operation at Tacolneston also came to Bristol for further training on the custom software which is used to operate the instruments and quality control the data.

Since the initial installation all the equipment has been operating well.

An unexpected power cut occurred during onsite work at Tacolneston in early December. Minimal data loss occurred as the site operator from UEA was able to go on site and restart instrumentation within two days.

8.2.3.1 Medusa-GCMS

Certain species on the Medusa, particularly the most volatile species like CF_4, degraded in precision from the 1st of January 2013 because of reduced amounts of refrigerant in the chiller unit which cools the adsorbent traps in the instrument. A site visit was made on the 30th of January 2013 the refrigerant was topped up and the oil-filter on the unit changed. This solved the problem resulting in 1 month of CF_4 data being lost. Other optimisations were carried out during this visit, they are detailed in the New Developments section of the main report. The lead technician who visits the site each week to service instrumentation also underwent additional training on the instrumentation, in particular the Medusa. A comparison of the ambient record for certain Medusa species with associated standard precision are shown in the main document.

8.2.3.2 TAC-MD

In early October 2012 H_2 and CO data measured on the Peak Performer 1 instrument became noisy due to a cross-port leakage on port 5. During this period a week of data was affected where precision for H_2 rose from 0.5 to 1.5% and CO precision rose from 1.5% to 7%. This was resolved on the 9th of October and normal data precision resumed.

In mid-October 2012 a cylinder of carrier gas for the ECD, which measures N_2O and SF_6, was attached and found to be contaminated with large amounts of SF_6. A spare cylinder was not available onsite, which resulted in a small delay in its replacement resulting in three weeks of lost data. To prevent this problem re-occurring, each cylinder of carrier gas for the ECD is now measured for contamination before it is used on the instrument.

8.2.3.3 CRDS

The CRDS instrument at Tacolneston ran without any problems during the measurement period. From July 2012 the CRDS was sampling from the lines at 54 and 100 m, in January 2013 the third sampling line at 185 m was plumbed to the instrument and measurements began at three heights.

Figure 158: The approximate location of the air sampling lines (185 m, 100 m, 54 m) on the tower at Tacolneston (right). The cups which cover the line inlets at the top of the tower (lower centre) and the mobile lab (bottom left) which will house instrumentation at Tacolneston.

8.2.4 Angus

A visit to the Tall Tower at Angus, 10 km north of Dundee, was made on Monday the 9th of May 2011 to see how the tower lines and instrumentation were set-up. Figure 159 shows the tower, which samples air from 222 m above ground level and instrumentation.

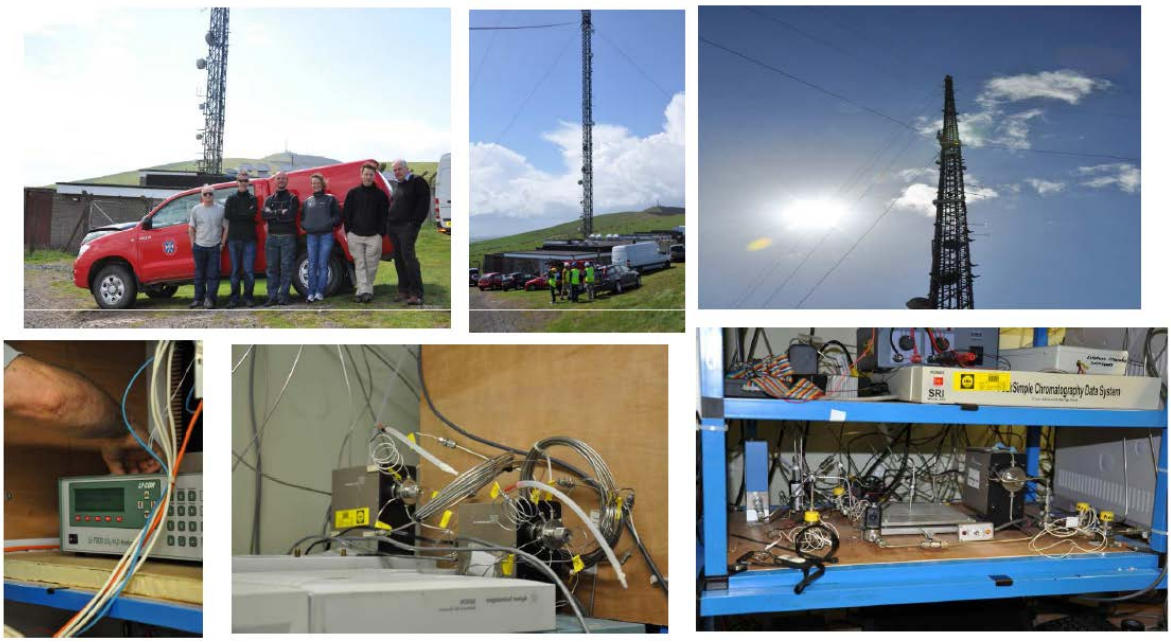

Figure 159: Picture of the tall tower at Angus, Dundee run by the University of Edinburgh (above) with instrumentation set-up (below): sampling valves for the GC-FID and ECD which measure CH_4, and N_2O and SF_6 respectively (lower centre) and the sample line split off into the three different instruments (lower right) are shown.

In December 2012 the University of Edinburgh decided they could no longer continue to run the Angus site. They suggested that the University of Bristol manage the site and run the instruments in the following months using the budget assigned to Edinburgh for the final year of the contract. Since December the site sharing agreement with Arqiva, internet and telephone accounts have been transferred to the University of Bristol. Only the Picarro CRDS instrument will continue measurements at the site for the final year of the DECC contract measuring CO_2 and CH_4 only. All other instruments have been mothballed until funds are available to allow their overhaul and update to the standard of existing equipment in the DECC network, or the purchase of new equipment.

The University of Bristol have recently been awarded £171K from NERCs capital equipment fund to purchase new sampling equipment for Angus - Picarro CRDS for CO_2 and CH_4, Los Gatos CRDS for N_2O and CO, and a flask-sampling package to provide the capability of isotope analysis (note there are at present no funds for the analysis of isotopes).

8.2.4.1 LiCor and CRDS

Until January 2013 CO_2 data from Angus was measured by a LiCor 7000 in line with the contract. However, data from a Picarro 1301 CRDS instrument which has been at the site since the beginning of the current DECC contract has been made available to the project. The CRDS provides measurements of CO_2 and CH_4. Data from this CRDS for the contract period has been transferred to the University of Bristol. UoB and Met Office personnel are in the process of automating the modification of the raw data output files to the correct format for calibration by the Integrated Carbon Observation System (ICOS) data server in the same manner which data from the CRDS instruments at Ridge Hill and Tacolneston are calibrated.

LiCor CO_2 data generally overlays well with Mace Head data however there appear to be many recent depletion events in CO_2 which are not seen at Mace Head. The validity of these low CO_2 measurements will also be clarified when calibrated CO_2 data from the Picarro 1301 CRDS is available.

8.2.4.2 GC-ECD

The GC-ECD at Angus, which measured N_2O and SF_6, was previously operating with problems (and a very high background signal). The ECD was replaced in December 2011. The new detector gave a low background and data quality improved for N_2O and SF_6. Recent N_2O data overlaid well with Mace Head measurements, albeit with a constant baseline offset. However due to irresolvable, frequent inconsistencies between Mace Head and Angus N_2O data inversions carried out at the Met Office to produce emission estimates cannot use the Angus data.

8.2.4.3 GC-FID

CH_4 data overlays well with Mace Head but the magnitude of pollution events are smaller at Angus than Mace Head - which is contrary to what would be expected considering the sites location closer to sources. One possible reason could be the difference in sampling heights, with Angus samples taken from 222 m above ground level being diluted compared with samples taken from 15 m above the ground at Mace Head. Yet another possible cause for this difference could be due to instrument calibration issues. When CH_4 data from the CRDS instrument is calibrated it will enable us to validate the CH_4 data from the gas chromatograph with flame ionisation detector. This will clarify whether pollution events are actually of a smaller magnitude or if it is an instrumental issue.

8.3 PFC point source analysis

8.3.1 Introduction

This section describes the ongoing work to investigate the point source inventory data that are available for two specific gases, namely PFC-14 and PFC-218. These gases were chosen as the number of defined sources within the UK and also across Europe are small and also, most importantly, known. The year 2004 was chosen for analysis because its emission in NWEU were more significant in 2004 than in later years. This analysis will be extended in future reports to include 2012 when observations from Tacolneston are also available.

PFC-14 has two significant categories of sources, from aluminium production and from the electronics industry. The former source is the dominant source. Release of PFC-14 occurs when there is an anode failure at a smelter. As there are hundreds of anodes at each plant and the plants are operated around the clock, it is reasonable to assume that the emissions of PFC-14 can be assumed to be uniform in time. The number, location and size of each smelter across Europe is readily known from the internet and so these emissions can be well defined. The emissions from each smelter in the UK were obtained directly from AEA Technology. The locations of emissions from the electronics industry are not defined. The emissions of PFC-14 from the production of aluminium have steadily fallen across Europe from 2004 to current day.

PFC-218 is emitted from only one chemical plant in the UK and so is ideal for point source analysis. The location of the plant is known and is near Preston in Lancashire. There are no declared emissions in Ireland. For the rest of Europe this is not the case and so when emissions from these countries are considered the emissions are spread uniformly across each country. It is assumed that the distance from Mace Head to these other sources is great enough to render the error of this simplification negligible.

This work is on-going. In future work, the emissions in 2012 will be investigated and compared against both the observations at Mace Head and at Tacolneston. The new observations at Tacolnestion will provide significant insight into the point source emissions of these gases.

8.3.2 PFC-14 (CF_4)

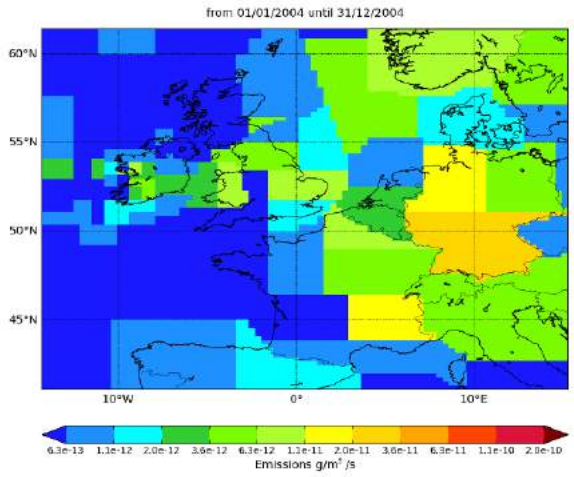

Figure 160: InTEM emission estimate for 2004.

The significant uncertainties in the InTEM results entirely overlap with the inventory estimates although the median results are consistently higher.

Year	RMSE (ppt)	Correlation	Max obs. above baseline (ppt)	% obs. above baseline noise	Mean obs. above baseline (ppt)
2004	0.14	0.35	1.50	22	0.13

Table 79: Statistical comparison between modelled and observed time-series for 2004.

Unit	Year	UK	(5th-95th)	NWEU	(5th-95th)
t/y	2004	46	(8.9- 91.)	430	(182.- 639.)

Table 80: InTEM estimates for 2004 for UK and NWEU with uncertainty (5^{th} – 95^{th} %ile).

8.3.2.1 Point source analysis of PFC-14

Country	Location	Aluminium Produced (kt/y) 2012	% Aluminium per country	Estimated emission of PFC-14 (t/y) 2004
UK	Anglesey			4.5
UK	Lynemouth			14.7
UK	Lochaber			0.7
UK	Lea (F2 chem)			1.1
Germany	Essen	170	27	20.5
Germany	Hamburg	135	22	16.7
Germany	Neuss	230	36	27.4
Germany	Voerde	96	15	11.4
France	Dunkirk	273	66	143.9
France	St Jean de M	141	34	74.1
Netherlands	Delfzijl	170	100	14.0
Total				329.0

Table 81: Aluminium smelters in NWEU (+ F2 chemicals in UK, by-product of halocarbon production). Non-UK emissions estimated based on size of smelter in 2012, and total country emissions reported to UNFCCC. UK electronic industry emissions of 3.33 t/y (14.3% of UK emissions) are not included. Non-UK smelter emissions elevated because emissions from halocarbon production and from the electronics industry are assigned to smelters.

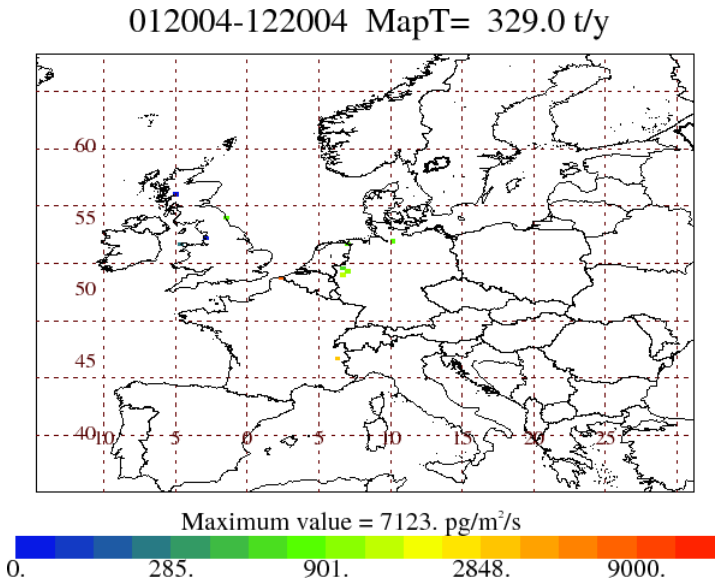

Figure 161: Location and magnitude of the PFC-14 emissions in NWEU from aluminium smelters (+ F2 chemicals in UK), see table above. The dominant emission point is Dunkirk in NE France.

Using the emission map shown in Figure 161 and the NAME dilution matrix that describes how emission dilution en route to Mace Head, it is possible to derive a time-series of modelled concentrations at Mace Head given these inventory emission estimates of PFC-14. The scatter plot of modelled versus observed (baseline removed) values is shown in figure 162.

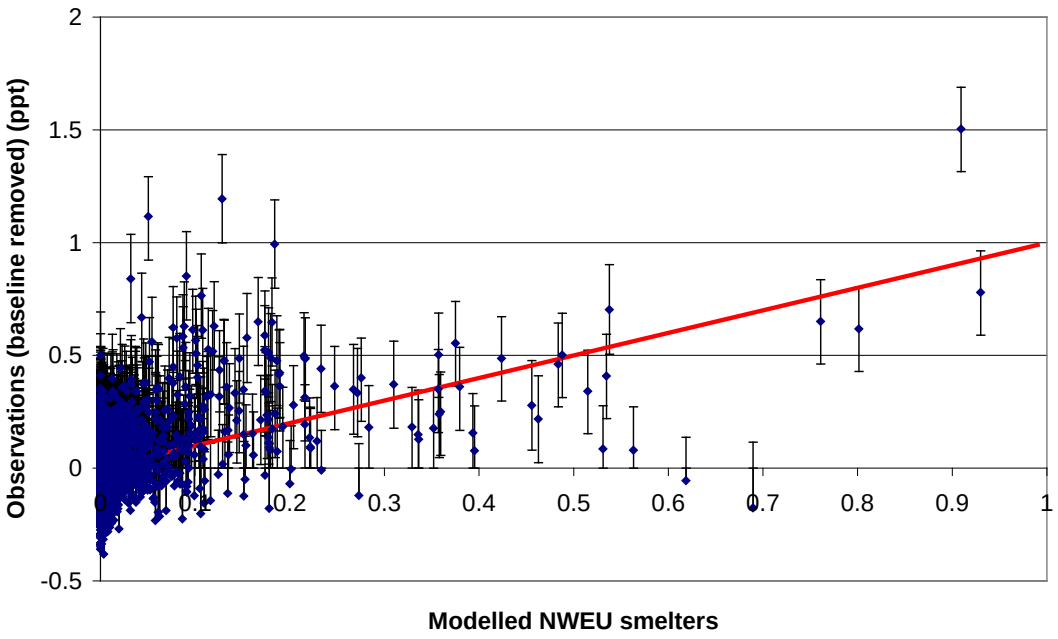

Figure 162: Scatter plot of modelled PFC-14 from NWEU smelters against Mace Head observations of PFC-14 (baseline subtracted). Red line is a 1:1 correspondence. The uncertainty bars on the observations reflect the uncertainty in the estimated baseline.

There is certainly reasonable correspondence between the elevated model and elevated observations. There are some notable exceptions, certainly there are significant occasions when the observations are elevated compared to the model. However only the NWEU smelters have been modelled here, the significant emissions from Spanish, Norwegian and Icelandic smelters are not modelled (see later), also the emissions from the UK electronics industry (14% of UK emissions) are absent (point source data are not available). The elevated points in both model and observation are discussed in more detail below. It should be noted that there are only relatively few elevated (above baseline uncertainty) events in the observations (see table 79).

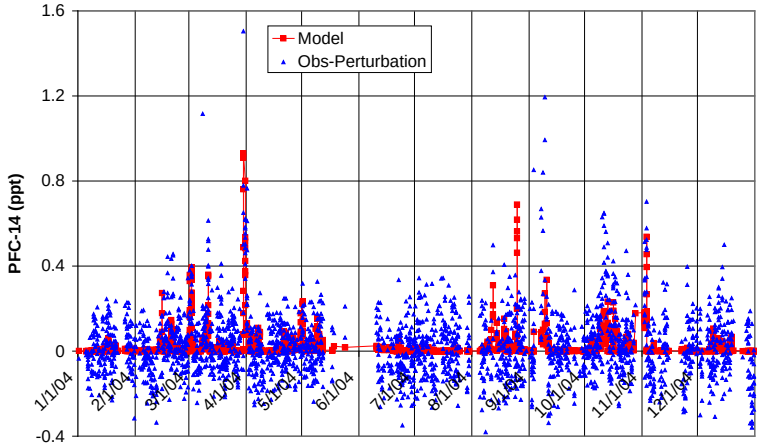

Figure 163: Time-series of PFC-14 of model (NWEU smelters only) and observations (baseline removed) at Mace Head in 2004.

Some of the significant pollution events shown in figure 163 are now discussed in more detail.

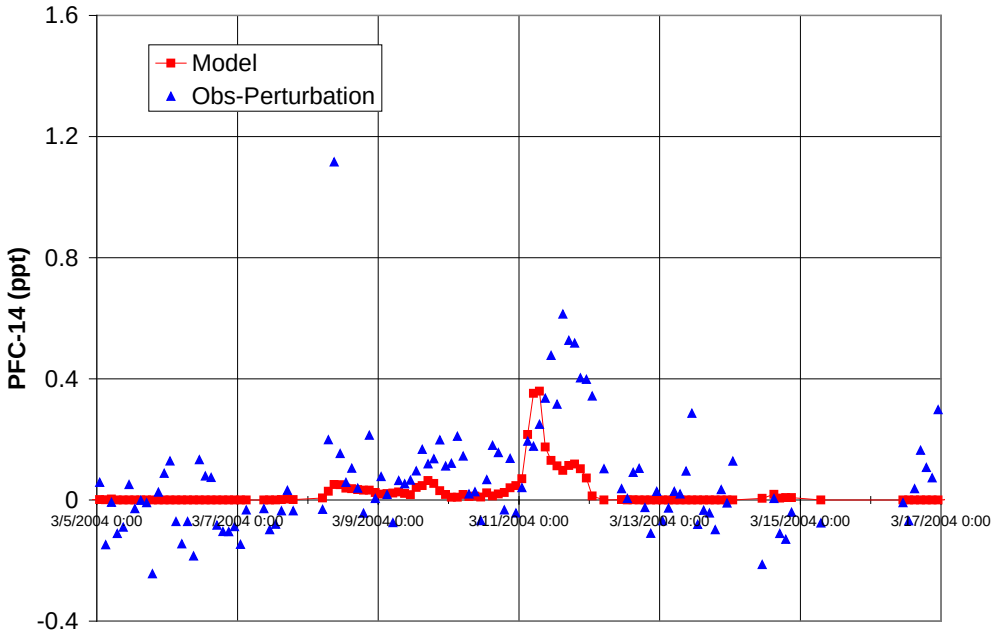

Figure 164: Mace Head observations (baseline subtracted) of PFC-14 compared to model values (NWEU emissions only exc. UK electronics), early March 2004.

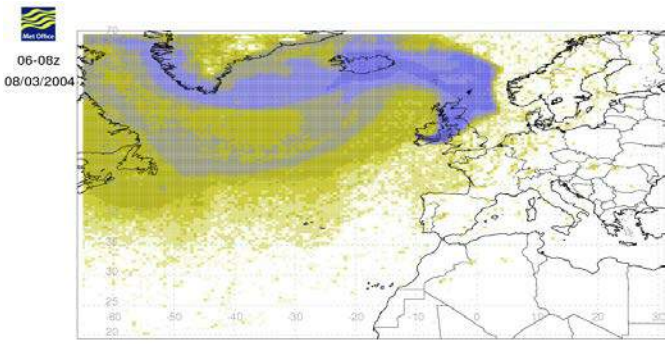

Figure 165: NAME air history map for 6-8am 8th March 2004

The high observation 6-8am 8th March 2004 is not seen in the model when only NWEU smelters are included. Considering the air history for this time, the likely sources are Anglesey (4.5 t/y), Lynemouth (14.7 t/y), Lochaber (0.7 t/y) or Iceland (5 t/y).

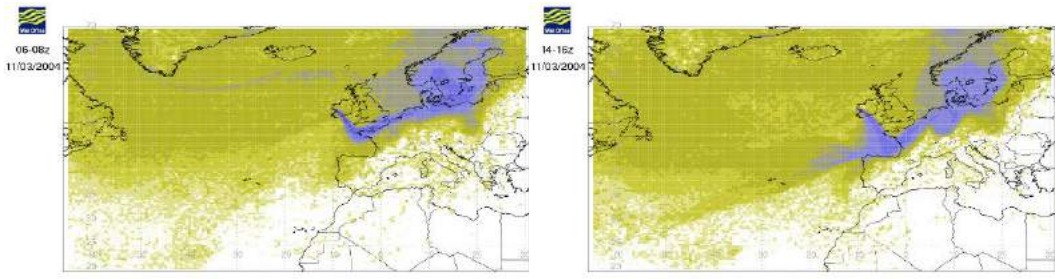

Figure 166: NAME air history map for 6-8am and 2-4pm 11th March 2004. The left shows a time when the model values are elevated above the observations, the right when the observations are elevated above the model values. The large Spanish smelter on the north coast may be responsible for the missing perturbation in the model values. The narrow modelled plume over the Dunkirk smelter may account for the elevated model value.

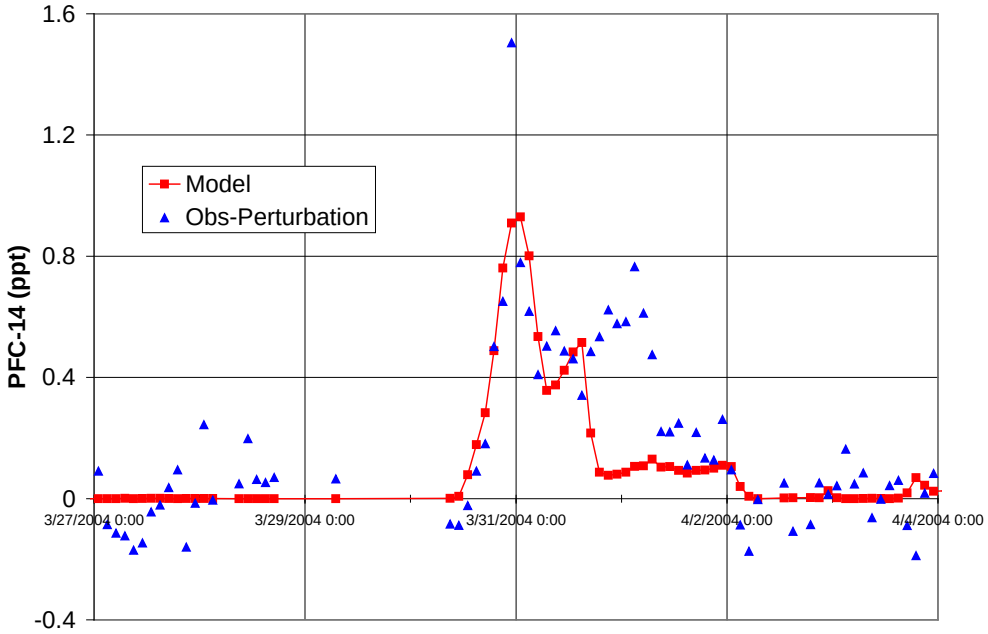

Figure 167: Mace Head observations (baseline subtracted) of PFC-14 compared to model values (NWEU emissions only exc. UK electronics), late March – early April 2004.

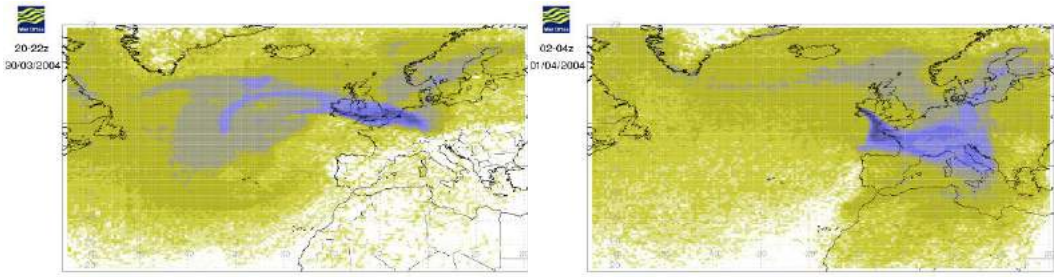

(a) (b)

Figure 168: NAME air history map for (a) 10pm-midnight 30th March 2004, (b) 2-4am 1st April 2004

Figure 168(a) above shows good agreement in terms of correlation between the modelled emissions and the observations, however the observation is 0.6 ppt higher. The tail of the elevated period (b) is not captured well by the modelled emissions. Possible explanations are; Incorrectly assigned French electronics industry, Spanish smelters or the air history map being a poor representation of reality at this time.

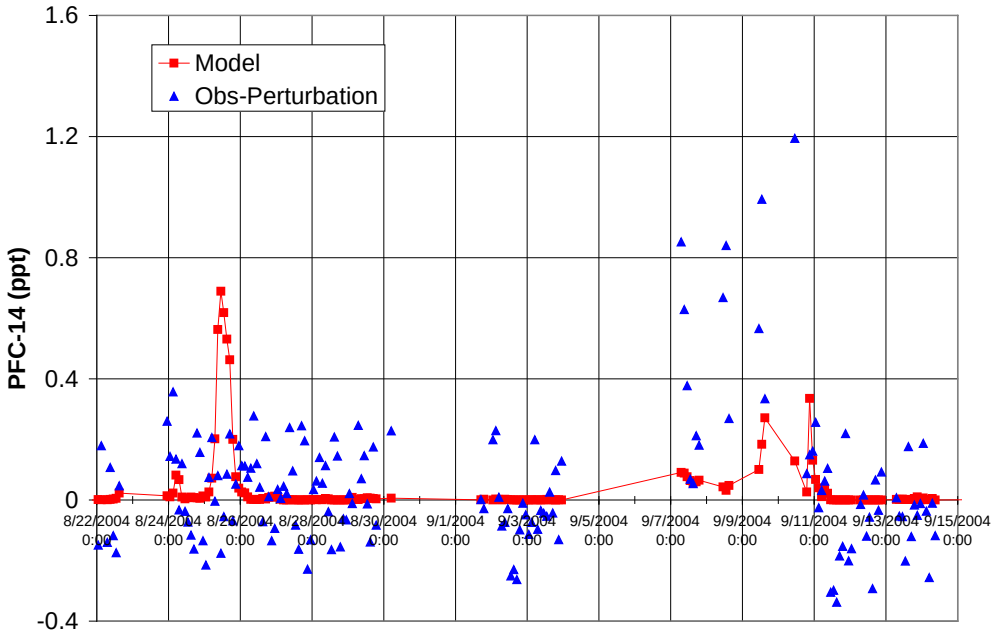

Figure 169: Mace Head observations (baseline subtracted) of PFC-14 compared to model values (NWEU emissions only exc. UK electronics), late Aug – early Sept 2004.

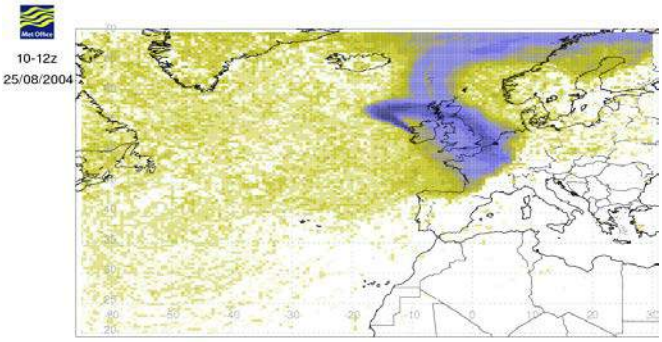

Figure 170: NAME air history map for 10am-noon 25th Aug 2004 (elevated model)

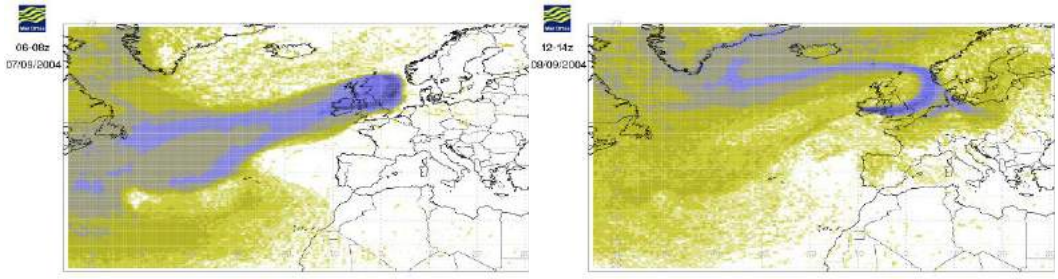

(a) (b)

Figure 171: NAME air history map for (a) 6-8am 7th Sept 2004, (b) noon-2pm 8th Sept 2004 (elevated observations)

On the 25th August 2004 the model is elevated above the observations. This could be due to the enhanced emissions given to the Dunkirk smelter. A significant proportion of these emissions will actually come from the electronics industry in France and be more widespread across the country.

The period in September of elevated observations is not well matched by the model. On the 7th and 8th Sept. the air is modelled to have passed over the UK and Ireland only before sweeping across the Atlantic. Possible reasons for mismatch: The excluded Norwegian or Canadian smelters (very significant sources), one-off release from UK sources, inaccuracy in the modelled air history.

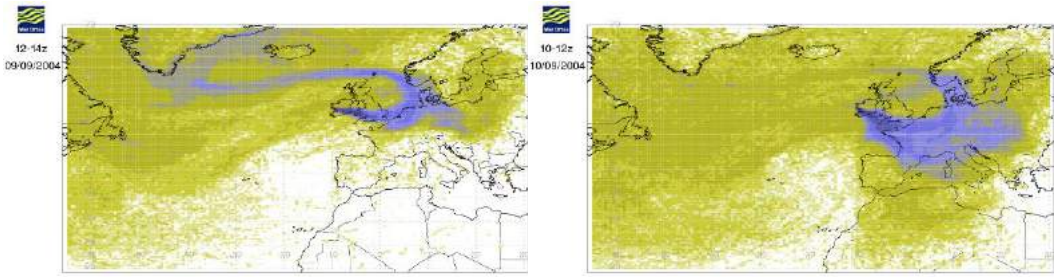

(a) (b)

Figure 172: NAME air history map for (a) noon-2pm 9th Sept 2004, (b) 10am-noon 10th Sept 2004 (elevated observations)

8.3.2.2 Adding in aluminium smelters in Norway and Spain

Country	Location	Aluminium Produced (kt/y) 2012	% Aluminium per country	Estimated emission of PFC-14 (t/y) 2004
Norway	Aardal	233	16.7	20.37
Norway	Hoyanger	60	4.3	5.25
Norway	Husnes	185	13.2	16.10
Norway	Karmoy	170	12.2	14.88
Norway	Lista	127.5	9.1	11.10
Norway	Mosjoen	221.5	15.9	19.40
Norway	Sunndalsora	400	28.6	34.89
Spain	Aviles	93	21.6	5.40
Spain	La Coruna	87	20.2	5.05
Spain	San Ciprian	250	58.2	14.55
Total				147

Table 82: Aluminium smelters in Norway (122 t/y in 2004, UNFCCC) and Spain (25 t/y in 2004, UNFCCC). Emissions estimated based on aluminium production of the smelter (en.wikipedia.org/wiki/List_of_aluminium_smelters) in 2012, and total country emissions reported to UNFCCC. The smelter emissions are marginally elevated because the reportedly small emissions from halocarbon production and from the electronics industry are assigned to smelters.

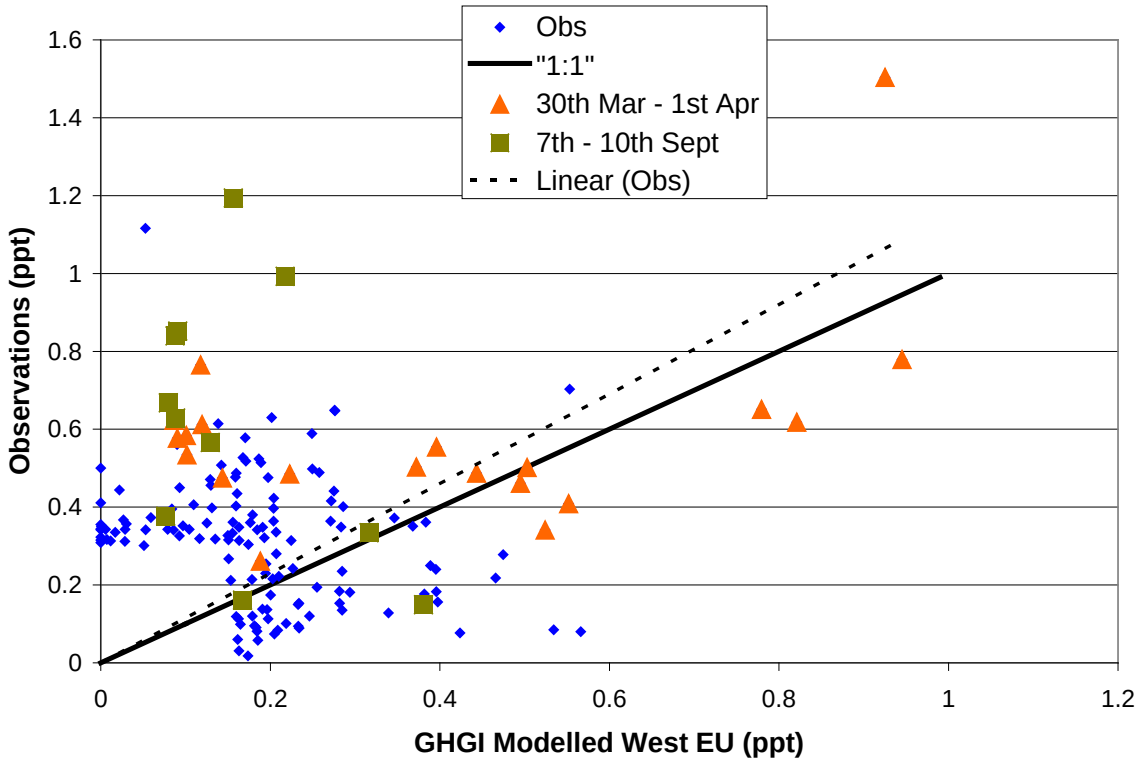

Figure 173: GHGI modelled PFC-14 from all Western EU sources (except UK electronics) compared to observed (baseline removed) in 2004 when either model or observation is elevated. Two specific pollution events are highlighted (discussed above). 1:1 line and the best-fit linear line (forced to zero) are shown for interest.

8.3.2.3 Summary on PFC-14 analysis

- Relatively few significant pollution events.
- Some events are reasonably well modelled by the GHGI emissions (UK electronic industry excluded) e.g. first part of 30th March – 1st April event, others not so, e.g. 7-10th Sept.
- Baseline uncertainty is relatively significant.
- Average modelled value when all significant Western European emissions are included is similar to average observed value.
- The geographically unspecified electronics industry emissions add uncertainty to this analysis.

8.3.3 PFC-218

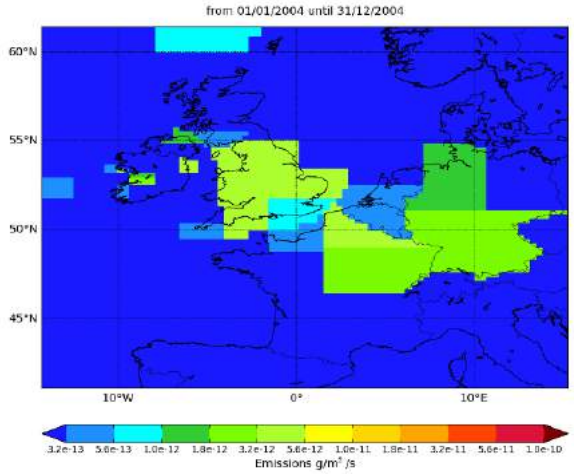

Figure 174: InTEM emission estimates for 2004.

Even with the relatively large uncertainty in the InTEM emission estimates they are still consistently elevated (by a factor of ~2) compared to the inventory both in the UK and in NWEU. The statistical match between the model time-series and the observations is fair.

Year	RMSE (ppt)	Correlation	Max obs. above baseline (ppt)	% obs. above baseline noise	Mean obs. above baseline (ppt)
2004	0.03	0.40	0.75	26	0.02
2012	0.02	0.40	0.23	23	0.01

Table 83: Comparison between modelled and observed time-series

Unit	Year	UK	(5th-95th)	NWEU	(5th-95th)
t/y	2004	31	(15.- 37.)	80	(35.- 92.)
t/y	2012	19.8	(6.- 23.)	36	(7.- 48.)

Table 84: InTEM emission estimates for UK and NWEU with uncertainty (5^{th} – 95^{th} %ile) for 2004 and 2012.

8.3.3.1 Point source analysis of PFC-218

The comparison between the observations and the InTEM solution and the reported GHG Inventory (GHGI) is further investigated in this section. The year 2004 was chosen as the reported UK emissions in this first complete year of Mace Head observation were estimated to be larger than in subsequent years.

An emission file was created from the reported GHGI data for 2004. It is shown in the figure 175. The UK emissions have a specific location. On the continent this information was unavailable and so the emissions for each country have been spread evenly across the country (For Spain, the emissions are spread across both Spain and Portugal for computational reasons). Only 2 countries in Western Europe, other than the UK (0.0103 Gg), have significant emissions of PFC-218 in 2004, namely Germany (0.0197 Gg) and Spain (0.0181 Gg). Ireland reports 0.0 emissions of PFC-218.

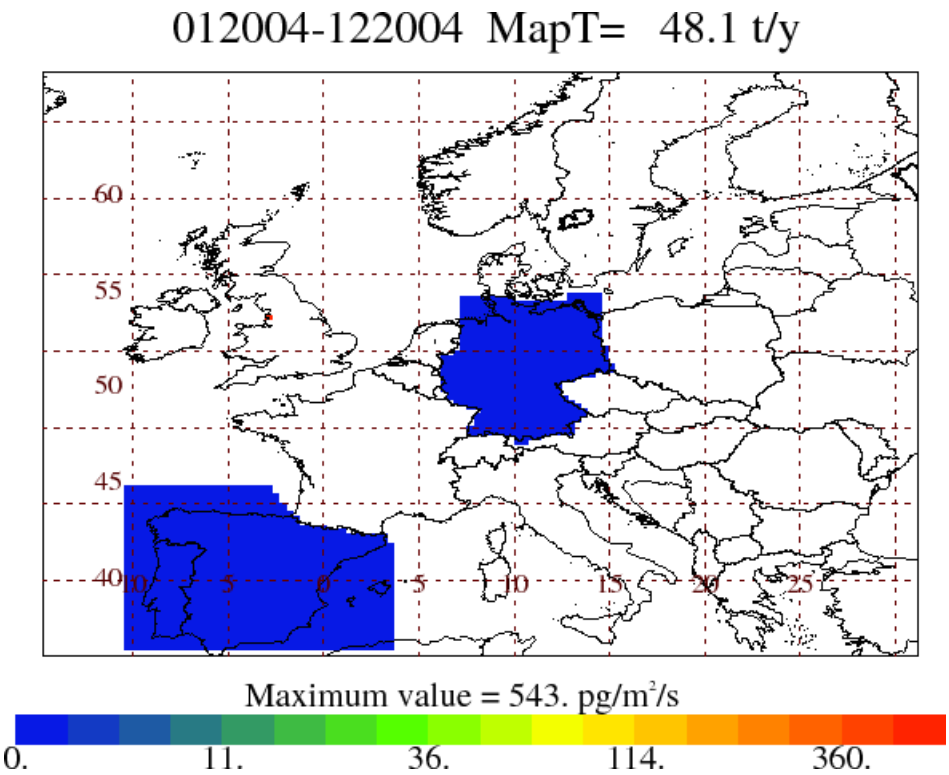

Figure 175: GHG Inventory (GHGI) emission map for PFC-218 for 2004. Emissions for UK (point source near Preston, NW England), Germany and Spain have been included.

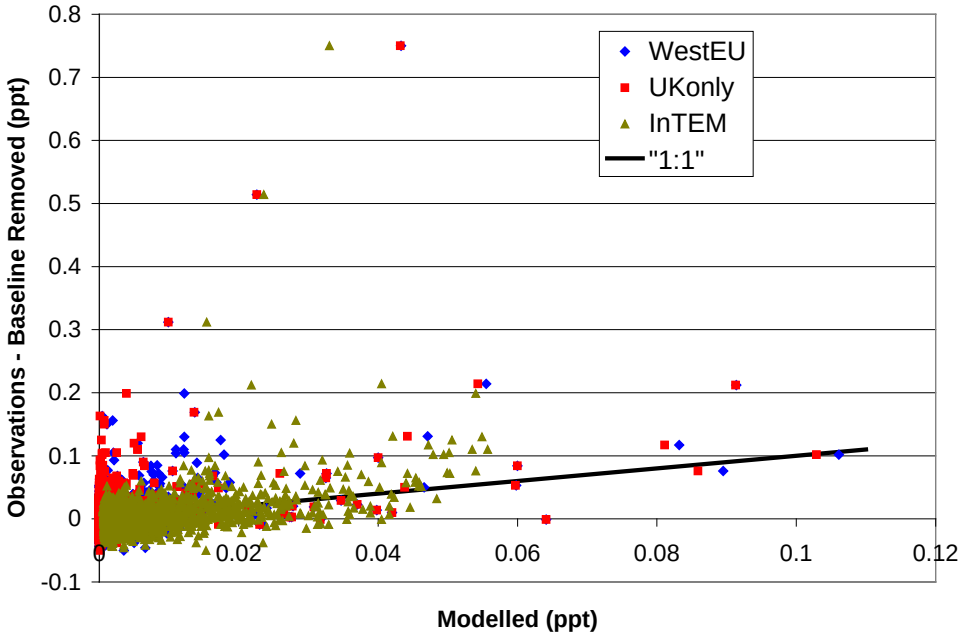

Figure 176: Scatter plot of modelled values against the observations (baseline removed). Time-series from three emission maps are shown; West EU = GHGI UK+Germany+Spain, UKonly = GHGI UK only and InTEM = Average InTEM solution for 2004. The 1:1 line is shown for interest.

As can be seen there are many observations above the 1:1 line showing that there are significant numbers of observations above the modelled values. There are many more modelled InTEM values to the right of 0.03 ppt than when the GHGI emissions are used, revealing the InTEM solution on the whole estimates higher values than the GHGI. There are also some very elevated observations considerably higher than modelled (by an order of magnitude). It is also worth noting that for many of the modelled values there is only a small difference between the GHGI WestEU

and UKonly solutions, this indicates that the UK emissions dominate the modelled signal seen at Mace Head.

It is also clear that the vast majority of observations and modelled values are very low in magnitude. Figure 177 only includes a comparison where either the observations are greater than 0.05 ppt or the modelled GHGI values are greater than 0.01 ppt. The best-fit line between the GHGI WestEU values and the observations has a gradient of more than two, in isolation this would imply the GHGI emissions are low by more than a factor of 2. However this line is strongly influenced by the three very elevated observations.

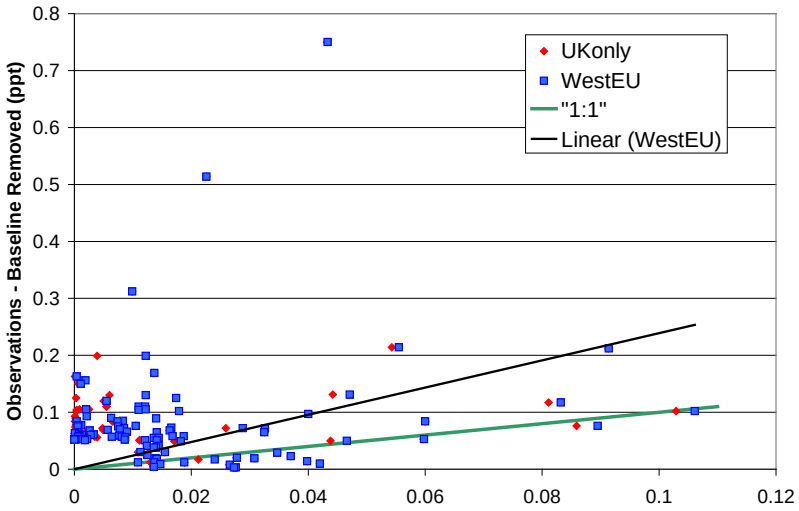

Figure 177: Scatter plot of modelled values against the observations (baseline removed) provided either the observations are > 0.05 ppt or the modelled values > 0.01 ppt. Two emission models are shown; West EU = GHGI UK+Germany+Spain, and UKonly = GHGI UK only. The 1:1 line is shown for interest, as is the linear best-fit line.

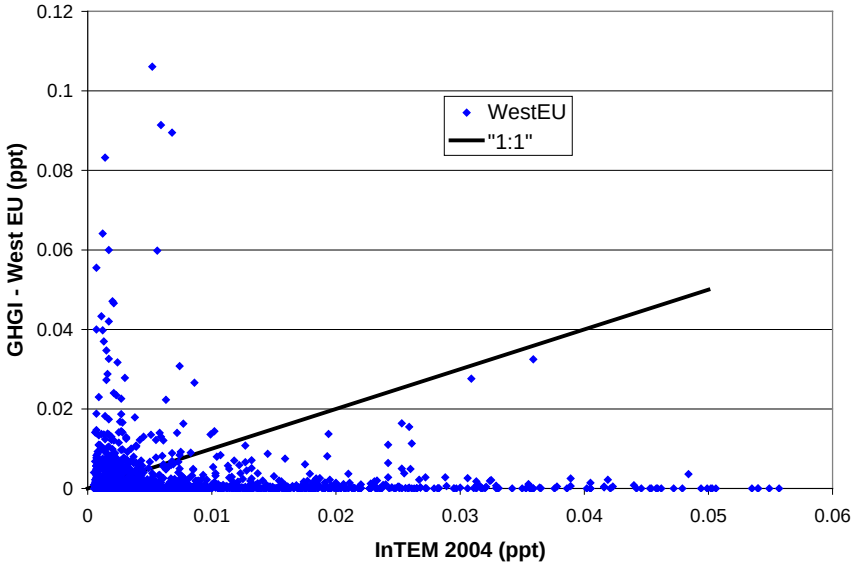

Figure 178: Comparing modelled times-series at Mace Head for 2004 from the two possible emission files; GHGI WestEU (UK + Germany + Spain) and InTEM 2004 inversion solution.

The comparison between the modelled time-series using the WestEU GHGI emissions and the InTEM solution for 2004 is very poor as shown in figure 178. It is clear that the InTEM solution has many more elevated values but also fails to replicate the limited number but elevated GHGI modelled values. In part this reflects the resolution of the InTEM solution. The GHGI emissions for the UK come from a single point source whereas the InTEM grid divides the entire UK into a limited

number (approximately 10) of sub-grids. It also reflects the large number of elevated observations above the GHGI modelled values and the fact that the InTEM solution is created purely from the observations (no a priori emissions).

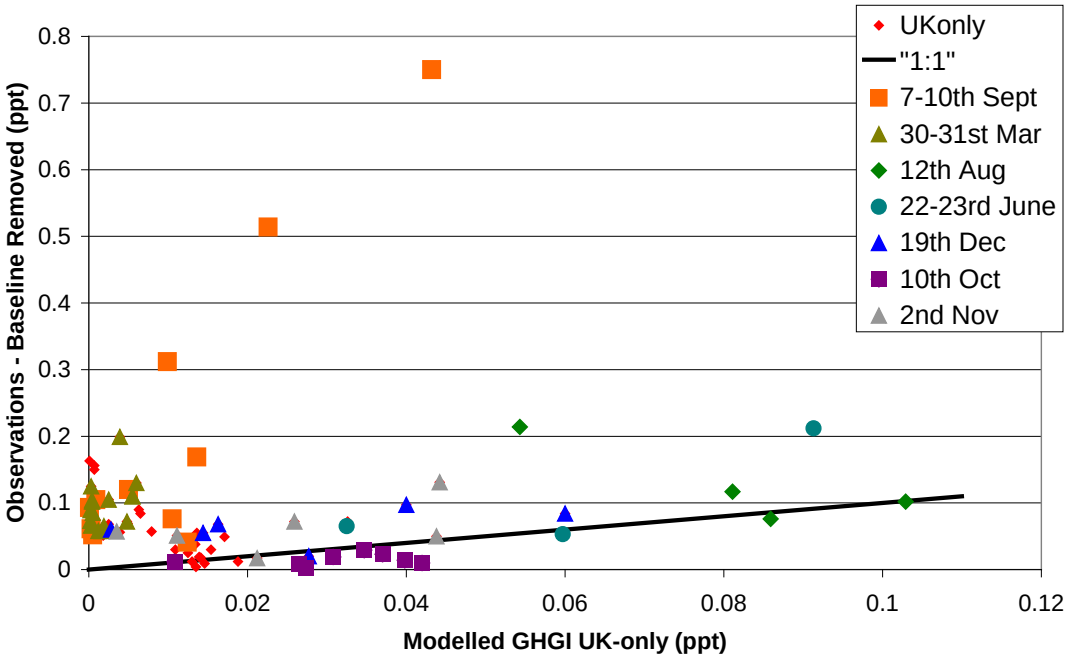

Figure 179: Elevated observations or modelled values colour coded by specific events.

Figure 179 shows the same values as shown in figure 177, i.e. only the elevated values are shown. However here they have been colour-coded by specific pollution events. This reveals some interesting features. The most important is that the elevated observations and modelled values arise for a limited number (seven) of events. The 7-10th Sept event has air histories that indicate that it is purely from NW UK with no continental influence (figure 180). The observations are around a factor of 20 greater than the GHGI modelled values at that time. Conversely the event on the 10th Oct has elevated GHGI modelled values above the observations. The events on 12th Aug, 22-23rd Jun, 2nd Nov and 19th Dec are all reasonably well modelled.

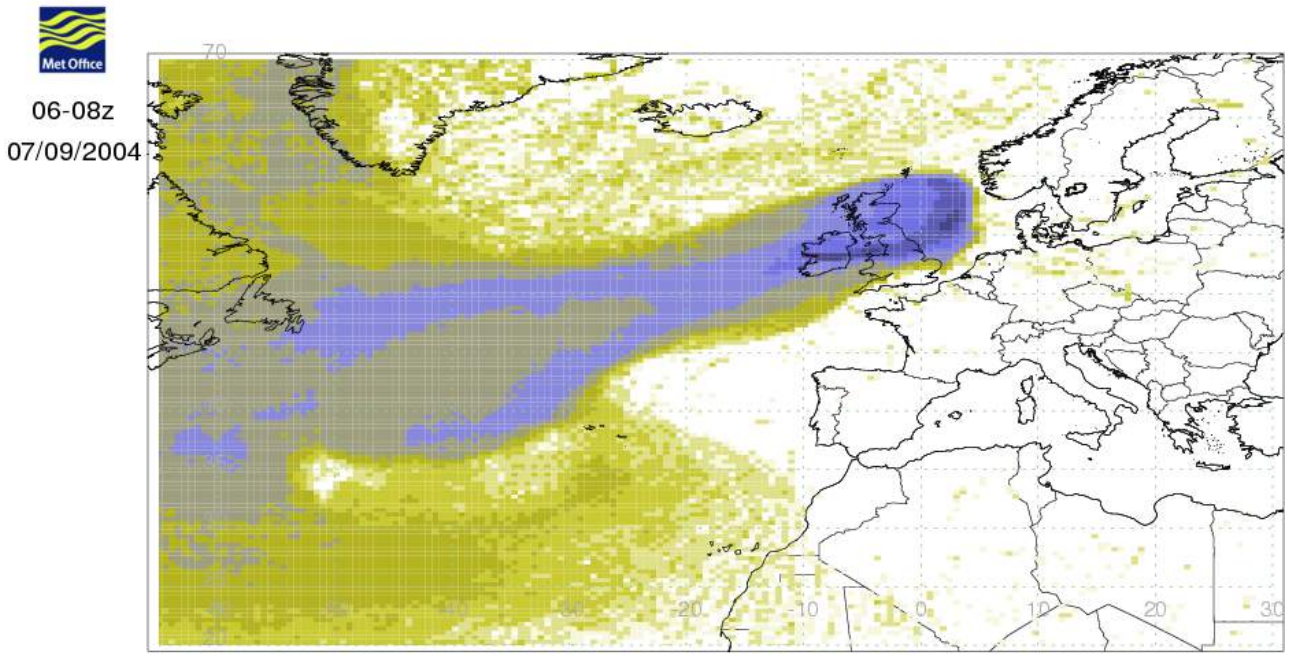

Figure 180: Air history map for 6-8 am 7th Sept 2004 for Mace Head.

8.3.3.2 Summary of PFC-218 analysis

- Few significant pollution events are seen at Mace Head.
- The point source emission in the UK dominates the significant pollution events seen at Mace Head.
- The release from the UK point source is not continuous. Sometimes it releases substantially more than (factor of 20) its annual average emission, other times less than its annual average release. Four out of the seven significant events indicate that the point source release is within a factor of two of its annual average and therefore these events are reasonably well modelled.
- 55% of the 2253 observations (after the baseline has been removed) are above the modelled GHGI WestEU values, however the average observation is more than three times the average modelled GHGI WestEU value. The average InTEM modelled value is within 2% of the average observation. This explains the elevated InTEM emissions relative to the GHGI estimates.
- The relatively coarse grid used in the inversion modelling is unable to capture the significant pollution events that arise from the single point source in the UK.

8.4 Stratospheric – Tropospheric exchange

8.4.1 Synopsis of paper submitted to the Journal of Geophysical Research

Interannual fluctuations in the seasonal cycle of nitrous oxide and chlorofluorocarbons due to the Brewer-Dobson circulation.

The tropospheric seasonal cycles of N_2O, CFC-11 (CCl_3F), and CFC-12 (CCl_2F_2) are influenced by atmospheric dynamics due to the inter-annual variations in mixing of stratospheric air (depleted in CFCs and N_2O) with tropospheric air with a few months lag. The amount of wave activity that drives the stratospheric circulation and influences the winter stratospheric jet and subsequent mass transport across the tropopause appears to be the primary cause of this interannual variability. By mass conservation the wintertime descent of stratospheric air in the extratropics, due to the Brewer-Dobson Circulation (BDC), is balanced by the upwards transport of tropospheric air in the tropics in a ~40^o latitudinal belt (20^{o}S-20^{o}N). The maximum STE occurs in late Winter/early Spring, primarily in the mid-latitudes (30^o-70^{o}N), and accounts for 67-81% of the annual input of air of stratospheric origin into the Northern Hemisphere (NH) extratropical troposphere.

We relate the observed seasonal minima of N_2O, CFC-11 and CFC-12 at three Northern Hemisphere sites Mace Head, Ireland (MHD); Trinidad Head, USA (THD) and Barrow, Alaska (BRW) with the behaviour of the winter stratospheric jet. As a result, a good correlation is obtained between zonal winds in winter at 10 hPa, 58^{o}N-68^{o}N and the de-trended seasonal minima in the stratosphere-influenced tracers. For these three tracers, individual Pearson correlation coefficients (r) between 0.51 and 0.71 were found, with overall correlations of between 0.67 and 0.77 when 'composite species' (average of N_2O, CFC-11 and CFC-12) were considered. These correlations could provide a useful observational measure of the strength of stratosphere-troposphere exchange and thus, could be used to monitor any long-term trend in the BDC which is predicted by climate models to increase over the coming decades.

Monthly mean baseline mixing ratios of N_2O, CFC-11 and CFC-12 are first calculated from the long-term observational record of trace gas measurements at the three observing sites. Baseline mixing ratios are defined here as those that have not been influenced by significant anthropogenic or local emissions within the past 30-days of travel, i.e. those that are well mixed and are representative of the mid-latitude Northern Hemisphere background concentrations. Baseline mixing ratios are calculated for each hour by interpolating; using a quadratic best-fit function, within a moving time window from all measurements recorded when the air is classified as 'baseline'. Points are defined as 'baseline' or not, through the use of air history maps calculated using the NAME (Numerical Atmospheric dispersion Modelling Environment) model. Three different detrending methods have been explored in order to define the long term and residual components and enable an estimation of the uncertainty. Working with the estimated hourly baseline values the time-series is split into 2 separate components, a long-term trend and a residual (seasonal cycle) component. Figure 181 illustrates the mass mixing ratio trend lines for MHD N_2O from the application of the three detrending methods and estimated seasonal variability mass mixing ratio for each method.

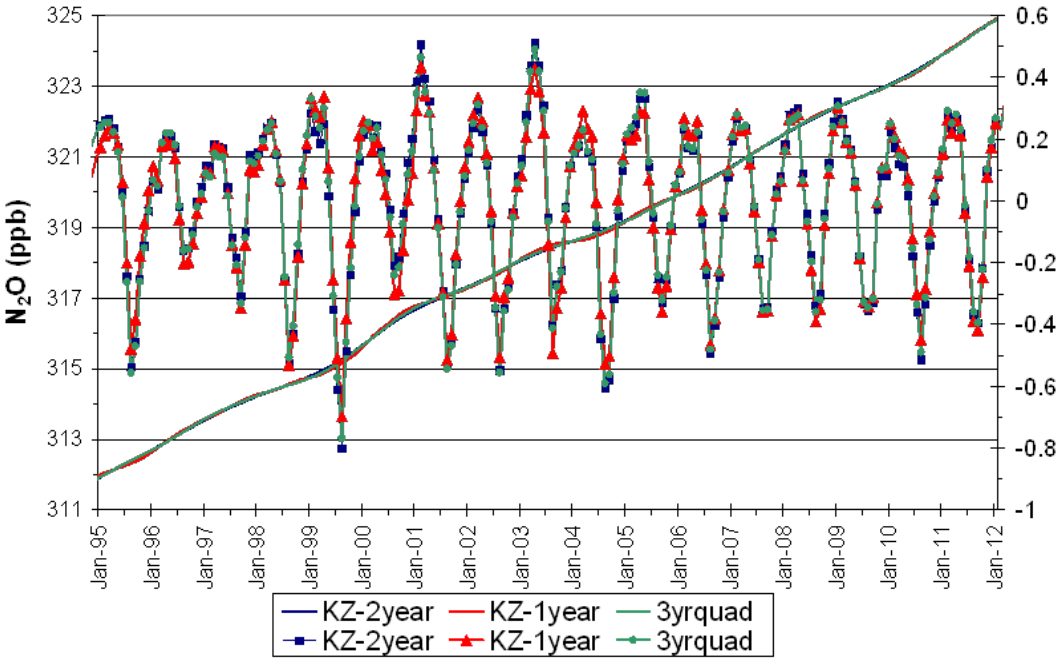

Figure 181: Mass mixing ratio trend lines for the Mace Head N_2O from the application of the three detrending methods (left-hand axis) and estimated seasonal variability mass mixing ratios for each method (right-hand axis).

We next correlated the species' residual seasonal variability at the surface with the jet's behaviour. Figure 182 compares the % variation of the residual from the long-term average of N_2O at Mace Head (MHD) for each detrending method with the median of the winds including uncertainty over the 58°N-68°N latitude band. In Figure 182b we average the residual components for N_2O from the three detrending methods including the uncertainty, versus the median of the winds. Overall there is a good correlation between the tracer residuals and the winds; however this relationship is weaker in some years and notably anti-correlated during 1995, 2003, 2009 and 2011. The winter of 2009/10 had a very weak polar vortex and exceptionally negative NAO and winter 2010/11 also showed unusual circulation patterns.

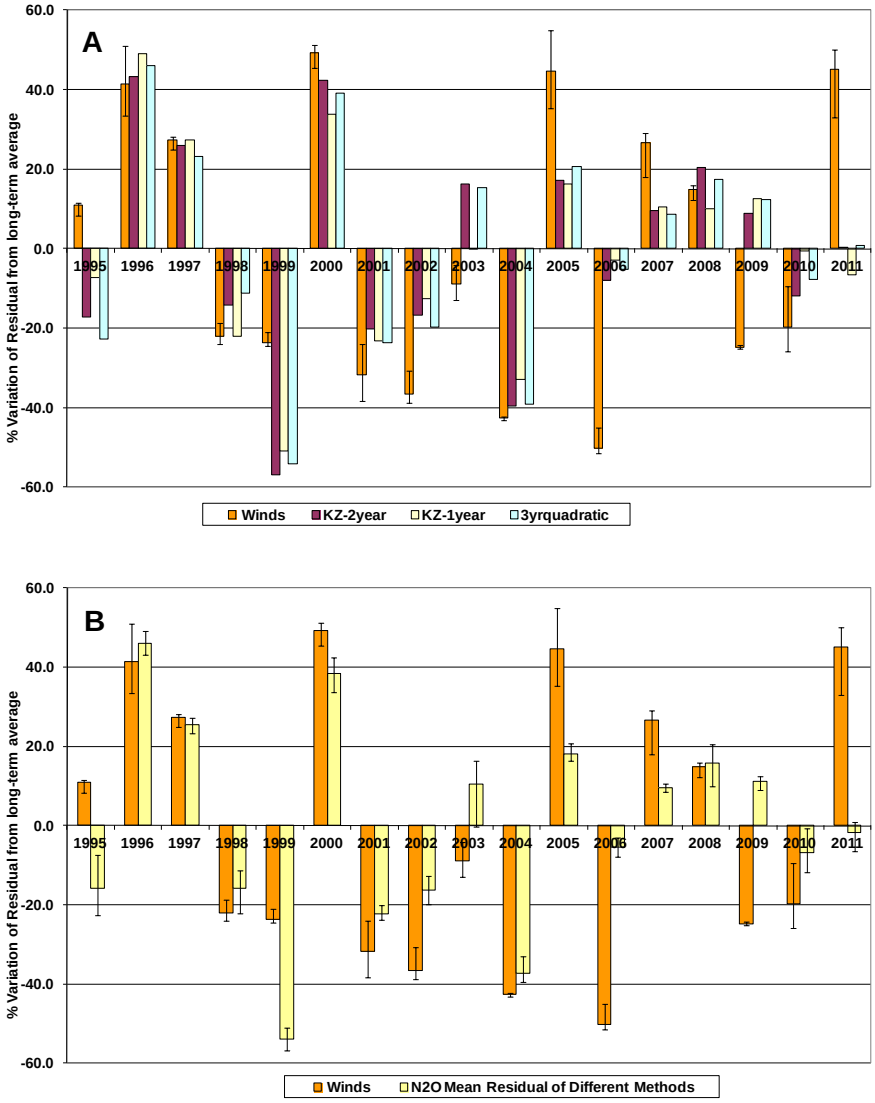

Figure 182 **(A)**: Comparison of the % variation of the seasonal variability from the long-term average of N_2O at MHD for each detrending method (K-1, K-2, 3yr Quad) with the median of the winds including uncertainty over the 58°N-68°N latitude band. **(B)** Average of the seasonal variability components for N_2O from the three detrending methods including the uncertainty, versus the median of the winds.

We next create an artificial new 'composite' tracer by averaging the component residuals of N_2O, CFC-11 and CFC-12 at MHD and in Figure 183 we relate this 'composite' tracer to the winds. We observe strong correlations between the 'composite' and the strength of the deviations of the previous wintertime (DJF) lower stratospheric winds in 12 of the 17 years of observations. This implies that a weak stratospheric jet and the resulting enhanced vertical transport leads to greater STE and thus a lower summer minima in the seasonal cycles of all of the stratospheric tracers. Correlations of this 'composite' tracer with the winds are 0.68 (1995-2011) and 0.82 (1995-2008). The years that show the largest summer minima for the 'composite tracer' were 1999, 2002, 2004, and 2006, while 2001 also has a significant minimum.

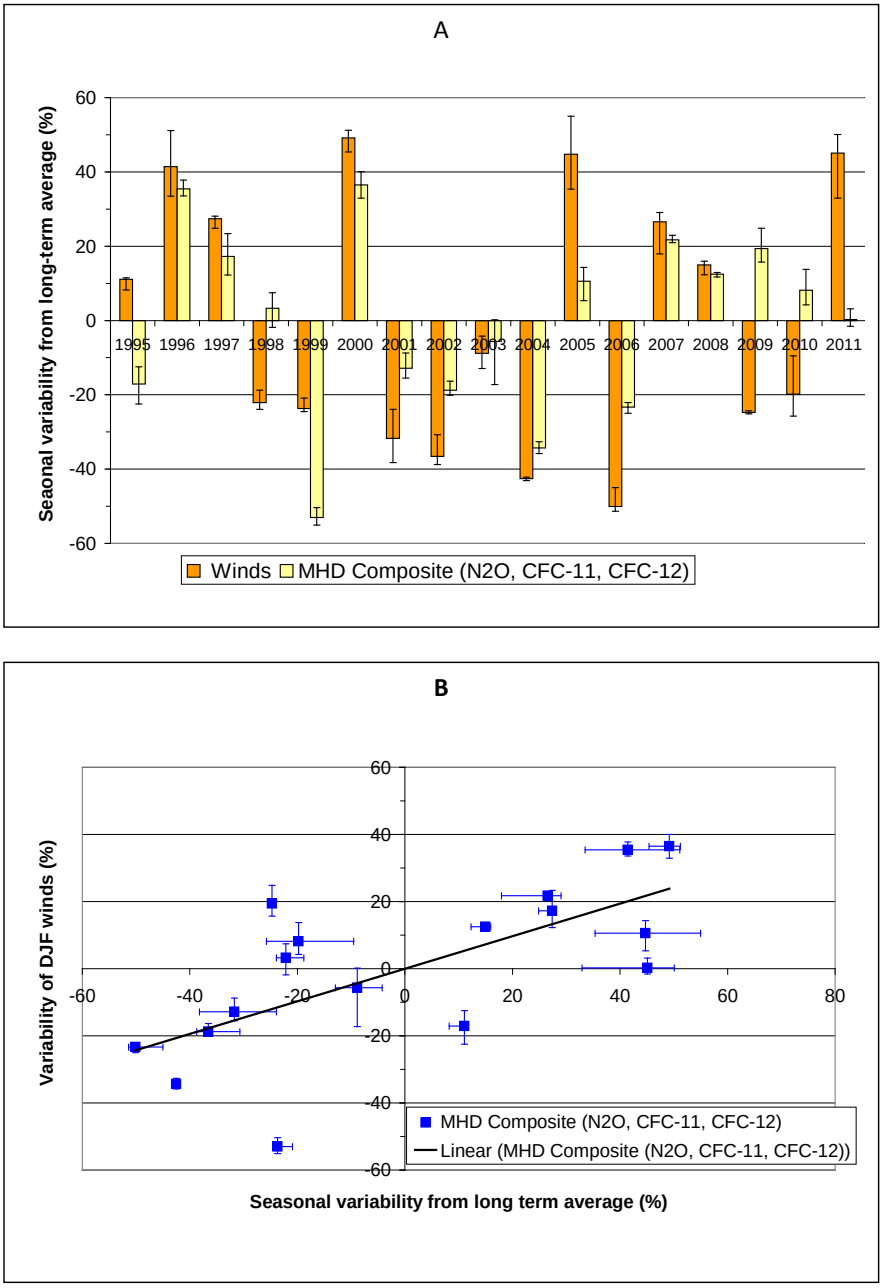

Figure 183: Comparison of the 'composite' tracer (mean of N_2O, CFC-11, and CFC-12 at MHD) by the three detrending methods with the median of the winds: (A) Bar graph showing comparison year by year and (B) scatter graph with the linear trend line.

We include in Figures 184A and B similar correlations of the 'composite' tracer with the winds for Trinidad Head (THD) and Barrow, Alaska (BRW), using the same three detrending methods as employed at MHD.

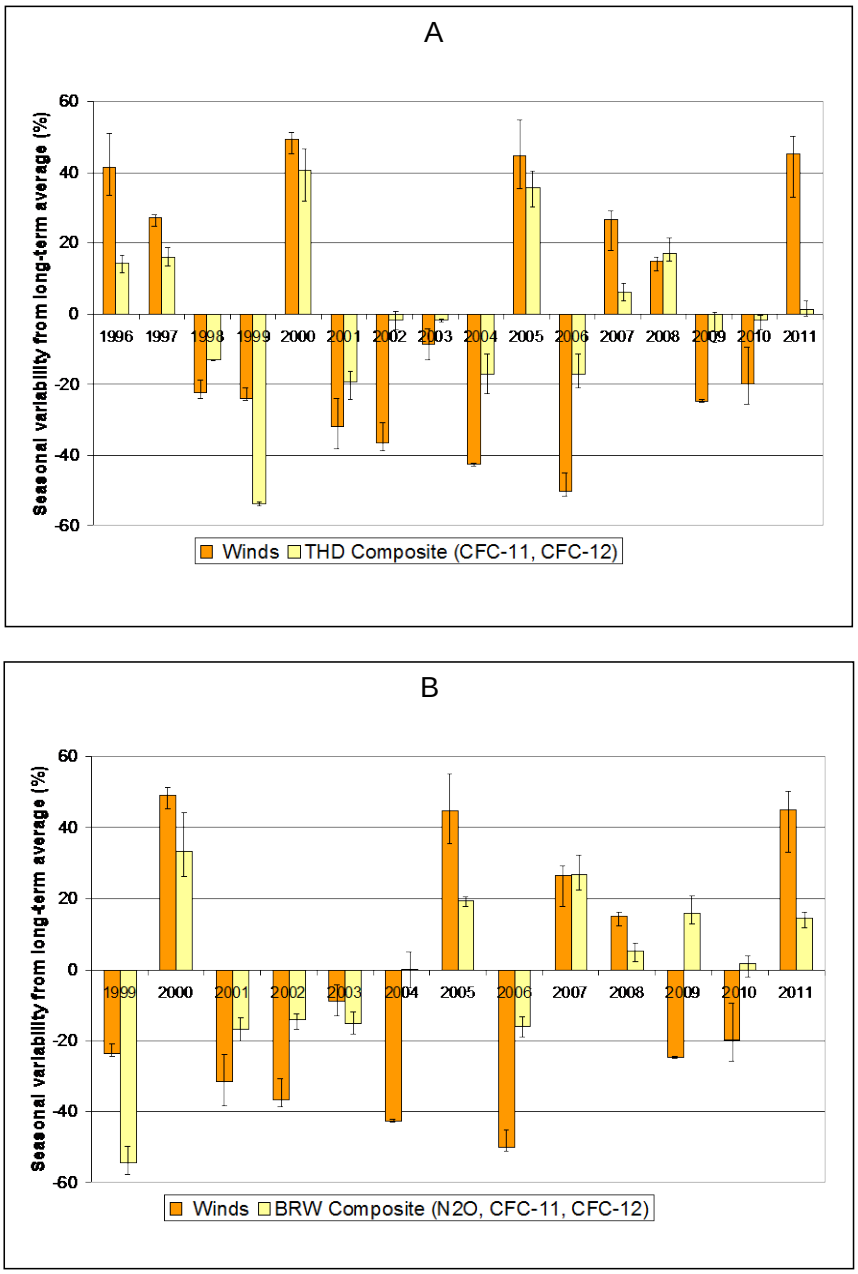

Figure 184**(A):** Correlation of THD 'composite' tracer (mean of CFC-11 and CFC-12) with the median of the winds. **(B)** Correlation of BRW CATS 'composite' tracer (mean of N_2O, CFC-11 and CFC-12) with the median of the winds. Composite is the mean of the three detrending methods as estimated at MHD.

We also briefly examined vertical profile measurements of N_2O and CFC-11 from the aircraft sampling program of NOAA/ESRL [http://www.esrl.noaa.gov/gmd] to see if they can provide a connection between STE and the lowermost troposphere. From the analysis of a very limited number of vertical profiles we conclude that these do not contradict our interpretation, i.e. STE can result in the transport of depleted mixing ratios of the stratospheric tracers into the lower regions of the troposphere, under conditions when there is a strong deceleration of the jet.

It is well established that other variations in atmospheric circulation, in particular, the El Niño Southern Oscillation (ENSO) and the North Atlantic Oscillation (NAO) are linked to the strength of the winter stratospheric circulation through dynamical coupling. A positive ENSO and a negative NAO are linked to stronger STE and thus deeper summertime minima of the stratospheric tracers. Figure 185 compares the residual component of the 'composite' tracer and the previous wintertime December-February (DJF) winds, the NAO and ENSO indices. Although N_2O is weakly correlated with ENSO and CFC-11 is also weakly correlated with NAO, these values are not statistically

significant. This suggests that tracer mixing ratios are better correlated with stratospheric winter flow than the major modes of tropospheric variability.

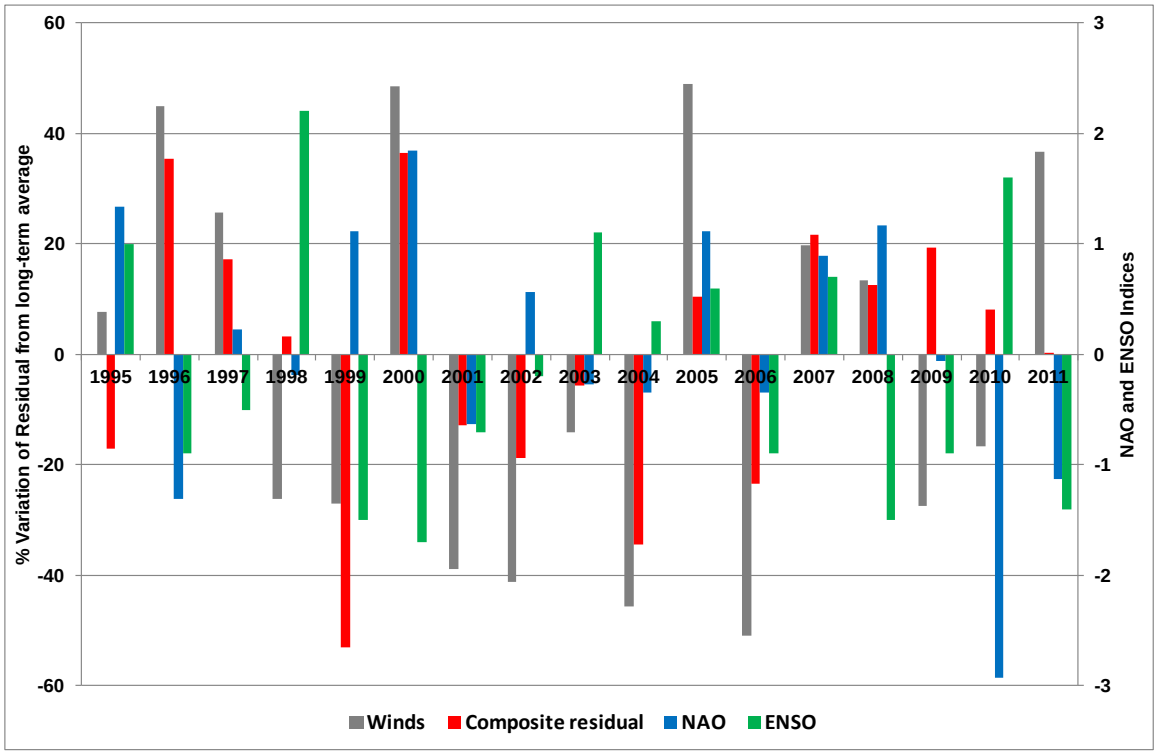

Figure 185**:** Comparison of the residual component of the MHD 'composite' tracer and the previous wintertime December-February (DJF) winds, NAO [*Hurrell and Deser.,* 2009; www.cgd.ucar.edu/cas/hurrell/indices.html] and ENSO [ENSO 3.4; www.cpc.ncep.noaa.gov] indices.

Table 85 summarises the Pearson correlation coefficient (r) for the individual tracers at MHD and the winds during 1995-2011. For the years when the stratospheric jet is strongly decelerated (relative to the climatological mean) we observe a deeper summertime minima (relative to the mean) in the species mixing ratios. The average individual correlation coefficients r (1995-2011) at MHD for N_2O, CFC-11 and CFC-12 were 0.71, 0.55 and 0.63, respectively with stronger winds corresponding to higher tropospheric tracer concentrations as expected. It is noteworthy that over the shorter time frame of 1995-2008 correlations were 0.80 (N_2O), 0.76 (CFC-11) and 0.74 (CFC-12).

Station / Tracer Species	Latitude, Longitude Network	Time-series
Mace Head, Ireland (MHD)	53.33°N, 9.9°W	1995-2011
N_2O	AGAGE	**0.71** (0.69-0.72)
CFC-11	AGAGE	**0.55** (0.50-0.59).
CFC-12	AGAGE	**0.63** (0.59-0.65)
'Composite Tracer'[1]	AGAGE	**0.68** (0.65-0.69)
Trinidad Head, USA (THD)	41.05°N, 124.15°E	1996-2011
N_2O[2]	AGAGE	0.41[2] (0.37-0.43)
CFC-11	AGAGE	**0.69** (0.60-0.73)
CFC-12	AGAGE	**0.59** (0.56-0.60)
'Composite Tracer'[3]		**0.78** (0.75-0.79)
Barrow, Alaska (BRW)	71.32°N,156.61°E	1995-2011
N_2O	NOAA,GCMG (HATS)	0.15 (0.01-0.25)
CFC-11	NOAA,GCMG (HATS)	**0.42** (0.37-0.43)
CFC-12	NOAA,GCMG (HATS)	0.26 (0.13-0.33)
Barrow, Alaska (BRW)	71.32°N,156.61°E	1999-2011
N_2O	NOAA,GCMG (CATS)	**0.53** (0.42-0.60)
CFC-11	NOAA,GCMG (CATS)	**0.68** (0.62-0.71)
CFC-12	NOAA,GCMG (CATS)	**0.51** (0.40-0.59)
'Composite Tracer'[1]		**0.67** (0.64-0.71)

Table 85: Correlations between the median of the (% deviation from the average) DJF 10 hPa winds in the 58°N-68°N latitude band and the mean tracer residuals (% deviation from the average) of the three detrending methods from 1995-2011 at MHD, THD, and BRW. The range in brackets shows the uncertainty in the correlation when the different methods are used individually.
Notes: [1] Mean N_2O, CFC-11, and CFC-12 residuals. [2] Seasonal cycle potentially influenced by summertime coastal upwelling. [3] Mean CFC-11 and CFC-12 residual seasonal variability. When N_2O is included in 'composite' r=0.77.

Table 86 lists the Pearson correlation coefficients (r) for each stratospheric tracer at MHD between the mean of the (% deviation from the average) three detrending methods versus the annual NAO] and ENSO indices.

Tracer	[1] ENSO (1995-2011)	[2] NAO (1995-2011)
N_2O	0.18	0.0
CFC-11	0.004	0.22
CFC-12	0.08	0.09

Table 86: Correlations between the mean tracer residuals (% deviation from the average) of the three detrending methods for N_2O, CFC-11 and CFC-12 and the NAO and ENSO indices.

In summary we have demonstrated strong correlations between the mid-stratospheric circulation at 10 hPa, 58°N-68°N and the de-trended residuals from the baseline monthly mean mixing ratios of the three stratospheric tracers N_2O, CFC-11 and CFC-12. There are a few years when the relationship between the species' residuals at the surface and behaviour of the jet is broken either collectively or as individual species. As noted previously there are other factors that cause climate variability in both the stratosphere and troposphere in addition to the stratospheric winds which will influence the depth of the tracer summertime minima. We would not therefore expect to see a perfect correlation in all years.

8.4.2 Potential Applications of this research.

We can see two potentially novel applications for this work. The first is seasonal forecasting of trace gas values in summer. While seasonal forecasts for many extratropical regions are unreliable with low forecast skill, the link between the previous winter circulation anomalies and the following summer minima in N_2O and CFCs appears to be strong enough to provide potentially high forecast skill for summer variations in trace gases strongly affected by STE. A further novel application of this work is monitoring the Brewer-Dobson circulation (BDC) by proxy. Given that the residual depth of the summer minimum is so well related to the strength of the winter and spring BDC, we can use it as a monitoring tool to test the climate model predictions of increasing BDC. This depth depends on the difference between summer and winter circulation. We can therefore estimate the uncertainty in any observed trend in the summer tracer minimum and calculate how many years of monitoring would be needed for this trend to be detectable above the climate variability "noise" using standard least squares fitting. The results show that it is not until the end of the 21st century that the increasing BDC is likely to be detected in observed tracer mixing ratios. However, if the noise could be attributed to other factors such as ENSO etc., as described above, then it may be possible to statistically remove these effects and better estimate the trends in the summer minimum, thereby allowing detection of the trend in the BDC on an a shorter timescale.

8.5 SPARC (Stratospheric Processes And their Role in Climate)

8.5.1 Re-evaluation of Lifetimes of Dominant Stratospheric Ozone Depleting Substances

The atmospheric lifetime of a trace gas is defined as the ratio of its global atmospheric burden to its annually averaged global loss rate. In the 1994 NASA assessment 'Report on Concentrations, Lifetimes, and Trends of CFCs, Halons, and Related Species' (NASA, 1994), lifetimes for numerous ozone-depleting substances (ODSs) were estimated based on observations and models. The report concluded that significant differences in model photolysis rates and transport led to at least a 30% range in lifetime estimates, and that the available observations were not sufficient to constrain the uncertainty in the model estimates. The calculated two-dimensional (2D) model lifetimes for $CFCl_3$ (CFC-11), for example, ranged from 40 to 61 years. The estimate inferred from observations and a 2D model with parameterized transport is 42 years (+7, -5, with 68% confidence). Later, Chapter 1 of the 1998 Ozone Assessment (Prinn and Zander, 1999) refined the figures (e.g., with a best estimate of 45 years for the CFC-11 lifetime).

Since then, three- dimensional (3D) chemical models (i.e., chemistry climate models or CCMs) have advanced significantly. Most CCMs use an agreed- upon set of photolysis rates, and many have fairly realistic transport, as judged by their ability to reproduce stratospheric distributions of long- lived trace gases. In addition, satellite, aircraft, balloon, and ground-based data sets for many important ODSs are now available for use in new estimates of inferred lifetimes.

Because the lifetimes of ODSs are used to predict their future evolution, to perform top down emission estimates, and to calculate the ozone-depletion potentials (ODPs) of those species, it is of critical importance to have the best possible estimates of ODS lifetimes. O'Doherty and Rigby are co-authors of Chapter 4 (Inferred Lifetimes from Observed Trace-Gas Distributions), where different methods have been applied to derive lifetimes of atmospheric trace gases based on measurements in the atmosphere. Some of these methods rely on a combination of modelling and observations while relative lifetimes of some species can be deduced from stratospheric correlations directly. The SPARC report will be published later in 2013. After publication it will be possible to provide DECC with updated figures illustrating the most recent global radiative forcing estimates in addition to figures illustrating global total chlorine and global total bromine [Objective 9].